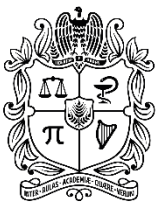

UNIVERSIDAD
NACIONAL
DE COLOMBIA

Durability Performance Assessment of Fly Ash Concrete Using Fine Recycled Aggregates

Andrés Felipe Barragán Ramos

Universidad Nacional de Colombia

Facultad de Ingeniería

Departamento de Ingeniería Civil y Agrícola

Bogotá, Colombia

2021

Durability Performance Assessment of Fly Ash Concrete Using Fine Recycled Aggregates

Andrés Felipe Barragán Ramos

Tesis de investigación presentada(o) como requisito parcial para optar al título de:

Magister en Ingeniería - Estructuras

Director:

I.C. MSc. Camilo Ríos Fresneda

Codirector:

I.C. PhD. MSc. Juan Manuel Lizarazo Marriaga

Línea de Investigación:

Materiales para construcción

Grupo de Investigación:

GIES – Grupo de investigación en Análisis y diseño

Universidad Nacional de Colombia

Facultad de Ingeniería

Departamento de Ingeniería Civil y Agrícola

Bogotá, Colombia

2021

Agradecimientos

Quiero dar gracias a mis padres por su constante apoyo, paciencia y amor durante todos estos años que he dedicado a estudiar.

A mi pareja, Mariana, quien me apoyó y acompañó en este proyecto como lo ha hecho con tantas cosas en mi vida.

Al Ing. Camilo Rios Fresneda, por haberme guiado y apoyado con su conocimiento, amistad y experiencia durante todo este proyecto de investigación. Quiero agradecerle además por la ayuda en la adquisición de materiales, equipos y asesorías que facilitaron la ejecución de este trabajo de grado.

Al Ing. Juan Manuel Lizarazo, sin cuyas enseñanzas, disposición y conocimiento no habría sido posible finalizar esta investigación.

A la Geóloga Nicole Hernández. Quien brindó su inestimable ayuda para la examinación petrográfica de agregados.

Al Ing. Jorge Olarte, del Laboratorio de cementos, Ing. Darío Moreno, del Laboratorio de Materiales y Tec. Edgardo Herrera, del laboratorio de Tecnología del concreto por su valiosa colaboración y disposición en la fase experimental de esta investigación.

A los ingenieros Jesús Omen y Luis Felipe Salazar con quienes compartí en los laboratorios, por sus múltiples favores y su ayuda en la fase experimental del proyecto.

Declaración de obra original

Yo declaro lo siguiente:

He leído el Acuerdo 035 de 2003 del Consejo Académico de la Universidad Nacional. «Reglamento sobre propiedad intelectual» y la Normatividad Nacional relacionada al respeto de los derechos de autor. Esta disertación representa mi trabajo original, excepto donde he reconocido las ideas, las palabras, o materiales de otros autores.

Cuando se han presentado ideas o palabras de otros autores en esta disertación, he realizado su respectivo reconocimiento aplicando correctamente los esquemas de citas y referencias bibliográficas en el estilo requerido.

He obtenido el permiso del autor o editor para incluir cualquier material con derechos de autor (por ejemplo, tablas, figuras, instrumentos de encuesta o grandes porciones de texto).

Por último, he sometido esta disertación a la herramienta de integridad académica, definida por la universidad.

Andrés Felipe Barragán Ramos

24/09/2021

Resumen

“Evaluación del desempeño por durabilidad de concreto con ceniza volante y agregados reciclados finos”.

En Colombia y el mundo, el uso de la fracción fina de los agregados reciclados derivados del concreto (RCA) es una práctica altamente restringida debido al efecto negativo que tienen los mismos en las propiedades mecánicas y de durabilidad. A pesar de que internacionalmente se ha concluido que pueden obtenerse resistencias satisfactorias usando estos agregados, no se ha estudiado extensamente el efecto que tienen los mismos en las propiedades de durabilidad, específicamente aquellas relacionadas a la corrosión debido a cloruros. En esta investigación, fueron realizadas mezclas de concreto con 0%, 20%, 60% y 100% de sustitución de agregados RCA y ceniza volante como cementante adicional con el fin de evaluar las propiedades físicas, desempeño mecánico, permeabilidad a cloruros y corrosión del acero de refuerzo con técnicas electroquímicas a distintas edades.

Los resultados indican que a pesar de que algunas propiedades se ven afectadas negativamente por la inclusión de finos reciclados, la ceniza volante es un mitigador altamente efectivo ante la penetración de cloruros a largo plazo y el uso de agregados reciclados no incrementa significativamente el riesgo de corrosión del acero de refuerzo a pesar de su alta alcalinidad. Basado en estos resultados, fue realizado un análisis de códigos de construcción internacionales con el fin de proponer lineamientos básicos que permitan usar estos agregados para la producción de concreto con fines estructurales.

Palabras Clave: Agregados reciclados, concreto reciclado, durabilidad del concreto, corrosión del acero.

Abstract

"*Durability Performance Assessment of Fly Ash Concrete Using Fine Recycled Aggregates"*

In Colombia and internationally, the use of the fine fraction of recycled concrete aggregates (RCA) is a highly restrictive practice due to the negative effect of its use in the mechanical and durability-related properties of new concrete. International research has concluded that a satisfactory compressive strength can be achieved using these aggregates, however, the durability effects related to steel bar corrosion by chlorides have not been extensively assessed. In this research, concrete mixes were produced with an RCA replacement of 0%, 20%, 60% and 100%, using fly ash as a supplementary cementing material to evaluate the physical properties, mechanical performance, chloride permeability and steel rebar corrosion using electrochemical techniques at different specimen ages.

Results indicate that while some properties are negatively affected by the inclusion of fine RCA; using fly ash is a highly effective mitigation technique to reduce long-term chloride penetration. It was also concluded that the use of recycled aggregates does not increase reinforcement steel's corrosion risk. Based on these results, an assessment of different international building codes was performed in order to suggest basic requirements for using recycled aggregates for structural concrete production.

Keywords: Recycled Aggregates, recycled concrete, concrete's durability, steel rebar corrosion.

Index

List of Figures

List of tables

Symbols and Abbreviations

Symbol	Name	Unit (SI)	Definition
A	Ampere	A	-
s	Second	s	-
mA	Milliampere	mA	10^{-3} *A*
C	Coulomb	C	$1\ A\ s$
V	Potential	V	$\Omega\ A$
Z	Impedance	Ω	-
y	Year	-	31536000 *s*
E_{corr}	Corrosion potential	V	-
ΔE	Potential differential	V	-
CR	Corrosion rate	-	µ*m/y*
i_{corr}	Corrosion current density	-	A/m^2
R_P	Polarization resistance	-	$\Omega\ cm^2$
J_i	Flux	-	
c_i	Mass concentration	-	

Symbol	Name	Unit (SI)	Definition
m	Meter	*m*	-
cm	Centimeter	-	10^{-2} *m*
mm	Millimeter	-	10^{-3} *m*
µm	Micrometer	-	10^{-6} *m*
N	Newton	*N*	-
kN	Kilonewton	-	10^{3} *N*
A'	Area	m^2	-
P_u	Ultimate compressive load	kN	-
Pa	Pascal	Pa	N/m^2
MPa	Megapascal	-	10^{6} Pa
f_c'	Concrete compressive strength	MPa	P_u/A'
g	Gram	-	-
Φ	Diameter	-	-
°*C*	Degree Celsius		
D_{nssm}	Non-steady-state migration coefficient	-	-

Abbreviations

Abbreviation	Definition
W/B	Water-to-binder ratio
RCA	Recycled concrete aggregate
RAC	Recycled aggregate concrete
RA	Recycled aggregate
f-RCA	Fine recycled concrete aggregate
FA	Fly Ash
ITZ	Interfacial transition zone
OPC	Ordinary Portland Cement
OAM	Old-attached mortar
pH	Potential of hydrogen
SCE	Saturated calomel electrode

1. Introduction

This research work was carried out to identify the effects of fine recycled concrete aggregates (fine-RCA) on the durability properties related to corrosion of hardened concrete. Despite its potential and environmental benefits, building codes and regulations worldwide and particularly in Colombia limit the use of this kind of aggregates as granular bases for road construction projects and non-structural concrete. As recycled aggregate concrete (RAC) is a sustainable alternative to conventional concrete, its mechanical and durability related properties must be fully assessed to allow the use of this material for structural purposes.

Scientific literature review shows that RAC mechanical performance is lower to conventional concrete, especially when including fine fractions, and additional products such as pozzolans must be used to improve the durability properties of this material. This work aims to establish the viability of employing fine recycled aggregates from a durability point of view while using fly ash as a mineral admixture. As reinforcement corrosion is considered the main issue to allow a generalized use of RAC, durability testing was focused on the main concrete properties related to this process. These tests included the measurement of concrete air permeability, chloride ion penetration, water absorption, porosity, density, Electrical Impedance Spectroscopy (EIS) and linear polarization resistance (LPR).

1.1 General Objective

Evaluate the effects of using fine recycled concrete aggregates obtained from construction and demolition waste and fly ash in concrete's durability performance related to steel rebar corrosion.

1.2 Specific Objectives

- To perform a comparative analysis between the properties of fine natural aggregates and fine recycled concrete aggregates.
- To identify the effects of incorporating different ratios of fine recycled aggregates in the durability performance of concrete.
- To evaluate the effects on corrosion-related durability properties of incorporating fly ash to concrete mixes made with fine recycled aggregates.
- To perform a mechanical and durability comparative analysis between the performance of conventional concrete, recycled aggregate concrete and recycled aggregate concrete with fly ash.
- To identify the viability of employing fine recycled aggregates with mineral additions according to national performance regulations.

2. Background and Justification

2.1 Background

Construction is one of the largest industry sectors as it is a manifestation of the economic and social developments of many countries. However, this industry is responsible for causing considerable environmental impact due to the massive extraction of natural resources and the associated pollution resulting from their processing activities [1]. Particularly, concrete production has a highly negative environmental impact as it requires large energy amounts, aggregate-extraction mining activities, and industrial processing for cement production. To produce one ton of Portland cement, approximately 1200 kg of limestone and marl, 400 kg of clay and 50 kg of gypsum are required. It is also estimated that cement production is responsible for 8% of the total CO2 released into the atmosphere. Out of this percentage, 65% is related to limestone extraction and clinkering, and the remaining 35% of emissions is caused by burning fossil fuels in cement production, as this process requires high temperatures [2].

Construction also generates large amounts of waste and debris due to the eventual demolition of buildings that have completed their life-cycle. Only in Europe, the construction industry generates more than 100 million tons of construction and demolition waste (CDW) per year [3]. In the USA, 569 million tons of CDW were generated in 2014, mainly from demolition activities and in China, 30% – 40% of total waste consists of CDW, producing around 3000 million tons. [4]. In Colombia, construction and demolition waste (CDW) are responsible for most of the country's solid waste production, corresponding to an estimate of 100 thousand tons per day (*Red Gestora de Residuos, 2016*). Most of these generated CDW are often incorrectly managed in waste deposits and is rarely reused, thus causing environmental deterioration, land encroachment, as well as potential soil damage. [4].

Colombia's biggest center of CDW production is Bogotá, where different public policies such as the Act No.1115 of 2012 (Resolución No. 1115 de 2012) "Utilización de elementos

reciclados provenientes de los Centros de Tratamiento y/o Aprovechamiento de RCD" and the City Development Plan 2012 – 2015 that includes the "Programa de Basuras Cero – Escombros Cero" have been formulated to control the disposal of these detrimental materials. However, these policies only focus on the final disposal location and ignore the possibility of reusing CDW for structural purposes on new buildings, therefore long-term production of CDW in Bogotá will cause an increasingly negative environmental effect due to the absence of an established reutilization program. Additionally, most of the aggregates used for concrete production in the city of Bogotá must be transported from different regions of Colombia, increasing environmental impact, and representing an additional cost that could be reduced if the local construction and demolition waste were reused for concrete production.

Using CDW as concrete aggregate has been proposed as a solution to reduce the amount of disposed waste and CO_2 emissions and allow sustainable production of concrete. Since CDW is a heterogeneous material, the quality of the resulting concrete is poorer in terms of mechanical and durability properties. However, it has been shown that when an adequate source separation is performed, using only recycled concrete aggregates (RCA), the resulting concrete can achieve similar properties than those of natural aggregate concrete [5].

Concrete produced from RCA is known as recycled aggregate concrete (RAC), and throughout the recent years, several studies have reported the effects from incorporating these aggregates in concrete's properties as the use of this material is economically feasible and environmentally friendly for structural applications [6]. In general, it has been shown that the concrete strength is reduced with a higher RCA replacement ratio (Guo et al. 2018; Kurda et al. 2018; Kwan et al. 2012; Lotfi et al. 2015; Matias et al. 2013; Mukharjee and Barai 2017; Pacheco et al. 2019; Rodrigues et al. 2013; Verian et al. 2018; Xiao et al. 2012). However, when the material is obtained from laboratory or field concrete samples without contaminants such as clay or masonry debris, the resulting strength can meet the expected behavior of natural aggregate concrete (Babu et al. 2014a; Lotfi et al. 2015; Marco 2014; Pedro et al. 2017a; Silva et al. 2019).

As durability-related properties are more affected by RA incorporation, little acceptance has been observed in the use of recycled aggregates for concrete production, especially when

employing fine RCA from CDW recycling plants, due to the variability of their composition [5]. Since most of these negative effects in concrete performance have not been controlled, most international regulations and codes in countries such as Spain, Portugal, U.K and Belgium allow a maximum replacement ratio of coarse recycled aggregates of 20% and forbid the use of RAC for structural purposes. Fine recycled aggregates are not allowed in most countries as they are responsible for a larger mechanical and durability performance loss. However, recent research has focused on developing enhancing techniques on both the aggregates and the concrete mix such as the use of mechanical grinding and mineral additions that could drastically reduce the negative effects of using RCA and allow it's structural use [21].

Finally, although some research has been reported on the RAC durability, especially when using the aggregate coarse fraction, it is still necessary to identify the effects of using fine recycled aggregates in concrete's rebar corrosion and the possible improvement caused by enhancing techniques such as the addition of fly ash. These enhancing techniques could allow the use of these aggregates to reduce the detrimental environmental effects of the construction industry and reduce transportation and extraction costs.

2.2 Justification and Problem Statement

The use of recycled aggregate concrete (RAC) has recently gained attention as it could be a long-term partial solution to the increasing production of construction and demolition waste (CDW) due to economic growth and the expansive development of urban centers. Extensive research has identified the negative effects of incorporating recycled aggregates in the mechanical and durability performance of concrete, however, the use of enhancing techniques has drastically improved RAC's viability.

Since the effects of using fine recycled concrete aggregates and mineral admixtures such as fly ash in concrete's durability to corrosion have not yet been fully studied in national and international research programs, the durability and basic mechanical properties of concrete mixes that include different replacement ratios of fine recycled aggregates and fly ash were compared in this research. A performance assessment was conducted on concrete mixes to evaluate different durability properties related to corrosion. From this assessment, the formulation of an optimal mitigation strategy could be formulated.

The results obtained are essential to further reduce the performance gap between conventional concrete and recycled aggregate concrete and could help to develop new mitigation strategies that could even result in the use of this material for structural purposes in different national and international building codes and regulations.

3. Research Framework

3.1 Aggregate-related properties affecting the durability of Recycled Aggregate Concrete

There are multiple factors affecting the durability-related performance of mixes made with recycled concrete aggregates such as aggregate substitution, content of adhered mortar, particle size, W/C ratio and recycled aggregate angularity. A qualitative summary of these effects in different durability properties, presented in Table 1, will be discussed in depth in this section.

Parameter	Parameter Change	Effect on RAC Durability Properties						
		Absorption	Permeability	Carbonation Resistance	Chloride Penetration	Freeze-Thaw Resistance	Drying Shrinkage	Abrasion Resistance
RA Substitution	↑	✗✗	✗✗	✗	✗	✗	✗✗	-
Adhered Mortar	↑	✗	✗	✗	✗✗	✗	✗	✓
Particle Size	↓	✗✗	✗✗	✗✗	✗	-	✗✗	✓
W/C Ratio	↓	✓	✓	✓✓	✓✓	✓✓	✓	✓
Aggregate Angularity	↑	✗	✗	✗	✗	✗	✗	✓

Remark:	↑	Increase	↓	Decrease
	✗	Negative	✗✗	Strongly Negative
	✓	Positive	✓✓	Strongly Positive
	-	No Significant Effect		

Table 1 – Effect of multiple aggregate and mix parameters in different durability properties of RAC.

3.1.1 Adhered mortar content of aggregates

There are multiple factors that may modify the mechanical and durability properties of concrete using recycled aggregates. The negative effects of incorporating RCA in the durability of concrete can be attributed to the high amounts of old adhered mortar (OAM) derived from parent concrete [22] or the presence of deleterious materials such as wood, clay or bricks [23]. OAM consist mainly of fully or partially hydrated cement particles with high porosity paste adhered to natural aggregates. The level of cement hydration and the surface area of the natural aggregates result in high concentrations of OAM for fine-RCA.

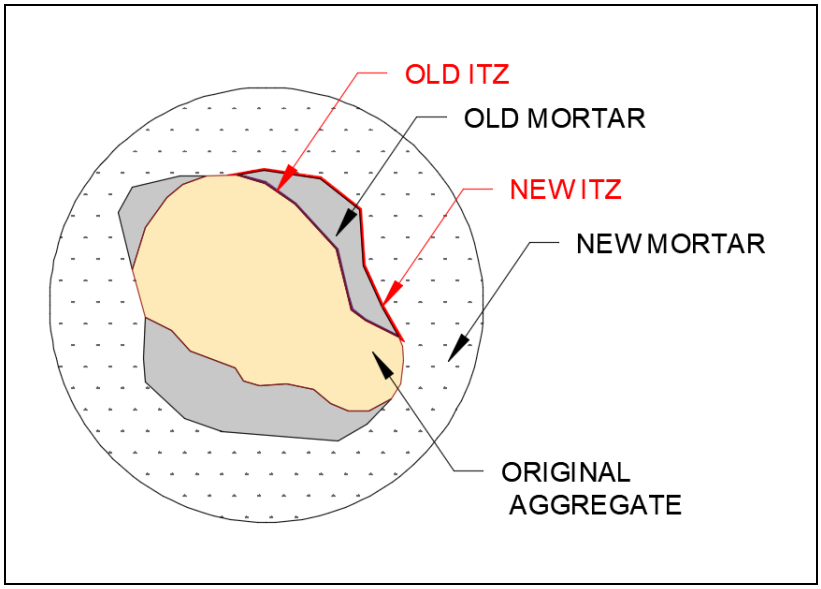

Figure 1 – Schematic of old and new ITZ in RCA. Adapted from *(Verian, 2018)* [8]

The microstructure of conventional concrete, also referred as Natural Aggregate Concrete (NAC), has a well-defined interfacial transition zone (ITZ) between the cement paste and the aggregates, whereas for RAC it can be identified three interphases, as shown in Figure 1: (1) ITZ between natural aggregate and old cement matrix (Old ITZ). (2) ITZ between natural aggregate and new cement matrix (New ITZ) and (3) ITZ between the new and the old cement matrices (New ITZ) [12], [24]. The presence of OAM drastically affects water absorption and density of RCA. In Figure 2, recycled aggregates present a gray color due to OAM and are expected to produce higher water absorption than natural aggregates.

Figure 2 - Fine recycled concrete aggregates (left) and fine natural aggregates (right)

Due to OAM, recycled aggregates show higher water absorption, lower density and lower abrasion resistance than natural aggregates [25], The presence of OAM is also responsible for the presence of micro-cracks, impurities and higher porosity in concrete's microstructure that reduce durability performance [8], [21], [26]. Recent research trends have focused on enhancing techniques to partially remove adhered mortar by further mechanical processing (Babu et al. 2014a; Dimitriou et al. 2017; Kazmi et al. 2019; Pepe et al. 2014), chemical treatment with different acid solutions [21], [29]–[31] and thermal techniques [32]–[35].

One of the main factors affecting the durability of RAC is the replacement ratio of recycled aggregates incorporated in the mix. There is a consensus in the literature about the negative effects on durability and mechanical performance of concrete when partially or completely substituting natural aggregates for RCA. Studies report a linear correlation between the incorporation ratio of recycled aggregate and the water absorption of concrete [10], this will result in more porous concrete mixtures with decreased durability. Compressive strength loss will also be greater for higher percentage ratios of both coarse and fine-RCA [36]–[41]. The mixtures with higher RCA replacement also present higher chloride intrusion [42] and Drying shrinkage deformation [43], [44].

Despite the apparent negative effect of incorporating recycled concrete aggregates, some studies carried out by Pedro de Brito & Evangelista (2017b) suggest that using RCA does not compromise the use of these aggregates in structural concrete as long as the RA's quality is guaranteed. In this study, the water absorption values, the carbonation and the chloride ion diffusion did not vary significantly when compared to natural aggregate concrete (NAC) and meet the requirements of most international standards since the aggregates were produced following strict laboratory conditions. Other than OAM content, there are different factors related to recycled aggregates that present significant impact in RAC's performance.

3.1.2 Particle Size of aggregates

The recycled aggregate size is one of the main factors affecting RAC mixtures' mechanical and durability related performance. Concrete mixtures made with fine-RCA have a limited performance compared to the corresponding coarse aggregate mixtures [26]. As fine-RCA are obtained by more intensive crushing processes, they have higher heterogeneity and contain more contaminants that could affect concrete's resulting properties [46]–[48], furthermore fine-RCA have a higher surface area and greater attached mortar that greatly increases water absorption.

A study performed by Evangelista et al. (2015) characterized the physical, chemical and mineralogical properties of fine-RCA by XRD, SEM/EDS and DTA/TG of individual size fractions. It was concluded that the recycled aggregate's smaller size fractions have higher bonded mortar contents and a reduced natural aggregate content. This results in more porous particles with water absorption levels up to 900% higher than natural fine aggregates. The higher water absorption by the recycled aggregates will result in lower density values, and a decrease in the mechanical and durability-related performance of the resulting concrete mixtures. Most international building standards and codes, exclude the use of fine-RCA due to their detrimental effects on concrete's durability and mechanical properties [35], [49].

Fine-RCA have a detrimental effect on the most important concrete's qualities, such as workability [50] compressive and tensile strength, modulus of elasticity, water absorption, shrinkage, carbonation and chloride penetration resistance [15], [49], [51]. There is a direct

relationship between RAC's durability and permeability-related performance, the latter being directly affected by the quantity and quality fine-RCA in the mixture [26], [47]. This is attributed to the higher porosity of fine recycled aggregates which allows the transport of fluids through them.

It has been reported that he replacement of 100% of fine-RCA increases water absorption by immersion and capillary action and reduces the carbonation and the chloride migration resistance [52]. However, some studies have obtained similar durability behavior between conventional concrete and RAC incorporating less than 30% fine-RCA [53]–[57].

3.1.3 Water to cement ratio of concrete and water content of aggregates

Another important factor affecting the RAC durability is the water/cement ratio (w/c). As expected, RAC has lower durability performance than its corresponding natural aggregate concrete (NAC) with the same w/c ratio. However, in low w/c ratio recycled aggregate concrete, the low porosity of the new paste is predominant so the flow of aggressive agents is delayed, thus obtaining similar results in some durability properties for both types of concrete [58].

The RCA's water absorption and porosity are higher than those of natural aggregates due to a higher porosity. This will lead to a decrease in concrete's mechanical and durability performance [25], [59] as well as reduced workability [60]. The water content of recycled aggregates is another important factor affecting the RAC durability. Since the RAC absorption levels are considerably high, water must be compensated to avoid a reduction in the effective w/c ratio that could result in a loss of mechanical resistance and durability performance. This can be accomplished by pre-saturating the recycled aggregates, by re-adding the absorbed water in the mixture [16], [51], [61] or by incorporating water-reducing admixtures [53].

Some studies have concluded that using recycled coarse aggregates in new concrete does not interfere with the effective w/c ratio as long as the additional amount of absorbed water is compensated in the mix [62]. Similarly, the use of superplasticizers and water reducing

admixtures can compensate for the loss in workability resulting from the incorporation of RCA [11].

Ferreira, et al. (2011), compared the effects of non-saturated aggregates and pre-saturated recycled coarse aggregates. In this study aggregates were saturated to approximately 90% of the potential water absorption by immersing them for 5 minutes. Conclusions showed that when the aggregates are fully saturated, potential bleeding may occur as the aggregates return part of the water to the paste. When comparing the pre-saturated aggregates mixes with the water-compensated mixtures, the first ones showed low mechanical performance and higher concrete water absorption due to less penetration of the cement paste into the pores of the saturated aggregates and a weaker interlock between the aggregates and the new paste.

3.1.4 Aggregate Shape

Another factor affecting RAC's performance is the recycled aggregate (RA) shape, which is directly related to its crushing or demolition process [64]. The use of rounder recycled particles may improve concrete's performance when compared to that provided by angular and elongated particles, as they improve its workability [11], [58].

The type of crushing devices and the number of processing stages influence the RA particle size and shape. Usually, jaw crushers are used in the primary stage of crushing and the they provide the best grain-size distribution; however, these aggregates will tend to be sharper [61], [65]. A second crushing stage is implemented by using cone crushers or impact crushers to produce more spherical particles with lower flakiness index and better grain-size distribution [46].

RCA originated from industrial crushing processing can also present fissures and micro-cracks that may contribute to the poorer mechanical and durability performance of RAC [48], [59]. Fine-RCA are angular and irregular and a significant number of fines is usually present in the pores of coarser particles, furthermore, the smaller size fractions presents high mortar content and low presence of natural aggregates [49].

The production process of recycled aggregates plays an important role in concrete's durability. A research by Bravo et al. (2015) studied the durability and mechanical

performance of concrete made with aggregates from different recycling plants in order to assess the effects of RA's composition. As expected, the properties of concrete vary greatly depending on the local construction activities of each recycling plant. The plants with the higher number of fine contaminants have the worst mechanical performance [15].

Another study by Alexandridou et al. (2017), assessed the mechanical properties and durability of recycled aggregates from three different recycling plants from Greece. As expected, each sample had different amounts of old bonded mortar, clay, soil and other contaminants due to the different origin and production process employed in every recycling plant. The concrete mixes made from these aggregates had different compressive strengths, but all were lower than NAC. According to the authors, the reduction of compressive strength is more notorious when the presence of clay minerals is higher. The durability was also lower when using recycled aggregates, having higher water absorption, higher carbonation depth and higher sorptivity, especially when the replacement ratio was higher than 75%.

3.2 Durability-related Properties of Recycled Concrete Aggregate

3.2.1 Absorption and permeability

Due to the high absorption levels of RCA, the resulting hardening concrete has workability difficulties and consequently lower mechanical and durability performance [50], [51], [59], [66]–[69]. This is attributed to the presence of high-absorption residual cement mortar bonded to the aggregate particles, which leads to a higher water requirement in the mixture, hence increasing the resulting concrete's permeability [56], [68], [70]. Other possible cause for the high absorption levels is the presence of micro-cracks in the concrete, which tend to create a path for water flow [9], [24].

Different studies cited by Verian et al. (2018) have reported that RAC has also a permeability higher than that of NAC, shown in values from two to five times above. When

the RCA replacement level is 100%, an RAC absorption increase of around 70% is also reported [67]. A study by Kurda et al. (2018) reported that the oven-dried density of concrete bearing RAC is lower than that of NAC, and also, when using fine recycled aggregates, the resulting concrete density will be inferior.

The aggregate size has been related to the high-water absorption level observed in RAC. Coarse aggregates have a smaller surface area than fine aggregates, which means less attached mortar and lower water requirement and absorption [9]. In the study conducted by Fan et al. (2015), it was reported that increasing the replacement ratio of fine recycled aggregates led to a reduction in flow values, density, compressive strength and ultrasonic pulse velocity.

The aggregate size has an important role in RAC's permeability and water absorption. Different concrete mixtures containing only fine-RCA obtained in laboratory conditions were tested by Evangelista & De Brito (2019), who showed that capillary water-absorption varies linearly with the increase of fine recycled aggregates in the mixture, having a difference of about 20%. The age of specimens did not seem to affect absorption by immersion, and the use of fly ash had a positive effect on this property.

Evangelista & de Brito (2010) reported that concrete made using a 100% replacement of fine recycled aggregate had a 46% increase in the absorption by water immersion, and a 70% sorptivity increase. This was expected as the concrete made with FRA has a more porous structure. Similar results were reported by Bravo et al. (2015), who concluded that the capillary water-absorption increases as the substitution RA ratio grows. When using 100% recycled aggregates from recycling plants, the same study reported a water absorption increase between 5.5% and 14.2%. Nevertheless, when using recycled coarse aggregates with a low replacement ratio (up to 25%), the water absorption values were similar to those of natural aggregate concretes.

3.2.2 Carbonation resistance

Concrete carbonation occurs due to the penetration of carbon dioxide present in the atmosphere (André et al. 2014; Li 2011; R. V. Silva et al. 2015). This gas can react with solid calcium hydroxide generated from the hydration of Portland cement, resulting in the

production of calcium carbonate. This reaction has considerable detrimental effects on concrete reinforcement, as it induces an alkalinity reduction by the consumption of calcium hydroxide. During the Portland cement hydration process, the concrete porous solution reaches a very alkaline pH of around 12 – 13.5, which is reduced through carbonation to values around 8.5 – 9 [75].

As the alkalinity decreases, the passive environment of steel bars could be lost, and the reinforcement turns susceptible to corrosion when oxygen and water are present. The concrete carbonation depth is proportional to the time square root, and it is expected that the concrete cover is enough to protect the reinforcement for as long as the structure life was defined [76]. Corrosion reduces the resistance, ductility and functionality of the steel rebar. When concrete has a denser microstructure, the carbonation rate is lower, this usually is accomplished by using a low w/c ratio and implementing intensive moist curing methods [77].

It has been shown that the RAC carbonation resistance is lower compared to that of NAC. A number of studies have concluded that increasing RCA levels can lead to a reduction of the RAC carbonation resistance [12], [51], [66], [67], [74], [78]. This has been attributed to the higher RAC porosity due to the presence of microcracks and a less dense cement matrix. It is expected that carbonation decreases as the w/c ratio decreases as well. Carbonation is increased when using fine recycled aggregates, since it results in higher-absorption concrete levels.

One of the main factors affecting RAC carbonation resistance is the replacement ratio of recycled aggregates. Silva et al. [74] performed a statistical analysis on the results of 600 mixtures made with coarse recycled aggregate and 360 mixtures bearing fine recycled aggregate from 10 different publications. This analysis concluded that mixtures using 100% coarse RA have a 95% likelihood of exhibiting carbonation depths up to 2.5 times greater than mixtures bearing only natural aggregates. When using fine recycled aggregates, the carbonation depth could be up to 8.7 times greater than that of the corresponding NAC.

The aggregate particle size has an important effect on the RAC carbonation resistance. A study conducted by Evangelista & de Brito (2010) concluded that when using fine recycled aggregates, the carbonation depth has a linear relationship with the replacement ratio, and

it can increase up to 110% at 21 days when comparing it to that of the natural aggregate mixture. A more recent study showed that concrete mixtures using fine recycled aggregates had higher carbonation depths than a reference concrete, ranging from 14 mm for 0% FRA to 20 mm for 100% FRA at 182 days [47].

The w/c ratio can also influence the carbonation resistance of the resulting RAC mixtures, as lower values result in denser mixtures and lower carbonation depths. Some authors suggest that by adjusting the mixture w/c ratio with high RCA replacement can lead to similar carbonation values when compared to NCA (Limbachiya et al. 2000.; R. V. Silva et al. 2015). It is recommendable to decrease the effective 0.05 w/c ratio to 0.1 points in order to obtain similar carbonation values for NAC and RAC made with 100% coarse aggregate [58].

Regarding curing and environmental conditions, concrete mixtures with inadequate curing conditions will be more likely to have an increased carbonation depth as the resulting matrix will be more porous due to the presence of water cracks caused by shrinkage around aggregate particles [76]. Recycled concrete mixtures cured in a drier environment show an increased carbonation depth. According to Silva et al. (R. V. Silva et al. 2015), under the right conditions, RAC mixtures can meet the carbonation resistance requirements to accomplish the target service life of concrete structures, and a detailed analysis on the needed concrete cover for reinforcement bars would be required.

3.2.3 Chloride penetration resistance

The presence of free chloride ions in the concrete matrix might also induce corrosion in the steel reinforcement bars. Chloride ions could be sporadically present in the aggregates or mixing water; however, they can also penetrate externally from different sources such as seawater, salt spray or de-icing agents [72]. When the chloride concentration in reinforced concrete is high enough, there is a significant risk of corrosion in a moist environment. The chloride-ion penetration rate is a concrete quality function, which tends to be higher in more porous materials [75].

Studies have shown that there is a linear relationship between the chloride penetrability and the increasing replacement of coarse RCA [51]. As RAC is more porous than NAC, a

reduction of chloride ion penetration resistance has been observed by different studies (Bravo et al. 2015; Kou 2007; Kou et al. 2012; Kurda et al. 2017; Kurda et al. 2019; Sim and Park 2011; Verian et al. 2018; Xiao et al. 2012). This negative effect can increase when the specimens are cured in a dry environment, as the lack of a proper hydration process can lead to a more porous microstructure; however, some studies claim that RAC can still be used for structural purposes since the target service-life can be achieved despite the detrimental effects in chloride penetration from incorporating recycled aggregates [47], [84].

According to Verian et al. (2018) , a rapid chloride permeability test (RCPT) on coarse RAC showed a passing charge 25% higher than that of NAC. This also indicates that RAC has a lower resistivity than NAC due to its more porous microstructure. There have been differences attributed to different experiment conditions such as w/c ratio or curing age and the values remain acceptable for structural RAC [67]. According to Kurda et al. (2017), the chloride ion penetration is more dependent on the cement matrix quality than on the aggregate's porosity. The chloride ion penetrability resistance has been reported to increase with the growth of the curing age and the reduction of w/c ratio [67], [81]. This can be attributed to the fact that and extended curing and low w/c ratios result in a denser and less porous cement matrix.

When incorporating coarse recycled aggregate, an increase in the chloride ion penetration depth of about 100% was observed [84]. According to the same study, the chloride penetration resistance improves over time, as mixtures with increasing coarse aggregate content presented a similar behavior than the corresponding NAC after 10 years. Also, in the previous research it was reported that the use of fly ash and other mineral admixtures can reduce the chloride ion penetrability.

A study conducted by Evangelista & de Brito (2010) reported that RAC made with 100% fine recycled aggregate has an increase of 33.8% in terms of the migration coefficient when compared to its natural aggregate counterpart. As the migration coefficient is directly linked to the concrete porosity, it is expected that RAC using fine recycled aggregates have a decrease in its chloride penetration resistance. It is also stated that there is a linear relationship between the proportion of the recycled aggregates and chloride penetration. Conclusions show that incorporating supplementary cement materials such as mineral

admixtures could compensate the negative effects from the presence of fine recycled aggregates. Another study by the same authors established a linear variability between the replacement ratio of fine-RCA and the chloride diffusion coefficient [47].

3.2.4 Freezing-thawing resistance

Concrete can be damaged from the effects of freezing-thawing cycles. As concrete is a porous material, water can accumulate in voids, fissures and surface pores. These voids are known as capillary voids and may range from 5 nm to 1 μm. When the temperature is low enough, water will freeze and expand. This expansion causes cracks in concrete which may increase with time as the damage accumulates. [75].

Freezing damage does not only depend on the exposure temperature. Since the concrete porous solution also includes different salts, its freezing point is lower than 0°. Moreover, freezing temperature is also a function of the pore size and it's not uniform in concrete. For multiple cycles, disintegration of concrete surface layers may occur [72].

Different studies have concluded that the RAC's freezing and thawing resistance is similar to that of the corresponding NAC with similar strength and that the freeze-thaw resistance of RAC will improve as the water/cement ratio decreases [67], [85], [86]. However, different studies have pointed out that RAC has a lower freezing-thawing resistance than that of NAC due to the presence of a higher porosity, which leads to poorer mechanical performance and higher absorption values [8], [87]. It has been reported that compressive strength and dynamic elastic modulus of RAC is lower than conventional concrete under the same number of freezing and thawing cycles [88] and the bond strength between RAC and rebar will decrease with an increased number of freeze-thaw cycles and lesser than conventional concrete [89]. A study performed by Ghorbani et al. (2019) reported an increase in freeze-thaw resistance when increasing the RCA substitution. Similar results were reported by Richardson et al. (2011), who measured the mean values of mass lost after 56 cycles of freeze/thaw. The results for conventional concrete indicated a mass loss of 25% while for RAC this value was less than 4%.

When employing fine-RCA, the freeze/thaw resistance of RAC does not present significant variations. Different studies have concluded that freeze/thaw resistance is more affected

by the w/c ratio than by the particle size of aggregate used as the higher porosity of fine recycled aggregates may contribute to increased hydraulic pressure dissipation [91]. The water content of recycled aggregates can also affect the frost resistance of concrete, as saturated particles could expel water into the surrounding environment during the freezing period [92].

The effects of the origin of concrete and mixing method on the resistance to freezing and thawing of air-entrained RAC have been assessed [93]. In this study, the coarse aggregates were obtained from parent concrete with different compressive strengths using a jaw crusher and the resulting RAC mixtures were submitted to 250 freeze-thaw cycles. The results showed that freeze-thaw resistance is greatly dependent on the parent concrete as RAC derived from high strength or air-entrained concrete presented similar resistance than conventional concrete. The OAM of recycled aggregates derived from non-air-entrained concrete presented an increase in cracks and fissures, eventually leading to a decrease in RAC's durability.

Gokce et al. (2004) investigated the demolished concrete's air content influence on RAC's freezing and thawing resistance. The results showed that when the recycled aggregates come from an air-entrained-concrete, the freeze-thaw resistance is lower. This is explained by the presence of micro cracks in the original mortar bonded to the non-air-entrained concrete, which reduces the resistance of the recycled coarse aggregate, leading to a poorer RAC microstructure [59].

3.2.5 Creep and drying shrinkage

Drying shrinkage causes cracking in concrete due to an early deformation which induces higher tensile stresses. This decreases the RAC durability and may lead to further deterioration. Several studies cited show that drying shrinkage increases linearly as the RCA replacement level increases as well. [8], [10], [43], [55], [67], [68], [81], [95]. As concrete containing RCA has higher paste content due to the presence of old adhered mortar, the resulting microstructure is less dense and leads to a higher volumetric instability.

As for creep, different studies have shown that the use of coarse RCA will lead to a higher concrete creep, depending on the replacement ratio and quality of the recycled aggregate. According to Silva et al. (2015), the curing conditions also seem to have an important role on creep behaviour, as sealed specimens have a similar creep behaviour than natural concrete mixtures, probably due to the porosity curing improvement and water loss to the environment. It has also been shown that creep is higher for recycled concrete when compared to regular concrete, and it increases when the replacement ratio increases as well [12]. According to Kwan et al. (2012), due to the higher absorption in RCA, a higher hydrostatic pressure develops and forces the specimen to expand even when it has been cured by immersion in water. Therefore, the higher the absorption is, the higher the expansion will be.

A study by Geng et al. (2016), reported that after 8 months under sustained loading, the creep deformation of RAC can be 50%-120% higher than that of the corresponding NAC. The detrimental effects were more noticeable for lower w/c ratios, or when using aggregates obtained from a previous concrete bearing high w/c ratios. Another study by Geng et al. (2019), reported that when using fine recycled aggregates and natural coarse aggregates, creep deformation increased as the replacement ratio increases as well; however, when using both, fine RA and coarse RA, creep deformation decreases as the replacement ratio of fine RA increases.

There seems to be a linear relation between RAC's shrinkage strain and the recycled aggregate's replacement ratio. When using 100% coarse RA, the resulting concrete mixture may exhibit up to 80% greater shrinkage than NAC, being this effect worse if RAC is cured in a dry environment. The use of water reducing admixtures and fly ash has proven to have a positive effect on this behavior [96].

It has been shown that increasing the W/C ratio results in higher drying shrinkage for RAC. However, the relationship among water to cement ratio, aggregate to cement ratio and drying shrinkage has not been stablished for the prediction of drying shrinkage strain. [43]. Different studies have shown that recycled aggregate concrete has greater creep than natural aggregate concrete due to the presence of old adhered mortar [8], [81].

The aggregate size seems to be another important factor that influences the RCA drying shrinkage behavior. Z. Guo et al. (2017) measured the volumetric changes of 36 RAC

mixtures with different replacement ratios of fine RA and coarse RA. As expected, conventional concrete exhibited the least drying shrinkage, while the mixture with 100% fine and coarse recycled aggregate showed the highest drying shrinkage. As the replacement ratio for the fine RA increased, the concrete drying shrinkage increased as well. This is attributed to the high absorption and porosity of the particles due to the larger presence of old attached mortar. When the fine RA ratio was less than 30%, the concrete mixture durability was acceptable even for a 100% coarse RA replacement. Similar results were reported by Cartuxo et al. (2015), who concluded that incorporating fine recycled aggregates in the mixture drastically increases the shrinkage and creep deformation, especially when the specimens were cured in dry conditions.

A study carried out by Manzi et al. (2013) measured the combined use of fine and coarse aggregate from a demolished building in the long term properties of concrete. It was found that concrete shrinkage strain is negatively influenced by increasing RCA replacement percentages. Since the resultant cement matrix is more porous, the resultant shrinkage deformation is expected to increase. Another study by Bravo et al.(2017) analyzed the shrinkage and creep performance of concrete made with recycled aggregates from different Portuguese CDW recycling plants. It was concluded that the use of recycled aggregates has a negative effect on concrete's shrinkage and creep performance, as a total replacement of natural aggregate bearing RA resulted in a shrinkage increase between 19% and 91% and a lesser creep increase. However, it is stated that there is a great result variability depending on the aggregate's source and chemical composition.

3.2.6 Effects of multi-recycling

The possibility to recycle concrete aggregate several times can further improve the sustainability of this material and drastically reduce the carbon footprint of different construction-related activities using concrete in the long-term. However, it is necessary to further identify the effects of multi-recycling on the durability and mechanical properties of concrete, in order to assess the use of this material for structural purposes as this particular application has not been widely studied.

As it is noted in the literature RCA obtained from multiple generations of recycling presents a loss of density and increase in closed porosity as a consequence of attached mortar and the reduction in size of the natural aggregate as the number of cycles increases [101]. After 5 - 6 recycling cycles the coarse natural fraction turns to sand and the performance of RAC will decrease as the mixture will have similar behavior to a mortar, therefore, there is a dependency between the production process, the natural aggregate maximum size and the RCA replacement ratio.

Studies have been carried out to identify the effects from recycling multiple generations of RCA in the durability-related properties of concrete. The study conducted by Zhu et al. (2019), aimed to identify the performance of three generations of RAC when using repeatedly recycled coarse aggregate. In this case, the durability performance decreased as the number of recycling cycles increased, thus obtaining less compressive and splitting tensile strength as well as lower freeze-thaw resistance, lower carbonation resistance and an increasing chloride ion penetrability. However, despite the decrease in mechanical and durability properties, the authors indicate that every generation of RAC could be used for structural concrete with a lifespan of at least 50 years.

Similar results were reported by Abreu et al. (2018), who assessed the effects of three generations of multi-recycled concrete on the mechanical properties of RAC made from coarse aggregate. Results indicated that a loss in mechanical performance can be expected as the number of recycling cycles increases; however, this decrease has an asymptotical behavior with the number of cycles that tend to stabilize. The maximum performance loss in compressive strength was (12.9%), tensile strength (19.4%) and modulus of elasticity (34%). Abrasion resistance also reported lesser values when compared to NAC. According to the authors, the asymptotical behavior can lead to establish a “minimum performance aggregate” that considers the minimum values for each property and enables the design of structures without concerning about the number of recycling cycles of concrete aggregates.

3.3 Enhancing Techniques to Improve Durability of Recycled Aggregate Concrete

Recent studies have focused on developing different techniques to improve the properties of recycled aggregate concrete. Many of these techniques aim to remove the mortar attached to recycled aggregates as shown in Figure 3, hence decreasing the RAC's porosity and permeability as the behavior of the aggregate greatly influences the behavior of the resulting concrete [58]. Other approaches focus on strengthening the bonded mortar by enhancing the RAC's microstructure [21]. In general terms, the enhancing techniques can be classified as: (a) use of mineral and chemical admixtures, (b) physical, chemical and thermal treatments, (c) impregnation and curing techniques, (d) bacterial deposition techniques and (e) mixing approaches.

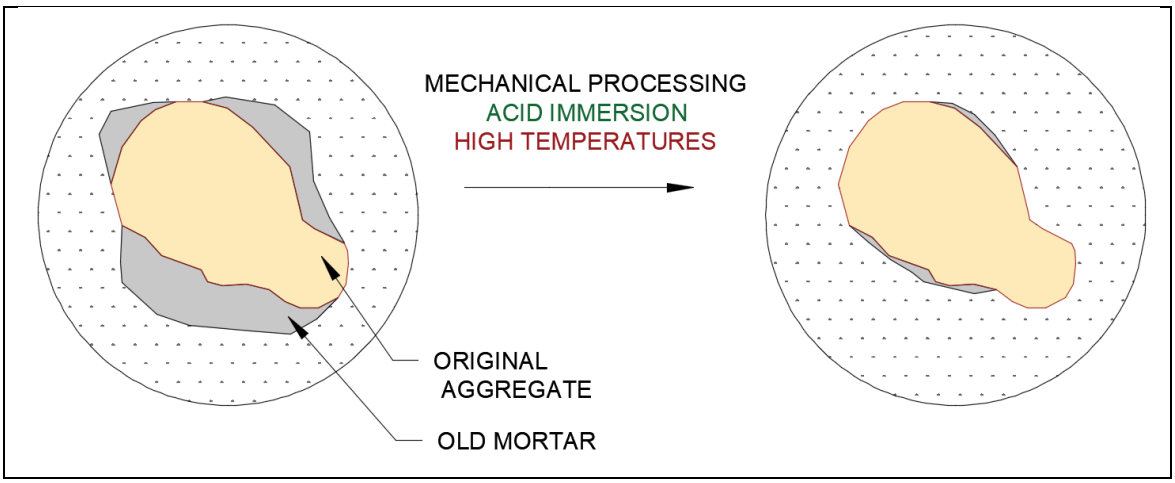

Figure 3 – Enhancing Techniques aimed to reduce old-attached mortar.

An overview of some of these techniques is presented in Table 2 and the advantages and disadvantages are discussed in Table 3. Each one of these strategies is reviewed in depth in this section.

Category	Enhancing Technique	Overview
Mineral Admixtures	Fly Ash (FA)	Adding mineral components to the RAC mix as a partial replacement of cement to enhance pozzolanic activity, improve bond strength and originate a filler effect within the recycled aggregates.
	Silica Fume (SF)	
	Nano – Silica (NS)	
	Metakaolin (MK)	
Chemical Admixtures	Water reducing admixtures	Adding chemical admixtures to improve workability, particle dispersion and reduce RAC pore size.
Mechanical Treatments	Milling – Grinding – Crushing	Further mechanical processing to minimize old-attached mortar.
Chemical Treatments	Acid Immersion	Use of chemical solutions (usually acids) to remove or minimize old-attached mortar.
Thermal Treatments	Conventional Heating	Recycled aggregates are heated at high temperatures to induce microcracks and fissures in the OAM due to thermal stress differential.
	Microwave-assisted beneficiation	
Impregnation and curing treatments	Accelerated carbonation curing	Induce enhancing chemical reactions that increase bond strength by adding a surface coating of finer particles that act as filler.
	Pre-coated recycled aggregates	
Bacterially Induced Precipitation	Bacterially Induced precipitation	Use of bacteria that naturally produce $CaCO_3$ to act as filler and minimize particle porosity.
Mixing Techniques/ Approaches.	TSMA – TSMAs – TSMsc – MMA - SEMA	Modifying the mixing times and proportions of RAC to enhance its properties.

Table 2 – Overview of advantages and disadvantages of different enhancing techniques for Recycled Aggregate Concrete production.

Category	Advantages	Disadvantages
Mineral Admixtures	- Easy to implement in concrete mixes and reduced cement consumption. - Enhance bonding and ITZ strength. - Positive environmental impact. -	- Increased production costs. - FA may increase carbonation rates. - Finer minerals negatively modify concrete's workability.
Chemical Admixtures	- Easy to implement. - Reduces water requirements. - Improves RAC density, durability, and strength.	- Increased production costs. - Additional waste production. - Reduced efficiency with fine aggregates.
Mechanical Treatments	- Highly effective, cheap, and possible at industrial scale. - Increase particle density and removes old-attached mortar. - Improves mechanical and durability performance.	- High energy consumption. - Additional waste production.
Chemical Treatments	- Increase particle density and removes old-attached mortar. - Improves mechanical and durability performance.	- Environmental deterioration. - Possible damage to aggregates. - Possible significant pH modification. - Increased production costs.
Thermal Treatments	- Possible at industrial scale. - High reduction of attached mortar due to cracks. - Improved bond strength and concrete performance.	- Higher energy consumption. - Increased production costs. - CO_2 emissions. - Possible degradation of aggregates.

Category	Advantages	Disadvantages
Impregnation and curing treatments	- CO_2 treatment has a positive environmental impact. - Coating reduces pore volume in aggregates. - Filler effect that enhances ITZ strength and densifies microstructure. - Enhanced RAC performance.	- Increased production costs. - Additional waste production. - Additional water and cementitious material consumption.
Bacterially Induced Precipitation	- $CaCO_3$ fills pores and enhances RAC performance. - Denser microstructure and ITZ. - Low environmental impact.	- Difficult to implement in industrial scale. - Specific pH and temperature requirements. - Increased production costs.
Mixing Techniques/ Approaches.	- Easy to implement and combine with other techniques. - Low cost and minimal environmental impact. - Stronger ITZ.	- Slightly lower improvement compared to other enhancing techniques.

Table 3 – Overview of advantages and disadvantages of different enhancing techniques for RAC.

3.3.1 Incorporation of Fly Ash (FA)

The use of fly ash (FA) may have positive effects in the performance of RAC such as permeability reduction, improved resistance to chloride penetration and reduced drying shrinkage [8]. The presence of fly ash reduces the amount of $Ca(OH)_2$ in the cement matrix, which is transformed into water insoluble hydration products that fill voids and reduce the RAC permeability [68]. Nevertheless, when employing high contents of fly ash and other ultra-fine spherical mineral admixtures, the relative pore size could increase due to particle distribution.

A critical aspect of using fly ash or similar pozzolanic materials is the low strength development at early ages in spite of the satisfactory long-term mechanical properties that is generally higher than concrete made with pure Portland cement [104].

Some authors claim that durability improves when higher FA levels are employed. According to Ahmed (2014), the scenario for concrete production in mixes with 50% fine recycled aggregates and 40% fly ash replacement, exhibited an improvement in RAC's water absorption when testing the samples at 56 days, being even lower than that of conventional concrete. It has also been reported that the incorporation of fly ash in RAC mixtures reduces the cracking due to high temperatures, but decreases its impact resistance [106].

The use of fly ash can improve RAC's durability to chloride penetration [38], [82], as the presence of fly ash can enhance pozzolanic reactions that result in a denser microstructure. The additional calcium silicate hydrate gel (C-S-H) produced from the pozzolanic reaction between fly ash, Portland cement hydrating products and old mortar attached to RCA densifies the cement matrix [8], [80]. According to Kurda et al. (2019), the use of fly ash is also notoriously favorable to the increase in RAC's electrical resistivity.

Incorporating RCA increases the concrete shrinkage, but this can be managed with the incorporation of fly ash [68]. The difference between the shrinkage of a conventional concrete and a mixture made with up to 40% of both fly ash and RCA was not significant. As for the creep behavior, the use of fly ash can also have a positive impact. Different authors have reported that the lower creep strain may be attributed to a lower stress/strength ratio since it is known that incorporating FA results in a slower strength rate gain, which results in a better volumetric stability [107].

Carbonation of concrete occurs when alkalinity decreases due to the penetration of carbon dioxide, as a result, the passive environment of steel bars could be lost, and the reinforcement turns susceptible to corrosion when oxygen and water are present (André et al. 2014; Li 2011; R. V. Silva et al. 2015). Different studies have concluded that the principal negative effect of incorporating fly ash to RAC is an increase in carbonation depth, as it causes a reduction in concrete's pH due to the pozzolanic reaction between portlandite and

fly ash, which reduces the amount of $Ca(OH)_2$, hence creating favorable conditions for carbonation to occur [8], [68], [78], [80], [83], [108], [109].

A study by Kou and Poon (2013), revealed that after a 10-year period, the use of fly ash in RAC resulted in a higher resistance to chloride penetration; however, the carbonation depth was about 1.9 times the carbonation depth of natural aggregate concrete. A recent study by Kurda *et al.* (2019) focused on the effects from incorporating high volumes of fly ash to RAC, and it was concluded that carbonation depth increased up to 3 and 6 times with the incorporation of 30% and 60% of fly ash respectively; however, it was stated that the service life of those mixtures was relatively high and the reinforcement was protected for up to 50 years. Since the incorporation of fly ash increases the carbonation depth, this problem could be manageable by increasing the concrete cover for reinforcement, as fly ash improves other mechanical and durability-related properties.

3.3.2 Silica Fume (SF)

Silica fume is a by-product of the silicon and ferrosilicon alloy production, the effectiveness of silica fume in RAC mixtures has proven to be variable and its durability effects have not been fully investigated. However, some studies have reported that the use of silica fume can lead to higher water absorption that could result in a decrease in the concrete's durability-related performance when using coarse recycled aggregate or both coarse and fine recycled aggregate [17], [110]. Other studies report that silica fume can increase compressive and tensile strength of RAC as this mineral decreases porosity due to the ultra-fine particle's filling effect and the production of calcium silicate hydrate. (Abd Elhakam et al., 2012; Gesoglu et al., 2015).

In the study performed by Pedro *et al.* (2017), different mixtures bearing 0%, 5% and 10% silica fume replacement were able to achieve compressive strengths between 70 and 85 MPa at 91 days. The recycled aggregates in this study were submitted to an industrial crushing process. However, it was reported that increasing the silica fume replacement percentage decreased RAC mixture's mechanical performance. In the same study, the incorporation of silica fume resulted in higher water absorption (18% when incorporating 10% SF compared to 9% without SF). According to the authors, the densification process

used in the production of silica fume leads to an agglomeration of particles that result in a performance loss in the concrete mixtures made with them.

3.3.3 Nano-Silica

Some studies have reported that the use of nano silica in concrete can improve its mechanical properties and durability. The nano material (nano-SiO2) has a smaller particle size, hence bigger surface area and improved activity [112], as it enhances the production of C-S-H gel which fills the voids in the microstructure, reducing porosity and increasing concrete's density [113]. The use of nano-silica could also improve concrete's hydration process, as it reduces the amount of $Ca(OH)_2$ in the ITZ [7]. It could also exhibit a higher pozzolanic activity than silica-fume [114]. Different studies revealed that RAC water absorption decreases with the incorporation of nano-silica and other nano materials, as they reduce the volume of pores and densify the microstructure [114]–[116].

In a study by Wang *et al.* (2019), nano-silica and basalt fiber were used to reinforce RAC mixes containing different replacement ratios of coarse RCA. Four different contents were tested for the basalt fiber: 0 kg $m^{-3,}$ 1 kg m^{-3}, 2 kg m^{-3}, and 3 kg m^{-3}, and the nano silica was applied in 0%, 3%, 6% and 8% ratios of the cement mass. It was concluded that basalt fiber and nano silica enhance concrete workability. Also, an optimal nano-silica content of 8% when the RCA replacement ratio was 100% resulted in higher compressive and splitting tensile strength.

According to the same research, the combined use of nano-silica and basalt fiber increases the RAC bonding properties and enhances the hydration process, resulting in higher density and reduced porosity for the concrete mixtures. However, when the nano-silica content is too large, the concrete's density and mechanical properties decrease.

3.3.4 Metakaolin (MK)

Metakaolin (MK) is a thermally activated aluminosilicate material with hig pozzolanic activity obtained from the calcination of kaolin clay at a temperature between 650°C and 800°C that has become widely used in concrete production due to the enhancement of

mechanical, durability and workability properties [117]. A variation of metakaolin, known as nano-metakaolin (NMK), has been developed by employing further mechanical grinding. NMK may also improve the mechanical properties, especially at early ages due to its filling effect and pozzolanic effect that improves concrete's microstructure [118].

The addition of metakaolin may improve the properties of RAC as the particles have a filler effect that reduces voids and enhance the pozzolanic reactions within concrete [119]–[121]. Microscopic analysis has also revealed that using metakaolin in RAC mixes reduces the peaks of portlandite and enhances the formation of C-S-H gel which is responsible for improving bond strength [122]. The use of metakaolin in RAC has proven to increase the compression strength of RAC [119], [123]–[125] and it may also improve the durability of concrete as some studies have reported an increase in resistance to high-temperatures [124], carbonation resistance and chloride penetration resistance [125]–[127] as well as freezing-thawing resistance [94], [128].

Studies have also shown that the use of metakaolin may reduce the workability of RAC due to the high water absorption of the finer particles that require an adjustment of the water content depending on the amount of metakaolin added [119]. Nevertheless, recycled aggregates and metakaolin have been used in self-compacting concrete mixes that require high flowability, obtaining comparable compressive strength at 120 days (45 MPa) for conventional concrete and RAC with 50% replacement ratios of recycled aggregates [126]. This resistance may be sufficient for most structural concrete applications.

The use of nano-metakaolin may also improve the compressive strength of RAC. A study by Xie *et al.* (2020), reported a maximum increase for 28-day compressive strength of 27% when using coarse recycled aggregates and a nano metakaolin replacement ratio of 7%. In this study, concrete mixes containing 100% coarse RCA and 7% nano metakaolin presented a similar compressive strength (45.9 MPa) than mixes with 30% RCA and 0% metakaolin (45.2 MPa) and mixes with 0% metakaolin and 0% recycled aggregates (47.4 MPa), proving that this option may be feasible from a technical point of view.

According to different authors, the use of metakaolin is viable solution for enhancing the properties of RAC as metakaolin production requires less energy than ordinary portland cement and despite the high production cost, the low replacement ratios of around 15%

allow the use of this mineral addition without significantly increasing the production cost of concrete [122].

3.3.5 Effects from incorporating Chemical Admixtures

It has been reported that the use of superplasticizers (SP) could improve recycled aggregate concrete's durability. A study by Kurda *et al.* (2019) concluded that the use of SP causes better dispersion and higher particle reaction, thus decreasing concrete pore size as a result. It is also stated that the efficiency of SP depends on the incorporation of fine RCA, as it modifies the effective water in the mixture due to the particle's high absorption.

A study by Barbudo *et al.* (2013), established the influence of plasticizers and superplasticizers (1%) in the mechanical performance of concrete made with different replacement ratios of coarse RCA (0% - 20% - 50% - 100%). The results showed that it is possible to use a 100% replacement ratio without affecting concrete's mechanical properties if a plasticizer is incorporated. This is attributed to the effect of the water-reducing admixture, which lowers the W/C ratio without affecting the concrete's flowability, further resulting in a denser cement matrix and a less porous material.

Another research by Matias *et al.* (2013), studied the effects of incorporating two types of superplasticizers based on lignosulphonate and polycarboxylate polymers to concrete mixtures with different recycled concrete aggregate ratios. It was concluded that the addition of SPs improves RACs workability and can compensate for the loss of compressive and splitting tensile strength resulting from the use of recycled aggregates.

The effectivity from incorporating water-reducing admixtures is affected if fine RCA are incorporated into the mixture. A study by Cartuxo *et al.* (2015), assessed the effects from incorporating a regular plasticizer and a high performance plasticizer in concrete mixtures containing fine RCA. A regular plasticizer is based on organic polymers that work by electrostatic repulsion, while a high-performance superplasticizer is chemically based on a combination of modified polymers such as polycarboxylates. As expected, fully replacing fine natural aggregates for fine RCA to the mixture decreased the effective W/C ratio and

compressive strength, while increasing shrinkage and creep up to 57% and 154% at 91 days respectively when compared to NAC. The effects of adding a high-performance superplasticizer to RAC mixes containing 100% fine RCA include the reduction of water absorption by immersion (25%), water absorption by capillarity (66%), carbonation depth (80%) and chloride migration coefficient (46%) when compared to RAC without superplasticizer.

Mixtures using regular superplasticizers had higher density and compressive strength. The creep and shrinkage decreased when compared to the mixtures without SP at 91 days. These positive effects were more pronounced when using high-performance superplasticizers, obtaining satisfactory rheological, mechanical and durability properties that could even offset the negative effects from incorporating fine RCA [52]. It has been also reported that the use of water-reducing admixtures could also have a positive effect on creep, as it reduces the W/C ratio while maintaining the same consistency and cement content [107].

3.3.6 Mechanical Treatments

Mechanical treatment of RCA generally consists of introducing an additional mechanical processing step by milling, crushing or grinding the coarse fraction in order to remove the original attached mortar (OAM). A study carried out by Pepe *et al.* (2014), conceived a physical treatment called "*autogenous cleaning",* in which the coarse RCA were placed in a rotating mill drum for 10 to 15 minutes to bump against each other. The aggregates were cleansed with water and dried to remove the remaining impurities after the rotating period was finished, finally the amount of detached mortar was measured to quantify the process efficiency. RAC mixes were produced with 100% replacement of both untreated and treated RCA. The results showed that autogenous cleaning can improve RAC properties as the original RCA water absorption of 12% was reduced to approximately 6% after a 15-minute cleansing period. This research reported that concrete's workability in fresh state improved and its compressive and tensile strengths increased 8% and 9% respectively.

A similar process was followed by Dimitriou *et al.* (2017). In this study, RCA were placed with water into an 8 m^3 modified concrete mixer and rotated for 5 hours at a speed of 10 rpm. Water was introduced to remove smaller particles and contaminants and saturate

OAM from the aggregates. After the rotation process was finished, RCA were sieved to discard particles with sizes lower than 4 mm. The treated aggregates presented higher particle density (2.49 g/cm^3) compared to untreated RCA (2.28 g/cm^3), furthermore water absorption improved from 7.2% to 3.7% and mortar content was reduced from 24% to 9%. Due to this treatment method, RAC mixes with RCA presented similar compressive strength and rapid chloride permeability than control mixes.

The incorporation of further mechanical processing has proven to be effective for enhancing RCA properties by removing OAM content. In a research by Babu *et al.* (2014), the aggregates were treated by grinding and then processing them using Los Angeles abrasion test machine for 200, 500 and 700 revolutions in order to measure the effects of a prolonged treatment. At 28 days, compressive strength of RAC containing 100% RCA treated for 0, 200, 500 and 700 revolutions decreased 58.%, 36%, 27% and 25% respectively when compared to control mix. The durability of treated RAC improved significantly, showing lower water absorption, sorptivity and chloride ion penetrability. Authors stated that there is a limit on the amount of OAM that can be removed using mechanical processing as the measured durability properties at 500 and 700 revolutions were similar.

3.3.7 Chemical Treatments

Different kinds of chemical treatments have been investigated to produce high quality RCA. In general, these treatments aim to remove or minimize the aggregate's OAM content by soaking them in different concentration of acids or other chemical solutions.

In a study by Kim *et al.* (2018), coarse RCA were treated using different solutions of hydrochloric acid (HCl) and sodium sulfate (Na_2SO_4) with a fixed aggregate-to-solution ratio of 1:4,5. The OAM content removed by HCl was twice (12%) the one removed by Na_2SO_4 (6%), furthermore, water absorption value for aggregates treated using HCl and Na_2SO_4 were 39% and 35% lower than untreated RCA. When using HCl, only a 5% reduction of compressive strength was reported, while carbonation depth decreased approximately 10% and chloride ion penetration resistance increased 12%.

Similar results have been reported by Ismail and Ramli (2013), who assessed the effects from soaking RCA in three different concentrations of hydrochloric acid (HCl) to remove OAM from the particles. The procedure involved immersing RCA in a plastic container holding HCl for 1, 3 and 7 days and, after the immersion time was completed, washing the RCA with distilled water, and removing the finer fractions using a 4.75 mm sieve. A linear relationship between the acid concentration and the amount of mortar removed was identified and the HCl concentration of 0.8M presented the highest value of mortar loss (5%). Aggregates treated with an HCl molarity of 0.8M for 3 days improved RAC's density by roughly 3% and reduced water absorption by 28% compared to untreated RCA. 28-day compressive strength was also improved as RAC produced with the same treated aggregates presented an increment of approximately 20%.

3.3.8 Thermal Treatments

Thermal treatments have been successfully implemented in different studies to further improve the quality of RCA. It has been reported that high temperatures can induce micro-fissures and cracks due to differential thermal stresses in the cement matrix sourrounding RCA, hence reducing the amount of old attached mortar (OAM) [21].

Conventional thermal treatment process consists of a sudden cooling of saturated aggregates that were previously heated at high temperatures for a certain amount of time. Particles are saturated to contribute to the formation of cracks as the heating process produces water vapour that induces thermals stress in the OAM agglomerates [35]. In general, higher heating temperatures allow the removal of more OAM, however, when the temperature is higher than 500°C, the aggregate properties may be degraded [21].

Thermal treatment procedure requires the remotion of impurities from RCA samples, once the material has been prepared, the aggregates are immersed in water for 2 hours to ensure a complete saturation of the residual attached mortar. The aggregates are heated at a temperature of 500°C for 2 hours and then quickly immersed in cold water. The sudden cooling of the particles induces volumetric changes that result in stresses and cracking of the OAM. Finally, the aggregates are washed and sieved to remove the lost mortar [35].

A variant of this thermal approach is known as microwave-assisted beneficiation and was described by Akbarnezhad *et al.* (2011). In this process, the use of microwaves to quickly increase the temperature of old mortar that surrounds RCA would result in significant differential thermal stresses within the mortar as its temperature increases much faster than the aggregate's. These stresses break up the surrounding mortar into its constituent materials, hence allowing the cleansing of RCA and the improvement of mechanical and durability performance of the resulting concrete mixtures. In this study, mortar content was reduced by almost 48%, which led to a 33% decrease in water absorption and a 4% increase in particle density. Other studies report a loss of 95% of adhered mortar using coarse RCA that were pre coated with iron oxide (Fe_2O_3) which induces higher temperatures and increases the amount of micro-cracks in the OAM due to an increase in void volume [33]. When combined with further mechanical rubbing, these benefits can be more notorious and prove to be a robust solution for treating recycled aggregates [34].

Unlike conventional heating methods, the microwave-assisted method does not seem to degrade the aggregate quality, as the temperature for the RCA reaches a much lower value (140°C) compared to the 300°C – 500°C range that is reached by conventional heating. Additionally, this method has proven to be more energy efficient since the required temperatures can be achieved much faster than conventional thermal treatments [32].

3.3.9 Accelerated carbonation curing treatment

Carbonation treatment may be one of the most effective methods to enhance RCA properties, and it is also an environmental-friendly approach that can further improve the sustainability of construction with recycled concrete [21]. CO_2 is able to penetrate the aggregate structure and react with hydration products from OAM such as calcium hydroxide and hydrated calcium silicate [21]. Carbonation treatment may be performed on the RCA or as a curing method for concrete mixtures.

Curing methods for RAC using CO_2 were proposed by Kou *et al.* (2014) and Zhan *et al.* (2014). This process aimed to densify the cement matrix by accelerating a carbonation reaction in the OAM. When the RCA are cured by this method, portlandite carbonation allows the formation of calcium carbonates that act as fillers and densify concrete's

microstructure. This method proved to enhance compressive and tensile strength, as well as durability-related properties such as chloride ion permeability and gas permeability.

Zhan *et al.* (2019) determined the effects of RCA carbonation treatment on concrete's transport properties and steel corrosion using cement mortars made with recycled aggregates that were treated for 1 and 7 days. RCA were subjected to accelerated carbonation using 100% CO2 atmosphere at a pressure of 1 bar for 1 day and for 7 days. This treatment reduced mortar water absorption from 11.22% down to 8.97% for the 1-day carbonated mortar and 7.90% for the 7-day carbonated mortar. Capillary absorption was also reduced, as sorptivity values were lower for carbonated mortars. In the same study, rapid chloride penetration tests (RCPT) were carried to measure chloride ion transport. The current flow decreased 18.2% for the 1-day carbonated mortar specimen and 26.1% for the 7-day treated specimen. This indicates an improvement in ion chloride permeability resistance produced by the densification of the microstructure due to the precipitation of calcium carbonate (CaCO3).

Another study by Lu *et al.* (2019), assessed the effects of carbonated coarse RCA on the properties and microstructure of concrete specimens. Carbonation treatment reduced RCA water absorption by roughly 18%. Concrete mixes with 100% carbonated RCA presented approximately 20% less drying shrinkage deformation and 50% higher micro-hardness. The mechanical properties were also positively affected as RAC mixes with 100% RCA content presented 30% higher compressive strength than mixes produced with untreated aggregates. The authors conclude that using carbonated RCA as concrete aggregates can also consume a significant amount of CO_2 and further improve sustainability for this material.

3.3.10 Pre-coated recycled aggregates

RCA can be treated by pre-coating methods to further improve their properties and enhance the hydration process. Zhao *et al.* (2013), assessed the physical properties of RAC mixtures whose aggregates surfaces were covered using different kinds of paste featuring Portland cement, sulfoaluminate cement, fly ash and silica fume. The coating method was accomplished by soaking the RCA in these different pastes for 5-10 minutes and subsequently letting the aggregates dry. Concrete mixes where RCA were pre-coated with

sulfoaluminate cement and fly ash presented the larger improvement, as the 28-day compressive strength and corrosion resistance coefficient increased roughly 35% and 20% respectively when compared to concrete mixes made with untreated RCA.

Martirena *et al.* (2017), conducted a "cement encapsulation" procedure for coarse RCA which consisted of covering the aggregates with a thin cement film ranging from 0.16 mm to 0.23 mm. By using this method, open pores and microcracks were covered, hence reducing aggregate water absorption by 55% when compared to untreated RCA. Compressive strength also increased 12% for concrete mixes using only treated RCA. Pore size distribution analysis indicated that the percentage of pores with a lesser area than 79 μm^2 increased from 13% for untreated RAC to 26% for RAC with treated aggregates. This demonstrates and increase of the density of the ITZ due to pre-coating cement hydration.

Liang *et al.* (2015), assessed the effect of different treatment methods on the RAC compressive strength. The aggregates were coated with cement slurry and cement slurry containing a silica fume solution, through different mixing methods. It was reported that pre-coating the RCA with cement slurry increases concrete's compressive strength, especially when using silica fume. When combining the impregnation method and two-stage mixing approach, a compressive strength of 43.3 MPa was reported, which is enough for most structural applications. According to the authors, the surface pretreatments should be applied seven days before concrete casting in order to ensure the formation of a cement layer over the aggregates which reduces their water absorption and strengthens the bond between the aggregate and the surrounding cement paste.

Micrographic images from different cross-sections of treated and untreated RAC have shown that pre-coating methods can improve the bond strength between the aggregates and the new cement paste, and drastically reduce water absorption, hence improving the resulting RAC's mechanical and durability properties [135].

3.3.11 Bacterially Induced Precipitation

Microorganism induced precipitation is based on bacterially $CaCO_3$ precipitation, which in the case of RAC decreases the water absorption values since it creates a natural barrier

that fills the voids in the RCA [136]. Certain micro-organisms have the ability to produce calcium carbonate on the surface of the cell wall due to the presence of adequate negative zeta potential, this means that under adequate charge and pH conditions, some kinds of bacteria may produce calcium carbonate [21].

The bacteria *S. pasteurii No DSM33,* which can be cultivated from a medium derived from urea has been used in different studies that have identified this calcium carbonate bio-deposition under appropriate temperature and pH conditions [136]–[138]. In the study performed by Qiu *et al.* (2014), a linear relation was identified between the bacteria concentration and the coarse RCA weight increase. Water absorption of treated recycled aggregates was reduced by 15% for the highest bacteria concentration and rate of $CaCO_3$ precipitation that occurred under a pH value of 9.5 and a temperature of 35°C. Another study performed by Sahoo *et al.* (2016), assessed the effects of employing coarse RCA and the bacteria *B. subtilis.* Compared to untreated RAC, a 20% compressive strength increase was reported due to microbial precipitation. Drying shrinkage for treated RAC was 82% lower than untreated RAC and 67% lower than control mixes with natural aggregates. A reduction capillary water absorption of RCA was also observed as calcium carbonate precipitation increases the density of concrete.

The use of microbial carbonate precipitation has also been reported when employing fine RCA [138]. In this study, the use of bacteria *S. pasteurii No DSM33* to enhance RCA resulted in an increase in particle weight of 3%, a reduction in particle water absorption of approximately 5% and an increase of 45% in mortar flexural strength and 12% in compressive strength when compared to non-treated fine RCA.

Abd Elhakam *et al.* (2012) reported that the use of a self-healing process can improve RAC's mechanical properties. In this study, for mixes made with a 75% replacement of coarse RCA, 56-day compressive strength increased by 37%, 56-day tensile strength increased by 34% and porosity was reduced by roughly 9% when compared to RAC without bacterial treatment. The positive effects were noted for all the RCA replacement ratios, and the enhancement was even more evident for mixtures with low water-cement ratios (W/C).

A study by Wang *et al.* (2017), assessed the effects from immersing RCA in different bacterial suspensions of *Bacillus sphaericus* LMG 22257. It was concluded that bio-deposition treatment improves the recycled aggregate quality since an improvement in the

fragmentation resistance was noted. It was noted that concrete mixes made with a content of 100% treated RCA presented a much higher density (2330 kg/m^3) than concrete made with untreated RCA (2250 kg/m^3) and even a close value to conventional concrete (2350 kg/m^3). As porosity and water absorption were reduced, compressive strength for treated RAC (76 MPa) was 40% higher than untreated RAC (54 MPa) and 25% higher than conventional concrete with natural aggregates (61 MPa).

Biodeposition may be an effective and more sustainable approach for enhancing RCA's properties and can also be applied to mortar mixes [138], as it requires less energy than other methods. Additionally, all the required components used for cultivating the microorganisms naturally occur in the environment [137].

3.3.12 Two-Stage Mixing Approach

Two-stage mixing approach (TSMA) was proposed by Tam *et al.* (2005) , to improve the RAC quality. The main difference with conventional concrete mixing is that TSMA divides the process in two parts and equally distributes the required water in two stages, while in regular mixing all the components are mixed in one stage. During the TSMA's first stage, a thin cement slurry similar to pre-coating treatment is formed around the recycled aggregate and acts as filler material reducing the volume of voids and cracks in the OAM. During the second stage, the rest of water is added to complete the concrete production process.

Examination of the ITZ by scanning electron microscopy (SEM) revealed that the cracks in RCA were also filled with hydration products when using TSMA, overall resulting in a stronger and denser ITZ that allows better mechanical performance [141]. Another study by Tam and Tam (2007), assessed the durability improvement when using the TSMA for RAC production. For a 100% replacement ratio, a reduction of 68% shrinkage, 46% creep, 35% water permeability and 30% chloride permeability were observed when compared to conventionally mixed RAC. Air permeability was also reduced by 52% for a 20% substitution of recycled concrete aggregate, thus demonstrating the effectiveness of this approach.

More researchers have identified the beneficial effects from employing the TSMA in RAC's mechanical and durability properties. Abd Elhakam *et al. (*2012), reported a 56-day

compressive strength and tensile strength improvement of 33% and 32% respectively for RAC mixes produced with TSMA and a 75% ratio of RCA when compared to normal mixing method.

3.4 Recycled Concrete Aggregate research in Colombia

The structural use of recycled aggregates in Colombia is still a new topic in the national construction industry and it has not been widely studied nor regulated. However, new initiatives regarding the use of recycled concrete aggregates have appeared in Colombia due to expanding urban development and renovation processes.

Most research has been focused in identifying the mechanical effects of different replacement ratios, water/cement ratios and curing conditions [143], where different studies have reported that concrete made with only coarse RCA, may present a compressive strength reduction compared to conventional concrete up to 25% [144]. However, different recent studies have also assessed the effects of incorporating fly ash, using enhancing methods and durability-related properties of concrete with fine and coarse recycled aggregates.

In Colombia, the effects of incorporating coarse recycled aggregate and fly ash in the compressive strength of concrete have been assessed [145]. In this study, concrete mixes with 25%, 50%, 75% and 100% coarse-RCA replacement ratios were tested at 7, 14 and 28 days. As expected, compressive strength was reduced for concrete mixes with higher RCA replacement ratios, however, specimens with 25% RCA replacement presented superior compressive strengths than cylinders from the control mix. Furthermore, replacement ratios up to 50% achieved the target strength of 28 MPa at 28 days. Compressive strength from concrete mixes with 20% fly ash substitution was reduced by more than 50%.

Durability studies performed in Colombia with replacement ratios of 20% and 40% coarse RCA have concluded that concrete's chloride resistance is not significantly reduced for RAC mixes [146]. The incorporation of RCA also resulted in higher carbonation resistance,

higher capillarity absorption and similar sulfate permeability. According to these authors, concrete with RCA substitutions lower than 40% can be used in construction projects as mechanical and durability performance is not significantly reduced. The incorporation of RCA has also resulted in higher permeability and chloride ion penetration, however, when less than 30% of coarse aggregates is substituted and mineral additions such as micro silica are used, there is not a significant durability difference between RAC and conventional concrete [143].

Electrical properties have also been assessed nationally, as it has been concluded that concrete resistivity from concrete mixes made with 100% RCA is approximately 25% lower than conventional concrete [144]. As higher RCA replacement ratios increase porosity, a higher ionic transport is expected to occur. In this research, every concrete mix with RCA presented high corrosion probability.

Enhancing methods such as accelerated carbonation treatment of fine recycled aggregates in mortar mixes has also been studied [147]. In this study, carbonation treatment reduced aggregate absorption by 20% and increased its density by 10% approximately, mortar mixes with carbonated aggregates also presented similar sulfate expansion levels than natural aggregate mixes. Mortar mixes with 25% and 50% replacement of fine RCA also presented increased compressive strength at 28 days when comparing to non-carbonated aggregates, specially for higher W/B ratios. The use of fine RCA for a W/C ratio of 0,505 in this study decreased capillary absorption, mix porosity and increased ultrasonic pulse velocity.

Due to national and international research and regulations allowing the use of recycled aggregates in structural concrete, in Colombia, the national standard **NTC 6421** – *"Coarse recycled aggregates for use in concrete"* [148], is currently being formulated to include additional specific requirements for the use of aggregates from construction and demolition waste. According to this standard, international research and guidelines have proved that some materials could be used for concrete production without a significant detrimental effect. Fine recycled aggregate inclusion is not included in this regulation since "international research has not reached a consensus regarding its viability in hydraulic concrete".

This Colombian standard classifies allowed aggregates from CDW into concrete derived aggregates (Rc), natural aggregates (Ru), and masonry or ceramic aggregates (Rb). Non-usable aggregates are derived from asphaltic waste (Ra), glass (Rg) and others such as plastic, magnetic, and organic materials or plastics (X). The relative proportions of each one of these components must be assessed to identify its applicability in new concrete production. Since there are no standardized procedures in national regulations, **NTC 6422** – *"Standard for classification of the constituents of recycled coarse aggregates"* [149], is being simultaneously formulated. This standard will present a simple method to identify and estimate the mass proportions of each component derived from coarse CDW by washing floating materials and establishing the weight of individual components.

The use of coarse recycled aggregates will be allowed for structural use for a maximum compressive strength of 35 MPa and 20% aggregate substitution. These aggregates must be composed of at least 92% of concrete derived aggregates and have a maximum content of 5% masonry aggregates and 2% non-usable materials. Additional requirements are a maximum of 5% aggregate absorption, 50% loss in Los Angeles machine and 25% flakiness and elongation indexes.

Proposals have also been made to allow the use of a 10% replacement of recycled concrete aggregates in another national standard being formulated by INVIAS – Instituto Nacional de Vias (National institute of roads) if a satisfactory performance comparable to natural aggregates is proven and durability testing is performed on concrete.

3.5 Corrosion of Steel in Concrete

3.5.1 Corrosion principles in metals

Metals exist in Earth's crust as minerals such as carbonates, sulfides, sulfates or oxides. In their natural state, metals are in a equilibrium state which corresponds to the lowest energy state. Once they are extracted, metals turn to a thermodynamically metastable state and depending on the environment, they will attempt to revert to a lower energy compound by Icorrosion or oxidation, corrosion is an electrochemical reaction that consists of anodic and cathodic half-cell reactions [104].

The stability of metal is described in terms of its electrochemical potential, which is a thermodynamic function defined as the ease of ionizing an atom of the metal. The electrochemical potential (EP) is dependent on the pH and factors such as oxygen availability. There are ranges of electrochemical potential and pH in which the products of corrosion are either dissolved ions such as Fe^{2+} or solid oxides or hydroxides. The Pourbaix diagram for iron, shown in Figure 4, indicate the regions of potential and PH in which the metals will be immune, will actively corrode or will form passive films.

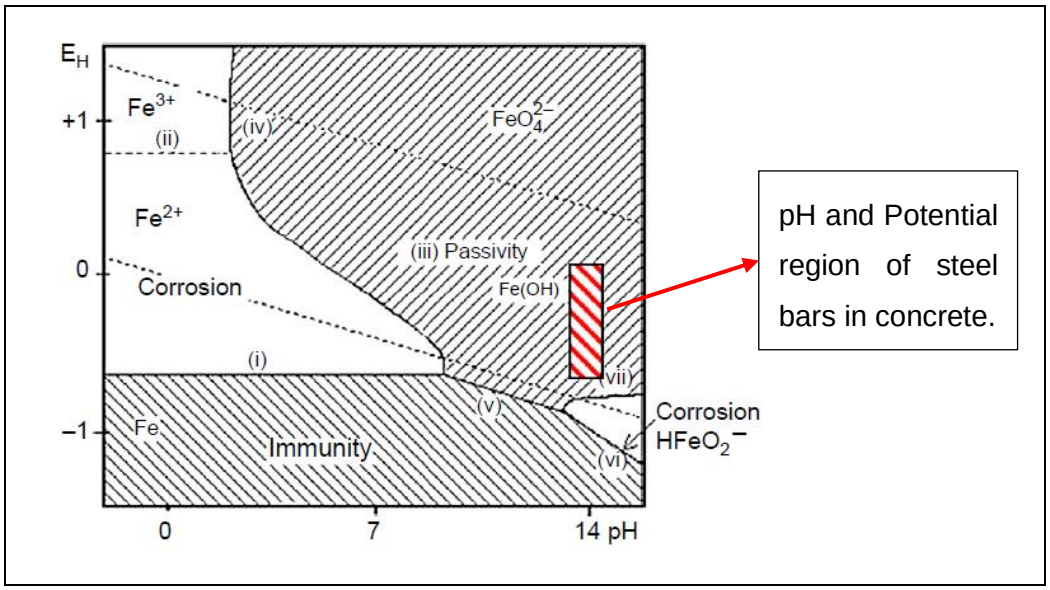

Figure 4 – Pourbaix diagram for Iron at 25°C. Retrieved from (*Poursaee, 2018)* [104].

Corrosion consists of electrochemical reactions at the surface between the metal and an electrolyte solution. During the anodic reaction, the metal is oxidized and releases electrons; these electrons are then consumed by the cathodic reaction in which the reduction occurs [104]. Since corrosion involves the exchange of electrons between the metal (anode) and the cathodic species (hydrogen ions or dissolved oxygen), it is an electrochemical process. The dissolution or oxidation of a metal (M) constitutes the anodic half-cell reaction:

$$M \rightarrow M^{2+} + 2e^-$$

The electrons released are immediately consumed by one of the cathodic half-cell reactions:

$$2H^+ + 2e^- = H_2$$

$$O_2 + 2H_2O + 4e^- = 4(OH)^-$$

The first reaction usually occurs in low pH conditions and with little oxygen available, while the second reaction is more common at neutral or high pH conditions and/or at higher oxygen concentrations.

The solid products of these reactions may form a thin layer, known as the passive film, over the surface and protect the metal from further corrosion. The length of the passive film is on the order of a few hundred nanometers. Regardless of the formation of this film, ions can still be transported and in practice, corrosion is never equals to zero but at a level considered insignificant for the service life of the metal [104].

Corrosion can occur in a metal in a general state or in a localized way. General corrosion happens in regions of potential and pH where the passive film is not stable and breaks down, forming corrosion products that can be either dissolved ions or nonprotective oxides/hydroxides. Localized corrosion, also known as pitting corrosion, can be observed in metals with passive films at high pH where the passive film breaks down by chloride adsorption. These pit form “local differential environmental cells” that grow since chlorides are not consumed in the process and travel through the metal reacting with water and oxygen to create hydroxyl ions [104].

3.5.2 Corrosion Mechanism of Reinforcement Steel

The durability of structures made from steel-reinforced concrete is related to its ability to reduce the rate of transport and ingress of aggressive ions. Concrete provides physical and chemical resistance to corrosion by acting as a barrier for ion ingress and a high pH environment that neutralizes corrosion reactions. As seen in Figure 4, steel embedded in concrete is usually in a passivity state where a ultrathin (<10 nm) protective film of oxides and hydroxides decrease the dissolution rate of steel to negligible levels.

Portland cement in concrete pore solution may present a pH higher than 13 due to the presence of Ca(OH)2, KOH and NaOH in the mix [150], for the corrosion rate of steel in mortar to drop to a rate typically considered passive after mixing, it takes approximately seven days, but the corrosion rate continues to decrease slowly for a long period after that [151].

Chloride ions or carbon dioxide penetrate the concrete cover depth to reach the reinforcement bars by capillary transport and moisture trough the interconnected pores in the cement paste. Porosity in cement paste consists of capillary pores, and calcium silicate hydrate gel (C-S-H) pores which are the remains of originally water-containing spaces that have not been filled up by products of hydration. Capillary pores are the largest with a diameter greater than 5 nm and their number and interconnectivity control the ingress of chloride ions, carbon dioxide, oxygen and moisture into concrete [152].

In the surface of steel bars, it is assumed that the outer layer that is mainly composed of Fe^{3+} rich oxides and hydroxides is nonprotective, while the inner oxide layer that is rich in Fe^{3+} is protective [153]. The loss of this films is known as depassivation and leads to active corrosion in the reinforcement steel bars. Corrosive products of iron are also expansive and may produce cracking and further deterioration in concrete [104]. Due to the nature of passive layers on metals, they usually exhibit the electrochemical properties of a semiconductor [154].

3.5.3 Chloride-induced Corrosion in Concrete

Chloride ions can be present in concrete due to the use of chloride-contaminated components, the use of de-icing salts or from environmental exposure in coastal areas. A localized breakdown of the passive film that initiates corrosion process in steel bars occurs when a sufficient amount of chloride ions reach the surface of the embedded bars in concrete [104].

When the chloride ions in concrete are dissolved in the pore solution, they are called free chlorides and when they are chemically and physically bound to the cement hydrates and their surfaces they are known as bound chlorides. Only the free chlorides are responsible for initiating the process of corrosion [155]. Figure 5 shows the corrosion process of iron in steel reinforcement due to the ingress of chlorides or carbon dioxide. In this process, ferrous ions (Fe^{2+}) are realized due to chloride ions (Cl^-) and react with free hydroxyls (OH^-) to produce iron (II) hydroxide ($Fe(OH)_2$).

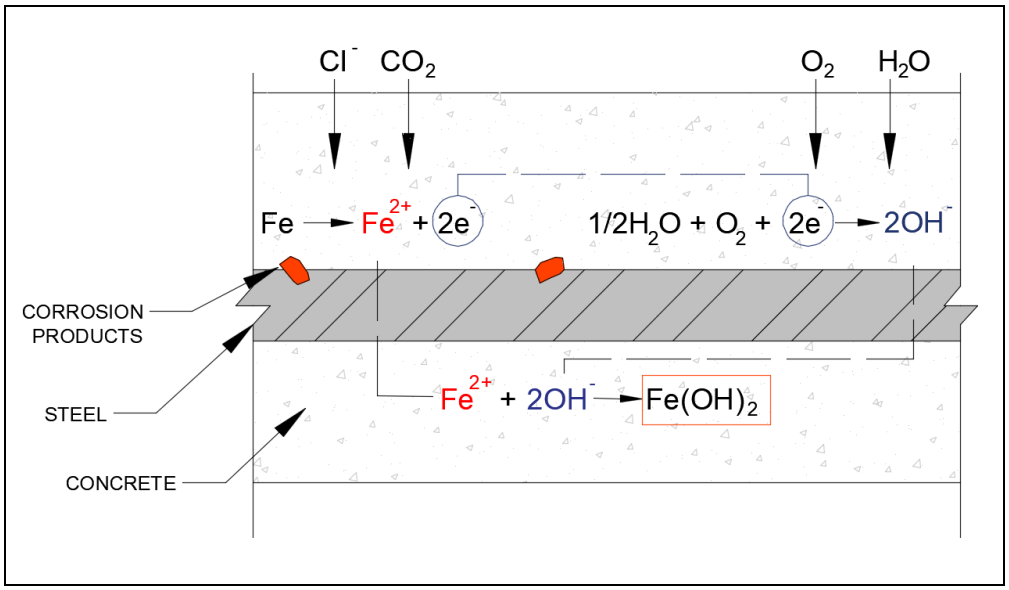

Figure 5 – Schematic illustration of corrosion in reinforcement steel bards. Adapted from (*Ahmad, 2003)* [156].

There are three theories about the chloride attack in concrete [104]:

1. Penetration of chloride ions though pores is easier than penetration of other ions.

2. Chloride ions are adsorbed on the metal surface in competition with O_2 or hydroxyl ions (OH^-).
3. Chloride ions compete with hydroxyl ions (OH^-) for the ferrous ions (Fe^{2+}) produced by corrosion and a soluble complex of iron chloride ($FeCl_2$ – $FeCl_3$) forms that diffuses away from the anode and destroys the protective layer of $Fe(OH)_2$, further allowing corrosion in the steel bar.

The usual approach to quantify chloride-induced bar depassivation is to limit the allowed content of chlorides in concrete since there are critical concentrations at which the passive film may be damaged, and corrosion initiated. However, there is uncertainty in these threshold values and other techniques should be applied. Chloride induced corrosion in concrete may be identified by cracking in the surface since the corrosion products are expansive [104].

3.5.4 Carbonation-Induced Corrosion

Carbonation in concrete occurs when calcium hydroxide ($Ca(OH)_2$) reacts with carbon dioxide as follows:

$$Ca(OH)_2 + CO_2 \rightarrow CaCO_3 + H_2O$$

Carbonation in concrete reduces pH to less than 8.3, which is enough to make the passive layer on the reinforcement rebar unstable [104], as seen in Figure 4. The depth of carbonation increases with time, and the rate at which it advances is a function of relative humidity, being the most rapid in the 50%-70% relative humidity range [76]. However, the rate of carbonation is slowed over time due to three factors: first, CO2 has to penetrate deeper into concrete, second, the concrete continues to hydrate and it's more impermeable over time and finally, carbonation itself decreases permeability due to the precipitation of calcium carbonate that acts as a filler [151].

Unlike chloride-induced corrosion, carbonation-induced corrosion is generalized and relatively homogeneous. The corrosion products are more soluble in the neutral carbonated concrete and diffuse to the surface as rust stains on the concrete rather than causing stresses and cracking [104].

Corrosion rates of carbonation are lower than those of chlorides, but over a long period of time, continuous depassivation may cause a significant loss in the cross-section of steel rebar even while there is little visible damage in concrete. The most aggressive environment for carbonation-induced corrosion is the alternation between wet and semidry cycles, which is more significant in areas where concrete is periodically subjected to saturation and drying by rainstorms [157].

3.5.5 Effects of Fly Ash in Steel Rebar Corrosion

Due to the high alkalinity of concrete's hydration products, steel reinforcement bars are considered to be protected by the formation of a passive oxide film. However, the addition of pozzolanic additions such as fly ash, can specifically reduce iron protection from corrosion by a pH reduction due to reactions between hydration products [104]. The inclusion of fly ash can also reduce concrete porosity and its permeability to aggressive agents such as carbon dioxide or chlorides [124], so the reduction of pH may not be sufficient to promote corrosion in the reinforcement steel of concrete since it depends on other factors such as W/B ratio and porosity.

Products without pozzolanic activity only act as fillers without modifying the alkaline environment in concrete, however, using a high volume of fly ash in concrete has no deleterious effect on the corrosion behavior of steel bars for similar concrete strength classes sin the morphology of the corrosive attack turns more diffuse and less penetrating [104].

3.6 Experimental Framework

3.6.1 Electrochemical Measurement of Corrosion

Corrosion consists of an anodic reaction in which a metal is oxidized end electrons are released, and a cathodic reaction in which the electrons are consumed, and the reduction occurs. By equating these two reactions, a corrosion current I_{Corr}, which is related to the corrosion rate, and a corrosion potential or open circuit potential, E_{Corr}, can be found.

On practice, potential is not measured absolutely, and is usually defined as the potential difference between the metal and that of a reference electrode chosen to have a stable potential. For example, magnesium-based electrodes are generally employed for potential measurements in concrete. The open circuit potential is equivalent to the voltage of a cell or battery versus a reference electrode and can be measured with a high impedance potentiometer [104].

The measurement of the current flowing between anode and cathode is a direct measurement of the rate of dissolution or oxidation of the metal, known as the corrosion current [104]. I_{Corr} cannot be measured directly but it can be estimated by using electrochemical techniques.

In electrochemical measurements, a cell consists of a working electrode (the corroding metal), a counter electrode, a reference electrode and electrolyte. All of the electrodes are connected to a potentiostat which changes the potential in a defined rate, and the resultant current is measured as a function of this potential. The change of potential is called “polarization”, when the polarization is done potentiostatically, the current is measured and when it’s done galvanotatically the potential is measured [104].

3.6.2 Polarization Resistance

When the relationship between potential and current in the region of the open circuit potential is plotted, there is an approximately linear region around the open circuit potential

as shown in Figure 6. This plot is known as the linear polarization resistance (LPR) curve, and it is obtained by applying a potential in the range of ±10 mV around the open circuit potential (E_{Corr}), as a constant pulse and measuring the current response.

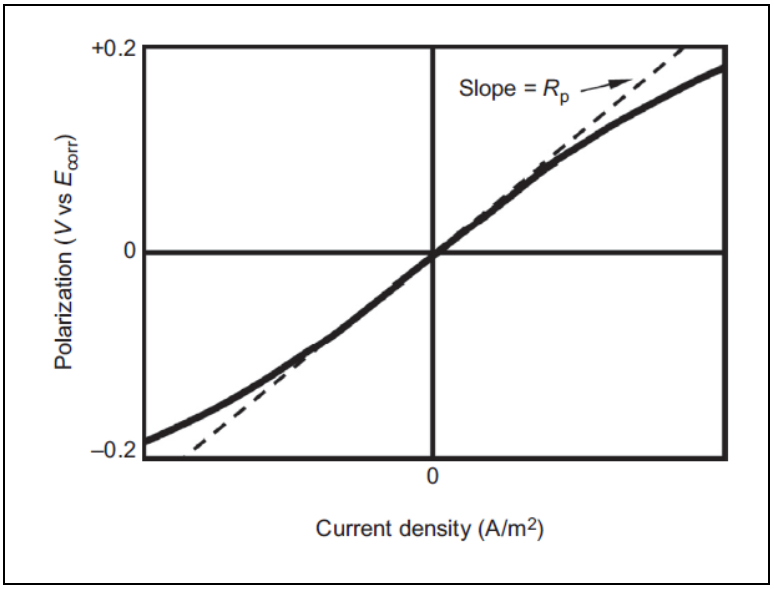

Figure 6 – Linear Polarization Curve. Retrieved from *(Poursaee, 2016)* [104].

Polarization Resistance (*Rp*) is the resistance of the specimen to oxidation while an external potential is applied, and the corrosion current (I_{Corr}) which is inversely correlated cam be calculated. The polarization resistance is defined as the slope of the linear region illustrated in Figure 6:

$$R_p = \frac{\Delta E}{\Delta I} \qquad \textit{Equation 1}$$

Where ΔE is the change in potential and ΔI is the change in current. The corrosion current and the corrosion current density (i_{Corr}) can be calculated from the polarization resistance using the mixed-theory potential developed by Stern and Geary, using the following equations:

$$I_{corr} = \frac{B}{R_p} \qquad \textit{Equation 2}$$

$$i_{corr} = \frac{B}{R_p A} \qquad \textit{Equation 3}$$

$$B = \frac{\beta_a \beta_c}{2.3(\beta_a + \beta_c)} \qquad \textit{Equation 4}$$

A is the surface area of the polarized zone, B is Stern-Geary constant and β_a and β_c are anodic and cathodic Tafel constants, respectively. The Stern-Geary constant should be determined empirically, however, for corrosion of steel rebar in concrete, B is assumed to be equal to 0.026V for active corrosion and 0.052 for passive corrosion [104].

The resistance measured by the LPR is the sum of the polarization resistance and the electrolyte resistance R_Ω. For environments such as concrete, R_Ω is significant in magnitude to the total polarization resistance and should be considered and subtracted in the measurements [158]. According to some researchers, corrosion current densities over 1 μA/cm^2 are identified as the level of high corrosion risk and corrosion current densities below are defined as passive corrosion in the system [104].

The corrosion current density can be related to the corrosion rate in μm/year by determining the mass loss during the polarization time and applying Faraday's law as following:

$$CR = \frac{i_{corr} * t_a * M_{Fe}}{Z_{Fe} * F * d_{Fe}} * 10^6 \left(\frac{\mu m}{year}\right) \qquad \textit{Equation 5}$$

Where $t_a$is the number of seconds in a year (31536000 seconds/year), $M_{Fe}$is the molar mass of iron (0.055847 kg/mol), Z_{Fe} is the number of loss electrons (2 for iron), F is Faraday's constant (96485 C/mol), and d_{Fe} is the density value for iron (7860 kg/m^3). Therefore, Equation 27 can be rewritten as:

$$CR\left(\frac{\mu m}{year}\right) = i_{corr}\left(\frac{A}{cm^2}\right) * 1161 \qquad \textit{Equation 6}$$

The main advantage of using LPR is that it is a non-destructive method and requires only a few minutes for corrosion rate determination, however, interpreting the values in concrete

is difficult since the actual corroding area of steel is almost impossible to determine and may cause an underestimation of the actual corrosion current density [104].

3.6.3 Electrochemical Impedance Spectroscopy (EIS)

An electrochemical process can be modeled as an electrical circuit with basic elements such as resistors, capacitors and inductors. Therefore, the alternate current (AC) circuit theory can be used to demonstrate the corrosion process and predict corrosion rates. In AC, Ohm's law can be described as:

$$V = I * Z \qquad \textit{Equation 7}$$

Where *V* is the applied voltage, *I* is the amplitude of the alternating current and *Z* is the impedance value. In AC circuits, the impedance is the resistance to flow of current, but it is dependent of the systems frequency. Direct current (DC) can be viewed as a particular case of AC when the frequency is equals to zero, in this case, the resistance is composed of only one or more actual resistors. When the frequency is not zero, all circuit elements that can affect the flow of current cause the impedance. The goal of AC EIS techniques is to measure the impedance and then model the response by using an equivalent simple circuit [104].

Mathematically, AC is described as a sinusoidal current or voltage that can be presented as a rotating vector as shown in Figure 7. In this plot, the x component shows the observed current, becoming the "real component" of the rotating vector, while the y component is a non-observed contribution named the "imaginary component" of the rotating vector [104].

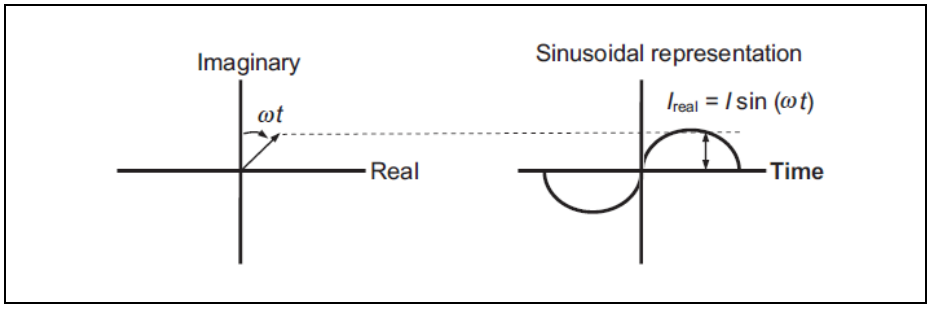

Figure 7 – Rotating vector representation of sinusoidal alternating current. Retrieved from *(Poursaee, 2016)* [104].

The real and imaginary components of the rotating vector are as following:

$$Real\ current = I_x = |I| \cos(wt) \quad \textit{Equation 8}$$

$$Imaginary\ current = I_y = |I| \sin(wt) \quad \textit{Equation 9}$$

Where *t* is time and w is the frequency in radians per second. The magnitude of the current can also be separated in its real and imaginary components and expressed as a vectorial sum:

$$E_{total} = E_{real} + E_{imaginary} = E' + jE" \quad \textit{Equation 10}$$

$$I_{total} = I_{real} + I_{imaginary} = I' + jI" \quad \textit{Equation 11}$$

$$Z_{total} = Z' + jZ" = \frac{E' + jE"}{I' + jI"} \quad \textit{Equation 12}$$

Where $j = \sqrt{-1}$. The phase angle *(θ)* is defined as the angle between the real and imaginary components of the impedance, as following:

$$\theta = \frac{Z"}{Z'} \quad \textit{Equation 13}$$

A simple corroding system representation is the Randles circuit, where the system can be assumed as a solution resistance in series with a combination of a resistor and a capacitor, which represents the polarization resistance and double layer capacitance [104], as shown in Figure 8.

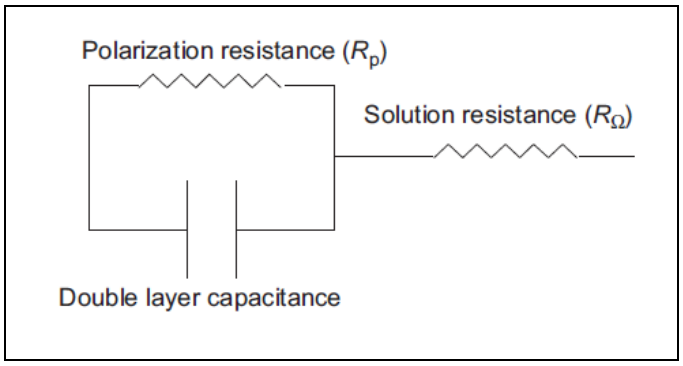

Figure 8 – Randles Simplified equivalent circuit for simple electrochemical circuit. Retrieved from *(Poursaee, 2016)* [104].

Due to its complexity, there are different ways to illustrate the response of an electrochemical system to an applied AC potential or current. The most common plot is called a “Nyquist Plot” where the real component is plotted on the x-axis and the imaginary component is plotted in the y-axis as shown in Figure 9. In this plot, each point is the impedance value for a single frequency.

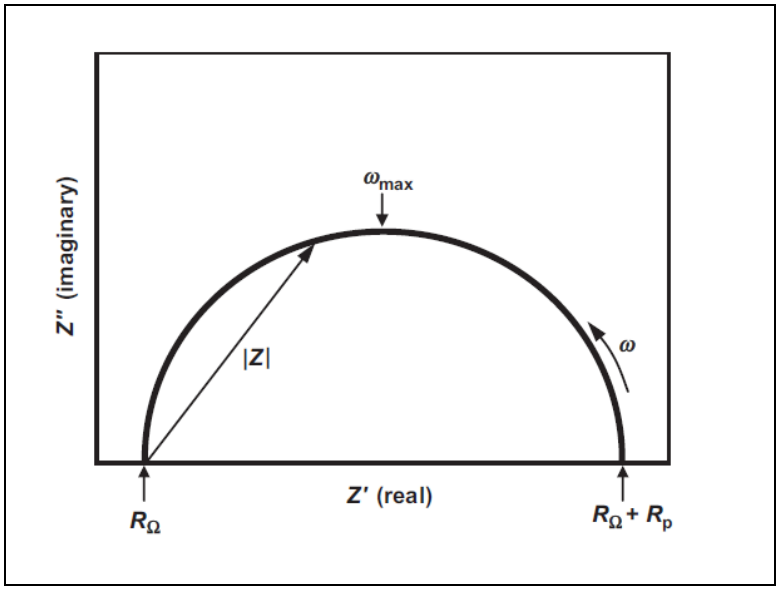

Figure 9 – Nyquist Diagram for simple electrochemical system. Retrieved from *(Poursaee, 2016)* [104].

From Figure 9 it is possible to identify that for high frequencies, at the leftmost end of the semicircle, the impedance is entirely produced by the ohmic electrolyte resistance (R_Ω), while at low frequencies, the value corresponds to the sum of the electrolyte resistance and

the polarization resistance of the corroding metal (R_P). The main disadvantage of a Nyquist Plot is that the frequency at which each impedance value was determined is not clearly shown. The electrolyte and polarization resistance values can also be determined directly from the plot but the electrode capacitance can only be calculated if the frequency information is known [104].

Bode Plots are also commonly used for data representation. In a Bode plot, the data are plotted with log of frequency on the abscissa and both the log of absolute value of the impedance and phase shift on the ordinate, as shown in Figure 10. From the Bode plot, it is also possible to determine the values of R_P and R_Ω, since at the highest frequencies, the ohmic resistance controls the impedance while at lowest frequencies, the sum of both resistances can be easily determined. The bode plot provides a more understandable description of the frequency-dependent behavior of an electrochemical system [104].

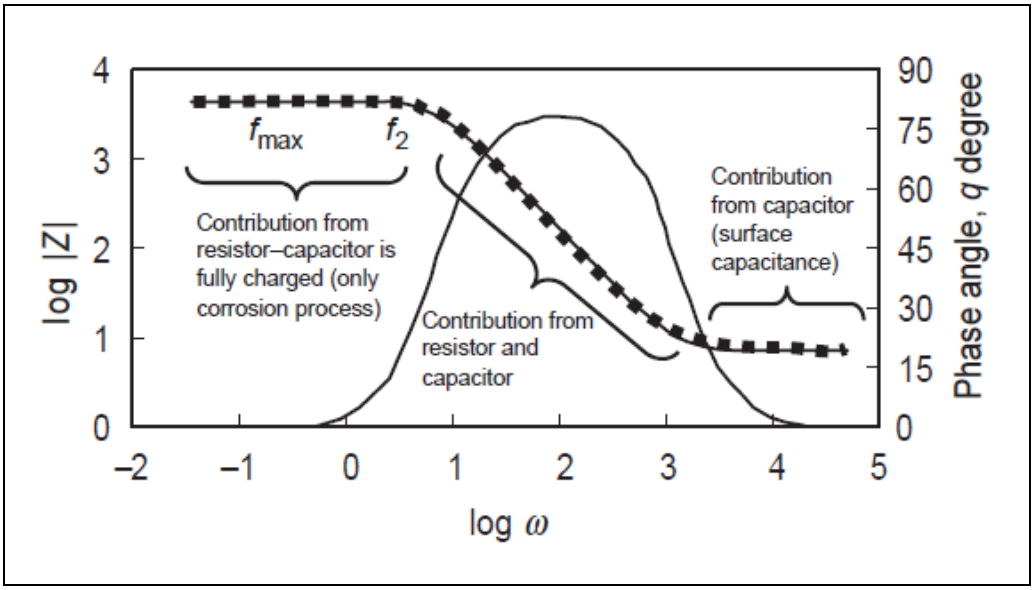

Figure 10 – Bode Plot for simple electrochemical system. Retrieved from *(Poursaee, 2016)* [104].

3.6.4 Chloride transport in concrete

Since concrete is a porous material, different transport mechanisms can originate ion movement. When this process is originated from a difference in chemical potential or concentration, the process is known as diffusion. On the other hand, when the flux is caused by a difference in electric potential, its called migration, and when the flux is originated from a difference in fluid pressure from capillary suction, the process is called permeability [159].

Flick's first law of steady state diffusion describes the relationship between flux *J,* and a constant concentration c_i, as follows:

$$J_i = -D_i \frac{\delta c_i}{\delta x} \qquad \textit{Equation 14}$$

Where D_i is the diffusion coefficient and $\delta c_i / \delta x$ is the change in concentration with distance. For non-steady state conditions, when the concentration is changing with time, *t*, the flux is defined by Flick's second law, as follows:

$$\frac{\delta c_i}{\delta t} = D_i \frac{\delta^2 c_i}{\delta x^2} \qquad \textit{Equation 15}$$

To obtain an approximate solution to Fick's second law, an ideal situation, shown in *Equation 16,* in which only chloride ions diffuse in a homogeneous semi-infinite medium, influenced by a constant concentration gradient is assumed [159].

$$c(x,t) - c_o = (c_s - c_o)\left(erfc\left(\frac{x}{\sqrt{4tD_a}}\right)\right) \qquad \textit{Equation 16}$$

In this solution, $c(x,t)$ is defined as chloride concentration for any time and position, c_o is the initial concentration of chlorides in the pore solution, c_s is a constant concentration on the external surface, D_a is the apparent diffusion coefficient and $erfc$ is the Gaussian error function.

When there is a combined effect of diffusion and migration originated from an electric field gradient, the ionic flux is determined using Nernst-Planck equation, which describes the

flow of any ion species by the action of a concentration gradient and an electric field as follows:

$$J_i = D_i \frac{\delta c_i}{\delta x} + \frac{Z_i F}{RT} D_i c_i \frac{\delta E}{\delta x} \qquad \textit{Equation 17}$$

Where Z_i is the electrical charge of species, R is the gas constant, F is the Faraday constant, T is the absolute temperature and E is the electrical potential. The Nernst-Planck equation is used in electrical migration tests on concrete samples such as **NORDTEST METHOD NT BUILD 492** – *"Chloride Migration Coefficient from Non-Steady-State Migration Experiments"* [160], in which the non-steady state migration coefficient is determined after an extended chloride migration period induced by a constant electrical potential.

3.6.5 Air Permeability in Concrete

Several researchers have developed methods to measure air permeability in concrete as it is a good indicator of the protective quality of the concrete cover that correlates very well with other durability parameters related to the rate of penetration of gases and liquids such as the coefficient of gas diffusion and the rate of water sorption [161].

Most of these methods consist in the creation of a vacuum inside a cell placed on the concrete surface by pumping over a period of time, and then increasing and measuring the increase in chamber pressure after pumping is stopped, however, most of these methods were limited since the geometry of the air flow is unknown and the results were strongly affected by the smoothness of the surface, resulting in misleading results [161].

A vacuum cell for measuring the coefficient of permeability to air in concrete was proposed by *Torrent (1992)* [161], using a two-chamber cell based on the guard-ring principle with an inner (*I)* and outer chamber (*O*) and a diaphragm pressure regulator whose role is to keep both chambers always at the same pressure ($P_i = P_o$). With this method, the geometry of the air flux is much better defined, and the air permeability coefficient, *k,* can be calculated based on the determination of the affected depth *L* at which atmospheric pressure still exists in the pores.

The calculation of the air permeability coefficient is based on the model shown in Figure 11, in which air flows through a “cylindrical” concrete tube, and it is assumed that at time *t* the affected depth *L* is the depth at which the air in the pores is still at the original atmospheric pressure P_a, with the additional assumption that the pressure varies linearly.

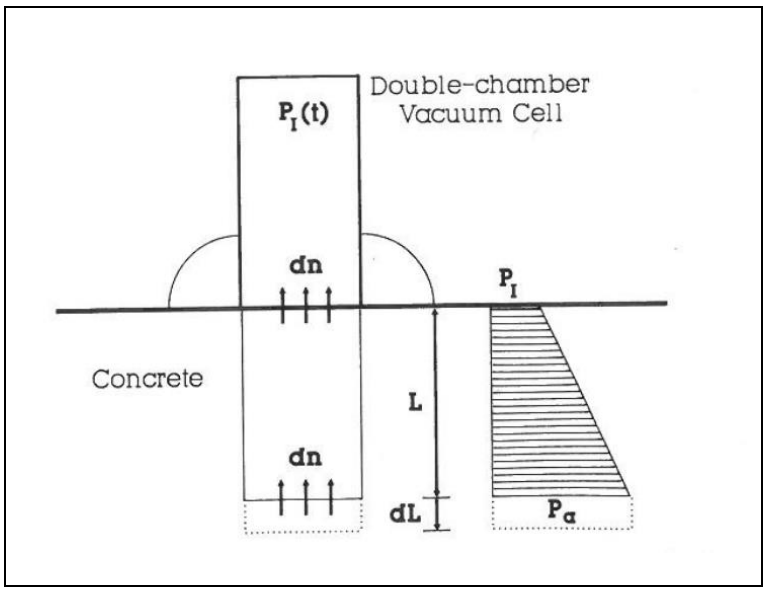

Figure 11 – Schematic description of the air permeability coefficient calculation model. Retrieved from *Torrent (1992)* [161].

The air-flow rate into the chamber is governed by Poisseuilles’s equation:

$$\frac{dV}{dt} = \frac{kA(P_a^2 - P_i^2)}{2\mu L P_i} \qquad \textit{Equation 18}$$

Where dV is the volume of the air entering the chamber during dt, A is the cross-sectional area of the concrete cylinder and μ is the dynamic viscosity of air. The equation for ideal gases is:

$$PV = nRT \qquad \textit{Equation 19}$$

Where *R* is the universal gas constant*, n* is the number of moles of gas existing in volume *V* at pressure *P* and temperature *T.* Combining both equations, the rate at which moles of air enter the chamber can be calculated as:

$$\frac{dn}{dt} = \frac{kA(P_a^2 - P_i^2)}{2\mu LRT} \qquad \textit{Equation 20}$$

The rate of increase in pressure P_i in a finite volume V_c can be calculated as:

$$\frac{dP_i}{dt} = \frac{dn}{dt}\left(\frac{RT}{V_c}\right) \qquad \textit{Equation 21}$$

By combining these equations, the coefficient of permeability can be derived as:

$$k = \frac{2V_c\mu L}{A\left(P_a^2 - P_i^2\right)}\left(\frac{dP_i}{dt}\right) \qquad \textit{Equation 22}$$

The solution of this equation leads to the following expression for calculating the coefficient of permeability after a defined time pressure change, *kT*:

$$kT = \left(\frac{V_c}{A}\right)^2 \frac{\mu}{2\varepsilon P_a}\left(\frac{\ln\left(\frac{P_a + \Delta P_{ieff}(t_f)}{P_a - \Delta P_{ieff}(t_f)}\right)}{\sqrt{t_f} - \sqrt{t_o}}\right)^2 \qquad \textit{Equation 23}$$

Where ε is the estimated porosity of the concrete cover, ΔP_{ieff} is the effective pressure raise in the inner cell at the end of the test and t_f is the time at the end of the test. The principle of the test is that more permeable concrete will lead to a faster ΔP_{ieff} grow, yielding a higher value of *kT*. The approximate depth affected by the test can be calculated as:

$$L \approx 1000\left(\frac{2\ kT\ P_a\ t_f}{\varepsilon\ \mu}\right)^{0{,}50} \qquad \textit{Equation 24}$$

4. Experimental Methodology

4.1 Research Phases

The research program was divided in three phases conducted according to a stablished time frame as presented in Figure 12. The methodology for each phase is described as follows:

4.1.1 Phase 1: Literature Review and experimental preparation

- Identification of the research problem by performing an extensive literature review of national and international scientific papers and thesis.

- Review process of different national and international regulations and codes regarding the use of recycled concrete aggregates.

- Experimental program definition and required material quantification and obtaining process.

4.1.2 Phase 2: Material identification and experimental execution

- Classification and testing of available natural and recycled aggregate material and execution of different tests on the mineral additions and cement.

- Mix design formulation according to material properties, accepted international methods and different aspects obtained from the literature review process.

- Mixing process of multiple concrete mixes with different fine recycled aggregates and fly ash replacement ratios.

- Multiple durability tests on all the concrete samples at different ages.

4.1.3 Phase 3- Statistical data processing and result analysis:

- Statistical analysis of experimental data. In this phase, test results were processed, and durability performance of each concrete mix was determined.

- Comparative analysis between the results for each concrete mixture and conclusion of the research process.

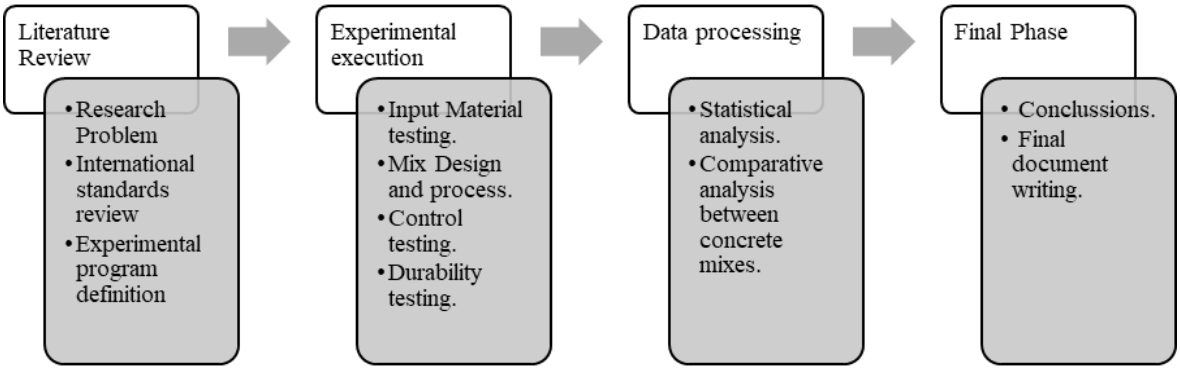

Figure 12 - Research phases definition

4.2 Experimental mix definition

Different concrete mixes were investigated in this research to identify the effects of including fine recycled aggregates and fly ash on the durability properties related to steel rebar corrosion of concrete as shown in Table 4. Each concrete mix is composed of coarse natural aggregates, a combination of natural and recycled fine aggregates and cementitious materials composed of fly ash and cement.

Mix	Mix	Water/Binder	Fine Recycled Aggregate	Fine Natural Aggregate	Fly Ash
ID	Name	Ratio	(%)	(%)	(%)
1	28-CONTROL		0	100	0
2	28-RA20		20	80	0
3	28-RA60		60	40	0
4	28-RA100	0,45	100	0	0
5	28-RA20-FA20		20	80	20
6	28-RA60-FA20		60	40	20
7	28-RA100-FA20		100	0	20
8	21-CONTROL		0	100	0
9	21-RA20		20	80	0
10	21-RA60		60	40	0
11	21-RA100	0,50	100	0	0
12	21-RA20-FA20		20	80	20
13	21-RA60-FA20		60	40	20
14	21-RA100-FA20		100	0	20

Table 4 - Experimental concrete mix proportions.

Each one of these mixes was cast by replacing the weight of the fine fraction (particles under sieve size No.4) of the natural aggregates with the desired proportion of fine-RCA. For the incorporation of Fly Ash in the selected concrete mixes, 20% of the cement weight was replaced.

The mixes were prepared using water/binder (W/B) ratios of 0,45 and 0,50, aiming for an average design resistance of 21 MPa and 28 MPa as these are the most produced concrete strengths in Colombia. These values of strength were also proposed to identify the relationship between water-to-binder ratio and each assessed durability property.

The replacement ratios of 20%, 60% and 100% were defined to identify the effects of incorporating incremental replacement ratios of fine recycled aggregates in different concrete properties related to steel corrosion. Low, medium, and full replacement ratios of RCA were proposed to detect the optimal ratio that could be added without significantly reducing concrete's performance.

Fly Ash contents of 0% and 20% were established to evaluate the effects of incorporating the maximum recommended fly ash dosage that is widely used in international construction practice. As different authors have reported, fly ash could enhance pozzolanic reactions and densify the microstructure of recycled concrete [105], [106], [124]. This mineral is also commercially available in Colombia and could be implemented in concrete mixes without significantly increasing production costs.

Average concrete compressive strength (f_c') was also involved as a variable in this research to assess the effects of two water-to-binder ratios (W/B). To achieve 21 MPa and 28 MPa compressive strengths, W/B ratios of 0,50 and 0,45 were also defined, respectively. The variation in W/B ratio could have a detrimental effect in RAC's durability since different authors have reported that fine recycled aggregates show high absorption levels that drastically modify concrete's workability and result in mixes with a highly porous microstructure [71], [162].

The target strength values of 21 MPa and 28 MPa are commonly used in structural concrete for low and medium resistance requirements and can be produced with most natural aggregates industrially at low cost. Additionally, a design strength of 21 MPa is commonly

used in Colombia since the local building code (NSR-10) requires 17.5 MPa as minimum compressive strength for concrete structures.

5. Materials and Testing

In this section, a description of materials and tests performed in concrete materials is presented. The same materials were used for all concrete mixtures. Commercially available materials were used to evaluate the applicability of recycled aggregate concrete in a conventional building project. Different national testing procedures were performed in each material as parameters for concrete mix design and material quality control.

5.1 Hydraulic Cement

Each recycled concrete mix was prepared using the same cement samples. The cement is classified in Colombian standards as Type GU – General use cement according to **ASTM C1157** – "*Standard Performance Specification for Hydraulic Cement"* [163], it is commercially available and widely used in building projects with different resistance and durability specifications. As seen in Figure 13, this cement is produced by CEMEX® and is branded as "super-resistant" structural cement with building applications.

Figure 13 – (a) Cement bags used in experimental program. (b) Cement particles used in concrete mixtures.

Different tests were performed on cement to identify properties such as fineness, setting time using Vicat needle, density, fluidity, and mortar bar strength. These tests and their results are shown in Table 5. Cement producers in Colombia are not required to specify the results of these tests if the material is produced and tested according to the national standard **NTC 121** – "*Portland Cement: Physical and Mechanical Specifications*" [164]. The required values for these properties according to NTC 121 are also shown in Table 5.

Cement property	Colombian Standard	ASTM Equivalence	Measured Property	Property limits NTC 121
Fineness Module (cm2/g)	NTC 33	ASTM C204	7041,25	Not specified
Cement Density (g/cm3)	NTC 221	ASTM C188	2,819	Not specified.
Water for normal Consistency (%)	NTC 110	ASTM C187	31%	Not specified.
Initial Setting Time (min)	NTC 118	ASTM C191	197	45 Min. Value
Final Setting Time (min)	NTC 118	ASTM C191	280	420 Max. Value
Fluidity using Flow Table	NTC 111	ASTM C230	111	Not specified
Water content (%)	-	ASTM D7348*	0,25 %	Not specified
Loss on Ignition (1000°C) (%)	-	ASTM D7348*	7,9 %	Not specified

Table 5 – Cement properties testing program and results.

Figure 14 shows a photographic record of different tests performed on the hydraulic cement used for the concrete mixes in this research program.

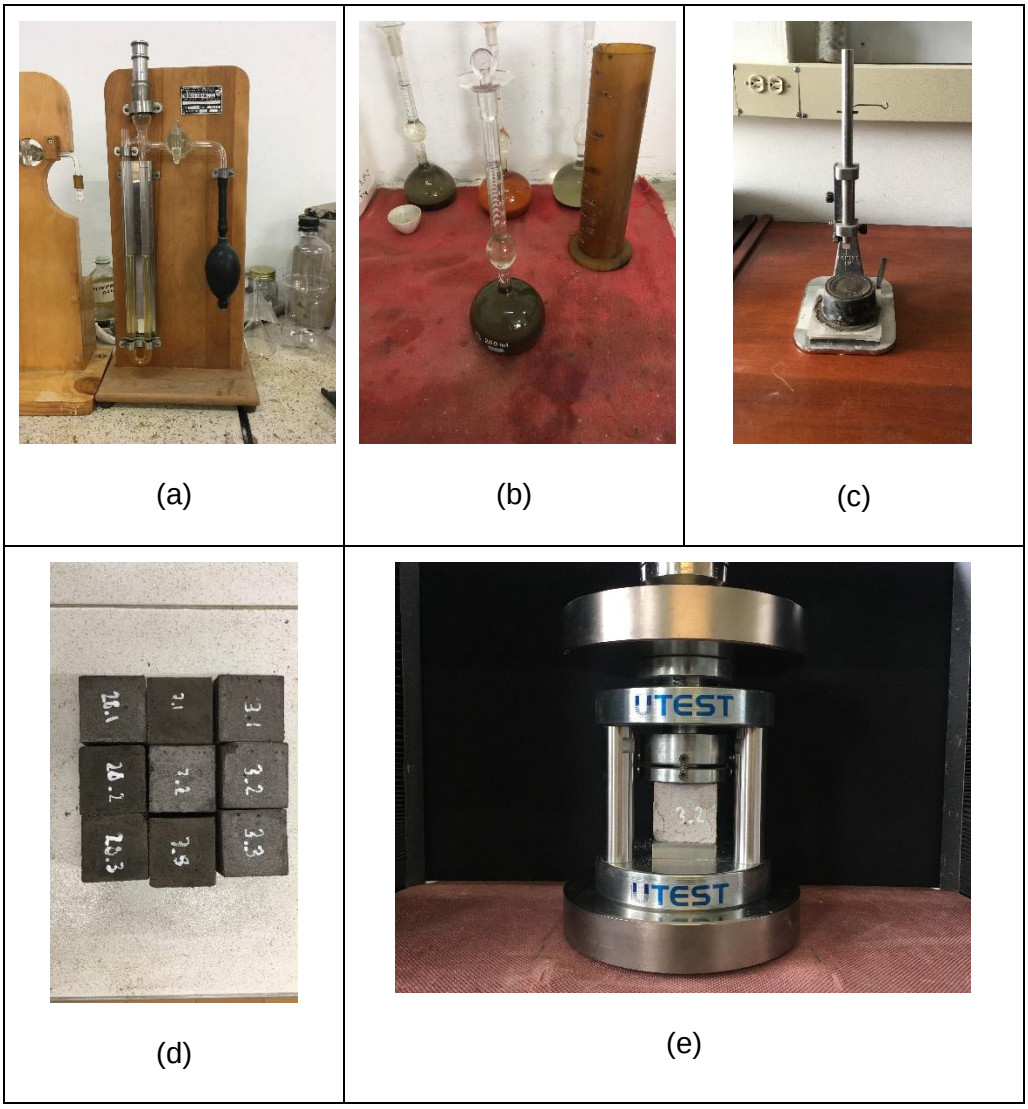

Figure 14 – (a) Fineness module test in cement. (b) Cement density test. (c) Setting time tests. (d) Mortar cubes for compressive test (e) Compressive strength of cement mortar test.

Compressive strength of the hydraulic cement was also determined according to the Colombian standard **NTC 220 –** *"Cements. Determination of compressive strength of hydraulic cement mortars, using 50 mm or 2 inches cube specimens"* [165], based on the American standard **ASTM C109** - *"Standard Test Method for Compressive Strength of Hydraulic Cement Mortars (Using 2-in. or [50 mm] Cube Specimens)*" [166]. Cement paste cubes were fabricated and tested at 3, 7 and 28 days and the results are shown in Table 6.

The mortar mixes were mixed by mass proportion using 2.75 grams of standard Ottawa sand per each gram of cement. According to NTC 220, enough mixing water must be used to produce a fluidity value of 110 ± 5 when testing the mortar mix in the flow table according to **NTC 111** – *"Cements. Specifications for flow table for use in tests of hydraulic cement."* [167]. The specimens were submerged in water for moist curing until testing time. The grading requirements for standard sand are described in **NTC 3937** – "*Cements. Standard Sand For Hydraulic Cement Tests*" [168], which was adapted and modified from the American standard **ASTM C778** – "*Standard specification for Standard Sand"* [169].

Mortar cubes Compressive Strength – ASTM C109 (NTC 220)

Sample	Age	Compressive Strength	Average Strength	Specified Strength by producer	Required Strength by NTC 121 (Min.)
	Days	MPa	MPa	MPa	MPa
3_1	3	4,54	-	-	-
3_2	3	7,03	-	-	-
3_3	3	4,89	6,92	17,0 – 21,0	8,0
7_1	7	6,74	-	-	-
7_2	7	7,08	-	-	-
7_3	7	6,95	9,54	17,0 – 21,0	15,0
28_1	28	9,56	-	-	-
28_2	28	10,07	-	-	-
28_3	28	9,00	20,23	26,0 – 32,0	24,0

Table 6 – Mortar cubes compressive strength results.

The compressive strength development for mortar cubes tested at 3, 7 and 28 days are presented in Figure 15. These mortar cubes were prepared using a 0,503 water-to-cement

(W/C) ratio and 2.75 parts of Ottawa sand per each part of cement. This W/C ratio defines the optimal water content for the fluidity requirements defined in NTC111.

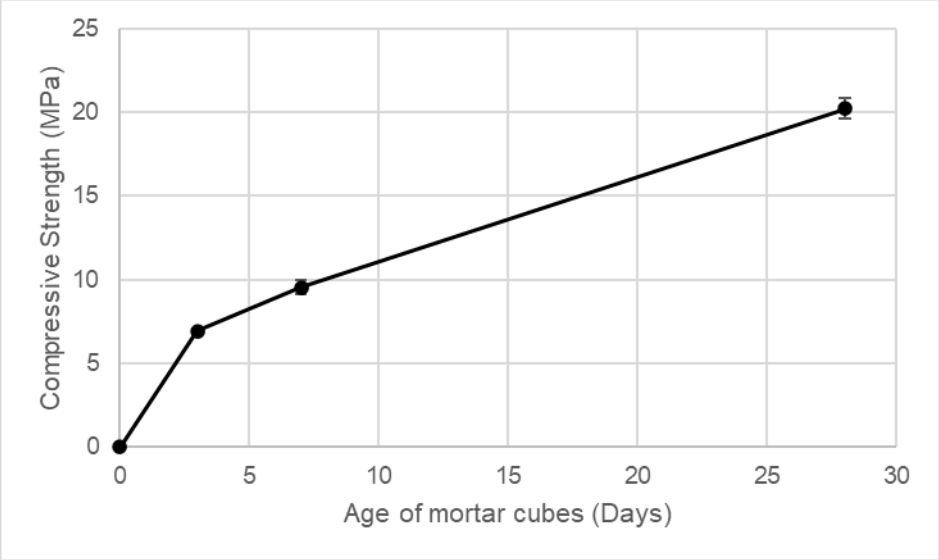

Figure 15 – Compressive strength development of hydraulic cement mortar.

The results from testing mortar cubes at different ages indicate lower compressive strengths when comparing to the values specified by the producer. At 28 days, the achieved average compressive strength (20,23 MPa) was approximately 78% of the expected value (26 MPa), nevertheless, Colombian standards allow the use of mineral admixtures in cement if the minimal physical requirements specified in NTC 121 are satisfied. Reference concrete mixes without recycled concrete aggregates were designed with a sufficient content of cement to achieve the desired mechanical performance and reduce the possible detrimental effects of using a commercially available binder material since other carried research works reported the use of ASTM Type I Portland or equivalent cement, which presents significantly more specific mass and less surface area [81].

5.2 Aggregates

5.2.1 Coarse Natural Aggregates

Coarse aggregates in the concrete mixes from the research program had a maximum aggregate size of ½ inch. The aggregates were obtained from a local concrete manufacturer where they are stored in open air conditions and used in structural concrete. These aggregates have a fluvial origin and are extracted close to the Saldaña river in Tolima, Colombia. The particles have a regular size and partially rounded edges as shown in Figure 16.

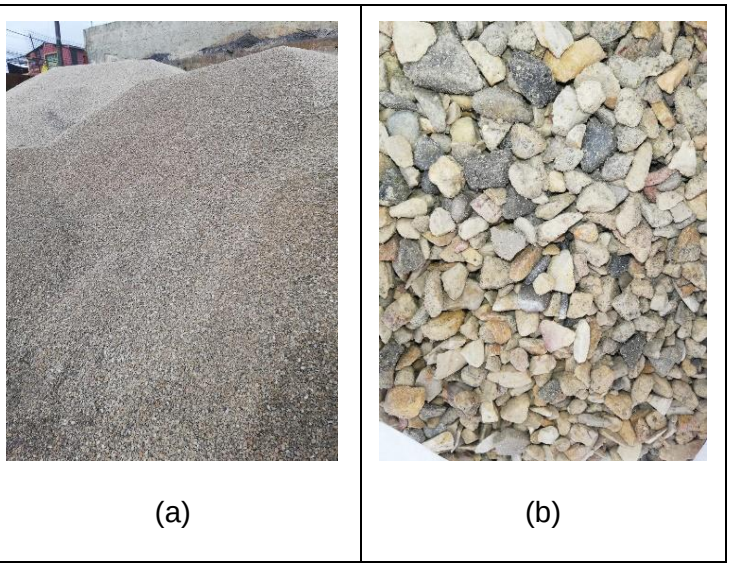

Figure 16 – (a) Coarse natural aggregates storage at source. (b) Coarse natural aggregate particles.

Different tests were performed on the natural aggregates according to national Colombian standards (NTC standards). These tests are useful for quality control and to identify different parameters used in the concrete design process. Table 7 shows the national standard and results obtained. The photographic record for the procedure of these tests is shown in Figure 17.

Aggregate Property	Colombian Standard	ASTM Equivalence	Measured Property
Total moisture content of aggregate by drying (%)	NTC 1776[1]	ASTM C566[4]	0,31
Specific gravity of coarse aggregate (g/cm^3)	NTC 176[2]	ASTM C127[5]	2,32
Absorption of coarse aggregate (%)	NTC 176	ASTM C127	4,62
Compacted Unit weight in aggregates (g/cm^3)	NTC 92[3]	ASTM C29-M[6]	1,39
Voids in aggregates (%)	NTC 92	ASTM C29-M	39,65

[1] NTC 1776 - Test method to determine the total evaporable moisture content of aggregate by drying [170].

[2] NTC 176 - Test method to determine the relative density (specific gravity) and absorption of coarse aggregate [171].

[3] NTC 92 - Test method for the determination of bulk density ("unit weight") and voids in aggregate [172].

[4] ASTM C566-19, Standard Test Method for Total Evaporable Moisture Content of Aggregate by Drying [173].

[5] ASTM C127- Standard Test Method for Density, Relative Density (Specific Gravity), and Absorption of Coarse Aggregate [174].

[6] ASTM C29, Standard Test Method for Bulk Density (" Unit Weight ") and Voids in Aggregate [175].

Table 7 – Natural coarse aggregate properties.

(a)

(b)

(c)

Figure 17 – (a) Dry-oven coarse aggregates for water content. (b) Saturated coarse aggregates for absorption and specific gravity. (c) Compacted aggregates for unit weight and voids.

5.2.2 Fine Natural Aggregates

Fine aggregates were obtained from the same concrete manufacturing facility as coarse natural aggregates. These particles have a maximum size of 4.76 mm (Sieve No.4) and are used in the production of structural concrete. The aggregates are extracted in the region of Tolima, Colombia. As seen in Figure 18, this material is stored in open-air conditions and the particle shape is mostly rounded.

(a)

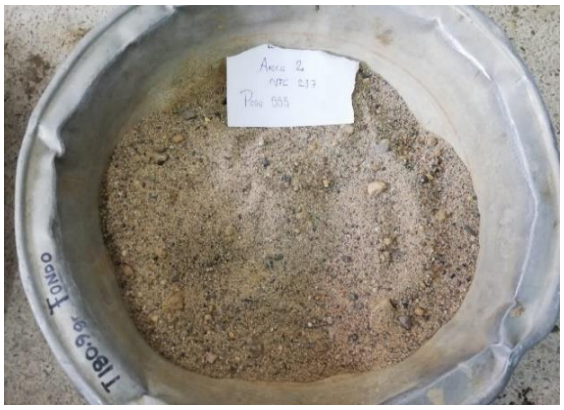

(b)

Figure 18 – Natural fine aggregates: (a). Aggregate storage at source. (b). Fine natural aggregate particles.

Similarly to coarse natural aggregates, fine particles were also tested according to national standards for quality control purposes and to identify different properties used in the concrete mixtures design process. The results of different tests performed in fine aggregate are presented in Table 8. Additionally, the photographic record of these tests is shown in Figure 19.

Aggregate Property	Colombian Standard	ASTM Equivalence	Measured Property
Total moisture content of aggregate by drying (%)	NTC 1776[1]	ASTM C566[5]	0,47
Materials finer than 75 µm (No. 200) sieve by washing (%)	NTC 78[2]	ASTM C117[6]	5,66
Specific gravity of fine aggregate (g/cm3)	NTC 237[3]	ASTM C128[7]	2,45
Absorption (%)	NTC 237	ASTM C128	2,09
Compacted Unit weight in aggregates (g/cm^3)	NTC 92[4]	ASTM C29-M[8]	1,53
Voids in aggregates (%)	NTC 92	ASTM C29-M	37,39

[1] *NTC 1776 - Test method to determine the total evaporable moisture content of aggregate by drying [170].*

[2] *NTC 78 - Test method to determine by washing the material that passes the 75 µm (no. 200) sieve in mineral aggregates* [176].

[3] *NTC 237 - Test method to determine the relative density (specific gravity) and the absorption of fine aggregate* [177].

[4] *NTC 92 - Test method for the determination of bulk density ("unit weight") and voids in aggregate [172].*

[5] *ASTM C566-19, Standard Test Method for Total Evaporable Moisture Content of Aggregate by Drying [173].*

[6] *ASTM C117-17, Standard Test Method for Materials Finer than 75-µm (No. 200) Sieve in Mineral Aggregates by Washing* [178].

[7] *ASTM C128-15, Standard Test Method for Relative Density (Specific Gravity) and Absorption of Fine Aggregate* [179].

[8] *ASTM C29, Standard Test Method for Bulk Density (" Unit Weight ") and Voids in Aggregate [175].*

Table 8 – Natural fine aggregates properties.

(a)

(b)

Figure 19 – Fine natural aggregates characterization. (a). Specific gravity testing. (b). Unit weight testing.

ASTM C40 “Standard Test Method for Organic Impurities in Fine Aggregates for Concrete” test was also performed to identify the presence of injurious amounts of organic impurities for natural aggregates that may cause a negative effect in the hydration process of concrete. In this test, fine aggregates are mixed with a 3% Sodium Hydroxide (NaOH) solution that reacts to the presence of organic materials by changing its color. After 24 hours, the solution color is compared to a standardized palette and when the solution is darker than the standard value, the possible presence of organic materials must be

assessed using the standard **ASTM C87** - *"Standard Test Method for Effect of Inorganic Impurities in Fine Aggregate on Strength of Mortar"* [180]. For this research program, natural fine aggregates presented a lighter color than the standard (Color #3), revealing a low content of organic impurities as seen in Figure 20.

Figure 20 – Organic Impurities testing in fine natural aggregates.

5.2.3 Fine Recycled Aggregates

Fine recycled aggregates were obtained from a local concrete manufacturer. Source concrete was designed to achieve a compressive strength of 35 MPa. These aggregates were produced by crushing prefabricated prestressed structural concrete slabs, removing steel rebar and other impurities, and further processing the aggregates by mechanical grinding to achieve the desired particle size. These aggregates are composed of natural aggregate particles with old-attached mortar in different states of hydration. A visual comparison of natural and fine particles is presented in Figure 21.

Figure 21 – Natural and recycled fine aggregates used in concrete mixes.

Fine RCAs were tested according to national standards to measure different properties related to quality control, water absorption and concrete design mix parameters. The results are shown in Table 9. Aggregate testing shows that fine RCA has a higher content of fine materials which drastically increases the water absorption rate, while decreasing specific gravity and unit weight. Additionally, Figure 22 shows the photographic record of these tests.

Aggregate Property	Colombian Standard	ASTM Equivalence	Measured Property
Total moisture content of aggregate by drying (%)	NTC 1776[1]	ASTM C566[5]	4,16
Materials finer than 75 µm (No. 200) sieve by washing (%)	NTC 78[2]	ASTM C117[6]	9,40
Specific gravity of fine aggregate (g/cm3)	NTC 237[3]	ASTM C128[7]	2,12
Absorption (%)	NTC 237	ASTM C128	9,48
Compacted Unit weight in aggregates (g/cm^3)	NTC 92[4]	ASTM C29-M[8]	1,48
Voids in aggregates (%)	NTC 92	ASTM C29-M	30,23

[1] *NTC 1776 - Test method to determine the total evaporable moisture content of aggregate by drying [170].*

[2] *NTC 78 - Test method to determine by washing the material that passes the 75 µm (no. 200) sieve in mineral aggregates* [176].

[3] *NTC 237 - Test method to determine the relative density (specific gravity) and the absorption of fine aggregate* [177].

[4] *NTC 92 - Test method for the determination of bulk density ("unit weight") and voids in aggregate [172].*

[5] *ASTM C566-19, Standard Test Method for Total Evaporable Moisture Content of Aggregate by Drying [173].*

[6] *ASTM C117-17, Standard Test Method for Materials Finer than 75-µm (No. 200) Sieve in Mineral Aggregates by Washing* [178].

[7] *ASTM C128-15, Standard Test Method for Relative Density (Specific Gravity) and Absorption of Fine Aggregate* [179].

[8] *ASTM C29, Standard Test Method for Bulk Density (" Unit Weight ") and Voids in Aggregate [175].*

Table 9 – Fine recycled aggregates properties.

(a)

(b)

(c)

(d)

Figure 22 – Fine recycled aggregates testing: (a) Unit weight testing. (b) Recycled aggregates after drying at 100°C for 24 hours. (c). Materials finer than sieve No. 200. (d). Specific gravity testing.

American standard ASTM C40 was also used to identify the presence of organic impurities in fine recycled aggregates using the procedure described for natural aggregates. The NaOH solution turned to a darker color for recycled aggregates but remained lighter than the limit defined in the standardized color palette (Color #3) as seen in Figure 23. Results show that both types of fine aggregates did not show a significant content of organic impurities and may be used without further assessment of detrimental hydration effects.

Figure 23 – Organic Impurities Testing in fine recycled aggregates.

5.2.4 Aggregate Size Distribution

Aggregate size distribution was determined by sieving according to the American standard **ASTM C136 –** "*Standard test method for sieve analysis of fine and coarse aggregates"* [181]. This parameter is used for concrete mix design and may modify fresh concrete workability and hardened concrete mechanical and durability properties. Figure 24 and Figure 25 present the size distribution for natural coarse and fine aggregates, additionally Figure 26 presents the size distribution for recycled fine aggregates used in concrete mixes. The required gradation limits established in **ASTM C33 –** "*Standard Specification for Concrete Aggregates"* [182], for concrete production are also plotted.

Sieve size	Retained fraction	Passing fraction
Inches	**%**	**%**
1 1/2	0,00	100,00
1	0,00	100,00
3/4	0,00	100,00
1/2	2,36	97,64
3/8	25,18	72,46
No. 4	62,90	9,56
Bottom	9,56	0,00

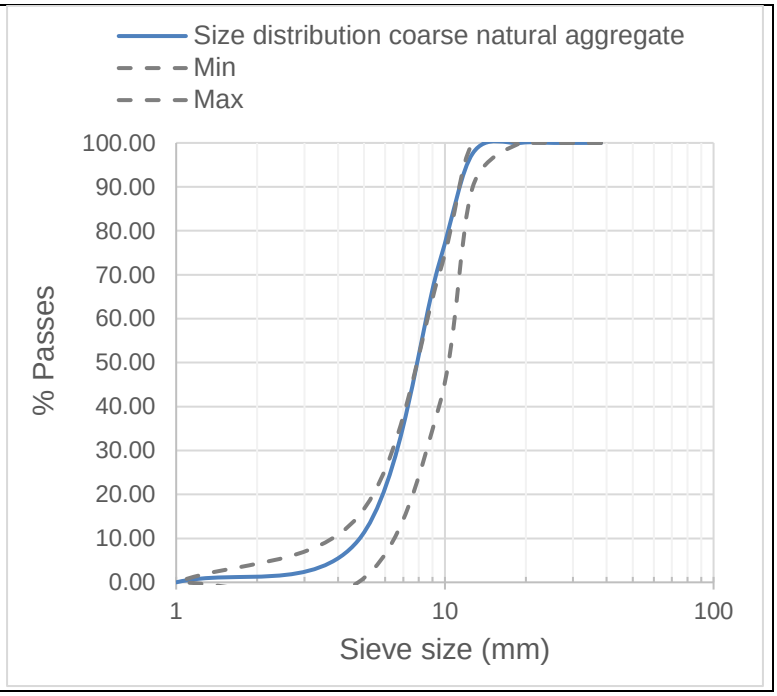

Figure 24 – Size distribution for coarse natural aggregates

Sieve size	Retained fraction	Passing fraction
Inches	**%**	**%**
No. 4	0,00	100,00
No. 8	3,00	97,00
No. 16	4,57	92,43
No. 30	8,71	83,71
No. 50	24,14	59,57
No. 100	35,14	24,43
No. 200	19,14	5,29
Bottom	5,14	0
Fineness Modulus		**2,38**

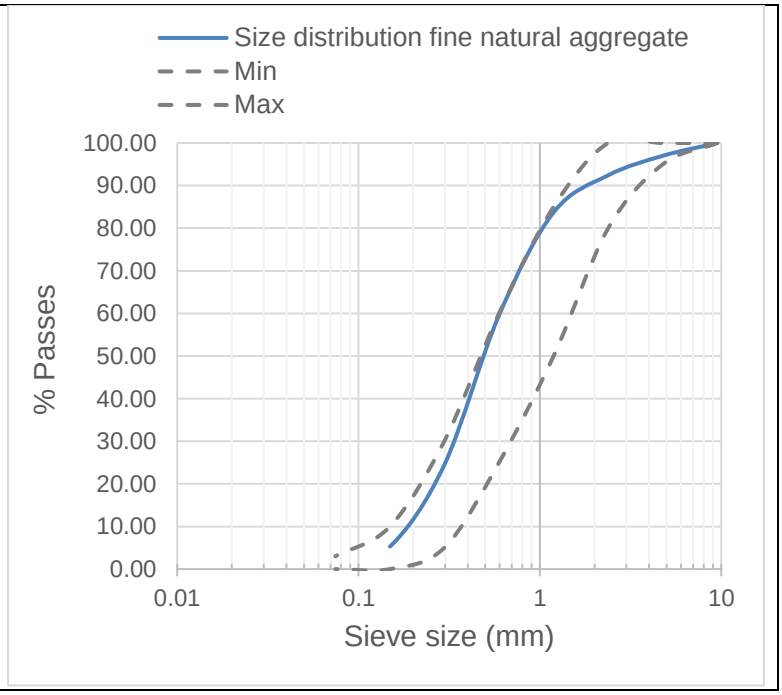

Figure 25 - Size distribution for fine natural aggregates

Sieve size	Retained fraction	Passing fraction
Inches	**%**	**%**
No. 4	1,54	98,46
No. 8	7,53	90,93
No. 16	15,25	75,68
No. 30	20,08	55,60
No. 50	17,18	38,42
No. 100	25,10	13,32
No. 200	10,62	2,70
Bottom	2,32	0,39
Fineness Modulus		**3,25**

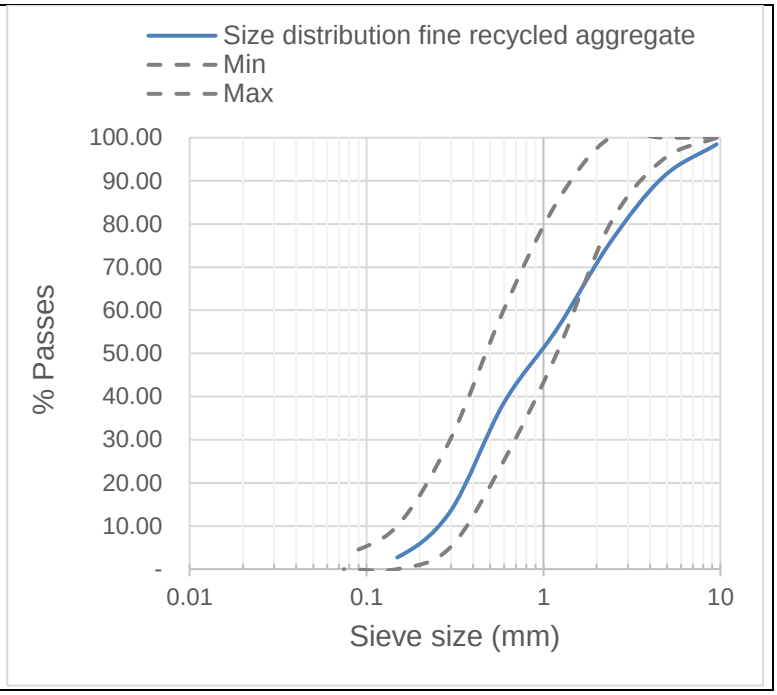

Figure 26 - Size distribution for fine recycled aggregates

Fineness modulus is an empirical estimation of the average particle size, ASTM C33 requires the Fineness modulus of fine aggregates to be between 2.3 and 3.1 as this is an indicator of a concrete with adequate workability properties. Fineness modulus is directly proportional to aggregate particle size as higher values are obtained from aggregates with larger particles.

A higher fineness modulus than the ASTM C33 limit was obtained from fine-RCA used in this research program, this can be noted when comparing the gradation curves from both types of aggregates in Figure 27. Both coarse and fine natural aggregates satisfy the size requirements of ASTM C33.

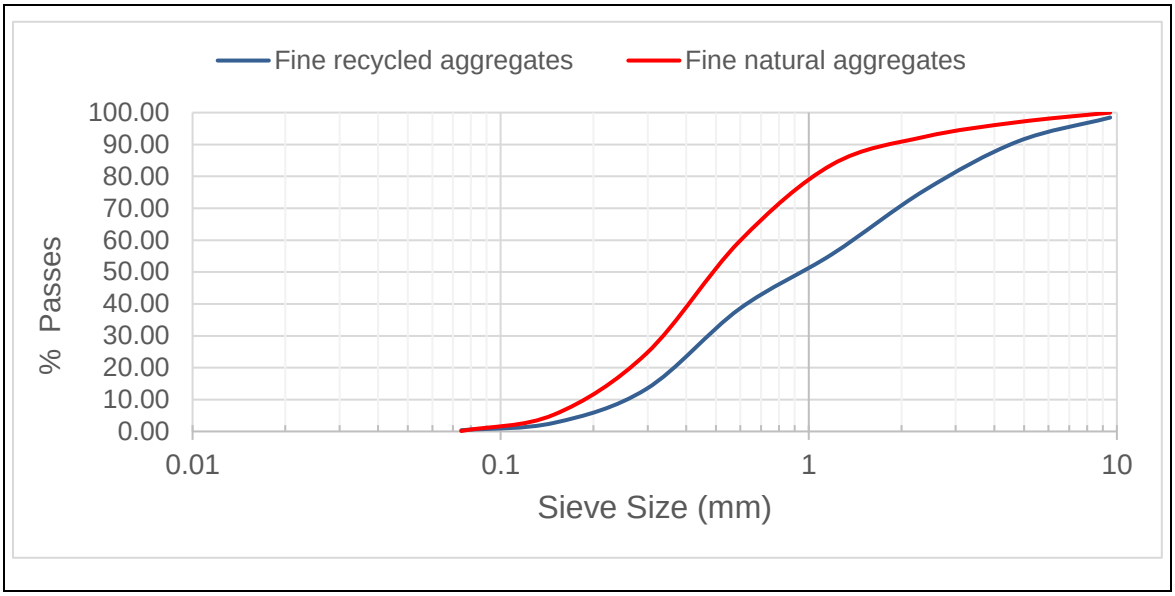

Figure 27 – Particle size comparison of fine aggregates.

Since combinations of fine-RCA and natural fine aggregates do not meet the specified grading requirements of ASTM C33, a modified Fuller-Thompson distribution method was used to obtain an ideal size distribution. In this method, defined by the Road Note Laboratory No. 4 (RNL), particle size is optimized by defining a combination of fine and coarse aggregates that best fits the optimal gradation range obtained from Equation 25.

$$p = 100 \left(\frac{d}{D}\right)^{0,50} \qquad \text{Equation 25}$$

Where *p* is the percentage of material that passes through the sieve size *d* in an aggregate mass where *D* is the largest particle size.

This size distribution method is widely used in national construction practice; however, empirical modifications have been proposed to improve workability properties by increasing the content of fine particles. This suggested grading range is presented in Table 10.

Recommended particle size distribution for different maximum aggregate sizes									
Sieve Size		Maximum aggregate size							
		25,4		19,1		12,5		9,51	
		1"		3/4"		1/2"		3/8"	
mm	Pulg	Inf.	Sup.	Inf.	Sup.	Inf.	Sup.	Inf.	Sup.
25,4	1	100	100						
19,1	3/4	85	90	100	100				
12,7	1/2	68	78	80	87	100	100		
9,51	3/8	58	71	68	78	85	90	100	100
4,76	No. 4	40	56	47	62	58	71	68	78
2,38	No. 8	27	44	32	48	40	55	46	61
1,19	No. 16	18	34	22	38	27	44	32	48
0,595	No. 30	13	27	15	30	19	34	22	38
0,297	No. 50	9	21	10	23	13	27	15	30
0,149	No. 100	6	17	7	18	9	21	10	23

Table 10 - Recommended particle size distribution for different maximum aggregate sizes using a modified Fuller-Thompson distribution.

By using the RNL method, an optimal content of fine and coarse aggregates that best fits the suggested range presented in Table 10 was defined for f-RCA contents of 0%, 20%, 60%, and 100% with a maximum coarse aggregate size of ½ inch. For all cases, a 51% content of fine aggregates and 49% content of coarse aggregates was defined. Grading results for aggregate combination and the optimal particle size distribution ranges are presented in Figure 28. The grading requirements are mostly accomplished with this content of fine and coarse aggregates, however, to achieve better workability and compensate for the low content of finer particles, for all concrete mixtures, a super plasticizer was incorporated.

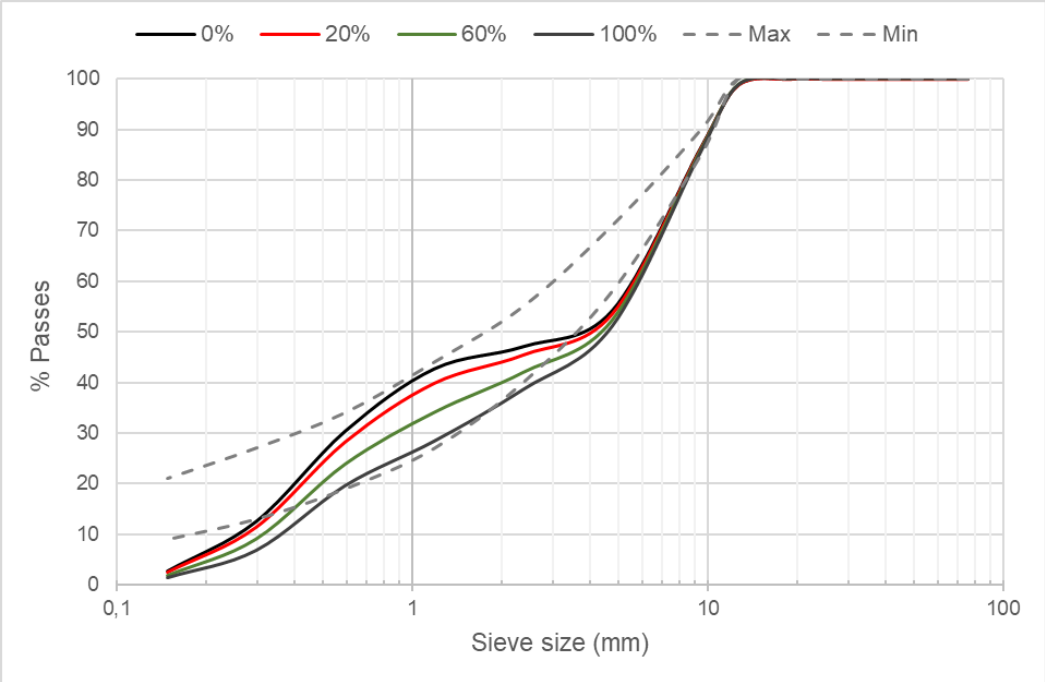

Sieve Size		Suggested Range		Combined gradation			
				% Fine recycled Aggregates			
mm	**Inch**	**Min**	**Max**	**0**	**20**	**60**	**100**
76,1	3	100	100	100	100	100	100
50,8	2	100	100	100	100	100	100
38,1	1,5	100	100	100	100	100	100
25,4	1	100	100	100	100	100	100
19,1	3/4	100	100	100	100	100	100
12,7	1/2	100	100	98,8	98,8	98,8	98,8
9,51	3/8	85	90	86,5	86,3	86,0	85,7
4,76	No. 4	58	71	54,2	53,5	52,3	51,1
2,38	No. 8	40	55	47,1	45,4	42,0	38,6
1,19	No. 16	27	44	42,7	39,8	34,1	28,4
0,595	No. 30	19	34	30,4	28,2	23,9	19,6
0,297	No. 50	13	27	12,5	11,3	9,1	6,8
0,149	No. 100	9	21	2,7	2,4	1,9	1,4

Figure 28 – Particle size distribution for 0%, 20%, 60% and 100% fine recycled aggregate replacement using 49% coarse aggregate content and 51% fine aggregate content.

5.2.5 Petrographic Examination of Aggregates

Petrographic analysis of aggregates was performed to identify and describe the minerals and general lithology of the aggregates used in this experimental program. Based on this composition, the potentially reactive mineral components with negative effects on concrete's durability can be assessed. A comparison of the mineral composition and microstructure of both types of fine aggregates is also presented to identify the main differences that may contribute to a reduction in the mechanical and durability performance of concrete mixes.

5.2.5.1 Methodology

Petrographic analysis was performed following the American standard **ASTM C295** – "*Standard Guide for Petrographic Examination of Aggregates for Concrete"* [183]*,* and its Colombian adaption, **NTC 3773** [184]*.* The samples were prepared selecting 150 particles for each sieve size. Three thin sections were prepared for each aggregate type as shown in Figure 29. The first one was prepared selecting particles retained on the #8 sieve, the second section was prepared with combined particles retained on the #16 and #30 sieve, and a third section was prepared with combined particles retained on the #50 and #100 sieves.

Petrographic examination for was performed focusing on mineral identification, the detection of potentially reactive minerals, weathering grade, porosity, shape and color. An **"OLYMPUS CX-31P"** microscope with 5x, 10x, 20x, 50x and 100x zooms and an adapted photographic camera was used for the analysis

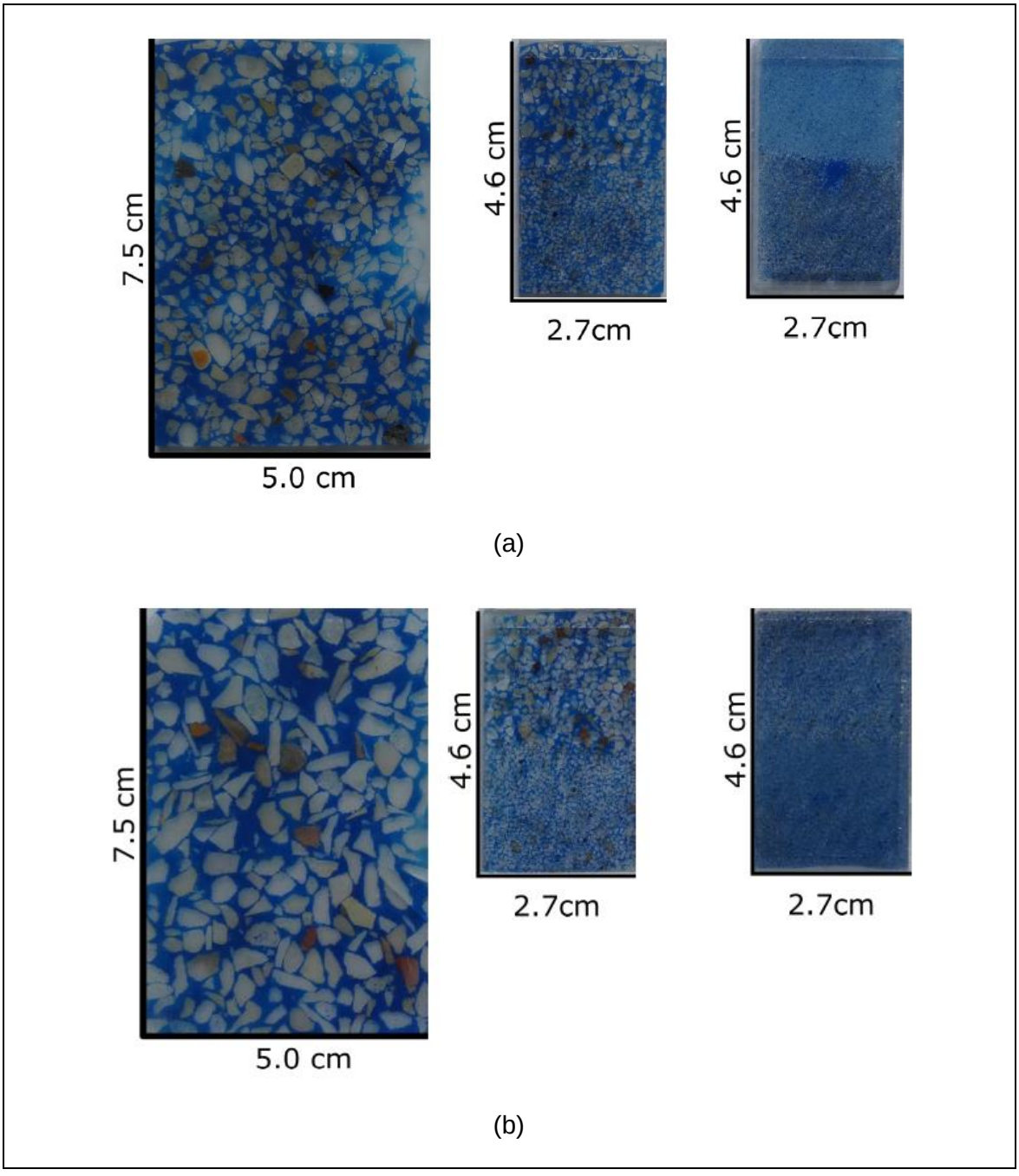

Figure 29 – Thin Sections for Microscopic examination prepared using (a) Fine recycled aggregates. (b) Fine natural aggregates.

For each thin section, the aggregate shape was classified using the roundness and sphericity scale proposed by *Powers (1982)*, presented in Figure 30. The porosity

percentage of aggregates was also determined using *Compton's* method (*1985)*, as shown in Figure 31. Weathering grade was classified in three categories: Unaffected rock particles (I), moderately weathered (II) and highly weathered (III). Weathering grade is determined based on the potential use of the particles as concrete aggregates, only categories I and II are considered adequate for concrete production.

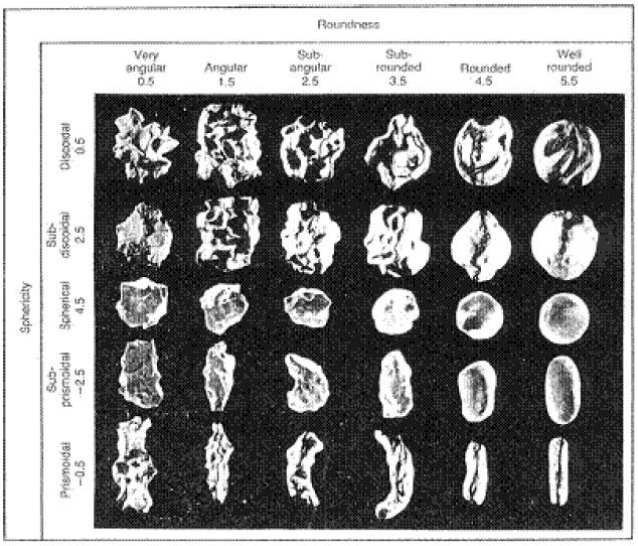

Figure 30 – Roundness and Sphericity Index. Retrieved from *(Powers, 1982).*

Porosity	**Range**
Very Low	< 4%
Low	4% - 8%
Medium	9% - 16%
High	17% - 32%
Very High	> 32%

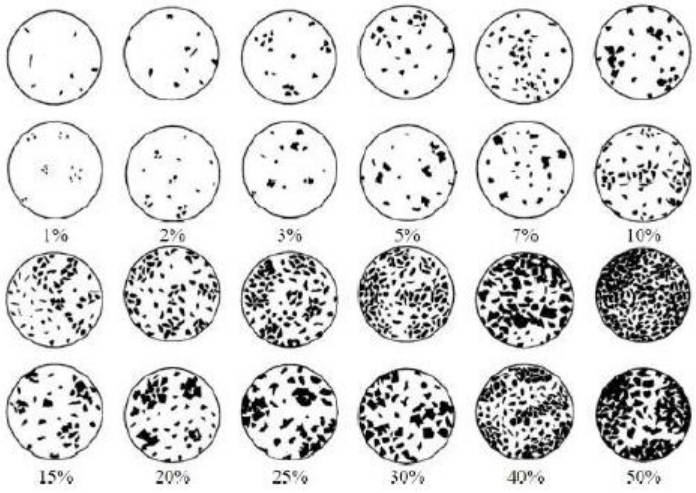

Figure 31 – Porosity estimation proposed by *(Compton, 1985).*

5.2.5.2 – Fine Recycled Concrete Aggregate Analysis

The examinate aggregates are mostly composed of recycled concrete (natural aggregates with old-attached mortar), followed by fragments of sedimentary rocks without OAM derived from the recycled concrete. The identified recycled concrete consists of aggregates with different lithologies which have been grouped as sedimentary (S), sedimentary and metamorphic (S+M) and Sedimentary and Igneous (S+I). For finer sizes, cement (C) was defined as particles derived from C-S-H gel hydration without any adhered aggregates. The possible aggregate compositions from the derived parent concrete are shown in Figure 32.

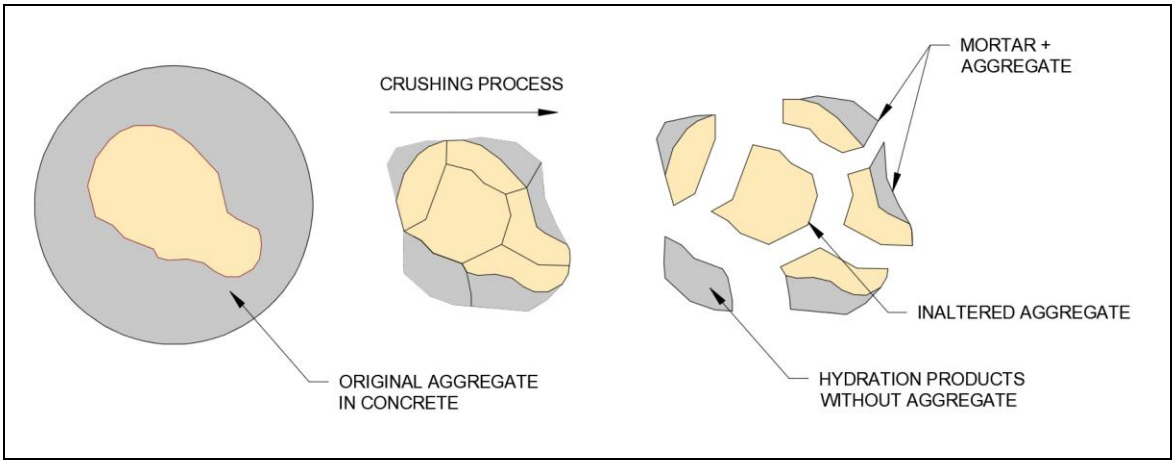

Figure 32 – Schematic representation of possible components of fine recycled aggregates identified by petrographic examination.

In general, the weathering grade of these particles is low (Grade I), and the porosity is low or very low. Particle shape presented a roundness between angular and sub-rounded and a sphericity between spheric and sub-prismoid. Carbonation was also observed on the OAM and cement particles of some particles.

A *"Concrete"* lithology was defined for the particles including fine aggregates, cementing materials and residual clinker and hydration products. The natural aggregates contained in these particles also include rocks from different lithological origins. The rocks contained in recycled aggregates are mostly from sedimentary origin, but igneous and metamorphic origins were also identified. It is important to determine the origin of the natural aggregates contained within recycled aggregates because multiple potentially alkali-silica reactive

lithologies such as chert, quartzites and phyllites were identified. Table 11 presents the content and origin of the predominant lithologies for each analyzed particle size, the predominant shape, porosity grade and weathering grade are also included. A complete list of all found lithologies is presented and discussed in further sections.

Sieve Size	Predominant Lithologies	Content %	Origin*	Predominant Shape	Porosity Grade	Weathering Grade
#8 (2,38 mm)	- Concrete - Chert - Silicate Siltstone	64,9 20,5 6,6	R S S	Sub-round & Sub-prismoid (12,6%).	- Very Low (79,5%) - Low (17,2%) - Other (3,3%)	I (54%) II (41%) III (5%)
#16 (1,19 mm)	- Concrete - Chert - Silicate Siltstone	61,2 11,2 8,6	R S S	Sub-round & Spheric. (14,0%)	- Very Low (80,3%) - Low (7,2%) - Medium (11,18%) - Other (1,32%)	I (41%) II (57%) III (2%)
#30 (595 µm)	- Concrete - Chert - Quartz	67,1 10,7 5,3	R S Min	Sub-round & Spheric. (17,6%)	- Very Low (84,0%) - Low (9,3%) - Other (6,7%)	I (26%) II (74%) III (0%)
#50 (297 µm)	- Concrete - Straight Quartz - Feldspar	43,3 10,7 12,7	R Min Min	Sub-angular & Spheric. (14,7%)	- Very Low (97,3%) - Low (2,7%) - Other (0%)	I (49%) II (47%) III (4%)
#100 (149 µm)	- Straight Quartz - Plagioclase - Feldspar	48,7 17,3 10,7	Min Min Min	Sub-angular & Spheric. (12,0%)	- Very Low (100%) - Low (0%) - Other (0%)	I (79%) II (21%) III (0%)

** R: Recycled Origin. S: Sedimentary Origin. I: Igneous Origin. M: Metamorphic Origin. Min: Minerals.*

Table 11 – Petrographic examination results for different particle sizes of recycled concrete aggregate.

In Table 12, the aggregate origin for different particle size of fine RCA is presented, these values were calculated as the sum of each lithology content with a common origin. A "*Recycled"* origin is defined for recycled aggregates with natural aggregates, old-attached mortar and remnants of cementing materials. In Table 13, the origin of the natural particles embedded in the recycled aggregates is presented.

Aggregate Origin	**#8 Content %**	**#16 Content %**	**#30 Content %**	**#50 Content %**	**#100 Content %**
Recycled	64,9	61,2	67,1	43,4	0
Sedimentary	32,5	27,0	17,4	18,0	3,0
Metamorphic	2,6	3,9	0	5,3	4,0
Igneous	0	4,6	1,3	0	0
Mineral	0	3,3	14,1	33,3	93,0

Table 12 – Calculated aggregate origin for different particle sizes of RCA samples.

From Table 12 it is possible to identify that most recycled aggregates had adhered mortar and hydration products. It is important to notice that an important content of sedimentary aggregates was identified for each particle size. These aggregates were derived from concrete, but due to the crushing process, some aggregates are obtained from bigger particles without presenting old-attached mortar presence. Results presented in Table 13 show that recycled aggregates were mostly derived from parent concrete made with sedimentary aggregates, but finer sizes also presented significant contents of metamorphic aggregates and cement.

RCA Composition	#8	#16	#30	#50
S	65,4	75,3	80	7,7
S+I	12,2	8,6	4	4,6
S+M	22,4	16,1	10	49,2
C	0	0	6	38,5
Total	***100***	***100***	***100***	***100***

S: Sedimentary Particles.
S+I: Sedimentary and Igneous Particles.
S+M. Sedimentary and Metamorphic Particles.
C: Cement and hydration products without aggregates.

Table 13 – Lithology of the recycled concrete fraction for different particle sizes of RCA samples.

Figure 33 shows a microphotography of the most common lithologies observed in recycled aggregates. In this photo, quartzite sandstone (Qa) can be observed with recycled aggregates (with OAM) derived from concrete with sedimentary aggregates (S) and combinations of sedimentary and metamorphic (S+M) and sedimentary and igneous (S+I).

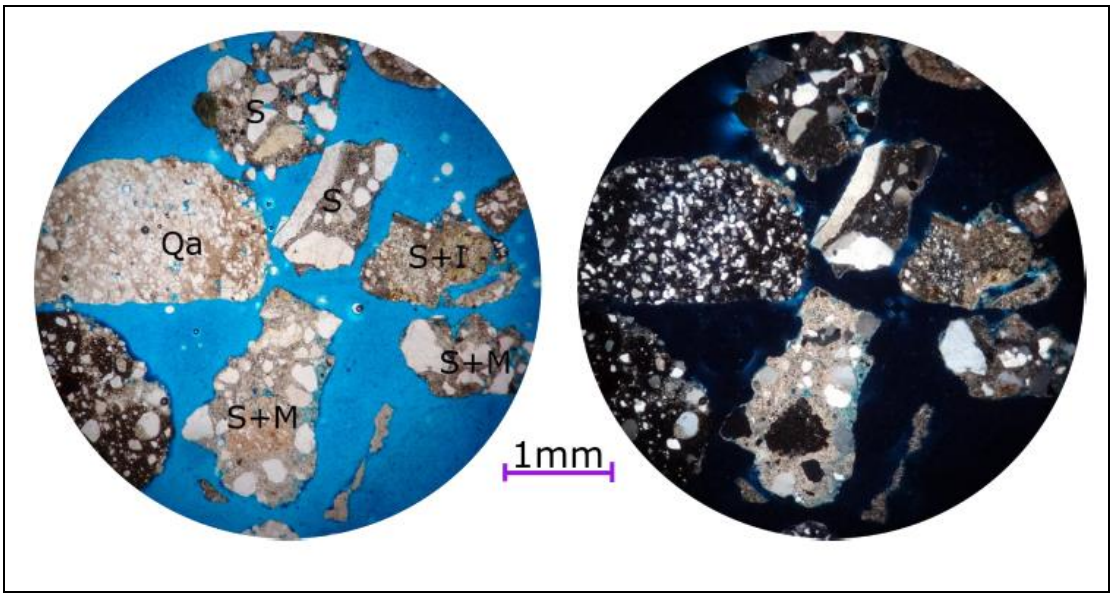

Figure 33 – PPL - XPL Microphotography of RCA with Quartz Sandstone (Qa), cement with sedimentary and metamorphic aggregates (S+M), Sedimentary and Igneous aggregates (S+I). and Sedimentary aggregates (S).

From Table 11 it is also possible to identify that the second most common lithology in fine RCA is "*Chert*". This sedimentary rock of fine grain size is composed of microcrystalline or

cryptocrystalline quartz. In some chert particles, a biogenic origin can be identified as some rock particles still present fossil fragments. This lithology is classified as potentially alkali-silica reactive according to the American standard ASTM C295. A microphotography of a typical chert particle with fossil remnants is shown in Figure 34.

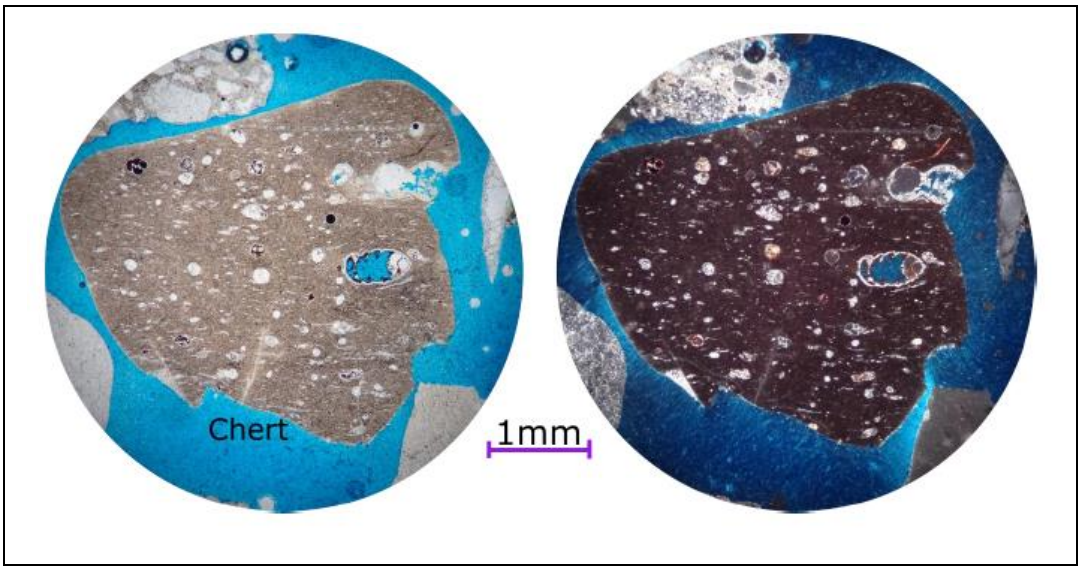

Figure 34 – PPL – XPL Microphotography (4X Zoom) of Chert particle in RCA with fossil remnants.

Regarding porosity, most aggregates presented a low or very low classification. The weathering grade for multiple recycled aggregates was classified as grade I (Unaltered particles), however, a significant portion of aggregates with “recycled” origin presented carbonation in the attached mortar or the cement component as shown in Figure 35. For aggregates without attached mortar, a weathering grade of II was defined with the presence of altering minerals such as sericite over the feldspar crystals. Despite the low general porosity, Figure 36 shows a recycled concrete particle with high porosity. These particles were more common for larger aggregates since smaller sizes present a higher presence of minerals and hydration products with low porosity.

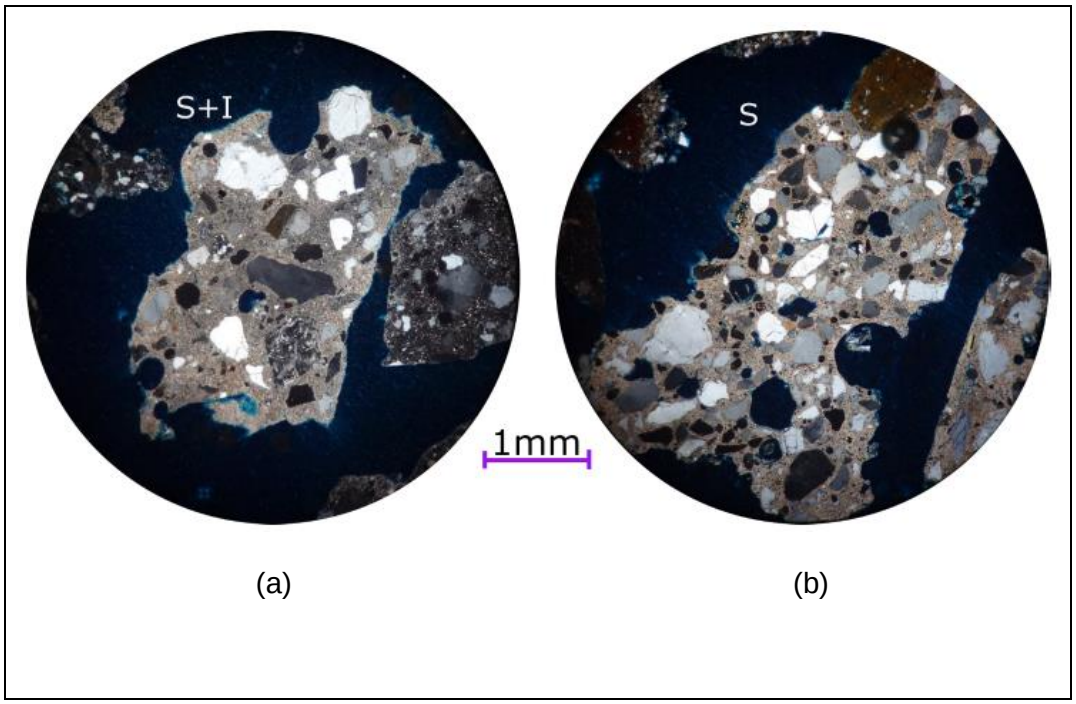

Figure 35 – XPL Microphotography of carbonated RCA with (a) Sedimentary and Igneous aggregates (S+I). (b) Sedimentary aggregates (S).

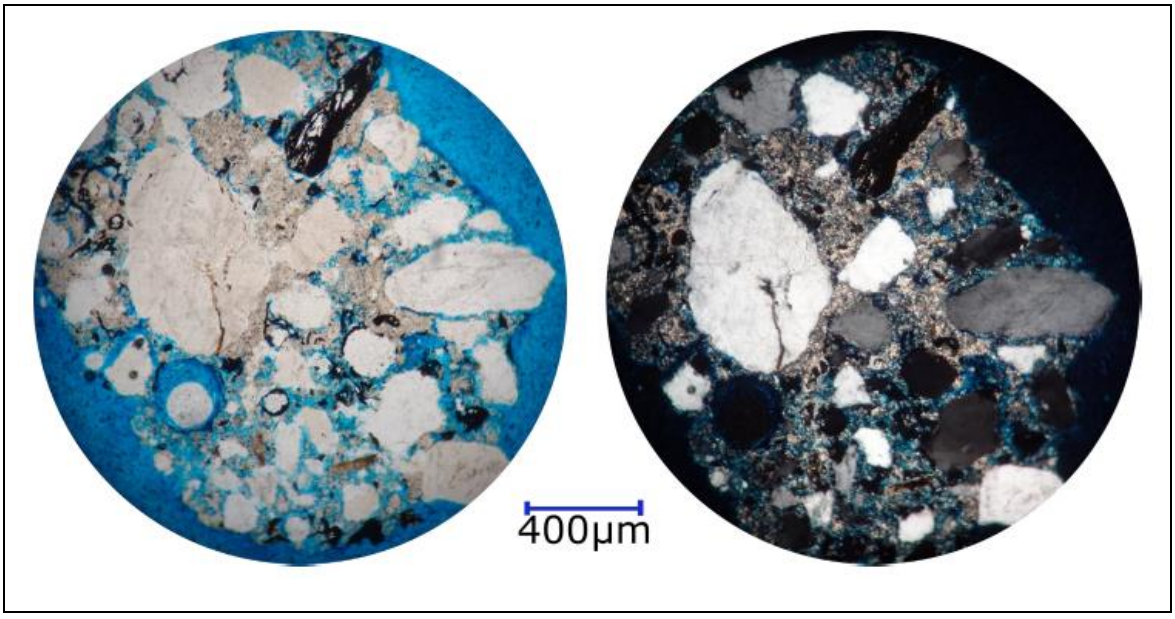

Figure 36 – PPL – XPL Microphotography (10X Zoom) of porous recycled concrete aggregates.

Regarding aggregate shape, the examined aggregates presented a large heterogeneity with different particle roundness and sphericity. Particles retained in the #8, #16 and #30 sieves were more heterogenous, presenting aggregates with all roundness and sphericity index classifications. For the smaller particles retained in the #50 and #100 sieves, most aggregates presented a rounded and more spherical shape. The heterogeneity in particle shape for different recycled aggregate sizes can be observed in Figure 37.

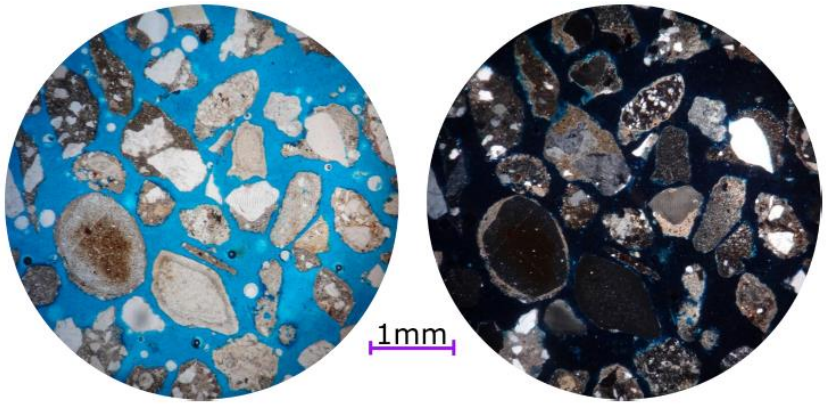

(a)

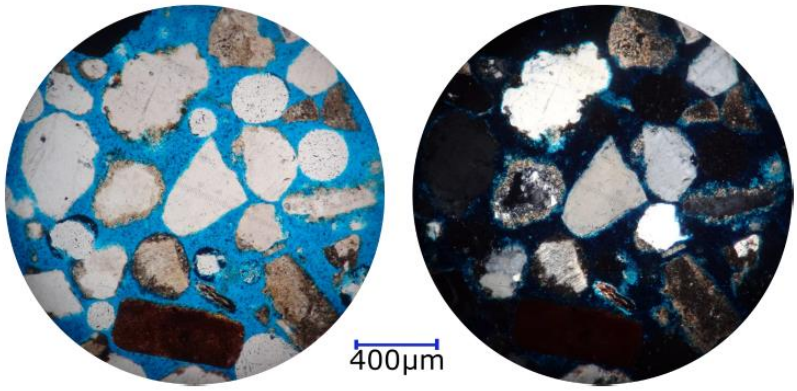

(b)

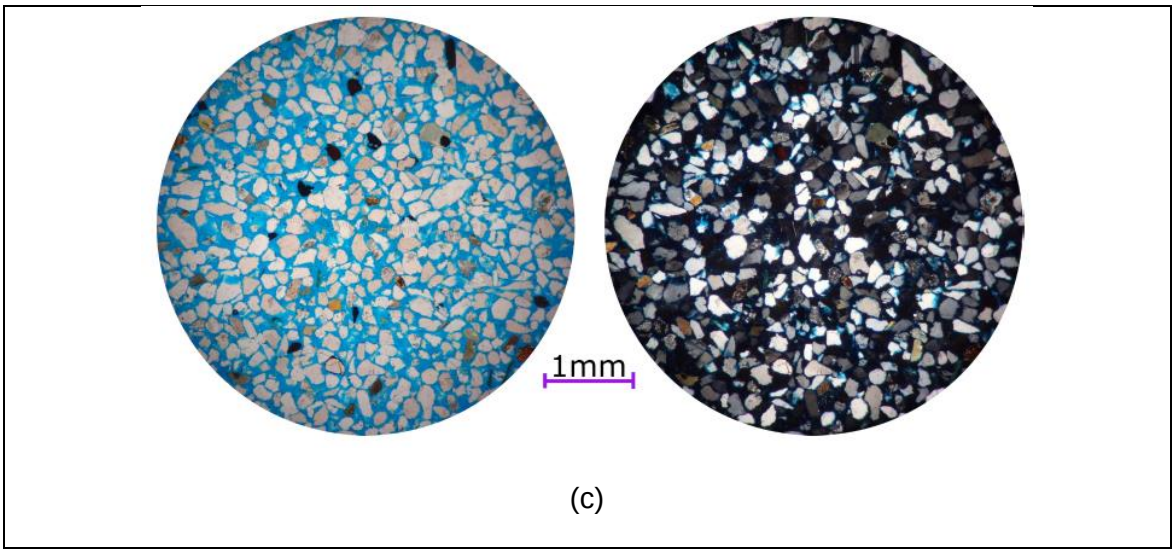

Figure 37 – PPL – XPL Microphotography (4X Zoom) of recycled aggregates retained on (a) #30 Sieve. (b) #50 Sieve. (c) #100 Sieve.

5.2.5.3 Fine Natural Aggregate Analysis

The examinated natural aggregates presented a more heterogeneous lithology with sedimentary, igneous and metamorphic aggregates in all particle sizes. Generally speaking, the weathering grade is lower than recycled aggregates, ranging between low and moderate. The main observed alteration is the sericitation of plagioclases and caolinization of feldspars. Particle shape presented a roundness between angular and sub-rounded and a sphericity between sub-discoidal and sub-prismoid. Table 11Table 14 presents the content and origin of the predominant lithologies for each analyzed particle size, the predominant shape, porosity grade and weathering grade are also included. A complete list of all found lithologies is presented and discussed in further sections.

Sieve Size	Predominant Lithologies	Content %	Origin	Predominant Shape	Porosity Grade	Weathering Grade
#8 (2,38 mm)	- Chert - Diorite - Quartz Sandstone - Silicate Siltstone	20,7 16,7 8,7 9,3	S I S S	Sub-round & Spheric. (11,3%).	- Very Low (95,3%) - Low. (3,3%) - Other (1,3%)	I (57%) II (42%) III (1%)
#16 (1,19 mm)	- Chert - Quartz Sandstone - Plagioclase - Quartz Shale	17,3 11,3 11,3 9,3	S S Min M	Sub-angular & Spheric. (12,0%)	- Very Low (98,0%) - Low (0,7%) - Other (1,33%)	I (67%) II (33%) III (0%)
#30 (595 µm)	- Straight Quartz - Undulose Quartz - Plagioclase	22,0 13,3 16,0	Min Min Min	Sub-angular & Spheric. (17,0%)	- Very Low (100%)	I (66%) II (31%) III (3%)
#50 (297 µm)	- Straight Quartz - Undulose Quartz - Feldspar	19,3 16,0 15,3	Min Min Min	Sub-angular & Spheric. (13,3%)	- Very Low (100%)	I (77%) II (23%) III (0%)
#100 (149 µm)	- Straight Quartz - Plagioclase - Feldspar -Hornblende	16,0 20,7 15,3 14,7	Min Min Min Min	Sub-angular & Spheric. (13,3%)	- Very Low (100%)	I (69%) II (31%) III (0%)

** R: Recycled Origin. S: Sedimentary Origin. I: Igneous Origin. M: Metamorphic Origin. Min: Minerals.*

Table 14 - Petrographic examination results for different particle sizes of natural fine aggregates.

The origin of the assessed aggregates is presented in Table 15. From this table, it is possible to identify that most aggregates have a sedimentary origin, however, the larger sizes presented a significant content of metamorphic and igneous origins. Individual minerals are the predominant lithology in smaller particle sizes.

Aggregate Origin	**#8 Content %**	**#16 Content %**	**#30 Content %**	**#50 Content %**	**#100 Content %**
Sedimentary	38,7	32,0	12,0	10,0	5,0
Metamorphic	26,0	19,3	10,7	6,7	3,0
Igneous	34,0	22,7	8,0	4,0	4,0
Mineral	1,3	26,0	69,3	79,3	88,0

Table 15 - Calculated aggregate origin for different particle sizes of NA samples.

Figure 38 shows a microphotography of some of the most common lithologies observed in natural aggregates. Sedimentary rocks such as Chert (Ch) was the most common, followed by igneous rocks such as Quartzite (Q), Diorite (D), Andesite (A) and Gabbro (Mg), and metamorphic rocks such as Quartz Shale (Eq).

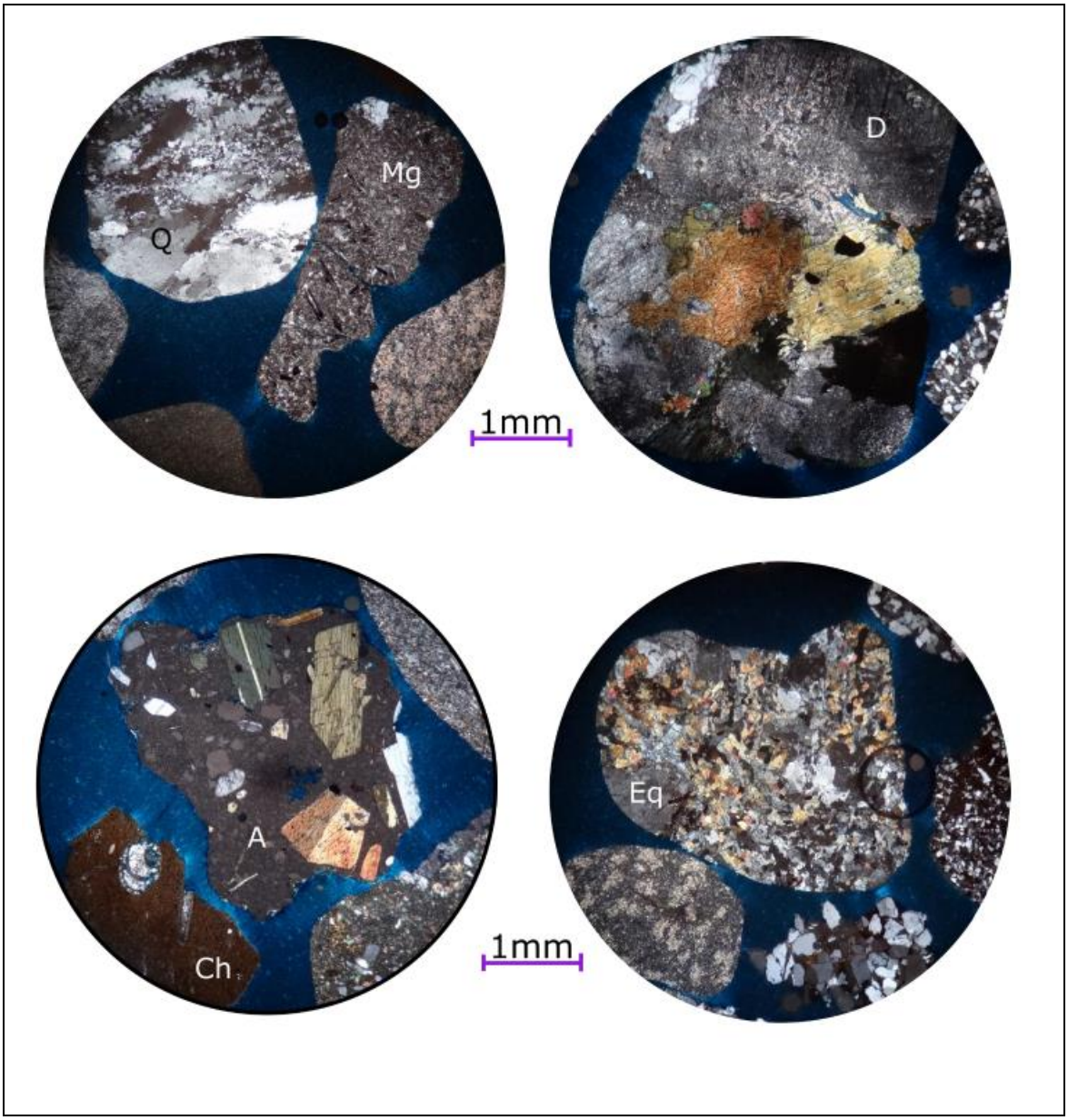

Figure 38 – (Eq) XPL Microphotography (4X Zoom) of frequent lithologies in fine natural aggregates. Q: Quartzite. Mg: Micro-gabbro. D: Diorite. A: Andesite. Ch: Chert. Eq: Micaceus Quartz Shale.

Particle shape is not homogeneous and for every sieve size, aggregates from each classification index were identified. Larger aggregates retained in the #8 and #16 sieves showed a round or sub-round roundness and a mostly spheric of sub-prismoid sphericity. Smaller aggregates retained in the #30, #50 and #100 sieves presented a mostly sub-

angular and sub-rounded shape. The shape heterogeneousness for natural aggregates can be observed in Figure 39.

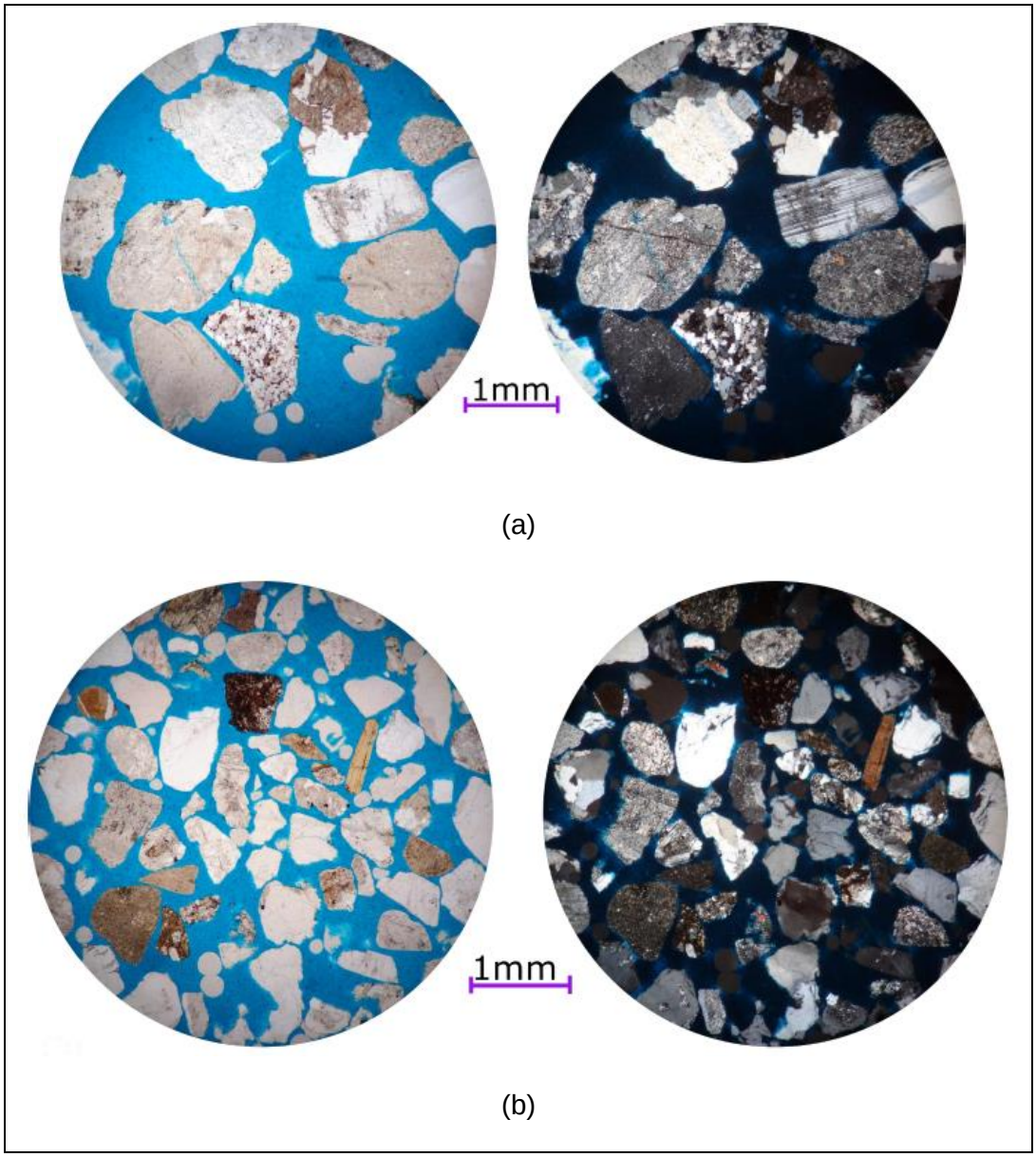

Figure 39 - PPL – XPL Microphotography (4X Zoom) of recycled aggregates retained on (a) #16 Sieve. (b) #30 Sieve.

5.2.5.4 Coarse Natural Aggregates Analysis

The used coarse natural aggregates were of sedimentary origin with Quartz Sandstone as the predominant lithology. Table 16 presents the content and origin of the predominant lithologies for each analyzed particle size, the predominant shape, porosity grade and weathering grade are also included. A complete list of all found lithologies is presented and discussed in further sections.

Sieve Size	Predominant Lithologies	Content %	Origin	Predominant Shape	Porosity Grade	Weathering Grade
#8 (2,38 mm)	- Quartz Sandstone - Silicate Mudstone - Chert	66,7 12,0 10,7	S S S	Sub-round & Sub-prismoid. (13,3%).	- Very Low (55,3%) - Low. (20,0%) - Medium (20,0%) - High (6,7%)	I (90,7%) II (9,3%) III (0%)

** R: Recycled Origin. S: Sedimentary Origin. I: Igneous Origin. M: Metamorphic Origin. Min: Minerals.*

Table 16 - Petrographic examination results for coarse natural aggregates.

Figure 40 shows a microphotography of the most common lithologies in the observed coarse natural aggregates. Regarding porosity, most aggregates presented a very low classification. However, some highly porous Quartz Sandstone particles with low grain cementing materials were identified as shown in Figure 41. The weathering grade of most assessed natural coarse aggregates corresponded to unaltered rock.

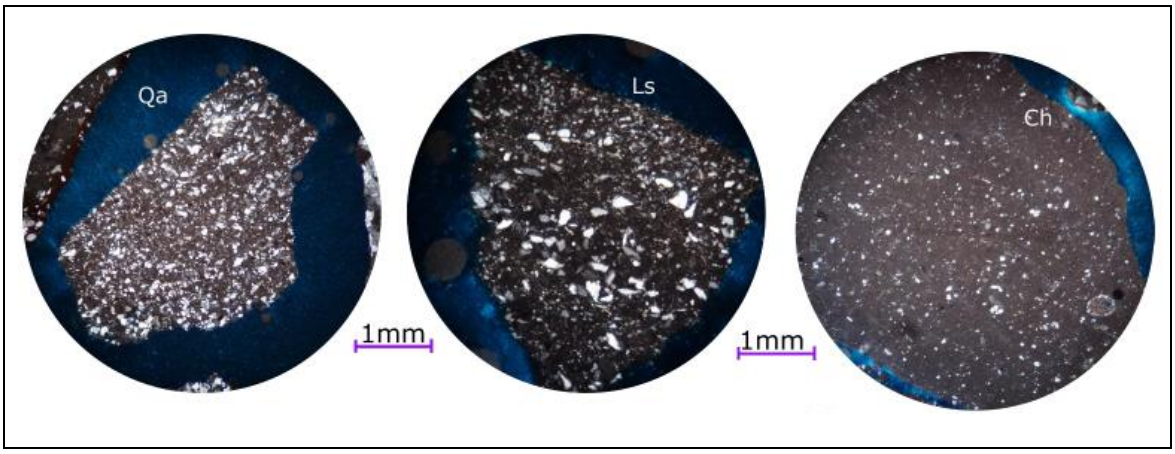

Figure 40 – PPL – XPL Microphotography (4X Zoom) of frequent lithologies on coarse natural aggregates. Qa: Quartz Sandstone. Ls: Silicate Siltstone. Ch: Chert.

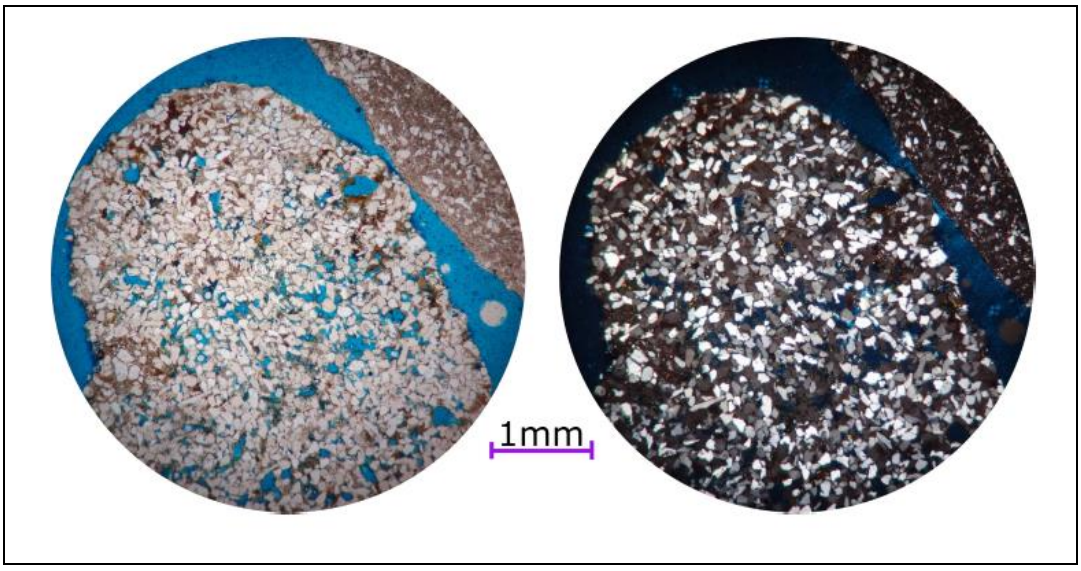

Figure 41 – PPL – XPL Microphotography (4X Zoom) of highly porous Quartz Sandstone in coarse natural aggregates.

5.2.5.5 Natural and Recycled Aggregate Comparison and Potential Reactivity

The full aggregate composition identified by microscopic examination for the assessed particle sizes of fine recycled aggregates (f-RCA), natural fine aggregates (f-NA) and coarse natural aggregates (c-NA) is presented in Table 17. The predominant lithologies with a content higher than 10% are highlighted in the table. Additionally, the names of the

potentially harmful components due to alkali-silica reactivity or organic content are also highlighted.

Type of Rock	Origin	#8 Sieve			#16 Sieve		#30 Sieve		#50 Sieve		#100 Sieve	
		RCA	c-NA	f-NA	RCA	f-NA	RCA	f-NA	RCA	f-NA	RCA	f-NA
Concrete	R	65,0			61,2		67,1		43,3			
Micaceus Quartz Shale	M	1,4		12,0	3,9	11,9				2,0	2,0	
Phyllite	M	1,4										0,7
Quartzite	M			8,7		6,0		6,7	5,3	4,7	2,7	2,0
Metadiorite	M			2,7				2,0				
Metasandstone	M			2,7		1,3		2,0				
Limestone	S	2,7										
Chert	S	20,5	10,7	20,7	11,2	17,3	10,7	4,0	9,3	5,3	2,7	2,7
Quartz Sandstone	S	2,6	66,7	8,7	5,9	11,3	1,3	3,3	3,3	2,0		2,0
Silicate Siltstone	S	6,6	8,0	9,3	8,6	1,3	2,7	1,3	1,3			
Mudstone	S		14,7		1,3	2,0	1,3	3,3	2,7	2,7		0,7
Litharenite	S						1,3					
Oxides	S								1,3			
Andesite	I			3,3	3,3	0,7	1,3	2				
Diorite	I			16,7	1,3	8		3,3		0,7		0,7
Granite	I			6,7		8		1,3		3,3		2,0
Microgabbro	I			5,3		4,7		1,3				1,3
Rhyolite	I			2		1,3						
Undulose Quartz	Min			0,7	1,3	2,7	1,3	13,3	1,3	16	6	13,3
Straigth Quartz	Min				1,3	5,3	4	22	10,7	19,3	48,7	16
Plagioclase	Min			0,7	0,7	11,3	4	16	4,7	15,3	17,3	20,7
Chalcedony	Min						0,7					
Feldspar	Min					5,3	4	12	12,7	15,3	10,7	15,3
Calcite	Min								4			
Hornblende	Min							4,7		8	4,7	14,7
Microcline	Min					1,3		1,3				
Biotite	Min									2	5,3	4,7
Muscovite	Min									3,3		2
Chlorite	Min											1,3
Total		***100***	***100***	***100***	***100***	***100***	***100***	***100***	***100***	***100***	***100***	***100***

** R: Recycled Origin. S: Sedimentary Origin. I: Igneous Origin. M: Metamorphic Origin. Min: Minerals.*

Table 17 – Petrographic examination results of recycled concrete aggregates (RCA), coarse natural aggregates (c-NA) and fine natural aggregates (f-NA) for different particle sizes.

From Table 17 it is possible to identify that the main difference between natural and recycled aggregates is the presence of a “concrete” aggregate type which contains aggregates with old-attached mortar and cement or hydration products in smaller particle sizes. For the remaining aggregates without attached mortar, a similar content of sedimentary rocks such as Chert was identified. For the aggregates retained on the #100 sieve, the “concrete” aggregate type was no longer identified and both fine and recycled aggregates presented a similar composition with a high presence of minerals such as feldspar, and plagioclase. A high content of straight and undulate quartz was observed for both types of aggregates due to the predominant sedimentary origin of the aggregates. The origin of the aggregates for different particle sizes is summarized in Table 18.

Particle Origin	#8 Sieve			#16 Sieve		#30 Sieve		#50 Sieve		#100 Sieve	
	RCA	c-NA	f-NA	RCA	f-NA	RCA	c-NA	f-NA	RCA	f-NA	RCA
Recycled	65,0	0,0	0,0	61,2	0,0	67,1	0,0	43,3	0,0	0,0	0,0
Metamorphic	2,7	0,0	26,1	3,9	19,2	0,0	10,7	5,3	6,7	4,7	2,7
Sedimentary	32,4	100,0	38,7	27,0	31,9	17,3	11,9	17,9	10,0	2,7	5,4
Igneous	0,0	0,0	34,0	4,6	22,7	1,3	7,9	0,0	4,0	0,0	4,0
Minerals	0,0	0,0	1,4	3,3	25,9	14,0	69,3	33,4	79,2	92,7	88,0

Table 18 – Particle origin of recycled concrete aggregates (RCA), coarse natural aggregates (c-NA) and fine natural aggregates (f-NA) for different particle sizes.

The apparent origin of the natural aggregates was more heterogeneous, presenting a significant content of metamorphic and igneous aggregates. However, the petrographic examination revealed that the “recycled” aggregates for the larger sizes also presented combinations of sedimentary, igneous and metamorphic aggregates bonded by hydration products from the parent concrete. Both types of aggregates presented low porosity and non-homogeneous shapes and carbonation was observed on the recycled aggregates. Since a similar angularity was observed for both types of aggregates, the negative effects on concrete durability of recycled aggregates with higher angularity is considered negligible in this research program.

For fine recycled aggregates, Table 19 summarizes the content of possible alkali-silica reactive minerals. This content was estimated based on the number of particles with each mineral regardless of its origin or classification. The main identified reactive minerals are undulous quartz and existing microcrystalline quartz in chert and silicate siltstone particles.

Reactive Components	**Mineral Content (%) for different Recycled Aggregate Sizes**					
	#8	**#16**	**#30**	**#50**	**#100**	**Average**
Undulous Quartz	48,7	37,3	38,7	16,0	7,4	***29,6***
Microcrystalline Quartz	27,3	21,3	16,0	13,3	2,7	***16,1***
Total	76,0	58,7	54,7	29,3	10,1	***45,7***

Table 19 – Content of potentially reactive components for fine recycled aggregates.

The results from the same analysis conducted for fine natural aggregates are summarized in Table 20. The main observed reactive minerals are also the undulous quartz in metamorphic aggregates and existing microcrystalline quartz in sedimentary particles such as chert, mudstone and silicate siltstone.

Reactive Components	**Mineral Content (%) for different Natural Aggregate Sizes**					
	#8	**#16**	**#30**	**#50**	**#100**	**Average**
Undulous Quartz	26,0	20,7	24,0	18,0	16,1	***21,0***
Microcrystalline Quartz	32,7	24,7	8,7	8,0	3,4	***15,5***
Volcanic Glass	1,3	0,7	0,0	0,0	0,0	***0,4***
Total	60,0	46,0	32,7	26,0	19,5	***36,8***

Table 20 – Content of potentially reactive components for fine natural aggregates.

For fine natural aggregates, potentially harmful organic components were also identified. Micas such as sericite and biotite may have high enough absorption levels to modify the hydration process of concrete mixes. The content of these organic components are summarized in Table 21.

Organic Components	**Mineral Content (%) for different Natural Aggregate Sizes**					
	#8	**#16**	**#30**	**#50**	**#100**	**Average**
Micas (Sericite and Biotite)	21,3	37,0	20,7	5,3	26,8	***22,2***
Organic matter	4,0	1,9	0,0	0,0	0,7	***1,3***
Total	25,3	38,9	20,7	5,3	27,5	***23,5***

Table 21 - Content of potentially harmful organic components for fine natural aggregates.

Regarding alkali-silica reaction, recycled aggregates presented approximately 10% higher content of potentially reactive minerals. For this research program, the concrete mixes made with both types of aggregates could be similarly reactive depending on the used cementing material and further assessment was formulated, however, no significant difference was observed on the mineral composition.

5.2.6 Alkali-Silica Reaction in Aggregates

Alkali-Aggregate reactions are detrimental chemical reactions in concrete that may produce a premature loss in durability. As the micropores in the matrix of hardened concrete are filled with a highly basic fluid (pH > 12.5) that consist mainly of dissolved alkali hydroxides (K^+-OH^-, Na^+-OH^-), in very aggressive environments with high pH, some mineral phases within the aggregates can react deleteriously producing internal expansion and loss of serviceability [185]. Alkali-Silica reaction occurs when the silica in the mineral phase of the aggregates reacts in high pH environments.

The use of fly ash can have a beneficial effect in reducing Alkali-Aggregate reactions, since it reduces the concentration of dissolved alkali hydroxides in the pore fluid, reduces concrete permeability and enhances the consumption of calcium hydroxide ($Ca(OH)_2$) through pozzolanic reactions [185].

Different studies have identified that alkali-aggregate reaction can occur in recycled aggregates when the attached mortar or the original natural aggregates were reactive; when RCA are composed of high alkali reactive aggregates, the expansion increases with the replacement ratio of natural aggregates, however, a 20% replacement level does not increase the reactivity significantly [186].

Based on the results from the petrographic examination and in order to assess the presence of deleterious alkali-silica reaction in aggregates, **ASTM C1260** – "*Standard Test Method for Potential Alkali Reactivity of Aggregates (Mortar-Bar Method)"* [187], was performed in multiple specimens. In this testing method, the longitudinal expansion of 254 mm long mortar bars cured in an aggressive environment is measured. The specimens are submerged in a 1N NaOH solution at 80°C during at least 14 days and regular length measurements are taken to calculate the bar expansion using a digital length comparator. Three testing specimens were cast for each mortar mix using Ordinary Portland Cement (OPC) and the grading requirements specified in this ASTM standard. OPC must be used since the cement material described in Section 5.1 and many commercially available cements in Colombia do not meet the requirements of ASTM C1260.

ASTM C1567 – "*Standard Test Method for Determining the Potential Alkali-Silica Reactivity of Combinations of Cementitious Materials and Aggregate (Accelerated Mortar-Bar Method)"* [188], was also performed to assess the effects of using fly ash as a supplementary cementitious material in mortar bars with combinations of natural and recycled fine aggregates. This test is performed using the same specimens than ASTM C1260, which are also submerged in a 1N NaOH solution at 80°C during at least 40 days for expansion measurements.

Both ASTM standards define the aggregate grading requirements and W/C ratio that must be employed in the mortar mixes. The digital comparator used for length measurements and the testing specimens are shown in Figure 42:

(a) (b)

Figure 42 – (a) Mortar bars used in ASTM C1260 and ASTM C1567. (b) Digital comparator for length measurement.

Five mortar mixes were assessed with different fine aggregate and binder composition, as shown in Table 22. For each of these mixes, three mortar bars were cast and submerged in a 1N NaOH solution at 80°C for 28 days. Mixes 1 and 2, incorporating only natural or recycled aggregates were defined to identify the Alkali-Silica reactivity of each type of fine aggregate. Since the experimental concrete mix program projected the use of 20% and 60% fine RCA replacement with 20% fly ash, mortar mixes 3, 4 and 5 were defined to assess the beneficial effects of incorporating fly ash and compare the effects of incremental fine RCA replacement ratios.

ID	Mix Name	Fine Aggregate Composition by mass	Binder Composition by mass	Testing Standard
1	100% NA	100% Natural	100% OPC	ASTM C1260
2	100% RA	100% Recycled	100% OPC	ASTM C1260
3	20%RA + 20%FA	20% Recycled + 80% Natural	80% OPC + 20% Fly Ash	ASTM C1567
4	60%RA + 20%FA	60% Recycled + 40% Natural	80% OPC + 20% Fly Ash	ASTM C1567
5	80%RA + 20%FA	80% Recycled + 20% Natural	80% OPC + 20% Fly Ash	ASTM C1567

Table 22 – Mortar mix composition used for Alkali-Aggregate Reaction testing.

Measurements were made at different ages for 28 days, the expansion results for each mortar mix calculated as the average of each three specimens are presented in Table 23.

	Expansion of mortar bars				
Day	**100% NA**	**100% RA**	**20% RA + 20% FA**	**60% RA + 20% FA**	**80% RA + 20% FA**
0	0,00%	0,00%	0,00%	0,00%	0,00%
3	0,02%	0,00%	0,01%	0,01%	0,01%
7	0,06%	0,15%	0,01%	0,02%	0,02%
10	0,09%	0,21%	0,02%	0,02%	0,02%
14	0,10%	0,24%	0,02%	0,03%	0,03%
19	0,12%	0,30%	0,03%	0,05%	0,04%
24	0,16%	0,33%	0,04%	0,06%	0,05%
28	0,18%	0,36%	0,05%	0,08%	0,07%

Table 23 – Expansion of Mortar Bars due to Alkali-Aggregate reaction.

According to ASTM C1260 and ASTM C1567, mortar bars made with potentially expansive aggregates will present an expansion larger than 0.10% after 16 days. The obtained bar expansion for each mix is plotted against specimen age in Figure 43. Results show that the used recycled aggregates are potentially expansive, presenting an expansion of approximately 0,25% at 16 days, while natural fine aggregates presented an expansion of approximately 0,11% at 16 days, staying slightly above the defined limit. Other studies have also reported an increase of expansion when incorporating higher levels of RCA, however, these studies were performed using microscopic analysis of polished concrete sections [189]. Nevertheless, different researchers have reported that RCA derived from parent concrete with non-reactive aggregates does not present detrimental expansion [190], this would suggest that the employed fine RCA was derived from slightly damaged concrete specimens.

Results from the mortar bars including fly ash, revealed an innocuous expansive behavior even when employing 80% replacement of fine RCA. This would indicate that fly ash is a very effective pozzolan for reducing the negative reactions of the expansive recycled aggregates. This has been observed by other researchers who claimed that fly ash reduces the alkalinity of recycled aggregates and neutralizes possible chemical reactions that result in bar expansion by reducing the pH of the fluids saturating the mortar bars [186], this study suggests that higher amount of supplementary cementitious materials such as fly ash, silica fume, metakaolin and ground granulated blast furnace slag are required for RCA since their constituent silica reacts with the alkalis in the pore solution.

As the use of recycled aggregates with fly ash will reduce the expansive potential of fine RCA, fine RCA should be incorporated in concrete mixes to prevent Alkali-Silica reactions. An enhancement in other durability properties of concrete is also expected when incorporating fly ash based on these results.

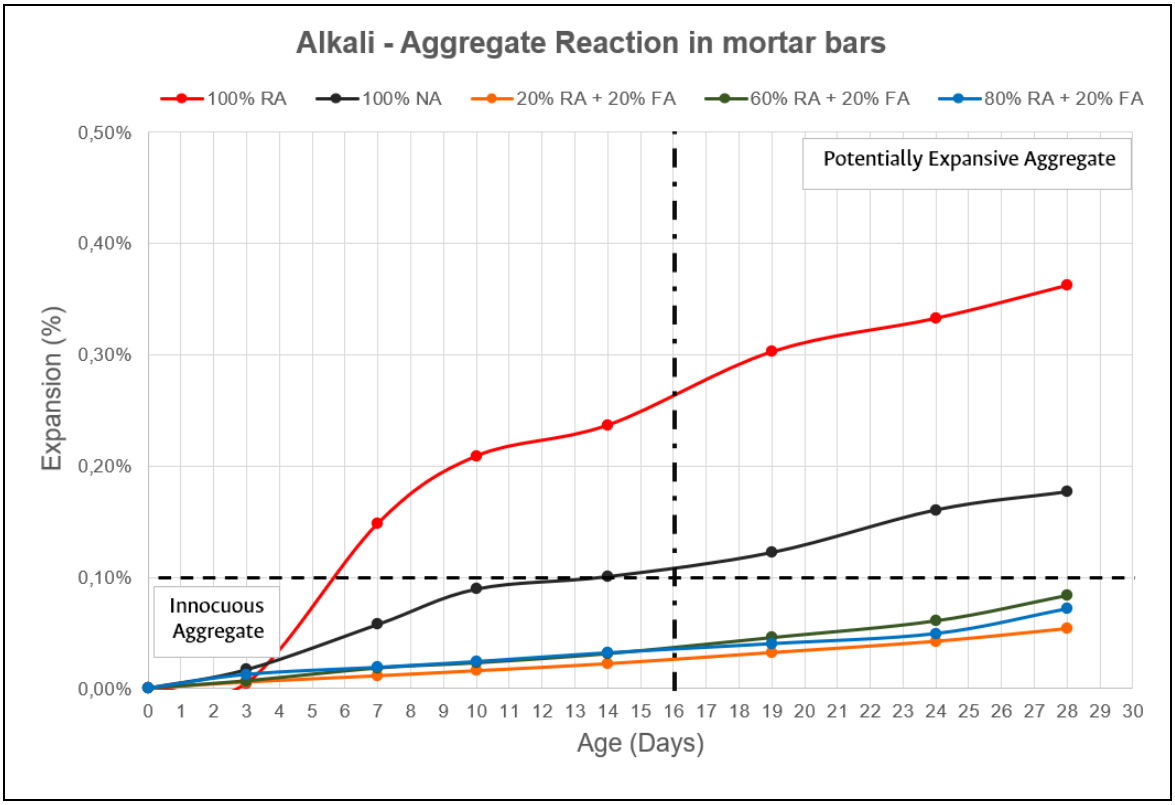

Figure 43 - Expansion of Mortar Bars for different mortar mixes.

5.3 Fly Ash

Fly ash (FA) was supplied by CEMEX® Colombia from the TERMOPAIPA IV thermoelectric power plant in Boyacá, Colombia. The provider conducted characterization tests in the material and defined a specific gravity of **2,05 g/cm^3** , this value was used in the mix design process to stablish the volume of cement and binder particles. The source of the raw material and the fly ash used in the experimental program for concrete mixing are shown in Figure 44.

(a)

Retrieved from https://bit.ly/3eOLDwi

(b)

Figure 44 – (a). TERMOPAIPA IV thermoelectric power plant. (b). Fly ash particles used in experimental program.

As fly ash is a byproduct of burning coal for power generation, possible residues of organic materials and unburnt fuel can be found. For quality control purposes, loss on ignition (LOI) testing was performed in fly ash. This test is conducted by heating the material at 1000°C for one hour and stablishing the mass loss, according to the American standard **ASTM D7348** - "*Standard Test Methods for Loss on Ignition (LOI) Of Solid Combustion Residues",* [191]. Loss on ignition results indicate **10,9%** mass loss at 1000°C and a water content of **0,41%** at 105°C. Fly ash chemical composition was obtained by the material producer using X-Ray Fluorescence (XRF) as presented in Table 24.

Fly Ash Component	**Chemical Formula**	**Units**	**Content**
Silicon dioxide	SiO_2	%	55,14
Aluminum oxide	Al_2O_3	%	25,33
Iron oxide	Fe_2O_3	%	7,76
Calcium oxide	CaO	%	1,43
Magnesium oxide	MgO	%	0,78
Sulfur trioxide	SO_3	%	0,43
Sodium oxide	Na_2O	%	0,18
Potassium oxide	K_2O	%	1,22

Table 24 – XRF results of fly ash chemical composition provided by producer.

The American standard **ASTM C618 -** "*Standard specification for Coal Fly Ash and Raw or Calcinated Natural Pozzolan for Use in Concrete"* [192], specifies different physical and chemical requirements for fly ash acceptance in concrete. For **class F** fly ash, produced from burning anthracite or bituminous coal, a maximum moisture content of 3,0% is required. The maximum loss on ignition value for this class of fly ash is 6,0%, however, this standard specifies that class F material containing up to 12% loss on ignition may be approved if laboratory testing indicates acceptable performance in concrete. The fly ash used in this experimental program meets the required physical properties for class F fly ash defined in ASTM C618.

5.4 Superplasticizer

A high-range water reducer admixture made from polycarboxylates known commercially as **MasterGlenium® 7990** was used. This superplasticizer is produced and distributed by BASF – Master Builders Solutions and according to the producer's specifications, it is highly effective to produce concrete mixtures with different levels of workability and slump and its properties meet the requirements of American standard **ASTM C494 -** "*Standard Specification for Chemical Admixtures for Concrete*" [193], for type A water-reducing admixtures and type F high-range water-reducing admixtures.

The specified dosage of this admixture is 150 ml to 1200 ml per 100 kilograms of binder material (0,15% to 1,2% of binder weight). The admixture is combined with the initial mixing water, and according to the producer, it is not a corrosive material as its chemical composition does not include chlorides. The superplasticizer used in the experimental program is shown in Figure 45.

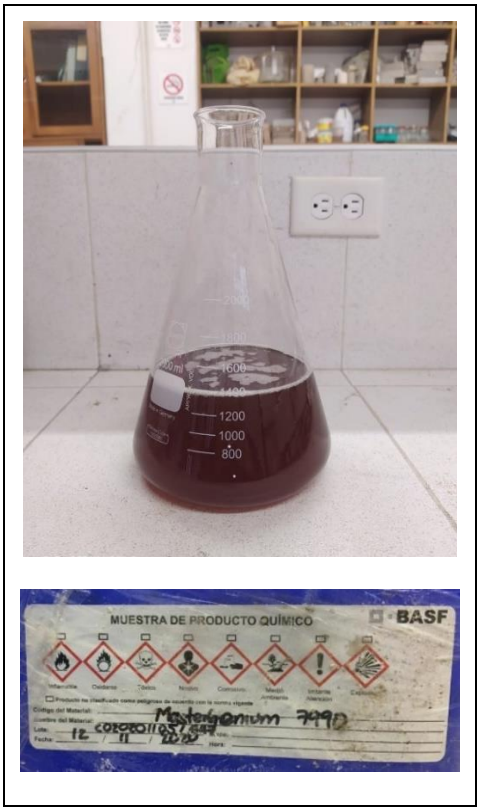

Figure 45 – High-range water-reducing admixture used in concrete mixes.

6. Mix Design and Specimen Casting

Mix proportions were obtained following the standard procedure proposed by **ACI – 211.1**: *"Standard Practice for Selecting Proportions for Normal, Heavyweight, and Mass Concrete"* [194]. In this procedure, an optimal amount of water is selected from the aggregate maximum size to obtain an ideal slump value. Using the selected water-to-binder (W/B) ratio, binder content is calculated from the amount of water and finally, using volumetric relations, the coarse and fine aggregate volume and weight can be stablished. Water content is finally adjusted from the aggregate's water content and absorption rates as non-saturated aggregates will modify the effective W/B ratio. A more detailed process of the mix-design procedure followed in the experimental program is presented in Figure 46.

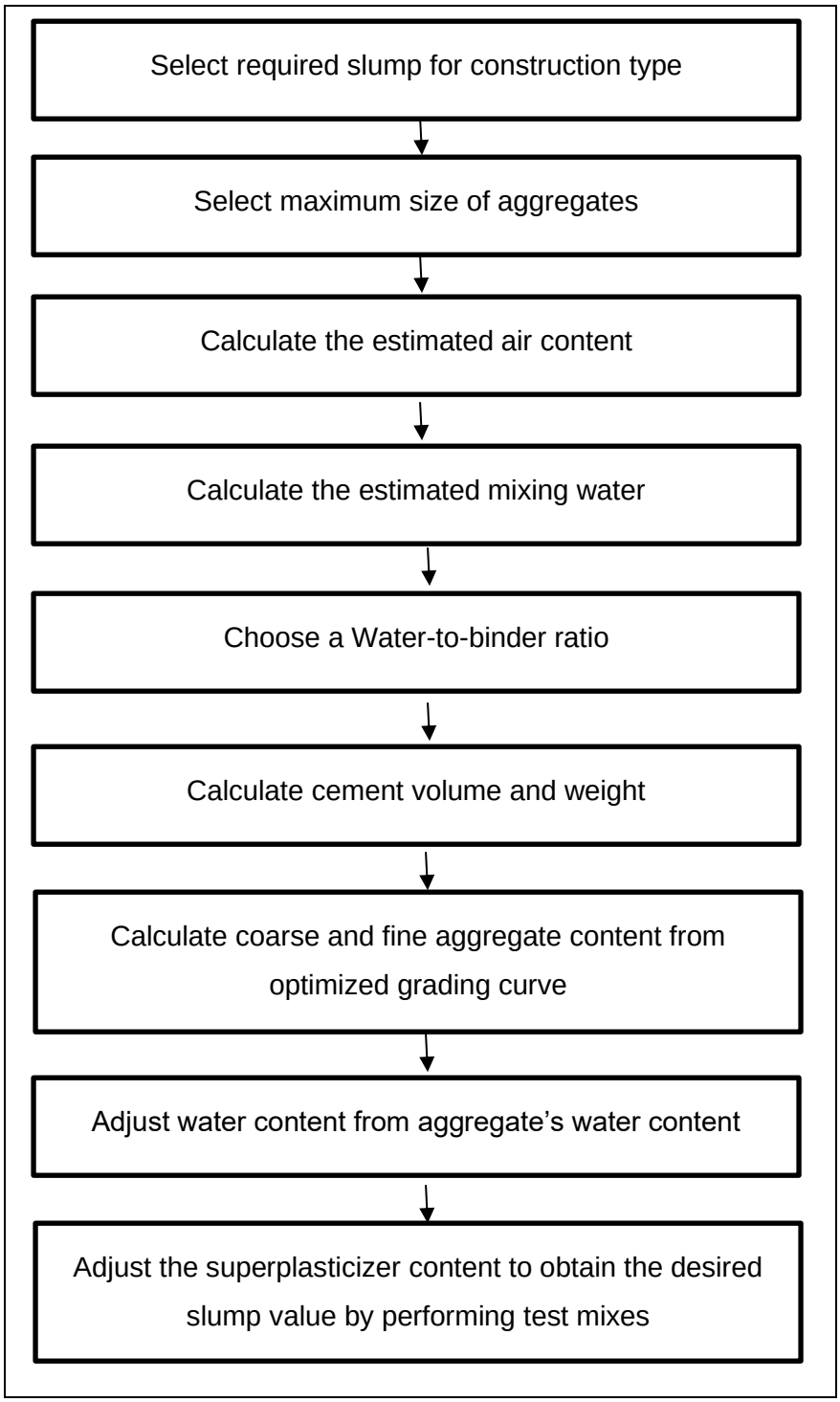

Figure 46 – Experimental Mix-design procedure based on ACI 211.1

6.1 Slump Definition

The selected slump for concrete mixtures was **5 ± 1 inches**. This slump value is accepted for different applications in international construction practice, as concrete mixtures will have the required workability to be used in highly reinforced structural elements. Since W/B ratio values of 0,45 and 0,50 were defined in the experimental program and a superplasticizer was used to achieve the desired slump value, the procedure was slightly modified by fixing binder content and obtaining the required mixing water.

A fixed content of binder (cement and fly ash) of 500 kg/m3 and 450 kg/m3 for W/B ratios of 0,45 and 0,50 respectively was defined. For concrete mixtures incorporating fly ash and cement, 20% of the total binder mass was replaced, in this case, the specific gravity of the binder was determined by arithmetic weighting, obtaining a value of **2,65 g/cm3**.

Aggregate volume was defined by volumetric relations using a content of 51% fine aggregates and 49% coarse aggregates as defined in the particle size optimization process described in section 5.2.4. The volume of aggregates was calculated using the values of specific gravity obtained in the characterization process (2,32 g/cm3 for coarse aggregates, 2,45 g/cm3 for fine natural aggregates and 2,12 g/cm3 for fine recycled aggregates). Fine recycled aggregates were incorporated by replacing the fine aggregate mass of control mixtures by the specified recycled aggregate content.

Finally, the superplasticizer (SP) dosage was defined in the range specified by the admixture producer (0,15% to 1,2% of binder weight) and different control mixes were performed with different dosage values until the desired slump was obtained. The material mixing proportions for the 14 concrete mixtures defined in the experimental program are presented in Table 25.

Mix	Mix	W/B*	Cement	Fly Ash	Water	Coarse Aggregate	Natural Fine Aggregates	Recycled Fine Aggregates	Super-Plasticizer	Super-Plasticizer
ID	Name		kg/m3	kg/m3	kg/m3	kg/m3	kg/m3	kg/m3	% Binder Mass	ml/m3
1	28-CONTROL	0,45	500	0	260,0	675,0	697,9	0,0	0,32	1600
2	28-RA20	0,45	500	0	269,6	660,7	551,0	142,8	0,35	1750
3	28-RA60	0,45	500	0	275,5	641,2	267,4	419,5	0,35	1750
4	28-RA100	0,45	500	0	281,1	621,2	0,0	677,3	0,35	1750
5	28-RA20-FA20	0,45	400	100	269,0	649,4	541,0	139,9	0,42	2100
6	28-RA60-FA20	0,45	400	100	277,9	630,8	262,7	407,8	0,42	2100
7	28-RA100-FA20	0,45	400	100	286,2	611,1	0,0	658,4	0,42	2100
8	21-CONTROL	0,5	450	0	266,2	691,1	719,6	0,0	0,18	810
9	21-RA20	0,5	450	0	271,3	682,2	568,3	145,9	0,18	810
10	21-RA60	0,5	450	0	282,9	662,7	276,0	425,1	0,2	900
11	21-RA100	0,5	450	0	283,7	639,7	0,0	698,6	0,2	900
12	21-RA20-FA20	0,5	360	90	273,0	669,5	558,7	144,3	0,25	1125
13	21-RA60-FA20	0,5	360	90	282,6	650,3	271,3	420,5	0,25	1125
14	21-RA100-FA20	0,5	360	90	284,6	631,9	0,0	683,9	0,25	1125

Table 25 – Concrete mixtures proportions

6.2 Mixing Process

Each concrete mix was performed following the Two-Stage Mixing Approach (TSMA), this method was proposed by *Tam et al. (2005)*, to improve recycled aggregate concrete quality and performance [141]. The main difference with conventional concrete mixing processes such as the described in American standard **ASTM C192-18** – *"Standard Practice for Making and Curing Concrete Test Specimens in the Laboratory"* [195], is that TSMA divides the process in two parts and distributes the required water in two stages, while in a regular mixing process all the components are mixed in one stage.

During the TSMA's first stage, the aggregates are uniformly mixed and saturated with approximately 50% of the water content for 1 minute. The binder material (cement and fly ash combination) is then added to the mix for 30 seconds. In this stage, a thin cement slurry is formed around the recycled aggregate that acts as filler material and reduces the volume of voids and cracks in the old attached mortar, accomplishing a beneficial pre-coating effect.

During the second stage, the other half of the mixing water is added to complete the concrete production process for 120 seconds.

Two minor modifications to TSMA were made in this research program: In the first stage, the aggregates were not homogenized in a dry state, instead approximately 20% of mixing water was added to prevent particle loss as fine-recycled aggregates had an important amount of material under 75 µm. Additionally, the water-reducing admixture was mixed with approximately 100 ml of the mixing water and added after the final mixing period. Concrete was mixed with the superplasticizer for additional 120 seconds to achieve the desired fresh state workability properties. This chemical admixture was included in this stage following the procedure suggested by the producer to increase its effectivity.

Figure 47 illustrates the difference between conventional concrete mixing, Two-stage Mixing Approach (TSMA) and the modified TSMA used in this experimental program to include a superplasticizer.

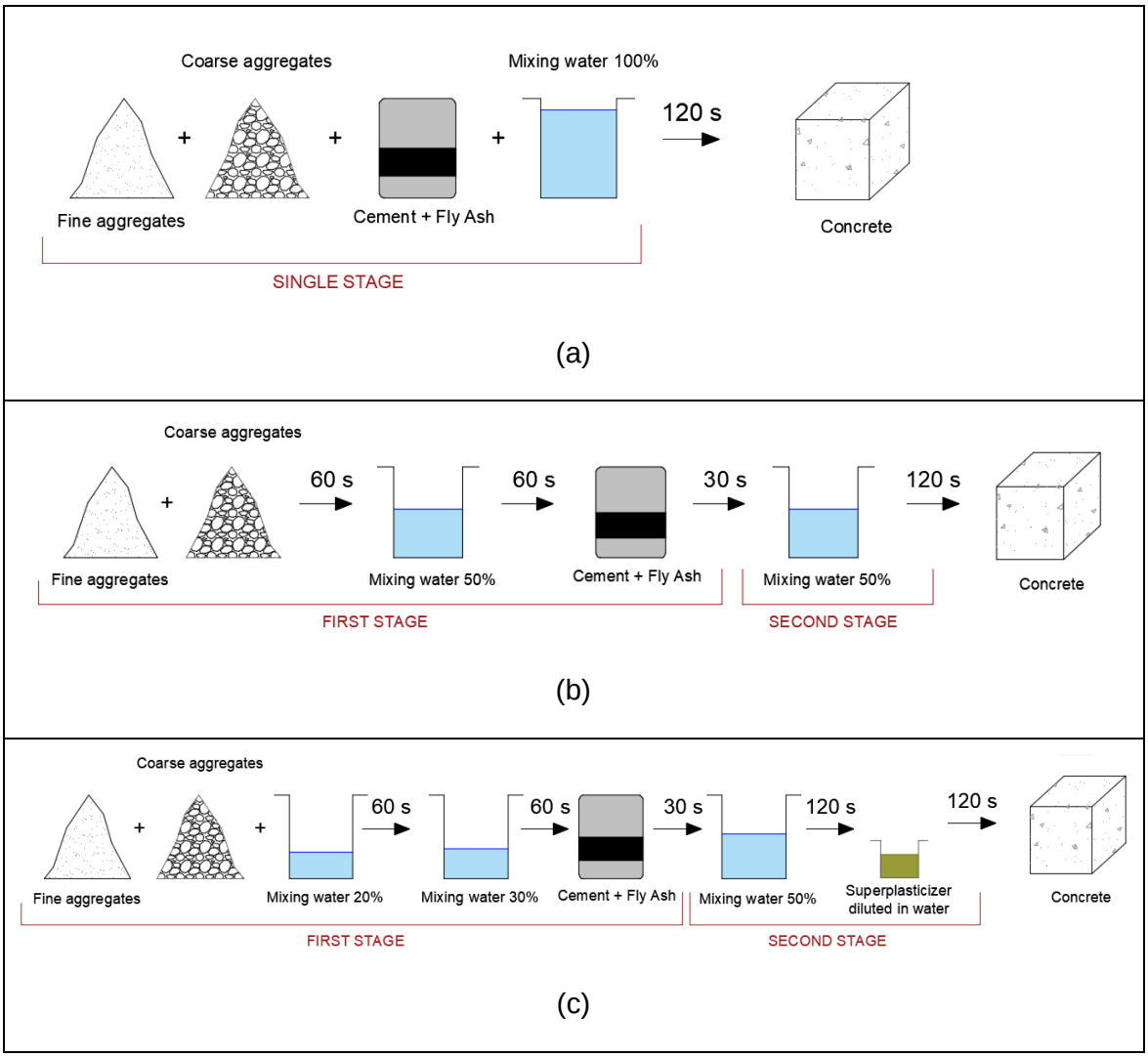

Figure 47 – Mixing procedure of (a). Conventional concrete. (b). Two-stage Mixing approach (TSMA). (c). Modified TSMA to include superplasticizer.

The mixing procedure was conducted in a 130-liter concrete mixer. Before starting the mixing process, the mixer walls were slightly damped with a towel to avoid the formation of lumps and loss of material. After the mixing time was finished, concrete slump was tested and immediately, the specimen mold casting was started. The mixer used for concrete production is shown in Figure 48.

Figure 48 – Concrete mixer used in experimental program.

6.3 Fresh Properties of Concrete

Slump value was measured using Abrams Cone as a control procedure to obtain concrete mixtures with similar workability and as an indicator of proper concrete mixing. The methodology for this procedure is described in the American standard **ASTM C143** - *"Standard Test Method for Slump of Hydraulic-Cement Concrete"* [196].

The test is performed with a metal mold shaped as a conical frustum known as Abram's cone. This cone has a superior internal diameter of 100 millimeters and an inferior internal diameter of 200 millimeters with a height of 305 millimeters. After the mixing procedure has been completed, the cone is damped using a towel and placed on a non-absorbent surface. While standing on the side metal flaps, the cone is filled in three layers and each slayer is tamped 25 times with a metal rod measuring 16 mm in diameter. After filling the cone, the superior surface is leveled, and excess concrete is removed. Finally, the cone is slowly lifted vertically upwards without any rotational movement that disturbs the conic shape of freshly poured concrete. This lifting movement is performed in 5 ± 2 seconds.

Immediately after lifting, the slump value is measured by placing the Abrams cone next to the concrete sample and determining the distance between the top of the metal mold and

the top of the collapsed concrete cone. This value must be recorded within 2,5 minutes of starting the procedure. The dimensions of Abrams cone and the slump measurement procedure for this experimental program are presented in Figure 49.

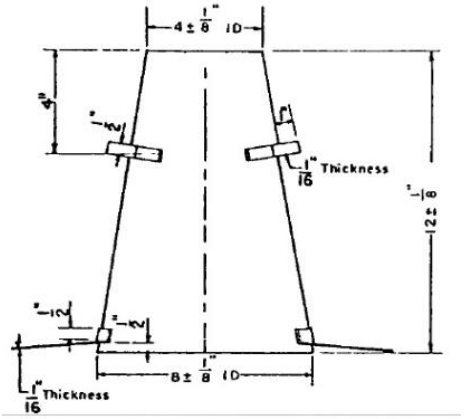

(a)

(b)

Figure 49 – (a). Abram's cone dimensions, retrieved from ASTM C143. (b). Slump measurement for experimental concrete mixtures.

As specified in the mix design process, the target slump value for all the concrete mixtures was 5 ± 1 inch. This value was achieved by using the high-range water reducing admixture with the dosage range described in section 5.4. As expected, concrete mixtures with 0,45 W/B ratio required a slightly higher dosage of superplasticizer than 0,50 W/B mixtures to achieve the target slump value. Mixtures with fly ash and cement also required a higher superplasticizer content as the water demand due to finer particles increases. The slump results for each concrete mix are presented in Table 26.

Mix	Mix	W/B*	Super-Plasticizer	Slump	Slump
ID	Name		%	in	mm
1	28-CONTROL	0,45	0,32	5,15	130,8
2	28-RA20	0,45	0,35	5,75	146,5
3	28-RA60	0,45	0,35	5,50	139,7
4	28-RA100	0,45	0,35	4,10	104,1
5	28-RA20-FA20	0,45	0,42	5,90	149,9
6	28-RA60-FA20	0,45	0,42	5,60	142,2
7	28-RA100-FA20	0,45	0,42	4,95	125,7
8	21-CONTROL	0,5	0,18	5,60	142,2
9	21-RA20	0,5	0,18	5,75	146,1
10	21-RA60	0,5	0,2	5,05	128,3
11	21-RA100	0,5	0,2	4,60	116,8
12	21-RA20-FA20	0,5	0,25	5,75	146,1
13	21-RA60-FA20	0,5	0,25	5,50	139,7
14	21-RA100-FA20	0,5	0,25	4,50	114,3

Table 26 – Slump values obtained for each concrete mixture.

6.4 Casting process and testing specimens

After completing the mixing process and evaluating the slump value for each concrete mix, test specimens were made according to the procedures specified in the American standard **ASTM C192-18** – *"Standard Practice for Making and Curing Concrete Test Specimens in the Laboratory"* [195]. Concrete was cast using different kinds of molds and consolidated by rodding.

Table 27 shows the total number of cylindrical samples that were cast according to the experimental program. In this section, a brief description of the making process of test specimens is described.

Standard	Measured Property	Specimens per Mix		
		Cylindrical Φ4	Cylindrical Φ3	Prisms
ASTM C39	Compressive Strength	8	0	0
ASTM C469	Elasticity Modulus**	(4)	0	0
ASTM C1202	Rapid Chloride Penetration	6	0	0
ASTM C642	Density, percent absorption, percent voids*	(6)	0	0
NT BUILD 492	Non-steaty-state Chloride Migration Coefficient*	(6)	0	0
ASTM G59	Corrosion Potential	0	3	0
SIA 262	KT Air Permeability	0	0	2
Total Specimens per Mix		14	3	2
Total Specimens for 14 Mixes		**196**	**42**	**28**

* ASTM C642 and NT 492 were obtained from the same cylindrical specimens.

** Elasticity modulus tests were performed on half of the compressive strength test samples.

Table 27 – Test specimens molded for each test

6.4.1 Cylindrical Specimens

To perform these mechanical and durability tests, different concrete cylindrical molded samples were cast in 4-inches diameter and 8-inches length plastic molds, as presented in Figure 50.

(a)

(b)

Figure 50 – (a) Plastic molds for concrete (Φ 4” x 8”). (b) Molded specimens after concrete mixing.

Following the procedure described in ASTM C192-18, concrete was poured into the cylindrical molds in 2 layers, each layer was rodded 25 times using a 10-mm diameter rod. A rubber mallet was used to consolidate the fresh concrete after rodding, by tapping lightly 15 times for each layer. After 24 hours, the molds were removed, and the resulting specimens were submerged in water for moist curing conditions. The resulting demolded specimen is presented in Figure 51.

Figure 51 – Demolded cylindrical specimen used in concrete testing (4 x 8 inches – 100 x 200 mm)

6.4.2 Cylindrical Specimens with Embedded Steel Bars

Corrosion potential and concrete resistivity were tested in 3-inch diameter cylindrical specimens with 6-mm diameter steel bars partially embedded. These specimens were cast in modified metallic molds with wooden supports to hold 100-millimeter-long steel bars.

The wooden supports have a 7 mm hole to hold the steel bars. These wooden supports are placed inside the metallic molds and concrete is poured inside once the steel bar has been placed. After concrete has hardened in a 24-hour period the specimens are demolded. Figure 52 presents the casting process and the resulting concrete specimens.

(a)

(b)

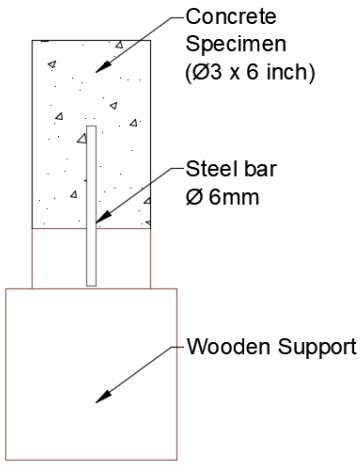

(c)

(d)

Figure 52 – (a) Metallic mold (Φ 3” x 6”) and wooden support with steel bar. (b) Assembled mold for concrete casting. (c) Specimen casting set-up (c) Resulting specimen after demolding.

Epoxy paint was applied in each steel bar to avoid corrosion in the discovered portion of the bar. Embedded in the concrete mix, a 4,5-centimeter zone was not painted to control the superficial area that was prone to corrode. The dimensions of the wooden supports and

testing specimens with the painted zones of the steel bars are presented in Figure 54 and Figure 53.

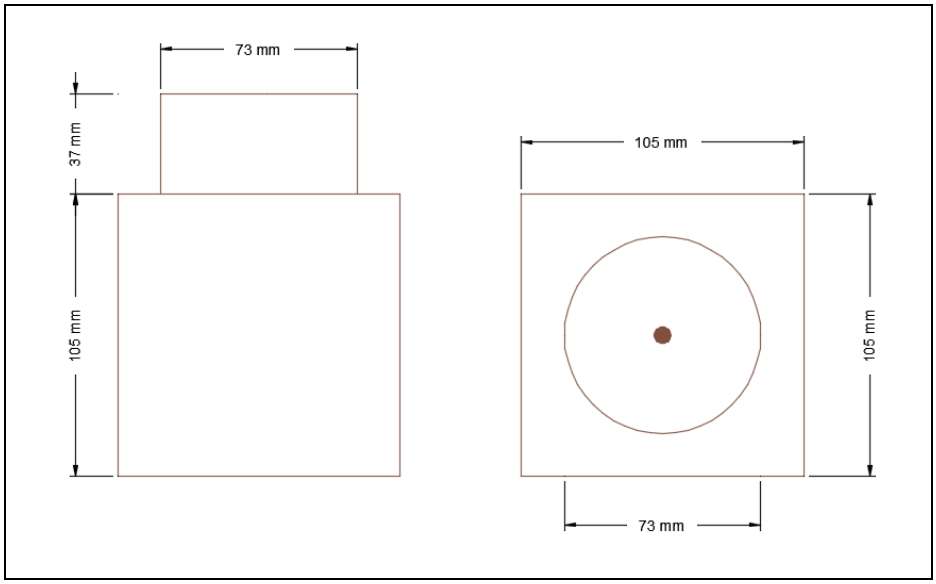

Figure 53 – Wooden support dimensions for concrete specimens with embedded steel bars.

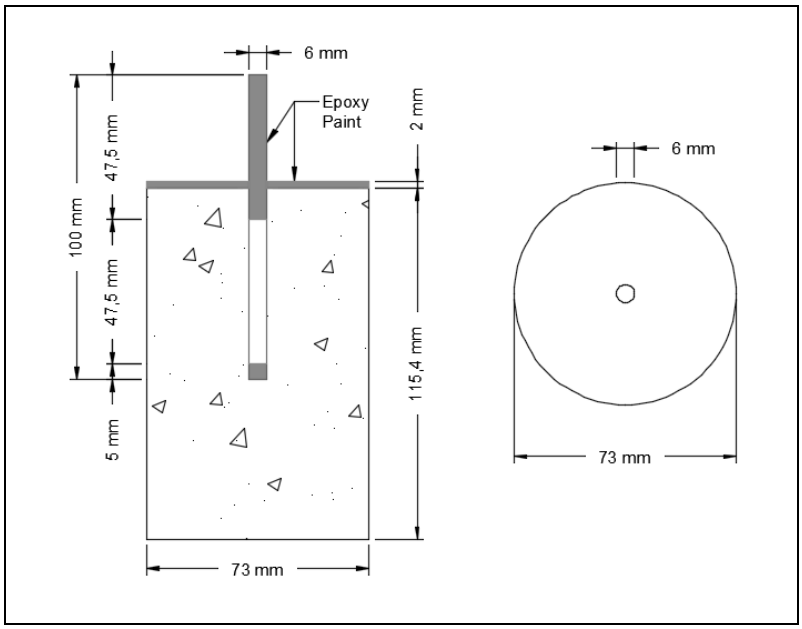

Figure 54 – Specimen dimensions and epoxy-painted zones.

Following the same procedure than 4 inch-diameter molds defined in ASTM C192-18, concrete was also poured in 2 layers and rodded 25 times with a 10-millimeter rod. A rubber mallet was also used to tap the molds 15 times after each layer was rodded. After 24 hours, the molds were removed and the moist curing process by immersion was started.

6.4.3 Rectangular Specimens

Air Permeability tests were performed in cubic concrete specimens. Fresh concrete was cast in prismatic wooden molds with dimensions of 15x15x55 centimeters, as shown in Figure 55. After the specimens were demolded, each concrete prism was submerged in water for the specified curing period. Using a diamond saw, the specimens are cut into 15-centimeter-long cubic specimens for testing.

(a)

(b)

(c)

Figure 55 – (a) Prism mold for concrete casting. (b) Molded specimens after concrete mixing. (c) Rectangular specimens after demolding.

The rectangular specimens were molded in 2 concrete layers. Each layer was rodded 60 times per layer using a 16-millimeter rod. A rubber mallet was used to tap the mold 15 times per layer to further consolidate the poured concrete. After 24 hours, the 15x15x55 centimeter specimens were demolded and submerged in water for the specified curing age.

6.5 Specimen Curing Conditions

The specimens were demolded according to the specifications of ASTM C192. Concrete specimens are removed from the molds 24 ± 8 hours after casting. Each cylindrical and prismatic specimen was demolded and cured in ideal conditions by submerging the samples in water at 23 ± 2 °C for 28, and 90 days according to the experimental program.

Specimens were stored for the curing period in a tank filled with tap water according to the requirements specified in the American standard **ASTM C511** - "*Specification for Mixing Rooms, Moist Cabinets, Moist Rooms, and Water Storage Tanks used in the Testing of Hydraulic Cements and Concretes"* [197]. In the storage water tank, special care is taken to the possible contamination of water by organic materials by applying Calcium Hydroxide ($Ca(OH)_2$) also known as slaked lime.

After the curing period was completed, all the specimens were taken out off the water tanks and prepared to be tested according to the experimental program. Specimen storage is shown in Figure 56.

Figure 56 – Specimens in curing conditions submerged in water tank at 21°C.

Different water tanks were used for the cylindrical specimens used for corrosion potential and concrete resistivity described in section 6.4.2 as submerging the specimens in water would result in general corrosion of the embedded steel bars. These specimens were stored in smaller tanks filled with tap water at 23 ± 2 °C for 28 days, the water level was always controlled, and the steel bars were painted with epoxy paint to maintain dry superficial conditions in the embedded steel bars. The curing conditions for these specimens is presented in Figure 57.

Figure 57 – 3-inch diameter specimens under curing conditions submerged in water tank at 21°C.

6.6 Specimen slicing for durability testing

Immediately after the moist-curing period of concrete samples was finished, the testing samples were sliced using a water-cooled diamond saw to obtain the required specimens for Rapid Chloride Penetration test, Non-Steady-State Chloride Ion Migration Coefficient test, density, porosity and water absorption tests and KT-air permeability coefficient test. This diamond saw, shown in Figure 58, has a rotating disc and a guiding system to make perpendicular cuts in concrete.

Figure 58 – Water-cooled diamond saw.

4-inch cylindrical specimens were sliced into discs with a thickness of 50 mm ± 5 mm. From each concrete cylinder, 3 discs were obtained and afterwards prepared for each durability test following the stablished procedure in reference standards. The resulting discs obtained from 4-inch cylindrical specimens are presented in Figure 59.

Figure 59 – Sliced 4-inch concrete cylinders.

Concrete prisms were also sliced using the same water-cooled diamond saw to obtain three quasi-cubical 15 cm x 15 cm x 15 cm specimens from each 15 cm x 15 cm x 55 cm concrete prism after the required moist-curing age was achieved. Since these specimens were used in KT air-permeability coefficient measurements, and this test is especially dependent on the surface conditions of concrete, special care was taken to secure the perpendicularity and uniformity of the sliced faces. Cubical sliced specimens can be observed in Figure 60.

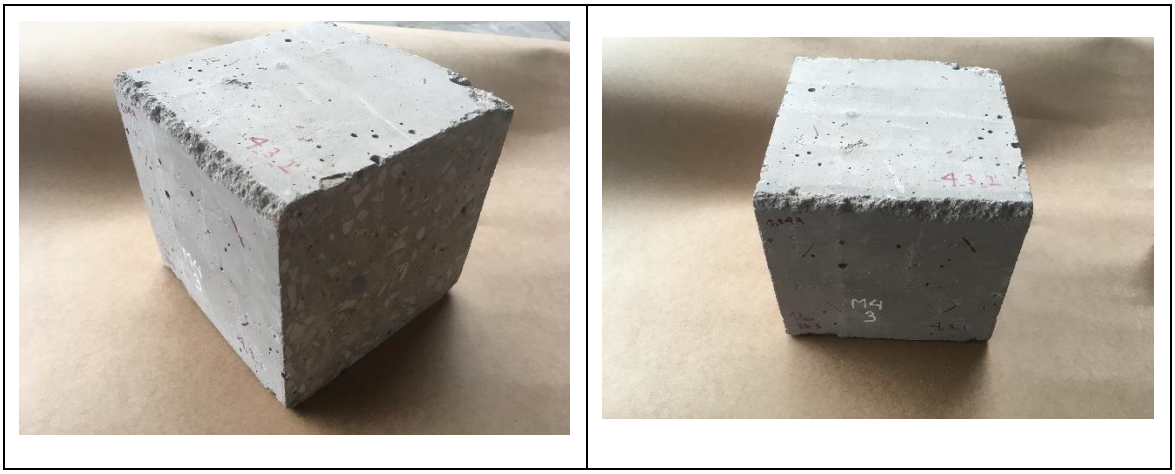

Figure 60 – 15 cm x 15 cm x 15 cm cubical specimens sliced with diamond saw.

7. Concrete Testing Program

Multiple tests were performed for each concrete mix at different curing ages, as shown in Table 28. Each one of these tests were performed to assess different durability properties such as chloride penetration, porosity, electrical resistivity, corrosion rate and air permeability. Compression strength and elasticity modulus were also measured as control parameters for mix quality and to establish a relationship between these factors and each durability property.

Standard	Measured Property	Test Ages Days
ASTM C39[1]	Compressive Strength	7 - 28 - 90
ASTM C469[2]	Modulus of Elasticity	90
ASTM C1202[3]	RCPT – Rapid Chloride Penetration	28 - 90
ASTM C642[4]	Density, percent absorption, percent voids	28 - 90
NORDTEST NT 492[5]	Non-steady-state Chloride Migration Coefficient	28 - 90
SIA 262[6]	Permeability to air of hardened concrete	28 - 90
ASTM G59[7]	Corrosion Potential and concrete resistivity	28- 56 – 90 - 120

[1] ASTM C39 / C39M-21, Standard Test Method for Compressive strength of Cylindrical Concrete Specimens [198].
[2] ASTM C469 / C469M-14e1, Standard Test Method for Static Modulus of Elasticity and Poisson's Ratio of Concrete in Compression [199].
[3] ASTM C1202-19, Standard Test Method for Electrical Indication of Concrete's Ability to Resist Chloride Ion Penetration [200].
[4] ASTM C642-13, Standard Test Method for Density, Absorption, and Voids in Hardened Concrete [201].
[5] NT BUILD 492 - Concrete, mortar and cement-based repair materials: Chloride migration coefficient from non-steady-state migration experiments [160].
[6] SIA 262/1 - Construction en béton - Spécifications complémentaires [202].
[7]ASTM G59-97(2020), Standard Test Method for Conducting Potentiodynamic Polarization Resistance Measurements [203].

Table 28 - Experimental program in concrete mixes

These durability tests are widely used in scientific literature and construction practice for quality control. As the main objective of this research is to identify the effects in corrosion durability of incorporating fine recycled aggregates and using fly ash as an enhancement method, multiple tests must be performed to measure the main properties that could be affected by the defined variables.

In this section, a brief description of each international standard and the procedures followed to perform the mechanical and durability tests in hardened concrete are presented. Each durability test was performed in concrete specimens cured in moist conditions for 28 and 90 days. Additionally, compressive strength was determined for each mix after 7 days of curing as a mix control parameter and to fully assess the development of resistance in concrete specimens. The equipment, experimental setup, and additional materials used in each test are also discussed in this section.

7.1 Compressive Strength

7.1.1 ASTM C39 – Standard Test Method for Compressive Strength of Cylindrical Concrete Specimens

This test method describes the measurement of compressive strength of cylindrical concrete specimens. The specimens are placed in a testing machine that applies a constant uniaxial force until failure is reached. The fracture pattern is registered as well as the maximal force applied by the testing machine. The value of compressive strength is defined as the relation between the maximal applied force and the cross-sectional area of the concrete specimen in units of pressure, usually megapascals (MPa), as shown in Equation 26, where *P* is the maximum applied force and *A* is the cross-sectional area of the specimen.

$$f_c' = \frac{P}{A} \qquad \text{Equation 26}$$

According to ASTM C39, values obtained are dependent of different conditions such as the size and shape of the specimen, batching and mixing procedures, methods of sampling, specimen fabrication and the age, temperature, and moisture conditions during curing. The specimens are tested in a moist condition.

The load is applied continuously at a rate of movement corresponding to a stress rate of 0.20 MPa/s and the fracture pattern is recorded according to Figure 61.

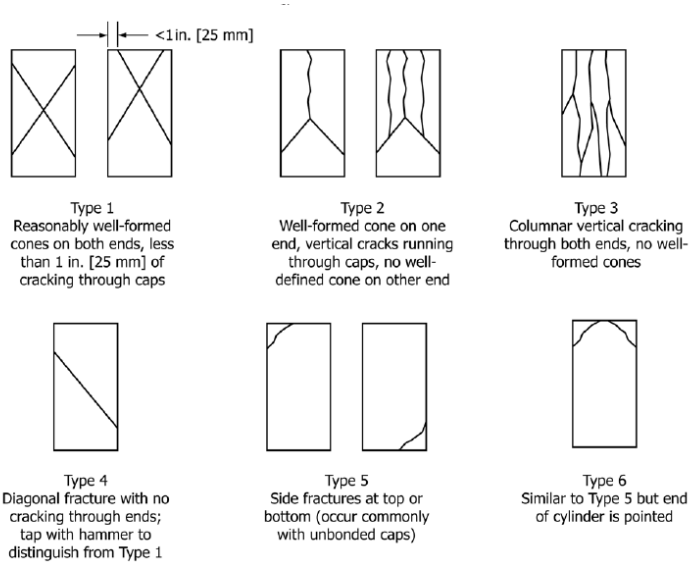

Figure 61 – Fracture patterns in cylindrical specimens. Retrieved from ASTM C192-18.

7.1.2 Experimental Procedure

Compressive strength tests were performed in hardened concrete specimens cast in the plastic molds described in section 6.4.1. Compression tests were performed in specimens cured in moist conditions for 7 days, 28 days and 90 days. After completing the curing period, each specimen is removed from submerged storage and tested in a saturated state.

Before applying the compressive force, the diameter and length of each concrete specimen were measured using a digital caliper with a precision of 0,01 millimeters. The cylindrical specimens are then tested in a hydraulic machine with a constant pressure increase of 0,20 MPa/s. The end-faces of the cylindrical samples are treated superficially to equally distribute the axial load in the cross-sectional area of the testing specimen.

For each cylindrical specimen, the failure load and the failure pattern are recorded according to the procedure described in ASTM C39. The experimental setup and the recorded values recorded from the testing machine are shown in Figure 62.

Figure 62 – Experimental setup for compressive strength testing.

The maximum load is automatically recorded by the testing machine and the compressive strength for each specimen is determined by using Equation 26. The strength correction employed for cylinders with a height to length ratio smaller than 2 was not applied for any of the concrete specimens as these were cast in molds with the adequate dimensions. The results and discussion for each concrete mix are presented in Section 8.1

7.2 Stress-strain Curves and Modulus of Elasticity

7.2.1 ASTM C469 – Standard Test Method for Static Modulus of Elasticity and Poisson's Ratio of Concrete in Compression

This method describes the determination of Young's modulus of elasticity and Poisson's ratio for concrete cylinders. A strain-measurement equipment known as a compressometer is attached to the sample and compressive load is applied with a testing machine to obtain the longitudinal stress-deformation curve as shown in Figure 63. The modulus of elasticity will be defined as the slope of the line between a longitudinal strain of 50 millionths and the stress corresponding to 40% of the ultimate load.

Figure 63 – Longitudinal strain-measurement equipment.

The modulus of elasticity is an important parameter to describe concrete's deformation capability and is used as a parameter for sizing of reinforced structural members. As the modulus of elasticity may vary with different load rates, a continuous movement of the compressive head is established at a rate of 1 mm/min. Multiple loading cycles with a maximum load of 40% of compressive strength are applied as usually the first cycle is primarily for the seating of the gauges. A linear trend must be observed in the strain-deformation curves as concrete should not exceed deformations in the elastic zone of the material.

7.2.2 Experimental Procedure

The modulus of elasticity was determined for each concrete mix from the stress-strain curves of multiple cylindrical specimens. To obtain these curves, the longitudinal deformation of multiple hardened concrete samples was measured for two compressive load-unload cycles.

Cylindrical concrete specimens were cured for 90 days in moist conditions, after completing the curing period, the samples were removed from submerged storage and the end faces were coated to uniformly distribute the compressive load across the concrete's cross-sectional area.

The compressive load was applied by a universal testing machine manufactured by **SHIMADZU®** as shown in Figure 64. This universal testing machine is equipped with a servo-controlled crosshead programed to descend at a 0,025 mm/s constant speed for this test. The testing machine automatically records the applied force and crosshead displacement. As specified by ASTM C469, once 40% of the maximum load applied to each cylindrical specimen was reached, the samples were unloaded with the same crosshead movement speed and subsequently submitted to a second load-unload cycle. The maximum load was previously determined for each concrete mixture in the compressive strength test.

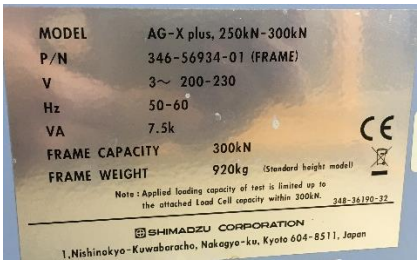

Figure 64 – Shimadzu universal testing machine used for Modulus of Elasticity testing.

During the loading and unloading cycles, an Averaging Axial Extensometer manufactured by **EPSILON®** was used to measure longitudinal strain of concrete samples. This extensometer has a gauge length of 150,00 mm and is designed for specimens with a diameter between 50 mm and 150 mm. The axial extensometer records the specimen's shortening distance at defined intervals of time, allowing the calculation of longitudinal strain using the initial gauge length. The experimental setup is presented in Figure 65.

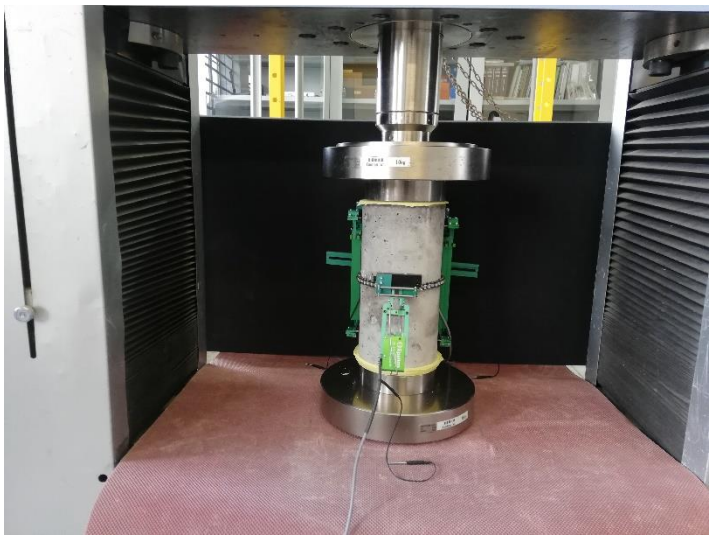

Figure 65 – Experimental setup for modulus of elasticity testing.

The modulus of elasticity was determined for each cylindrical specimen according to the procedure described in ASTM C469 as the slope of the line in the stress-deformation curve between a deformation of 5 millionths and 40% of the maximum compressive strength. In these curves, the correlation between stress and strain should be quasi-linear for both load and unload cycles as the specimens are always loaded under elastic conditions as shown in Figure 66. The modulus of elasticity of each concrete mix was calculated as the arithmetic average of the results from the test specimens. The results and discussion for each concrete mix are presented in Section 8.2.

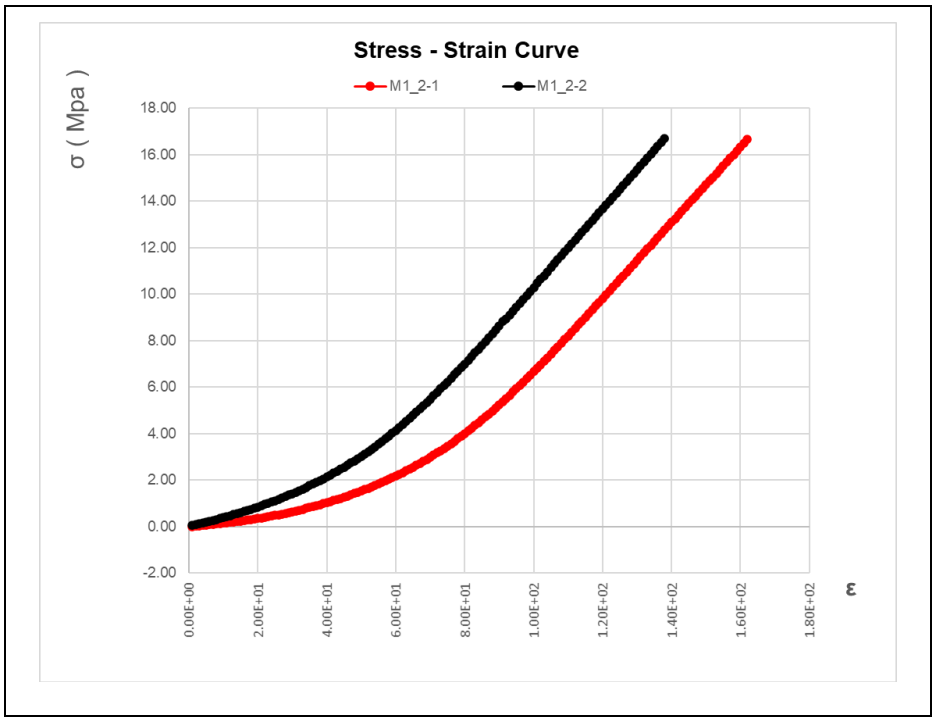

Figure 66 – Stress-Strain curves obtained from Modulus of Elasticity testing.

7.3 Concrete Density, Absorption and Porosity

7.3.1 ASTM C642 – Standard Test Method for Density, Absorption, and Voids in Hardened Concrete

This test method is used to measure the water absorption, density, and porosity of concrete samples by establishing volumetric relations between saturated and non-saturated weight. The sample mass is determined in different saturation conditions, such as dry, saturated while superficially dry, saturated after boiling and immersed in water. A brief scheme of the test procedure is presented in Figure 67.

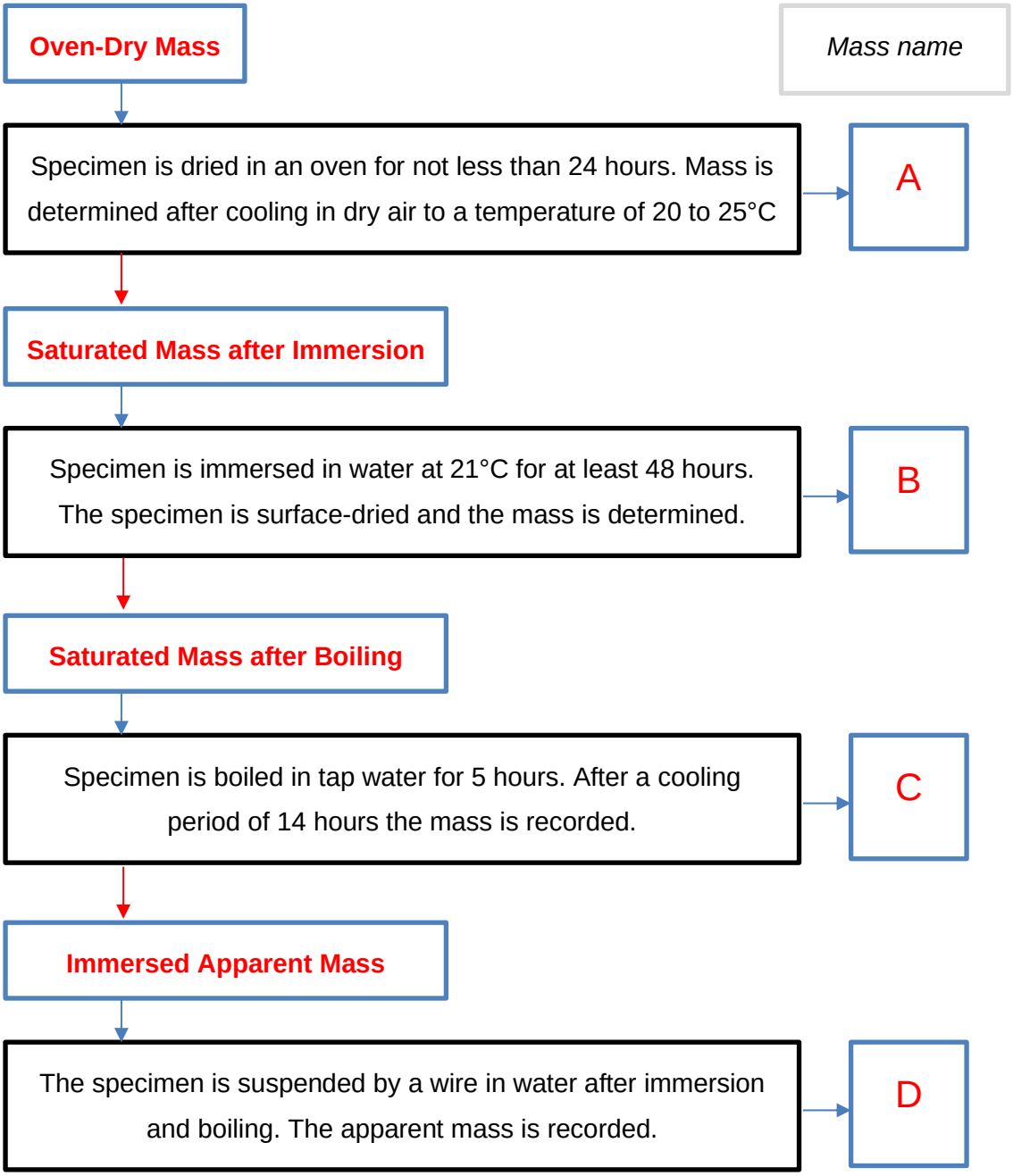

Figure 67 – Testing procedure for ASTM C642.

From these recorded masses, the following concrete properties are calculated using Equation 27 to Equation 33:

$$Absorption\ after\ immersion\ (\%) = \frac{B - A}{A} * 100 \quad \text{Equation 27}$$

$$Absorption\ after\ immersion \text{ and boiling } (\%) = \frac{C - A}{A} * 100 \quad \text{Equation 28}$$

$$Bulk\ density, dry\ \left(\frac{g}{cm^3}\right) = \frac{A}{C - D} * \rho = g_1 \quad \text{Equation 29}$$

$$Bulk\ density\ after\ immersion \left(\frac{g}{cm^3}\right) = \frac{B}{C - D} * \rho = g_1 \quad \text{Equation 30}$$

$$Bulk\ density\ after\ immersion\ and\ boiling \left(\frac{g}{cm^3}\right) = \frac{C}{C - D} * \rho = g_1 \quad \text{Equation 31}$$

$$Apparent\ density \left(\frac{g}{cm^3}\right) = \frac{A}{A - D} * \rho = g_2 \quad \text{Equation 32}$$

$$Volume\ of\ voids\ (\%) = \frac{g_2 - g_1}{g_2} * 100 \quad \text{Equation 33}$$

Where ρ is the density of water (1 g/cm^3).

The most significant parameters for this research are absorption after immersion, apparent density, and volume of voids since the research variables are directly associated with the change in concrete microstructure that results in higher concrete's porosity.

7.3.2 Experimental Procedure

For each concrete mix, multiple specimens with a thickness of 50 mm were tested following the procedure described in Figure 67. Before the initial drying period, all the samples were cleaned to remove potential surface impurities from the slicing process that could modify the recorded weight. The specimens were dried in an oven at 105°C for 24 hours and the dry weight was recorded. The concrete samples were dried at the oven for additional 24 hours until the difference between recorded dry weights at 24 hour-intervals was less than 0,50%. At this point, the specimen was considered completely dry, and its final weight was

recorded as variable “A”. The specimens drying in oven conditions can be observed in Figure 68 (a).

(a)

(b)

Figure 68 – (a) Concrete specimens’ oven-dried at 105°C. (b) Concrete specimens positioned on boiling reservoir.

Once the dried specimens had reached room temperature, they were immersed in a water tank for 48 hours after which the surface-dry saturated mass was determined. Concrete samples were submerged for additional 24-hour periods until the difference between recorded saturated weights was less than 0,5%. The specimens were considered saturated at this point and each sample’s weight was recorded as variable “B”.

After saturation was achieved, each concrete sample was boiled in water for 5 hours, after this period, the specimens were cooled at room temperature and the mass after boiling was recorded as value “C”. The boiling reservoir of concrete samples is presented in Figure 68 (b). Boiled samples were finally suspended in water and the immersed apparent mass was recorded as value “D”.

Once values A, B, C, and D were determined, absorption after immersion, absorption after immersion and boiling, bulk density, apparent density and volume of voids were calculated using Equation 27 to Equation 33. The results and discussion for each concrete mix are presented in Sections 8.3, 8.4 and 8.5.

7.4 Rapid Chloride Penetration Test – RCPT

7.4.1 ASTM C1202 – Standard Test Method for Electrical Indication of Concrete's Ability to Resist Chloride Ion Penetration

This test method is used to establish the electrical conductivity of concrete that is directly related to chloride penetration resistance. The test specimens are 50-millimeter-thick discs obtained from 4-inch-diameter cylindrical molds. Specimens are prepared in a vacuum desiccator with an absolute pressure lower than 6650 Pa for 3 hours, while maintaining the vacuum, de-aired water is added to fully saturate concrete's pores for 1 hour. The specimens are finally soaked in water for 18 hours before starting the test. This preparation must be performed to enable an appropriate flow medium for the chloride ions.

One of the surfaces of the specimen is in contact with a 3% sodium chloride (NaCl) solution and the other is in a 0.3N sodium hydroxide solution (NaOH). Sodium solutions are stored in voltage cells (Figure 69), that will be directly connected to a power supply.

Figure 69 – Voltage cell with specimen for Rapid Chloride Penetration Test.

A 60-volt direct-current potential is passed through the specimen and the total charge passed in coulombs is tracked for a period of 6 hours, this value is directly related to chloride

ion penetrability. Table 29, retrieved from ASTM C1202, correlates Chloride Ion Penetrability for hardened concrete with the total charge passed in Coulombs. These values were obtained from multiple tests carried in laboratory conditions. The tests results are highly dependent on curing conditions and sample age as concrete becomes less permeable with time.

Charge Passed (coulombs)	Chloride Ion Penetrability
>4,000	High
2,000–4,000	Moderate
1,000–2,000	Low
100–1,000	Very Low
<100	Negligible

Table 29 – Chloride Ion Penetrability Based on Charge Passed. Retrieved from ASTM C1202.

7.4.2 Experimental Procedure

Rapid Chloride Penetration Tests were performed after 28 and 90 days of moist curing. To perform this test, a 60V DC potential is applied across the concrete specimens positioned in test cells that act as reservoirs for the catholyte and anolyte solutions. A ***PROOVE'it***® system manufactured by GERMANN INSTRUMENTS was used to perform RCPT tests in three specimens from each concrete, this device is capable of providing the required potential for 6 hours while recording the electrical current in the system. The test cells are two fluid reservoirs with an open side for contact between the specimen's end faces and the contained liquid solutions. The used source of potential and testing cells are shown in Figure 70.

(a)

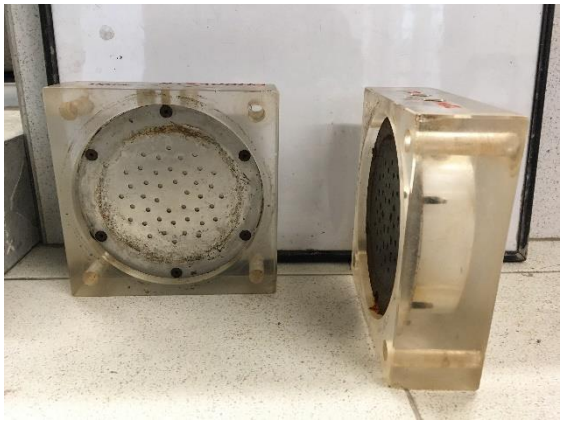

(b)

Figure 70 – (a) Proove'it device for Rapid Chloride Permeability Testing. (b) Testing Cells for 4-inch diameter specimens.

Concrete Cylindrical specimens were sliced in 50-mm thick discs and prepared for testing following the procedure prescribed in ASTM C1202. Each specimen was placed inside a testing cell and sealed using rubber bands and mechanical tightening. For each test, the reservoirs were filled the anolyte and catholyte solutions described in ASTM C1202. The mounting of concrete specimens in the testing cells and the connection to the potential source are shown in Figure 71.

(a)

(b)

Figure 71 – (a) Specimen mounting in testing cells for RCPT testing. (b) Connected cells under RCPT testing for 6 hours.

Once the cells were connected to the Proove'it device, a 60V DC potential was applied separately for each cell and the current was recorded for 6 hours. Once the testing time was finished, the current was plotted against time, as shown in Figure 72, and the total charge passed in Coulombs was calculated as the area beneath the curve using Simpson's method.

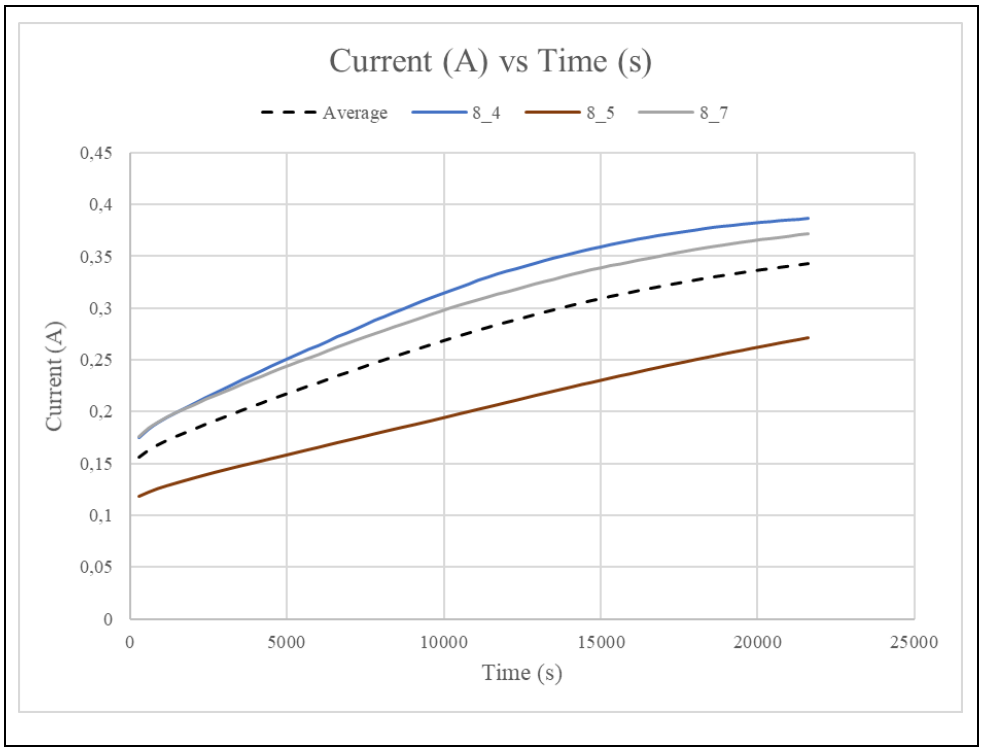

Figure 72 – Current VS. Time curves recorded in RCPT testing of concrete samples.

The resulting total charge passed in Coulombs is directly related to the chloride ion penetrability of concrete mixes, as more permeable samples will present higher ion migration and a higher current will be recorded. The results were adjusted for a standard specimen diameter of 95 mm and the permeability class was determined using the classifying criteria presented in Table 29. The results and discussion for each concrete mix are presented in section 8.6

7.5 Non-Steady-State Chloride Migration Coefficient Test

7.5.1 NORDTEST METHOD NT BUILD 492 – Chloride Migration Coefficient from Non-Steady-State Migration Experiments

This test method is used for determination of the non-steady-state chloride migration coefficient in concrete using the principle of diffusion, were ions move under a chemical potential from a high concentration zone to a low concentration zone. The movement of ions is accelerated by the application of an external electrical field.

Similarly, to ASTM C1202, the specimens are preconditioned in a vacuum desiccator with a pressure in the range of 1-5 kPa for 3 hours, followed by a moist vacuum treatment with calcium hydroxide ($Ca(OH)_2$) for another hour. The specimens are left in the $Ca(OH)_2$ solution for 18 hours after the vacuum conditioning is finished to fully saturate the specimen pores and allow the migration of ions.

According to NT 492, an external electrical potential is applied axially across the specimen and forces the chloride ions outside to migrate into the specimen. Chloride ions migrate because of electrical potential from the catholyte, a 10% sodium chloride (NaCl) solution by mass, to the anolyte, a 0.3N sodium hydroxide (NaOH) solution. The experimental set-up and the plastic support geometry, retrieved from NT BUILD 492, are displayed in Figure 73.

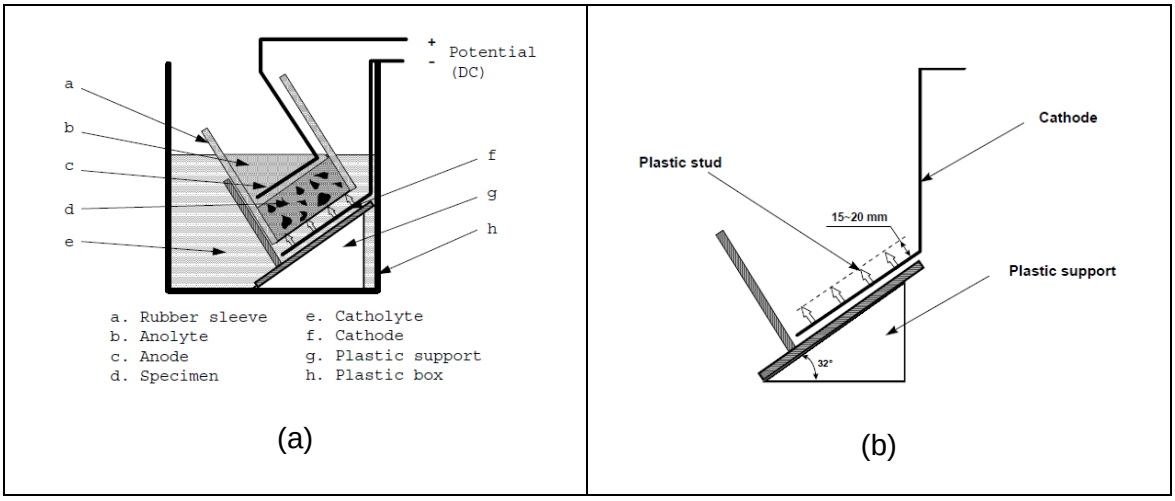

Figure 73 – (a) Chloride migration set-up. (b) Support geometry and cathode. Retrieved from NT BUILD 492.

An initial external potential of 30 volts direct-current (V DC) is applied between the two electrodes and the initial current is recorded. Catholyte temperature is also recorded at the start and after the test completion. To keep the power consumption of the concrete specimen lower than 2 Watts, the potential is adjusted to a range between 10V and 60V and the test duration is adjusted according to Table 30, retrieved from NT BUILD 492.

Initial current I_{30V} (with 30 V) (mA)	Applied voltage U (after adjustment) (V)	Possible new initial current I_0 (mA)	Test duration t (hour)
$I_0 < 5$	60	$I_0 < 10$	96
$5 \le I_0 < 10$	60	$10 \le I_0 < 20$	48
$10 \le I_0 < 15$	60	$20 \le I_0 < 30$	24
$15 \le I_0 < 20$	50	$25 \le I_0 < 35$	24
$20 \le I_0 < 30$	40	$25 \le I_0 < 40$	24
$30 \le I_0 < 40$	35	$35 \le I_0 < 50$	24
$40 \le I_0 < 60$	30	$40 \le I_0 < 60$	24
$60 \le I_0 < 90$	25	$50 \le I_0 < 75$	24
$90 \le I_0 < 120$	20	$60 \le I_0 < 80$	24
$120 \le I_0 < 180$	15	$60 \le I_0 < 90$	24
$180 \le I_0 < 360$	10	$60 \le I_0 < 120$	24
$I_0 \ge 360$	10	$I_0 \ge 120$	6

Note: For specimens with a special binder content, such as repair mortars or grouts, correct the measured current by multiplying by a factor (approximately equal to the ratio of normal binder content to actual binder content) in order to be able to use the above table.

Table 30 - Test voltage and duration for concrete specimen with normal binder content. Retrieved from NT BUILD 492.

After the test time has been completed, the specimen is axially split, using a brasilein test or with manual splitting techniques. A 0,1M silver nitrate ($AgNO_3$) solution is sprayed as a chloride indicator, the reaction between silver nitrate and the chloride ions in the specimen produce a change in color that indicates the penetration depth due to ion migration. The penetration depth can then be measured, and the chloride migration coefficient is calculated from this penetration depth, using Nernst-Planck equation as follows:

$$D_{nssm} = \frac{RT}{zFE}\frac{x_d - \alpha\sqrt{x_d}}{t} \qquad \textit{Equation 34}$$

$$E = \frac{U - 2}{L} \qquad \textit{Equation 35}$$

$$\alpha = 2\sqrt{\frac{RT}{zFE} * \text{erf}^{-1}\ (1 - \frac{2c_d}{c_o})} \qquad \textit{Equation 36}$$

Where D_{nssm} is the non-steady-state migration coefficient $\left(\frac{m^2}{s}\right)$, z is the absolute value of ion valence (1 for chloride), F is the Faraday's constant (9,648 x 10^4 J/(V mol)), U is the asolute value of the applied voltage, R is the universal gas constant (8,314 J/(K mol)), T is the average value of the initial and final temperatures in the anolyte solution, L is the thickness of the specimen, X_d is the average value of the chloride penetration depth, t is the test duration in seconds, *erf*$^{-1}$ is the inverse of error function, c_d is the chloride concentration at which the colour changes (0.07N for OPC concrete) and c_o is the chloride concentration in the catholyte solution.

7.5.2 Experimental Procedure

Non-Steady-State Chloride Migration Coefficient was determined for three specimens of each concrete mix. Initially, the specimens were sliced into 50-mm thick discs and vacuum-prepared following the procedure prescribed in NT BUILD 492. For the mounting of the chloride migration test, each specimen was placed inside rubber sleeves and adjusted using tightening clamps as shown in Figure 74 (a). Three 12-liter plastic reservoirs were

filled with a 10% NaCl solution and inclined plastic supports were placed inside each reservoir as shown in Figure 74 (b).

(a)

(b)

Figure 74 – (a) Rubber Sleeves and tightening clamps used for NT BUILD 492 testing. (b) Plastic support and plastic reservoir for catholyte solution.

The specimens inside the rubber sleeves were positioned in the inclined plastic supports and filled with approximately 300 ml of 0,3N NaOH solution. Finally, the cathode and anode were connected to the source of potential's positive and negative terminals respectively and the adjusted voltage was determined and applied for the time specified in Table 30. The experimental setup is presented in Figure 75.

Figure 75 – Non-Steady-State Chloride Migration test experimental mounting.

As multiple specimens were tested simultaneously, a circuit with the same potential gradient was proposed. All cathodes were connected to the positive terminal and all anodes were connected to the negative terminal of the source, resulting in a parallel circuit with a uniform potential. In this circuit, the negatively charged chloride ions migrate from the NaCl solution to the NaOH solution as presented in Figure 76.

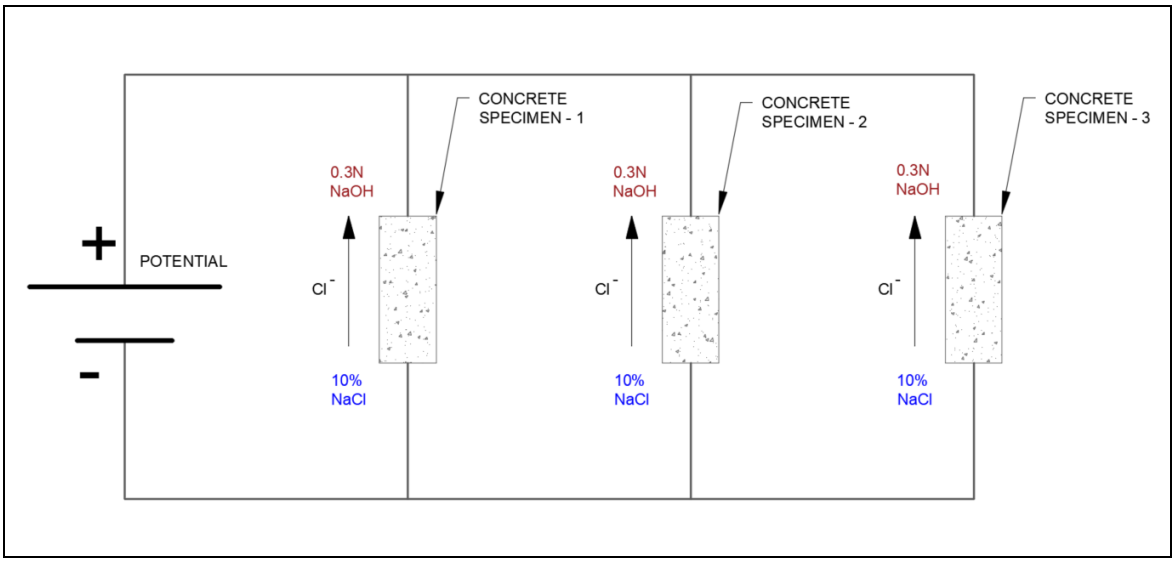

Figure 76 – Parallel circuit used for non-steady-state chloride migration test.

After the testing period was finished, each concrete specimen was axially split and a 0,1N solution of Silver Nitrate ($AgNO_3$) was sprayed on the freshly discovered face. Finally, 9 penetration distances were recorded for each specimen and the average value was defined as the chloride penetration depth. In Figure 77, the change of color after spraying the silver nitrate solution can be observed.

Figure 77 – Concrete specimens after spraying Silver Nitrate solution for Chloride ion indication.

Using the average penetration depth and the recorded values of temperature, voltage, current and specimen thickness, the non-steady-state migration coefficient was calculated for each concrete mix using *Equation 34* to *Equation 36*. The results and discussion for each concrete mix are presented in Section 8.7.

7.6 Polarization Resistance and Steel Corrosion Rates

7.6.1 ASTM G59 – Standard Test Method for Conduction Potentiodynamic Polarization Resistance Measurements

This test is used to obtain the corrosion potentials and potentiodynamic polarization resistance of steel rebar in reinforced concrete. For the testing setting, a steel bar that acts as an electrode is embedded in a concrete cylindrical sample and connected to a potentiostat to measure the current density for different potentials. Using the current density versus potential curve, polarization resistance can be obtained as the slope of the tangent

line at the point where current density is equals to zero, as this will be the point near corrosion potential.

According to ASTM G59, polarization resistance can be related to the rate of general corrosion of metals and it is a quality control test commonly used to rank materials as corrosion inhibitors. Figure 78 shows the basic electrochemical cell required to measure the corrosion potential of metal specimens.

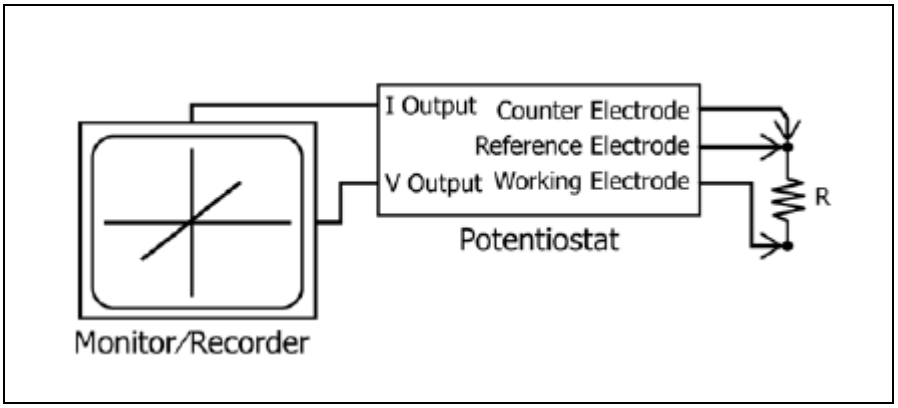

Figure 78 – Electrical resistor experimental set-up. Retrieved from ASTM G59.

7.6.2 Experimental Procedure

Polarization resistance was measured for three specimens of each concrete mix after 28 days of moist curing conditions in water. Once this period was completed and the initial polarization resistance tests were performed, specimens were submerged in a 3% NaCl solution to assess the effects of corrosive conditions in the corrosion rate of steel bars embedded in concrete. Polarization resistance tests were performed after 1, 2 and 3 months of chloride solution immersion.

A **GAMRY®** potentiostat was used to perform Polarization resistance tests in concrete samples. In these tests, the potentiostat measures current for incremental potential values at defined time periods. This device is also equipped with a command software to control voltage scan rate and define multiple parameters in each experiment. A data analysis software is also used to visualize the results and obtain the desired polarization curves. The **GAMRY®** potentiostat experimental connection to testing samples must be performed in four electrodes or leads named after a color-coded system as “working” (green), “working

sense" (blue), "reference" (white) and "counter" (red). Two of these leads carry the current ("working" and "working sense") and the other two are sense electrodes used to measure potential.

The working electrode is defined as the specimen under testing, in this case the cylindrical concrete specimens with embedded steel bars. The counter electrode is a graphite bar that completes the current path. The used reference electrode is a saturated calomel electrode, commercially known as a SCE, which is based in the reaction between elemental mercury and mercury chloride (Hg_2Cl_2) and during potentiostatic testing, can hold a constant potential, acting as a reference point. The used **GAMRY** potentiostat and saturated calomel electrode are shown in Figure 79.

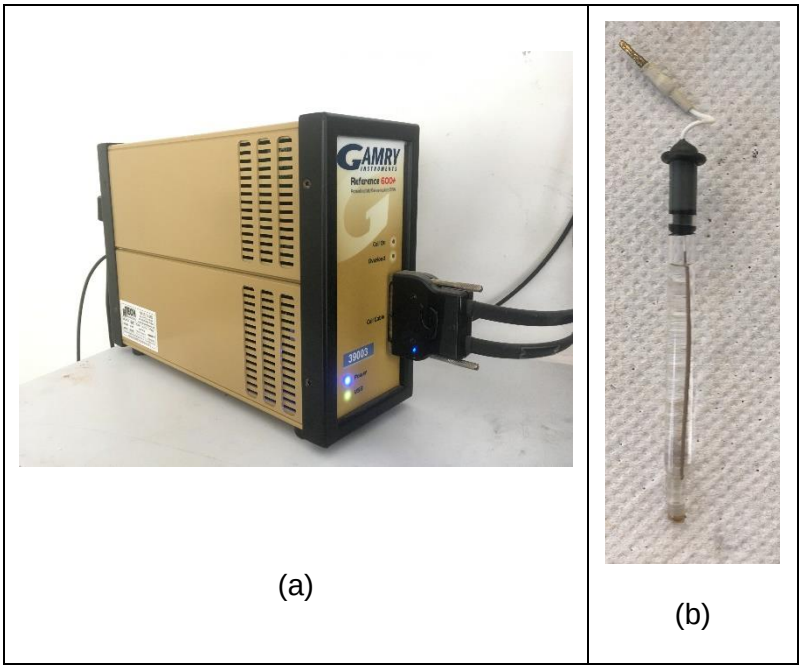

Figure 79 – (a) GAMRY potentiostat used in polarization resistance testing. (b) Saturated calomel electrode used in experimental program.

The system electrodes can be connected in different setups depending on the performed test. For polarization resistance testing, a three-point electrode system is used. In this mode, the change in potential is measured as the difference between potential in the working and reference electrodes while using the counter electrode to close the circuit. The experiment is performed in a Faraday Cell with an additional "floating ground" lead

connected to the cell's wall to suppress external electromagnetic noise. Figure 80 shows the set-up for the conducted three-electrode experiment in the concrete specimens.

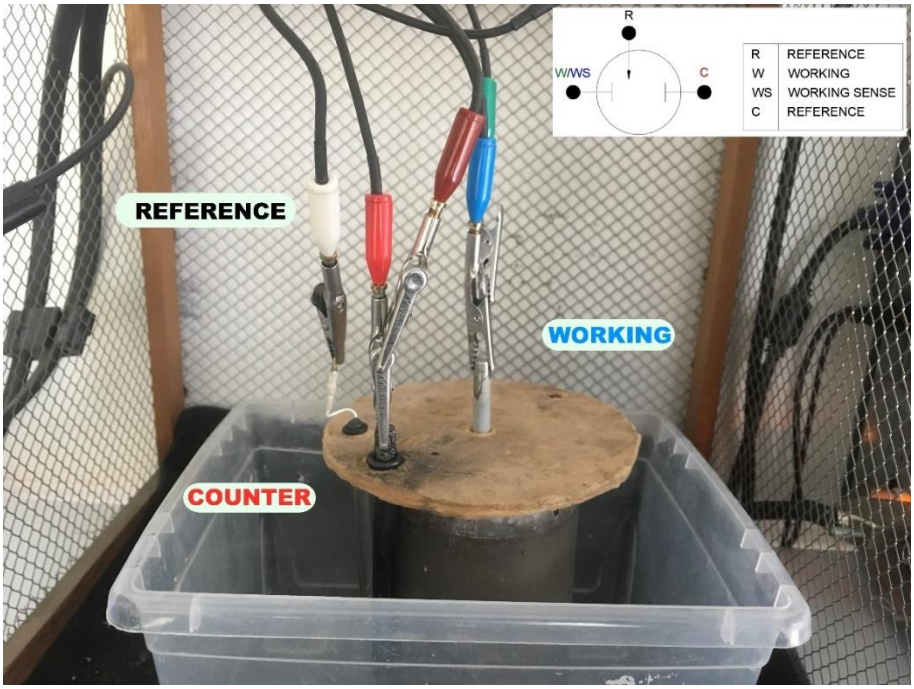

Figure 80 – Three-point electrode system used for polarization resistance measurement.

During testing, concrete samples are immersed in a plastic reservoir filled with a 3% NaCl solution that acts as an ion bridge between working, reference and counter electrodes, allowing the flow of current in the system. A sufficient volume of solution was present in the plastic reservoir to fully cover the end faces of the reference and counter electrodes. Each testing specimen was placed inside Faraday's cell and connected using the described three-point electrode system to the **GAMRY** potentiostat which automatically performed the voltage variation and recorded the resulting current. The experimental set-up and electrode connection to the source of potential are presented in Figure 81.

Figure 81 – Electrochemical cell for measuring polarization resistance connected to GAMRY potentiostat.

Experiments were performed at a voltage scan rate of 0,36 V/h (0,1 mV/s) from a potential of -30 mV to 30 mV. However, initial testing revealed that the current of corrosion could be determined for most specimens in a range between -10 mV and 10 mV. GAMRY software was used to obtain the polarization curves for each concrete specimen at each testing age, these polarization curves presented the typical behavior shown in Figure 82.

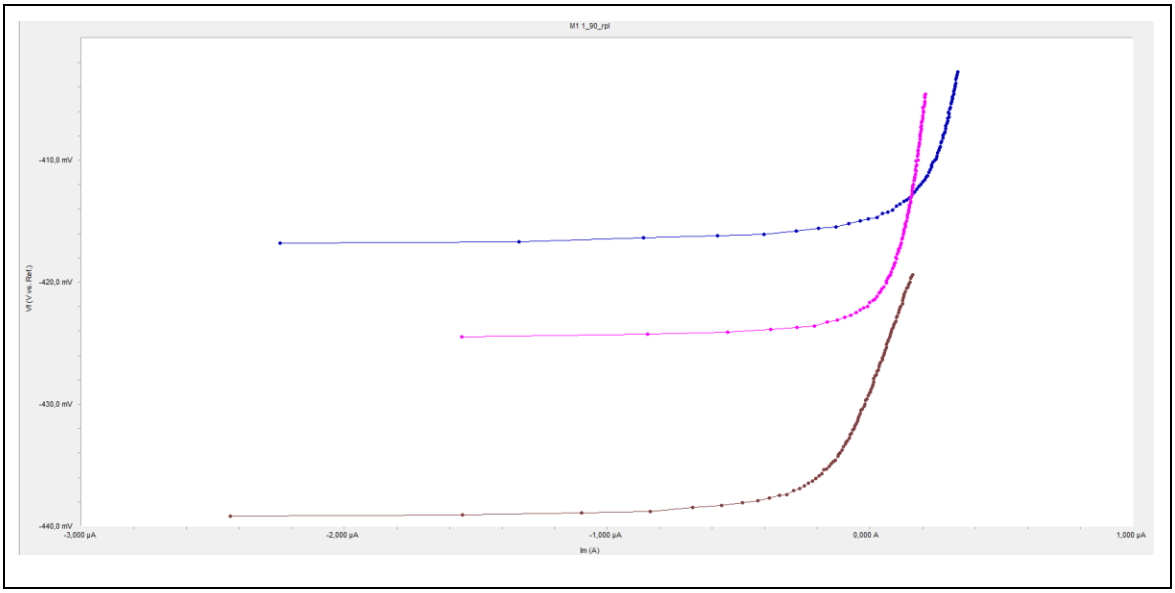

Figure 82 – Polarization curves from Polarization resistance testing in concrete samples.

The polarization curves were processed in a data analysis software to obtain the polynomial regression that best fitted each curve. As polarization resistance is defined from mix-theory potential as the slope of the line tangent to the polarization curve at a current value of 0, for a nth-grade polynomial expressed as Equation 37, polarization resistance can be calculated as the derivative of this function evaluated at 0 as shown in Equation 38.

$$P(x) = a + bx + cx^2 + dx^3 + \cdots + kx^n$$ Equation 37

$$P'(0) = b + c(0)^1 + d(0)^2 + \cdots + k(0)^{n-1} = b$$ Equation 38

Polarization resistance curves and polarization resistance values were obtained for each concrete specimen at different testing ages. Figure 83 shows an example of the obtained curves from polynomial fitting and the line tangent to the curve at a current value of 0 whose slope is computed as the polarization resistance of the specimen.

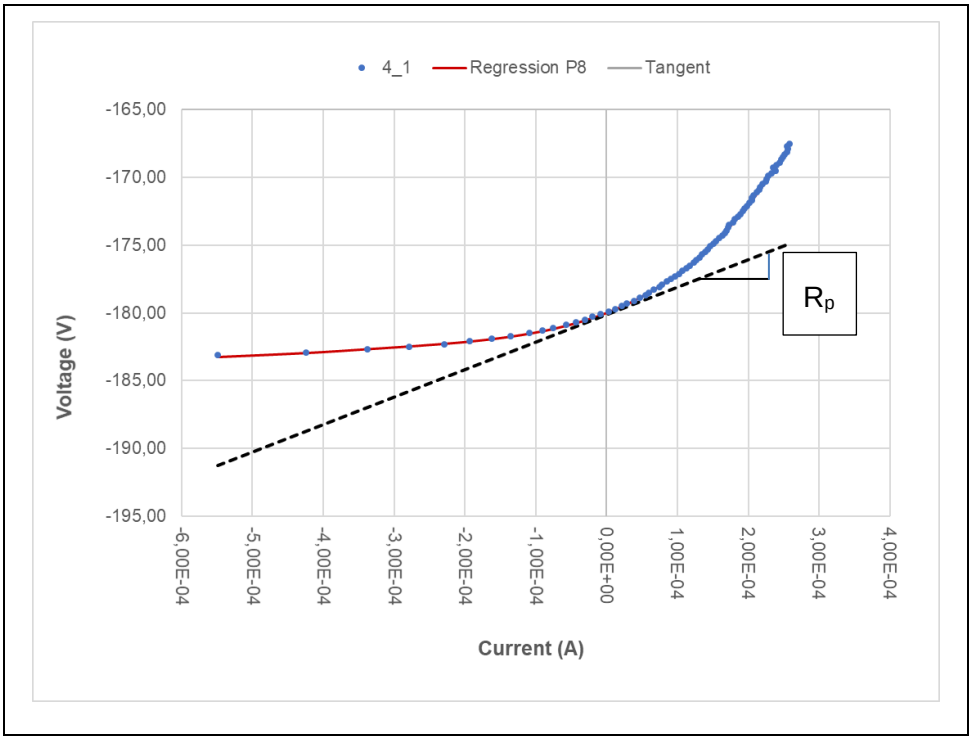

Figure 83 – Polarization curve fitting by polynomial regression and polarization resistance values.

Since Polarization Resistance was assessed for cylindrical specimens with steel bars embedded in concrete, the test results are an indicator of the current flowing through the specimen due to change in potential. The measured resistance of the working electrode ($R_{electrode}$) can be discretized as the sum of its individual components; hence the resistance value of the specimen is equal to the sum of resistance values for concrete ($R_{concrete}$) and steel (R_{steel}) as described in Equation 39.

$$R_{electrode} = R_{steel} + R_{concrete}$$ Equation 39

To identify the resistance value of the embedded steel bar alone, the resistance provided by the concrete cover must be previously measured using electrochemical techniques and subtracted as shown in Equation 40.

$$R_{steel} = R_{electrode} - R_{concrete}$$ Equation 40

Electrochemical Impedance Spectroscopy (EIS) tests were performed to measure each concrete mix ability to resist the flow of electrical current in an alternate current (AC) circuit. Since electrical resistance values for concrete samples are not independent of frequency, specimens cannot be assumed as idealized resistors following Ohm's Law and impedance measurements must be performed. EIS tests were conducted using a **GAMRY** potentiostat following the same three-point electrode system using concrete specimens with steel bars, a graphite counter electrode, and a SCE reference electrode. From EIS testing, Bode plots can be constructed by plotting log frequency on the X-axis and the value of impedance on the Y-axis as seen in Figure 84.

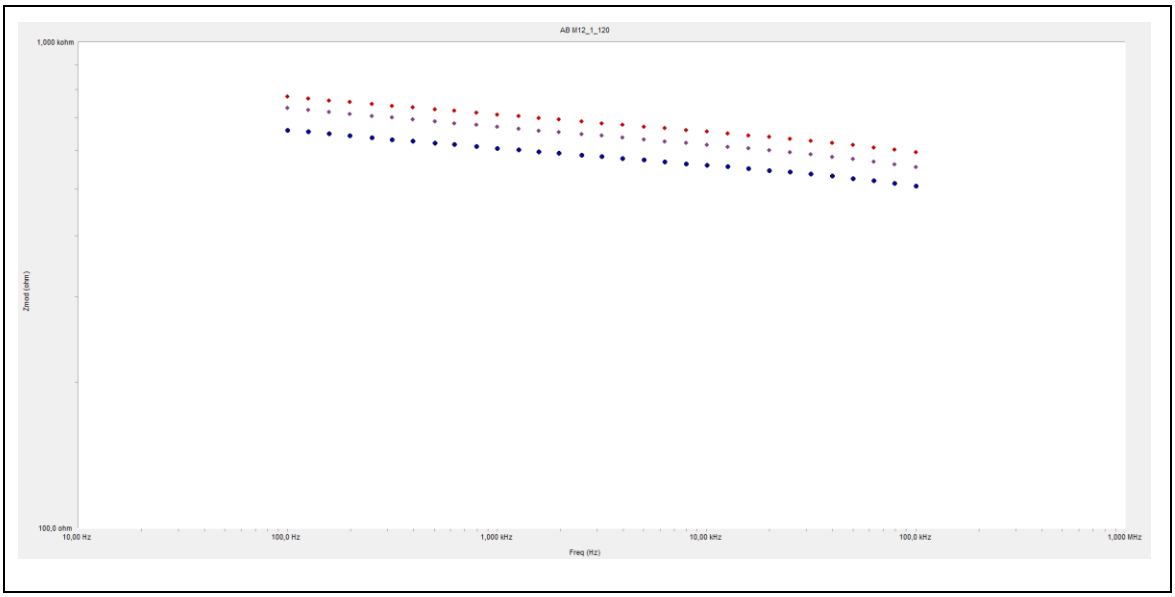

Figure 84 – Bode diagram obtained from Electrochemical Impedance Spectroscopy (EIS) testing in concrete samples.

Bode plots of concrete samples reveal a linear behavior of impedance for multiple orders of magnitude of frequency. From these tests, the value of resistance used in Equation 40 was established as the impedance for a frequency of 10 KHz. Once the resistance value of steel was calculated, the current of corrosion for each specimen was determined using *Equation 3*. Finally, rate of corrosion was computed for each concrete specimen using *Equation 6*.

López, Pérez et al. (2006) [204] have formulated a corrosion risk classification based on the measured corrosion current density as presented in Table 31. These values were used to give an indicator of possible corrosion in specimens from the assessed concrete mixes. The results and discussion for each concrete mix are presented in Section 8.8 and 8.9.

Current Density – i_{corr} (μA/cm^2)	**Risk of Corrosion**
<0,1	Low
0,1-0,5	Moderate
0,5-1	High
>1	Very High

Table 31 – Corrosion risk according to corrosion current density. Retrieved from *López, Pérez et al. (2006)* [204].

7.7 Air-Permeability of Concrete

7.7.1 SIA 262 – Air Permeability in Structures

This test method is performed to obtain the coefficient of permeability to air of hardened concrete (kT) using the "Torrent Method". A vacuum is created in a double-chamber cell that adheres to the surface of the specimen, and under non-steady state conditions, the flow rate of gas entering the inner chamber is measured through the rise in its pressure with time.

The penetrability of concrete's pore system is directly related to its transport properties, such as diffusion coefficient of gases, diffusion of aggressive ions in the liquid phase and rate of water absorption. This parameter is highly influenced by the age of the specimen, the composition of concrete mixtures, the consolidation and finishing method of fresh concrete, the type of curing and the presence of microcracks.

Measurements are made using a vacuum cell composed of two concentric vacuum chambers and soft rubber rings that seal the cell onto the concrete surface when the vacuum is applied. As the relative pressure between the chambers gets balanced, a

unidirectional flow of air from the pores occurs into the inner chamber. This air-flow mechanism is depicted in Figure 85.

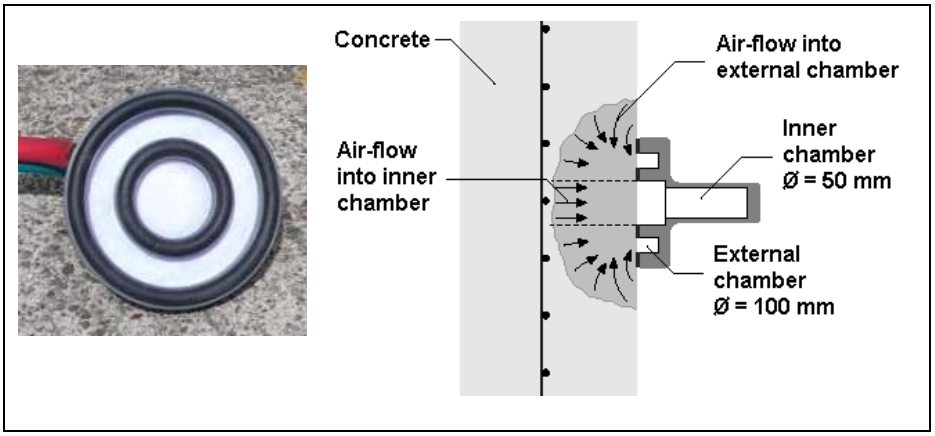

Figure 85 – Vacuum Cell for measurement of permeability to air. Retrieved from SIA 262.

The test specimens are concrete cubes of at least 150-millimeter side length or 150-millimeter diameter cylinders. The specimens are cast and cured under appropriate conditions for the desired time. Before testing, the specimens are conditioned in an oven at 50°C for 4 days, as the permeability measures are strongly affected by the moist conditions of the surface.

The coefficient of permeability to air (kT) of hardened concrete is measured in m^2 using the measurements of pressure in the inner chamber by applying *Equation 23*. SIA 262, presents a classification for concrete's permeability and equivalence with other standard tests from the value of the coefficient kT, as presented in Table 32.

kT (10^{-16} m²)	*kT* Permeability Class		Equivalence to	
			ASTM C1202	EN 12390-8*
< 0,001	PK0	Negligible	Negligible	
0,001 – 0,01	PK1	Very Low	Very Low	≤ 30 mm
0,01 - 0,1	PK2	Low	Low	≤ 50 mm
0,1 - 1,0	PK3	Moderate	Moderate	
1,0 - 10	PK4	High	High	
10 - 100	PK5	Very High		
> 100	PK6	Ultra High		

* M*aximum penetration*

Table 32 – Permeability class classification and correlation with other international standards. Retrieved from SIA 262.

7.7.2 Experimental Procedure

Air permeability was measured in prismatic samples of all concrete mixes using a **PermeaTORR®** testing equipment after 28 days and 90 days of moist curing. Testing was performed in three 15x15x15 cm samples obtained from slicing 15x15x55 cm prismatic beams. For each cubical specimen, two measurements were made in opposite faces since air permeability is highly dependent on the surface conditions of the sample.

The used **PermeaTORR** device is controlled by an integrated software which automatically performs conditioning, calibration and measurements when connected to the vacuum active cell. This software also automatically performs calculation of KT air-permeability coefficient and plots the results against the classification limits defined in international standard SIA 262. The testing equipment and the connection to the active cell are presented in Figure 86.

Figure 86 – PermeaTORR device used for Air-Permeability testing of concrete samples.

Before performing a group of measurements in concrete samples, a conditioning process was conducted using PermeaTORR's acrylic calibration plate. In this process, both chambers of the active cell are fully evacuated during 20 minutes as pressure measurements can be affected by residual pockets of air from previous testing. After conditioning, the active cell is automatically calibrated by measuring the increase in pressure of the inner chamber for 6 minutes holding the active cell against the calibration plate. PermeaTORR's software displays the increase of pressure against elapsed time for user control. A second calibration process is established by standard SIA 262, testing of specimens can be started if the final value of increase in pressure during calibration does not exceed 5,0 mbar and the difference in values between first and second calibration do not exceed 0,5 mbar. The calibration plate and calibration process of the active cell are shown in Figure 87.

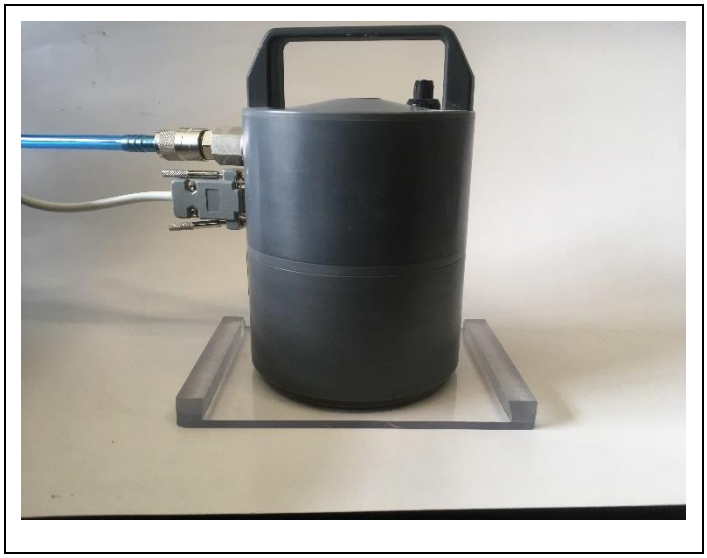

Figure 87 – (a) Calibration plate of PermeaTORR instrument. (b) Calibration process of the active cell.

Once the conditioning and calibration process was completed, testing in the concrete samples was performed. Each of the specimens was previously surface-cleaned and oven-dried at 50°C for at least 4 days as shown in Figure 88. This process must be performed to ensure a dry surface since measurements results will be affected by moisture and impurities in the specimen.

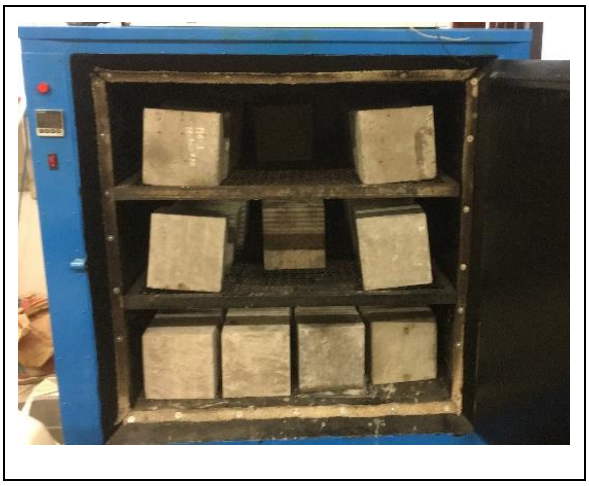

Figure 88- Cubical specimens oven-drying at 50°C for 4 days.

The active cell was placed in the surface point and the test was initiated automatically by using PermeaTORR's integrated software. During testing, the pressure in the inner chamber rises due to air flow from the concrete pores into the evacuated chamber. Pressure increase in the inner chamber is measured and graphically displayed for 12 minutes, however, after 6 minutes the air permeability coefficient is displayed when sufficient measurements have been made and recorded as *"**KT6**"*. For a homogeneus concrete, this plot should be quasi-linear and the values of *KT6* and KT after 12 minutes should not be significantly different. The testing process of concrete samples is shown in Figure 89.

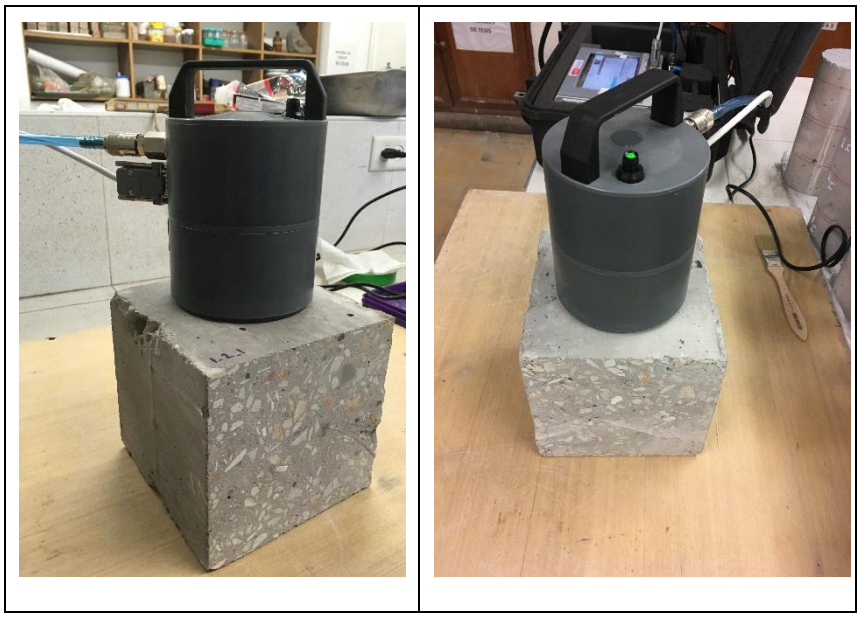

Figure 89 – Air-Permeability testing of concrete cubical samples.

The test results for each 12 min (or 6 min) measurements are displayed in the PermeaTORR display as a pressure evolution graph were the increase in the effective pressure of the inner chamber ($\Delta P_{i\ eff}$) is plotted as a function of the square root of change in time ($t^{1/2} - t_0{}^{1/2}$). The permeability class limits defined in SIA 262 (Table 32) are included in the plot to easily identify the classification of the concrete sample according to its air-permeability coefficient. A pressure evolution graph for a concrete specimen is displayed in Figure 90.

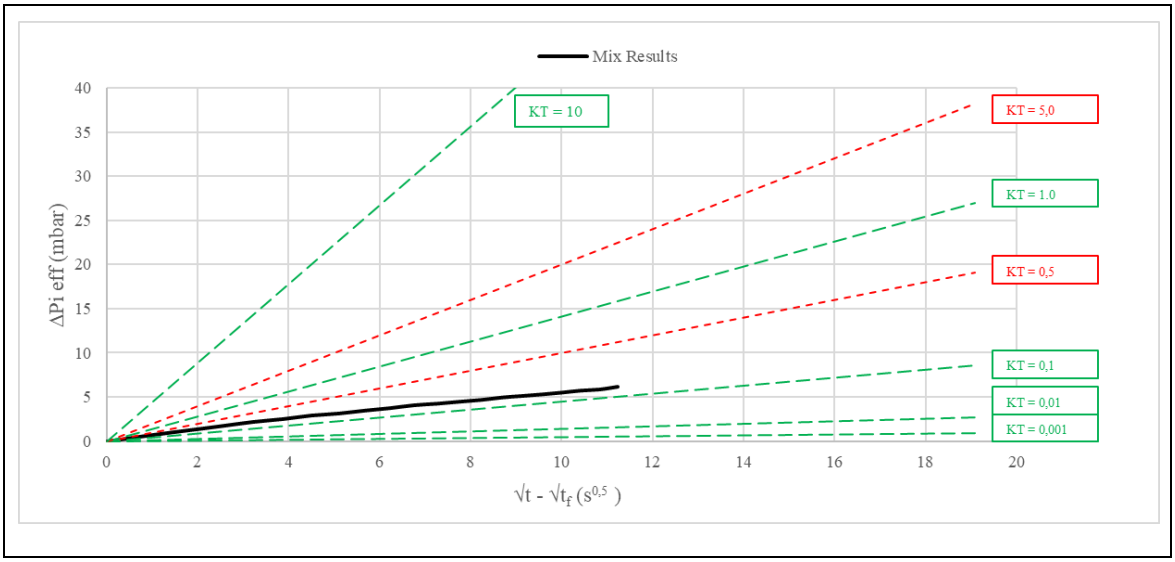

Figure 90 – Effective pressure VS. Variation of time curve for calculation of Air-Permeability KT coefficient.

The KT air-permeability coefficient is automatically calculated and displayed by the PermeaTORR instrument. Two measurements were recorded for each concrete sample and 3 cubical specimens were tested for all concrete mixes, resulting in 6 recorded measurements per mix and testing age. The conditioning and calibration process was performed before starting every group of tests to reduce possible errors related to instrument use. The results and discussion for each concrete mix are presented in Section 8.10.

7.8 Statistical analysis of data

For each concrete mixture, a statistical analysis of outlying data detection was performed to obtain a single test result from the multiple tests performed in concrete specimens. Initially, results were determined as the average of multiple values obtained in at least three concrete specimens for each performed test, however, possible outlying data was detected

and rejected using the procedure described in American Standard **ASTM E178 – "***Standard Practice for Dealing with Outlying Observations"* using the "*Criterion for a single outlier".*

In this criterion, based on a Gaussian distribution assumption, a critical value "T_n" is defined as the value exceeded by chance with a specified small probability defined as the "significance level". The critical value was calculated for every observation "X_n" using Equation 41.

$$T_n = (X_n - \bar{X})/s \qquad \text{Equation 41}$$

Where $\bar{X}$ is the arithmetic average of the population and s is the estimate of the population standard deviation based on the sample data.

This critical value is compared to a defined limit presented in Table 33, based on the number of observations and a defined significance value. If the calculated Tn value exceeds the critical value "T", the observation can be defined as "outlying" and its rejection evaluated. For this research, a significance level of 1% was defined for outlying data rejection since for most concrete tests performed, three results were obtained for each concrete mixture and the exclusion of a value could significantly modify the obtained result.

Number of Observations, *n*	Upper 10 % Significance Level	Upper 5 % Significance Level	Upper 1 % Significance Level
3	1.1484	1.1531	1.1546
4	1.4250	1.4625	1.4925
5	1.602	1.672	1.749
6	1.729	1.822	1.944
7	1.828	1.938	2.097
8	1.909	2.032	2.221
9	1.977	2.110	2.323
10	2.036	2.176	2.410
11	2.088	2.234	2.485
12	2.134	2.285	2.550
13	2.175	2.331	2.607
14	2.213	2.371	2.659
15	2.247	2.409	2.705
16	2.279	2.443	2.747
17	2.309	2.475	2.785
18	2.335	2.504	2.821
19	2.361	2.532	2.854
20	2.385	2.557	2.884
21	2.408	2.580	2.912
22	2.429	2.603	2.939
23	2.448	2.624	2.963
24	2.467	2.644	2.987
25	2.486	2.663	3.009
26	2.502	2.681	3.029
27	2.519	2.698	3.049
28	2.534	2.714	3.068
29	2.549	2.730	3.085
30	2.563	2.745	3.103
35	2.628	2.811	3.178
40	2.682	2.866	3.240
45	2.727	2.914	3.292
50	2.768	2.956	3.336

[A] Values of *T* are taken from Grubbs (1),[3] Table 1. All values have been adjusted for division by $n - 1$ instead of n in calculating s. Use Ref. (1) for higher sample sizes up to $n = 147$.

Table 33 – Critical Values for T using the Criterion for a Single Outlier – Retrieved from ASTM E 178.

8. Results and Discussion

The results obtained in the tests performed for each concrete mixture are summarized in this section, a brief description on the effects of incorporating fine RCA and fly ash to concrete mixes is also discussed.

8.1 Compressive Strength

Compressive Strength results (f_c') evaluated for each concrete mixture after 7 days, 28 days and 90 days of moist curing are presented in Table 34. As expected, results show an increase in compressive strength as the specimen age increased. The calculated population standard deviation (σ) after statistical data analysis is also presented.

Mix	Mix	7 Days		28 Days		90 Days	
ID	Name	F'c (MPa)	σ (MPa)	F'c (MPa)	σ (MPa)	F'c (MPa)	σ (MPa)
1	28-CONTROL	19,86	0,99	30,78	0,01	34,92	0,00
2	28-RA20	20,37	0,09	27,43	1,70	33,66	0,00
3	28-RA60	19,72	0,24	26,21	0,28	32,09	0,00
4	28-RA100	17,75	0,60	25,90	2,30	30,36	0,86
5	28-RA20-FA20	13,38	0,13	19,16	0,53	28,48	0,65
6	28-RA60-FA20	12,59	0,35	20,43	1,96	25,79	1,24
7	28-RA100-FA20	11,05	0,47	21,53	0,89	25,69	0,36
8	21-CONTROL	13,98	0,09	25,94	0,54	25,17	0,02
9	21-RA20	18,59	0,10	28,30	1,17	30,57	0,66
10	21-RA60	14,70	0,02	23,95	0,59	25,06	1,65
11	21-RA100	14,79	0,00	22,55	1,22	24,36	1,01
12	21-RA20-FA20	10,50	0,23	20,07	0,37	23,29	0,30
13	21-RA60-FA20	9,92	0,08	17,41	1,17	21,04	0,31
14	21-RA100-FA20	10,18	0,22	17,41	0,67	20,37	2,33

Table 34 – Compressive test results.

The effects of increasing the replacement ratio of fine RCA in concrete mixes for different testing ages can be assessed from Figure 91. Through these values, it can be confirmed

that compressive strength is negatively affected by the inclusion of fine RCA as mixtures with 100% fine RCA presented lower compressive strengths for all testing ages than control mixes. This is consistent with the results reported by multiple researchers who also have described a loss of strength when including only fine RCA in concrete [45], [53].

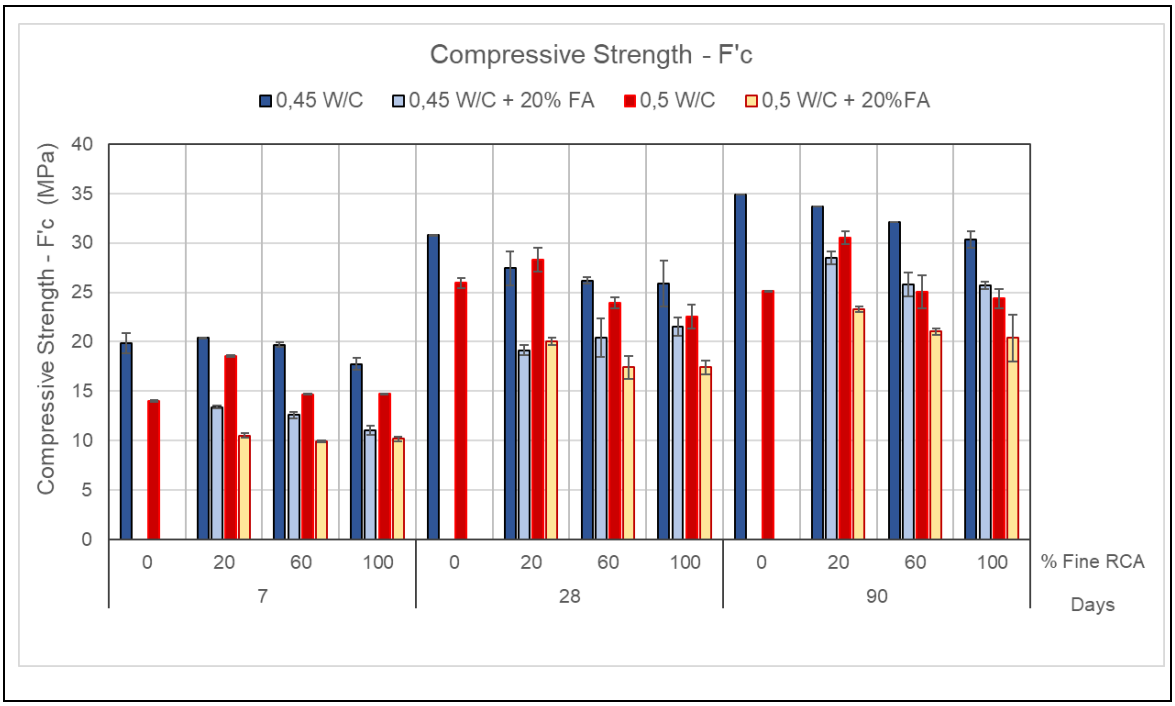

Figure 91 – Compressive strength (F'c) for increasing replacement ratios of fine RCA at different testing ages.

For each testing age, results were normalized by dividing the obtained strength by the 0,45 W/C and 0,50 W/C control mixtures strength, as an indicator of the performance of each RAC mixture compared to conventional concrete, the results are presented in Table 35.

Mix ID	Mix W/B	Mix Name	7 Days $\frac{F_c'}{F'c_{ctrl}}$	28 Days $\frac{F_c'}{F'c_{ctrl}}$	90 Days $\frac{F_c'}{F'c_{ctrl}}$
1	0,45	28-CONTROL	1,00	1,00	1,00
2		28-RA20	1,03	0,89	0,96
3		28-RA60	0,99	0,85	0,92
4		28-RA100	0,89	0,84	0,87
5		28-RA20-FA20	0,67	0,62	0,82
6		28-RA60-FA20	0,63	0,66	0,74
7		28-RA100-FA20	0,56	0,70	0,74
8	0,50	21-CONTROL	1,00	1,00	1,00
9		21-RA20	1,33	1,09	1,21
10		21-RA60	1,05	0,92	1,00
11		21-RA100	1,06	0,87	0,97
12		21-RA20-FA20	0,75	0,77	0,93
13		21-RA60-FA20	0,71	0,67	0,84
14		21-RA100-FA20	0,73	0,67	0,81

Table 35 – Compressive strength results compared to natural aggregate control mixes.

This comparative analysis is also presented graphically in Figure 92. From these results, it is possible to identify a reduction in compressive strength at all testing ages for 0,45 W/B mixes without fly ash incorporation. At 28 days, 0,45 W/B mixes with 20%, 60% and 100% fine RCA presented a strength reduction of 11%, 15% and 16% when compared to the control mix while at 90 days these reduction values were 4%, 8% and 13% respectively. On the other hand, the compressive strength for 0,50 W/B mixes did not present significant reduction due to fine RCA inclusion, and 20% fine-RCA replacement even resulted in an increase of strength of 10% at 28 days and 21% at 90 days. As expected, decreasing the W/B ratio increases the compressive strength as has been reported in other studies [55].

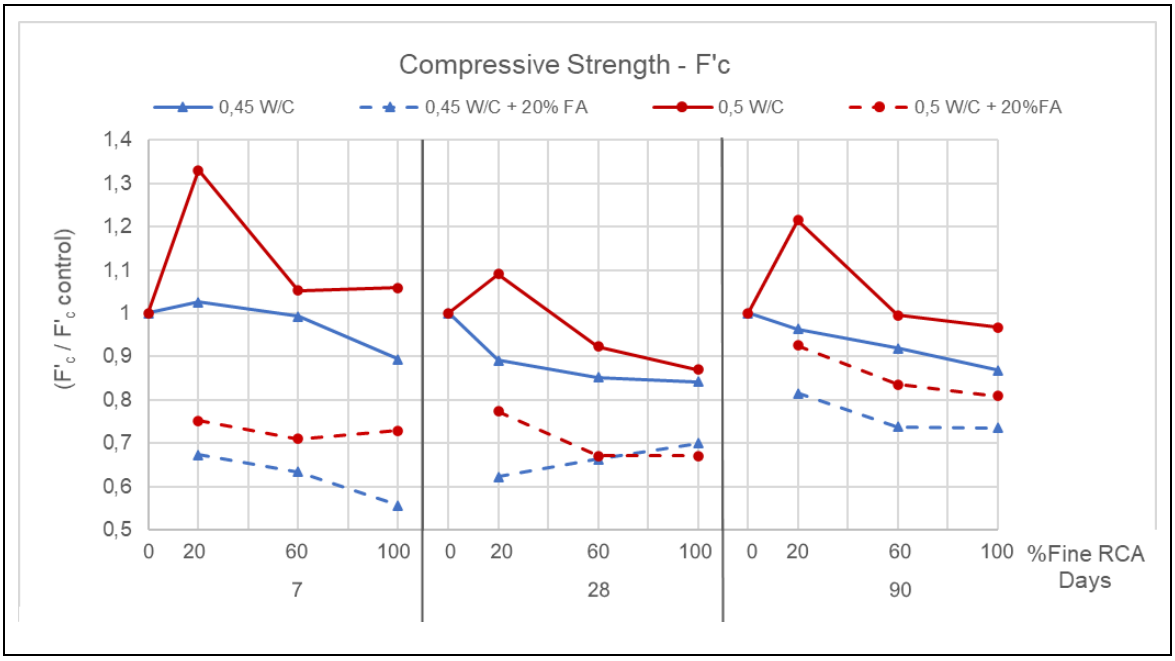

Figure 92 - Compressive strength results compared to natural aggregate control mixes.

At 90 days, 0,50 W/B mixtures presented similar strength values than natural concrete and at 7 days, mixtures containing 20%, 60% and 100% fine RCA presented an increase of 33%, 5% and 6% respectively in compressive strength when compared to 0% control mix. The possible increase of strength by incorporating fine RCA with a W/B ratio of 0.48 has also been described in other works, and attributed to proper assortment and processing in the aggregate production method [50], [54], [100]. A different study, indicated that the increase of strength for low replacement ratios of could be attributed to an improved microstructure of the Interfacial Transition Zone with increased bond strength between the new cement paste and particles [81].

Results also indicate that fly ash inclusion did not improve recycled concrete's compressive strength since both 0,50 W/B and 0,45 W/B mixtures with fine RCA and fly ash presented worst performance when compared to mixtures with only cement as binder material. This effect was more notorious at 7 days for a fine RCA replacement of 100% since mixes 28-RA100-FA20 and 21-RA100-FA20 presented a reduction of 44% and 27% respectively when compared to control mixes. Nevertheless, at 90 days, the negative effect of including fly ash was reduced, revealing the same low early strength effect that has been observed

by multiple authors in international researches [150]. These results are consistent with numerous studies that have shown that incorporating FA to mixes with fine RCA has a harmful effect in the compressive strength but may contribute to higher rates of resistance gain [68]. This is attributed to the delayed pozzolanic reaction that occurs between the FA and $Ca(OH)_2$ in RCA, which absorbs CaO and produces CSH which is the main contributor to strength development. Colombian studies have also obtained reduced compressive strengths when incorporating RCA and fly ash [145].

The strength development curve against specimen age for 0,45 W/B mixes is presented in Figure 93. From this figure, it is possible to identify that early age 7-day strength values for all concrete mixes are similar when not incorporating fly ash as a binder. At 28 days, only the control mix had achieved the strength design value of 28 MPa, however, at this age all recycled concrete mixes without fly ash achieved a strength higher than 25 MPa. At 90 days, all mixes with only cement as binder had surpassed the F'c 28 MPa design value and the mixes with fly ash and 20%, 60% and 100% fine RCA presented strengths of 28.48, 25,79 and 25,69 MPa respectively.

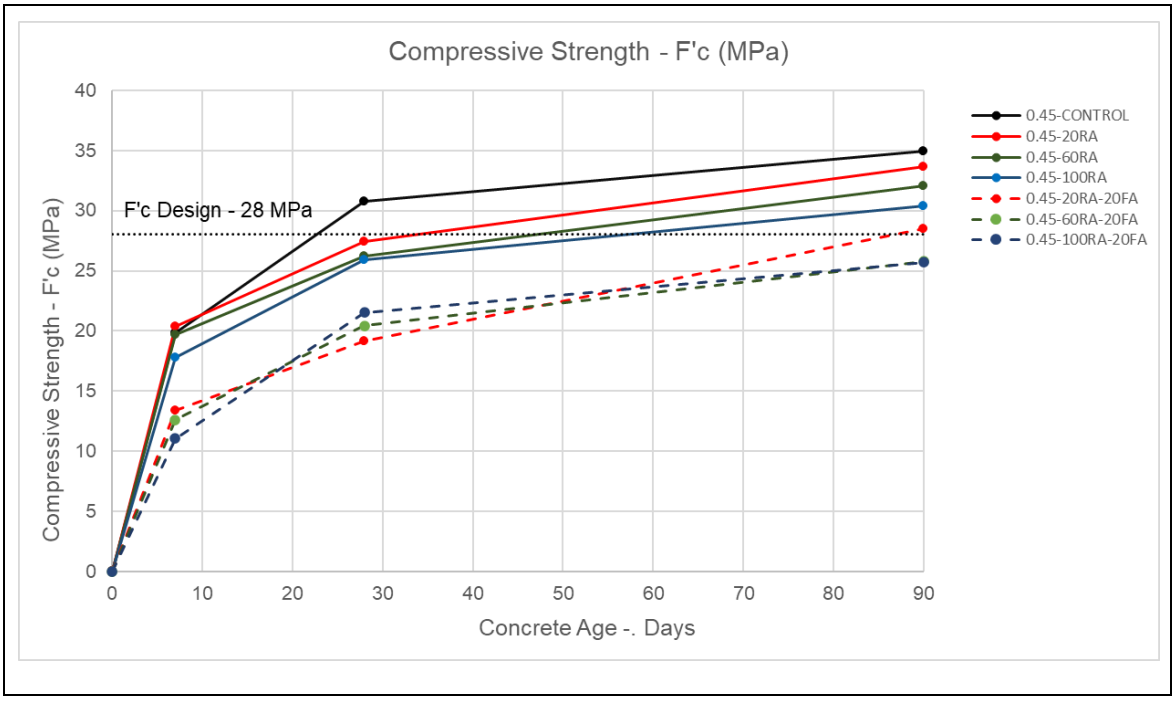

Figure 93 – Compressive Strength VS. Specimen age for 0,45 W/B mixes.

A similar analysis can be performed on the 0,50 W/B strength development curves, presented in Figure 94. These concrete mixes were designed for a compressive strength of 21 MPa. The highest F'c at all ages was obtained for the mix incorporating 20% RCA and only cement as binder which achieved a strength of 28,3 MPa at 28 days. At 28 days, all mixes with only cement as binder had surpassed the design F'c of 21 MPa and at 90 days, mixes made with both types of binder materials achieved strengths between 20,37 and 30,57 MPa, presenting a satisfactory behavior even for concrete specimens with 100% fine RCA and 20% fly ash.

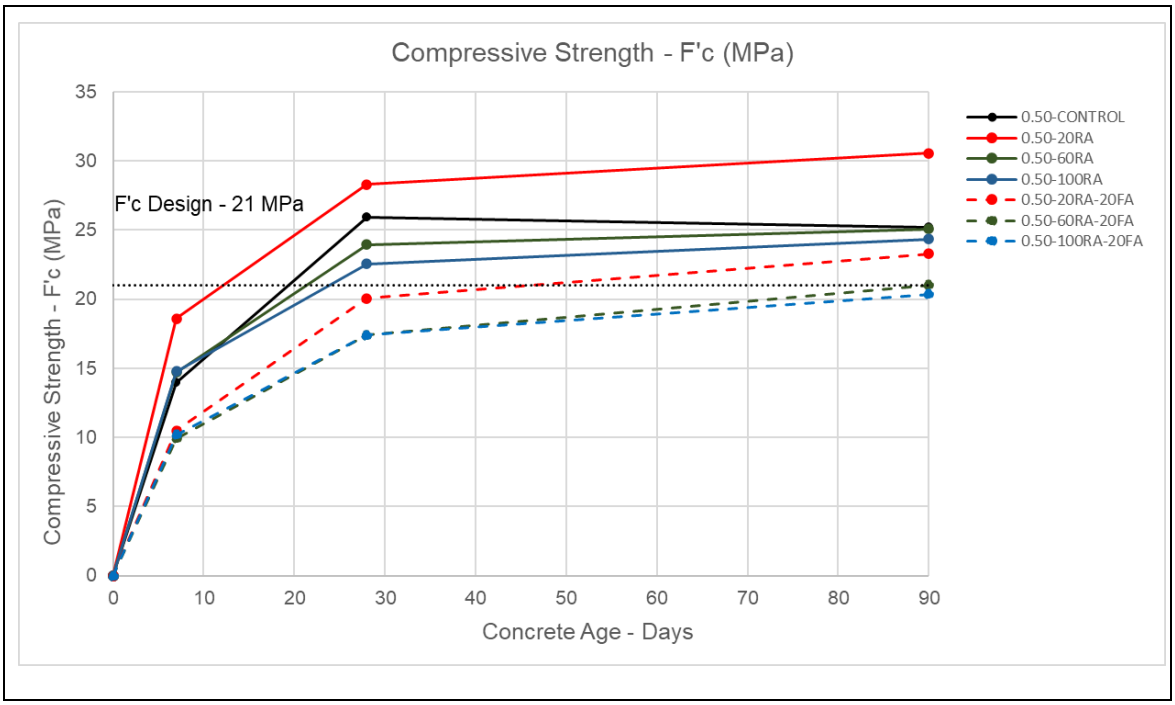

Figure 94 - Compressive Strength VS. Specimen age for 0,50 W/B mixes.

0,50 W/B mixes were less affected by the inclusion of fine RCA than 0,45 W/B mixes and even improved compressive strength for a 20% replacement ratio. As these aggregates have an important amount of cement attached as old mortar, these particles could hydrate and contribute to the binding strength of the microstructure, especially for mixes with a higher water content that could enhance the hydration of old attached mortar, as has been described by other researchers [54]. However, there appears to be a balance point for this positive effect, as higher fine RCA replacement ratios than 20% could drastically increase

water absorption and workability, resulting in more porous mixes with reduced mechanical properties. The effects of incorporating only fine RCA in the strength development of concrete specimens for both W/B is presented in Figure 95.

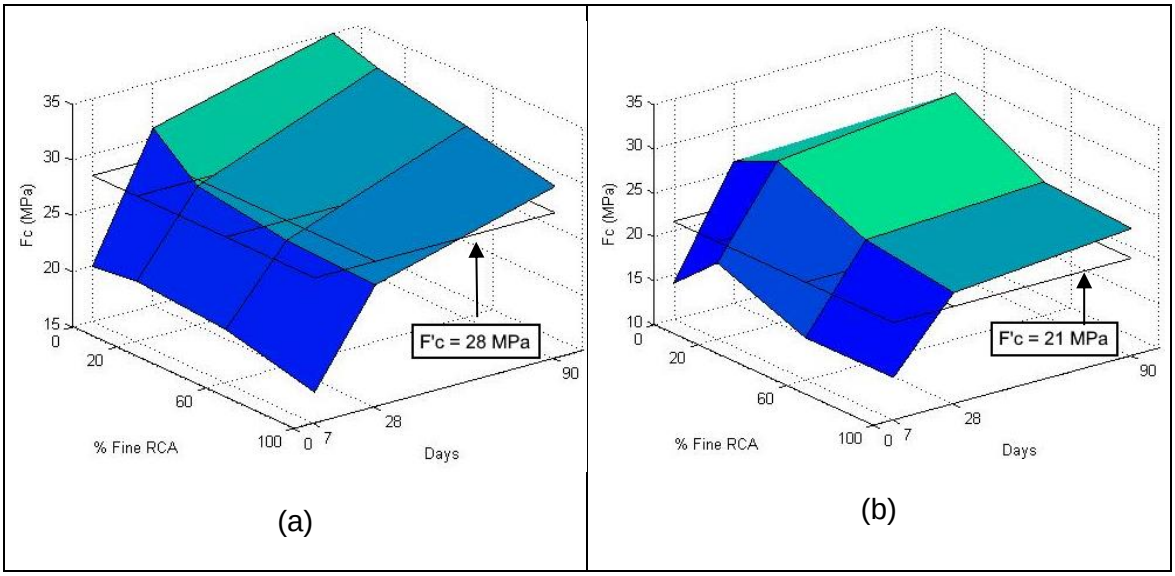

Figure 95 – Strength development curves for increasing ratios of fine RCA of (a) 0,45 W/B mixes. (b) 0,50 W/B mixes.

The inclusion of fly ash had a negative effect in compressive strength of all concrete mixes, specially at younger specimen ages. This effect has already been reported by other researchers [68] who had identified that high contents of fly ash reduce the water content in early hydration and cause a reduction in compressive strength due to a delayed strength development. This effect could be increased using commercially available cement in Colombia, which presented reduced density and higher fineness, probably due to the inclusion of fly ash during grinding.

Despite the overall reduction of F'c values for 0,45 W/B mixes when compared to 0% fine RCA control mixes, most specimens achieved and surpassed the 28 MPa design compressive strength at 90 days and most 0,50 W/B had already achieved the 21 MPa design strength at 28 days. This may indicate that fine RCA could replace natural fine aggregates in low replacement ratios (up to 20%) without significantly affecting strength. Replacement ratios higher than 20% could be formulated for concrete applications that do not require high early-age strengths if enough attention is paid to fine RCA attached mortar

content and concrete mixes are formulated with a sufficient W/B ratio to balance the aggregates absorption.

8.2 Modulus of Elasticity

The results obtained from the modulus of elasticity (Ec) test and the population standard deviation (σ) for each concrete mix at 90 days are summarized in Table 36. These test results were obtained from the statistical processing of the results of 3 concrete specimens for each concrete mix.

Mix	Mix	90 Days	
ID	Name	Ec (MPa)	σ (MPa)
1	28-CONTROL	20.115	228
2	28-RA20	21.630	1.654
3	28-RA60	20.474	610
4	28-RA100	17.991	759
5	28-RA20-FA20	19.392	1.123
6	28-RA60-FA20	15.995	2.584
7	28-RA100-FA20	16.579	1.104
8	21-CONTROL	21.110	399
9	21-RA20	20.737	1.592
10	21-RA60	19.906	215
11	21-RA100	17.530	390
12	21-RA20-FA20	17.994	430
13	21-RA60-FA20	17.418	1.128
14	21-RA100-FA20	14.706	301

Table 36 – Modulus of elasticity test results.

The effects in the modulus of elasticity of increasing the replacement ratio of fine RCA in concrete can be assessed in Figure 96. Results indicate similar behavior for 0,45 and 0,50 W/B mixes when incorporating 20% and 60% fine RCA, however, as higher ratios of fine RCA are employed, the modulus of elasticity decreases, especially for mixes containing

100% fine RCA. The negative effects of replacing 100% RCA aggregates is consistent with the observations made by different researchers [45].

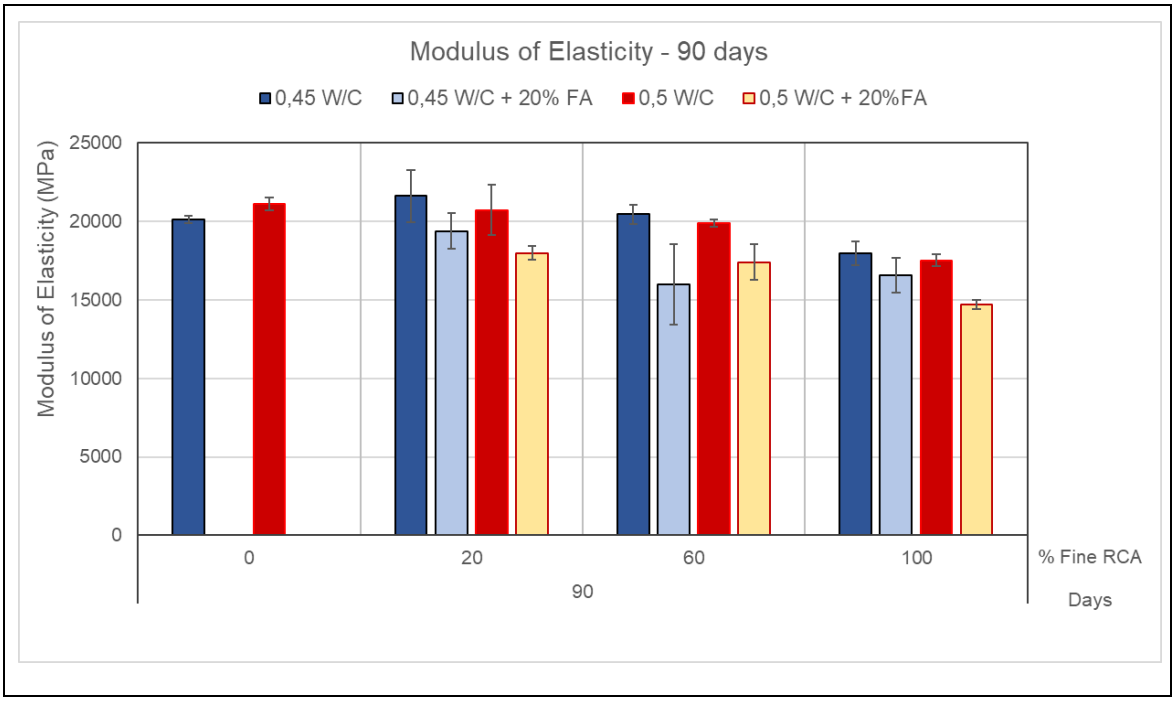

Figure 96 – Modulus of Elasticity (Ec) for increasing replacement ratios of fine RCA at 90 days.

In order to compare the effects of incorporating different ratios of fine RCA to natural aggregate concrete, the results were normalized dividing by the modulus of elasticity of control mixes for each W/B ratio. Table 37 presents a quantitative comparison between the modulus of elasticity results of each RAC mix and the conventional concrete control mixes.

Mix ID	Mix W/B	Mix Name	90 Days $\frac{E_c}{E_c ctrl}$
1		28-CONTROL	1,00
2		28-RA20	1,08
3		28-RA60	1,02
4	0,45	28-RA100	0,89
5		28-RA20-FA20	0,96
6		28-RA60-FA20	0,80
7		28-RA100-FA20	0,82
8		21-CONTROL	1,00
9		21-RA20	0,98
10		21-RA60	0,94
11	0,50	21-RA100	0,83
12		21-RA20-FA20	0,85
13		21-RA60-FA20	0,83
14		21-RA100-FA20	0,70

Table 37 – Modulus of Elasticity results compared to natural aggregate control mixes.

The results of this comparative analysis of modulus of are also presented graphically in Figure 97. For 0,45 W/B concrete mixtures without fly ash, incorporating 20% and 60% fine RCA increased the value of “Ec” by 8% and 2% respectively, while replacing 100% of natural aggregates reduced the modulus of elasticity by 11%. On the other hand, 0,50 W/B mixes presented reductions in “Ec” of 2%, 6% and 17% when incorporating 20%, 60% and 100% fine RCA, respectively.

These results indicate that the incorporation of fine RCA up to 60% did not have a significantly negative effect in the modulus of elasticity of 90-day-old concrete samples since only the concrete mixes made with exclusively fine RCA presented a noticeable reduction in modulus of elasticity. These results differ from most references who had reported a decreasing relation between the content of fine RCA and the modulus of elasticity of concrete samples [17]. This reduction is attributed to the fact that the modulus of elasticity depends on the stiffness of both the aggregates and the mortar and the incorporation of fine RCA reduces this mortar stiffness.

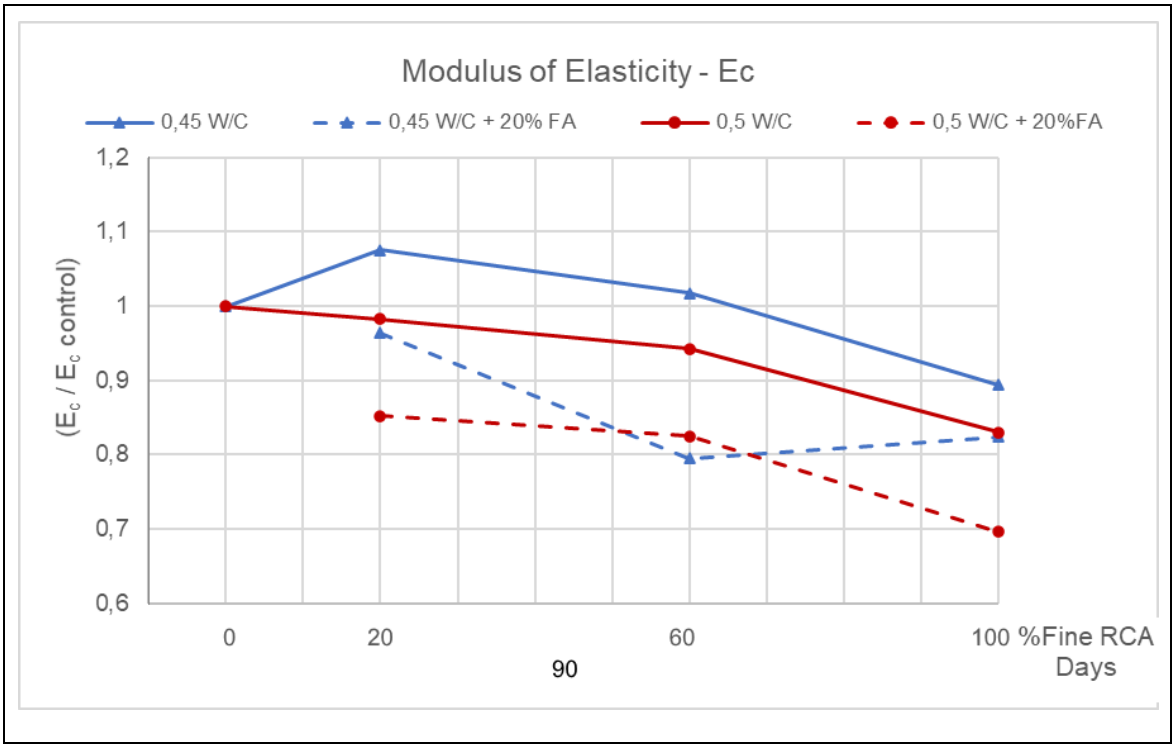

Figure 97 – Modulus of elasticity results compared to natural aggregate control mixes

Similarly, to the compressive strength tests, results indicated a reduction of the modulus of elasticity for RAC mixes including fly ash for all concrete mixes made with both 0,45 W/B and 0,50 W/B. All concrete mixes with fly ash presented worst performance than mixes made with the same replacement ratio of fine RCA but with cement as only binder material. Mix 21-RA100-FA20 presented the higher decrease in modulus of elasticity, having a reduction of 30% when compared to the control mix and 26% when compared to the mix with the same fine RCA content and no fly ash. These results are not consistent with the reported in international literature, where including levels of 25% of fly ash did not reduce the modulus of elasticity in recycled mixes with coarse aggregates [68], this would suggest that the negative effect in the modulus of elasticity of fly ash is more notorious when using fine RCA.

In Figure 98, the stress-strain curve for the specimen with the highest modulus of elasticity of each mix is presented. From this figure, it can be observed that the inclusion of 20% RCA increased the modulus of elasticity for both mix groups, and the worst performance was observed for mixes with high replacement of fly ash and fine RCA.

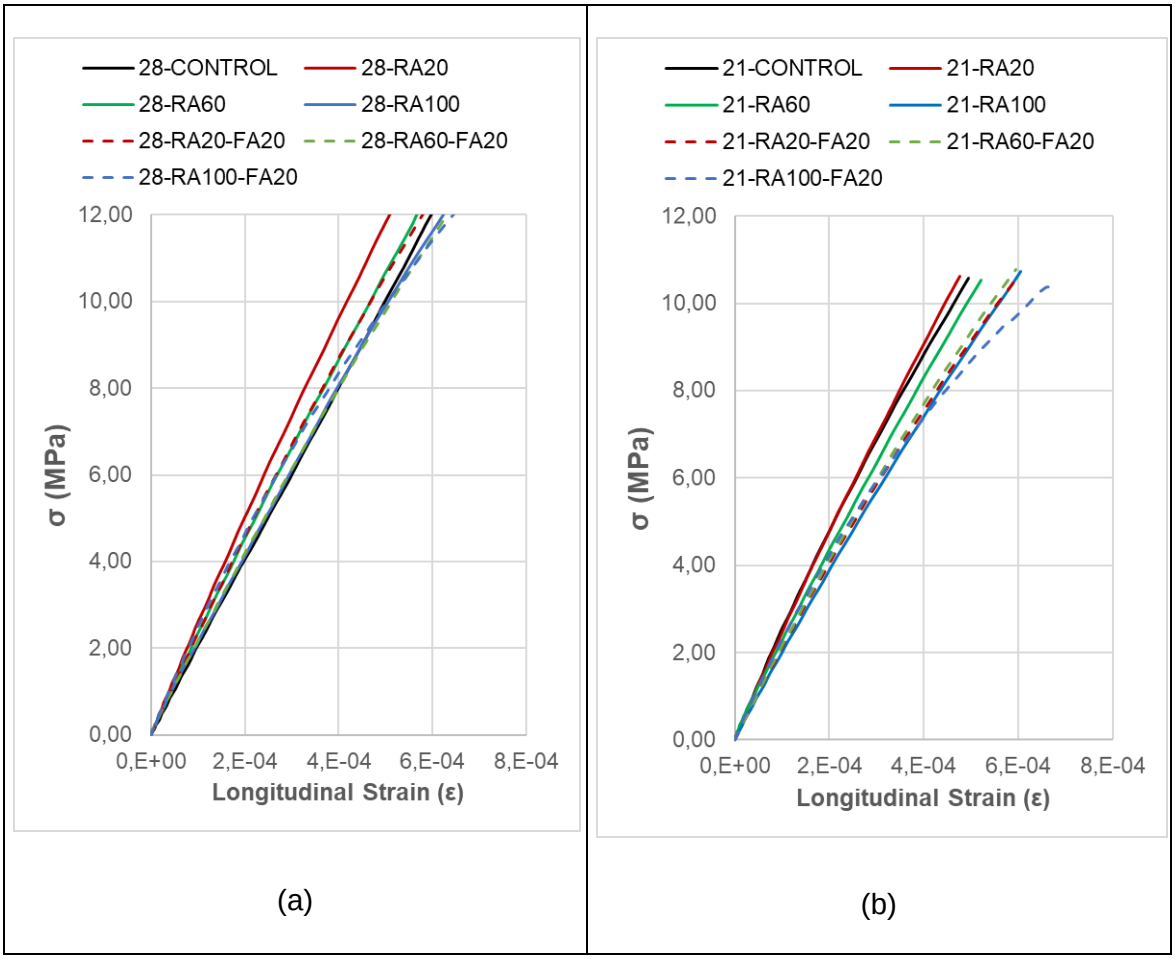

Figure 98 – Average Stress-Strain curves obtained for each concrete mix for (a) 0,45 W/B mixes and (b). 0,50 W/B mixes.

Since modulus of elasticity was only measured at 90 days, the modulus of elasticity development curve versus time could not be formulated. However, given that compressive strength results showed a positive effect of incorporating up to 20% fine RCA at early ages, a similar behavior could be expected for modulus of elasticity as both properties are highly correlated. Results show that all concrete mixes incorporating up to 60% fine RCA have a satisfactory mechanical performance with a similar modulus of elasticity than conventional concrete. Based only on the results obtained from modulus of elasticity and compressive strength, fine RCA could be used for structural concrete applications when a low-to-medium content of fine RCA is incorporated.

8.2.1 Factor for Modulus of Elasticity Estimation

According to the American Concrete Institute building code ACI318-19: "*Building Code Requirements for Structural Concrete"* and the Colombian code NSR-10: "*Reglamento Colombiano de Construcción Sismo Resistente"*, it is permitted to calculate and estimation of the modulus of elasticity using Equation 42.

$$E_c = k\sqrt{f_c'} \qquad \text{Equation 42}$$

Where f_c' is the compressive design strength of concrete and k is a coefficient which mainly depends on the aggregate type but is also affected by concrete constituents, mixture proportions, bond strength and age of concrete samples. Since the modulus of elasticity is an important design parameter in structural engineering which affects the calculated values for deflection, drifts and dynamic response, coefficient k was determined for each concrete mix using the average compressive strength results of 90 days. The obtained coefficient results and the values suggested by NSR-10 and ACI-318 are summarized in Table 38.

Factor for modulus estimation $k = E_c/\sqrt{f_c'}$ (MPa)			**Mix**	**Mix**	**90 Days**	
Type of Aggregate/Concrete	**NSR-10**	**ACI 318-19**	**ID**	**Name**	**Ec MPa**	**k**
Normal Weigth Concrete	4.700	4.700	1	28-CONTROL	20.115	3.801
			2	28-RA20	21.630	3.728
			3	28-RA60	20.474	3.614
Igneous	5.500	-	4	28-RA100	17.991	3.265
			5	28-RA20-FA20	19.392	3.634
			6	28-RA60-FA20	15.995	3.150
Metamorphic	4.700	-	7	28-RA100-FA20	16.579	3.271
			8	21-CONTROL	21.110	4.208
			9	21-RA20	20.737	3.751
Sedimentary	3.600	-	10	21-RA60	19.906	3.976
			11	21-RA100	17.530	3.552
			12	21-RA20-FA20	17.994	3.729
Any type	3.900	-	13	21-RA60-FA20	17.418	3.798
			14	21-RA100-FA20	14.706	3.258

Table 38 – Factor for modulus estimation "*k"* recommended values according to ACI-318 and NSR-10 and results for each concrete mix.

The calculated coefficients along with the values suggested by NSR-10 and ACI-318 are also shown in Figure 99. From these results it is possible to identify that *k* is similar to the suggested value for sedimentary aggregates in Colombia's building code (3.600), however, when compared to the value suggested by the American code (4.700), all of the mixes from both mix groups presented a lower coefficient. It is also noted that for the used aggregates and mix proportions, a reduction in factor *k* can be observed as the replacement ratio of fine RCA increases.

All mixes including full replacement of fine RCA presented a lower value for *k* than the indicated in the reference building codes. These results would suggest that the inclusion of fine RCA would reduce concrete's ability to deform despite of reaching the target compressive strength. Based on these results, for low replacement ratios up to 20%, the modulus of elasticity could be calculated with the same coefficient of estimation *k* than natural aggregate concrete without expecting a significant overestimation of this parameter. For medium or high replacement ratios, a more conservative factor could be formulated but this would result in larger structural elements in concrete buildings. Nevertheless, since only one type of recycled aggregate was tested, it was not possible to establish how the calculated coefficient is related to the aggregate type or the source concrete.

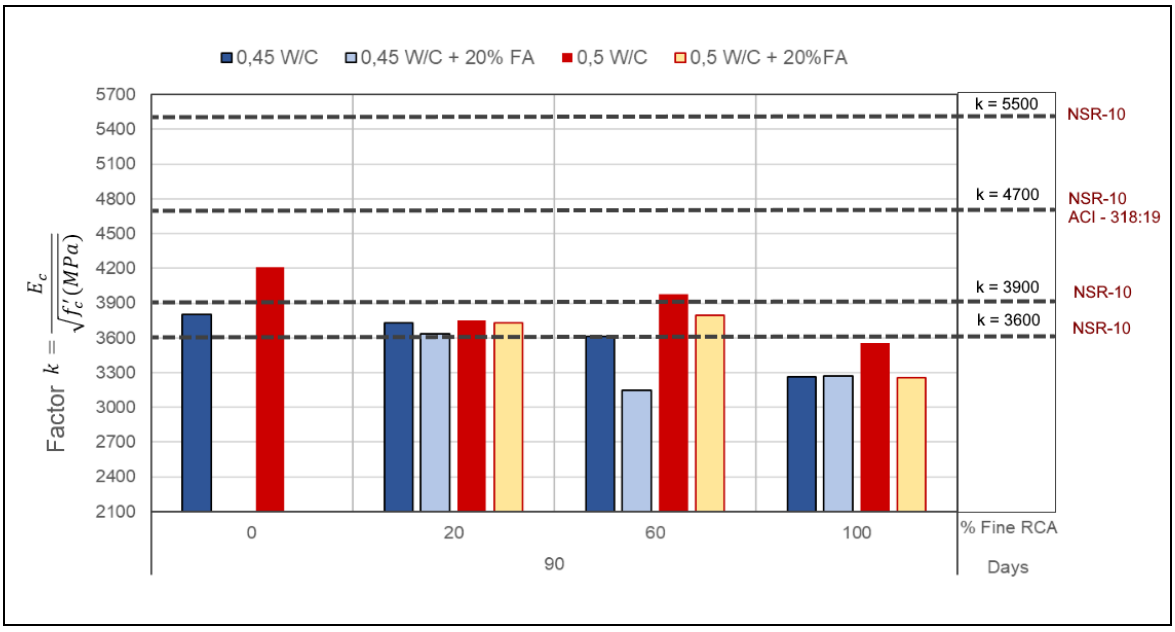

Figure 99 - Factor for modulus estimation "*k*" recommended values according to ACI-318 and NSR-10 and results for each concrete mix.

8.3 Apparent Concrete Density

The apparent density “D” of concrete samples was determined for specimens cured for 28 days and 90 days. The results obtained for this test after statistical analysis and the population standard deviation are presented in Table 39.

Mix	Mix	28 Days		90 Days	
ID	Name	D (g/cm^3)	σ (g/cm^3)	D (g/cm^3)	σ (g/cm^3)
1	28-CONTROL	2,42	6,0,E-03	2,43	6,3,E-03
2	28-RA20	2,47	4,7,E-03	2,42	1,4,E-02
3	28-RA60	2,46	1,6,E-02	2,39	3,7,E-03
4	28-RA100	2,47	1,7,E-03	2,37	4,5,E-03
5	28-RA20-FA20	2,41	5,2,E-03	2,39	3,9,E-03
6	28-RA60-FA20	2,49	8,3,E-03	2,37	3,9,E-03
7	28-RA100-FA20	2,49	1,1,E-02	2,36	8,2,E-03
8	21-CONTROL	2,55	3,8,E-03	2,39	1,2,E-02
9	21-RA20	2,53	1,2,E-02	2,35	9,4,E-03
10	21-RA60	2,50	8,8,E-04	2,30	4,7,E-03
11	21-RA100	2,32	1,1,E-02	2,32	2,5,E-03
12	21-RA20-FA20	2,52	6,4,E-03	2,36	4,7,E-03
13	21-RA60-FA20	2,49	3,0,E-03	2,35	3,6,E-03
14	21-RA100-FA20	2,30	2,0,E-02	2,34	5,6,E-03

Table 39 – Apparent density of concrete test results.

Figure 100 shows the effects in apparent density of increasing fine RCA content in concrete mixes for testing ages of 28 and 90 days. Results indicate at 90 days that concrete’s density is reduced as higher ratios of fine RCA are incorporated into the mix for both 0,45 W/B and 0,50 W/B mixes. From this figure, it is also possible to identify that fly ash reduced the apparent density of the 0,45 W/B mixes but increased it for 0,50 W/B mixes.

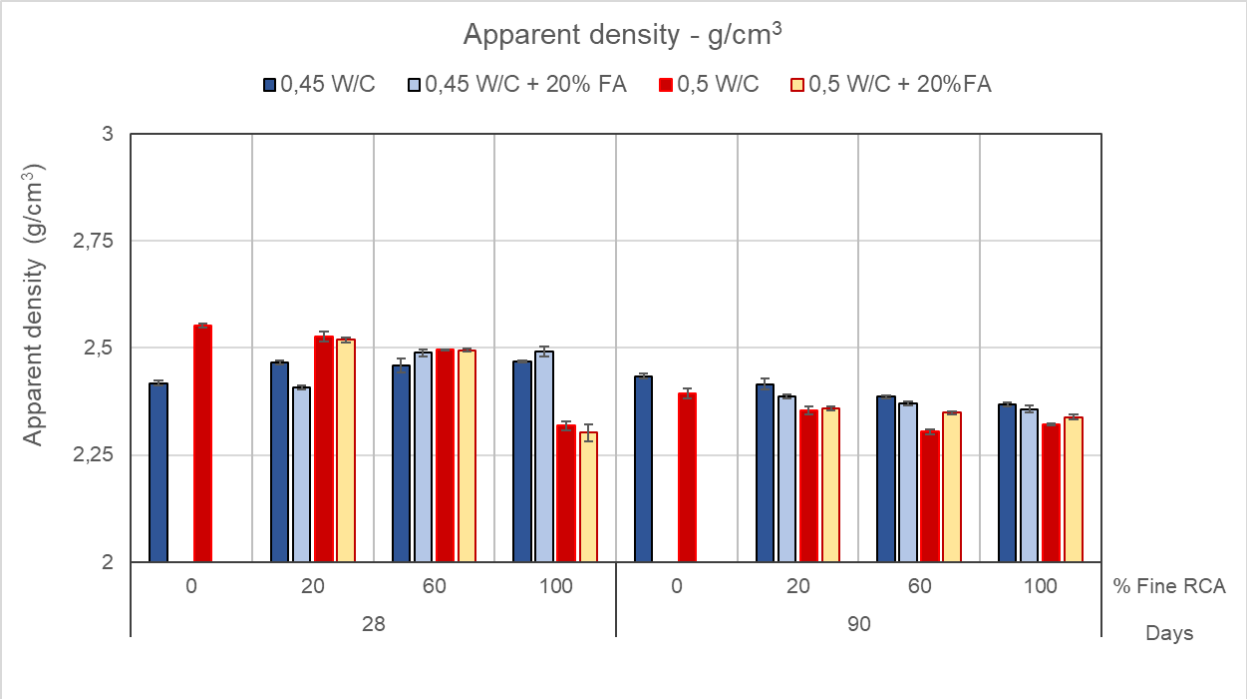

Figure 100 – Apparent density (ρ) for increasing replacement ratios of fine RCA at 90 days.

Similarly, to the mechanical performance tests, results were normalized by dividing each density value by the obtained for the 0,45 and 0,50 W/B mixes. These results are presented in Table 40.

Mix ID	Mix W/B	Mix Name	28 Days $\frac{D}{D_{ctrl}}$	90 Days $\frac{D}{D_{ctrl}}$
1		28-CONTROL	1,00	1,00
2		28-RA20	1,02	0,99
3		28-RA60	1,02	0,98
4	0,45	28-RA100	1,02	0,97
5		28-RA20-FA20	1,00	0,98
6		28-RA60-FA20	1,03	0,97
7		28-RA100-FA20	1,03	0,97
8		21-CONTROL	1,00	1,00
9		21-RA20	0,99	0,98
10		21-RA60	0,98	0,96
11	0,50	21-RA100	0,91	0,97
12		21-RA20-FA20	0,99	0,99
13		21-RA60-FA20	0,98	0,98
14		21-RA100-FA20	0,90	0,98

Table 40 – Apparent density results compared to natural aggregate control mixes

It is possible to identify a slight tendency of apparent density reduction for higher replacement ratios of fine RCA as incorporating 20%, 60% and 100% fine RCA caused a density reduction of 1%, 2%, and 3% respectively for 0,45 W/B mixes and 2%, 4% and 3% respectively for 0,50 W/B mixes.

Despite the observed behavior, as results indicate a high similarity, it is not possible to identify a clear detrimental effect of fine RCA incorporation in apparent density of concrete at 90 days using this method. From this analysis, high contents of fine RCA and even full replacement could be made in concrete mixes without significantly modifying its density. However, different researchers have reported a loss in concrete density for incremental RCA replacement ratios [51].

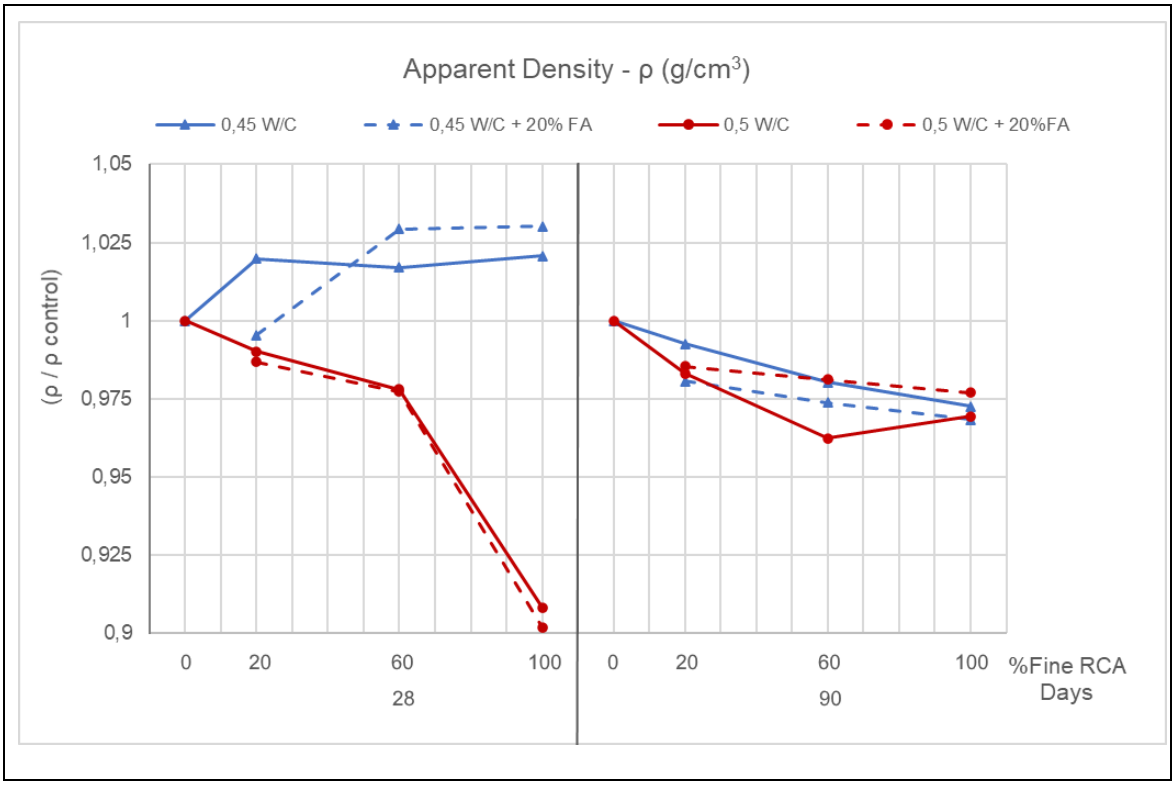

Figure 101 – Apparent density results compared to natural aggregate control mixes.

The results in Figure 101 reveal that fly ash had a different effect in RAC's apparent density for 0,45 W/B and 0,50 W/B mixes. For the lower ratio, mixes with 20%, 60% and 100% fine RCA and fly ash presented a reduction in density of approximately 1% when compared to mixes with the same replacement ratio but only cement as binder. For 0,50 W/B, mixes with fly ash and these replacement ratios presented a density increment of approximately 1%. Nevertheless, these variation values are so low that, for practical effects, no significant change can be assessed from incorporating fly ash at 90 days.

The results indicated in international literature have shown that fly ash can increase the apparent density of RAC, however no important change has been observed between RAC and conventional concrete in this work. Similar results have been compiled for low FA incorporation ratios [68], according to these studies, for low incorporation ratios of FA a favorable effect may be observed since this mineral fills the voids between particles, but for

higher incorporations, negative effects have been observed as the total voids between the FA particles (themselves) increase and the density decreases.

8.4 Concrete Porosity

Concrete Porosity (P) was measured for all concrete mixes after 28 days and 90 days of moist curing. The test results and the population standard deviation (σ) for each mix are presented in Table 41.

Mix	Mix	28 Days		90 Days	
ID	Name	Porosity %	σ %	Porosity %	σ %
1	28-CONTROL	18,70	0,15	18,67	0,53
2	28-RA20	18,60	0,35	19,03	0,44
3	28-RA60	21,20	0,16	21,08	1,00
4	28-RA100	23,25	0,54	23,26	0,05
5	28-RA20-FA20	17,39	0,04	19,70	0,19
6	28-RA60-FA20	25,36	0,30	21,66	0,32
7	28-RA100-FA20	27,37	0,18	23,36	0,59
8	21-CONTROL	22,92	0,43	18,49	0,22
9	21-RA20	22,03	0,32	18,63	0,32
10	21-RA60	24,44	0,07	20,74	0,06
11	21-RA100	24,63	0,02	20,77	0,48
12	21-RA20-FA20	24,32	0,68	19,61	0,17
13	21-RA60-FA20	25,52	0,41	21,53	0,41
14	21-RA100-FA20	19,93	0,14	22,87	0,61

Table 41 – Porosity of concrete test results.

These results are presented graphically in Figure 102. Results show an overall reduction in porosity in concrete mixes with a longer sample age and curing duration. An increase in concrete porosity can also be assessed for incremental values of fine RCA incorporation. As mechanical testing indicated a delayed effect of fly ash in concrete's properties, the 90-day measurements are considered to be a better indicative of this property, since significant microstructure changes from the hydration process can still be occurring in 28-day-old concrete specimens.

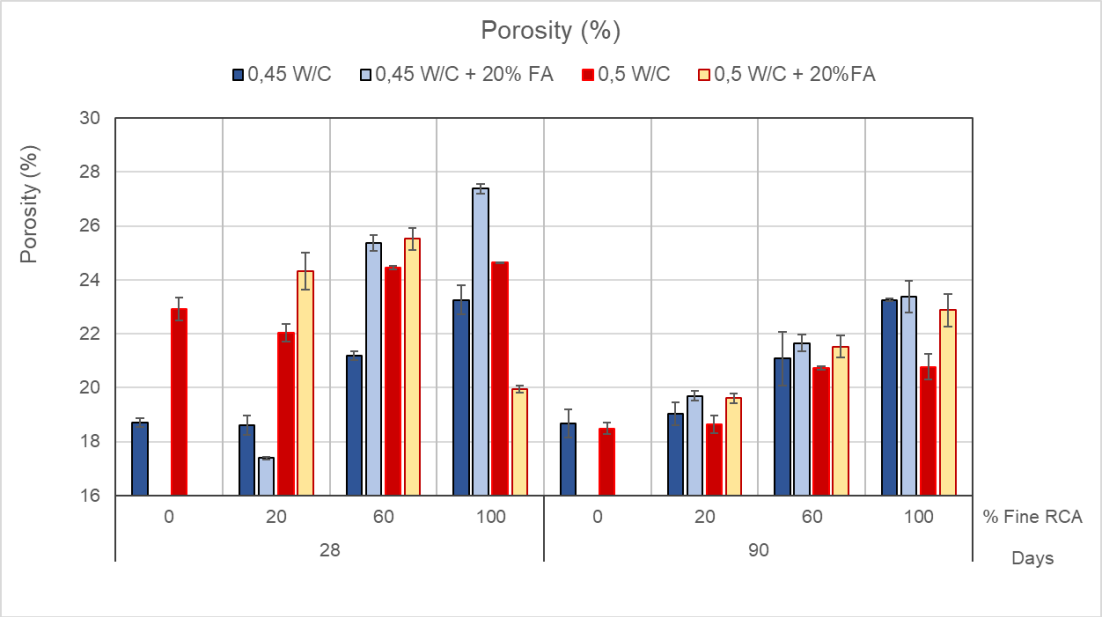

Figure 102 – Porosity of concrete values for increasing replacement ratios of fine RCA at 28 and 90 days.

The normalized results of concrete porosity at 28 and 90 days are presented in Table 42.Similarly to previous tests, these values are presented as a quantitative indicative of the performance of each concrete mix when compared to the mix without fine RCA and the same W/B ratio. Testing shows higher porosity for higher replacement levels of fine RCA. At 90 days, concrete mixes made only with fine RCA presented a porosity increase of 12% for 0,50 W/B and 25% for 0,45 W/B mixes. However, for both groups, replacing 20% of fine RCA increased porosity by less than 2% at 90 days. These results are consistent with the conclusions made by other researchers who have observed an increase in porosity for higher contents of fine RCA [66].

Mix ID	Mix W/B	Mix Name	28 Days $\frac{P}{P_{ctrl}}$	90 Days $\frac{P}{P_{ctrl}}$
1		28-CONTROL	1,00	1,00
2		28-RA20	0,99	1,02
3		28-RA60	1,13	1,13
4	0,45	28-RA100	1,24	1,25
5		28-RA20-FA20	0,93	1,05
6		28-RA60-FA20	1,36	1,16
7		28-RA100-FA20	1,46	1,25
8		21-CONTROL	1,00	1,00
9		21-RA20	0,96	1,01
10		21-RA60	1,07	1,12
11	0,50	21-RA100	1,07	1,12
12		21-RA20-FA20	1,06	1,06
13		21-RA60-FA20	1,11	1,16
14		21-RA100-FA20	0,87	1,24

Table 42 – Porosity of concrete results compared to natural aggregate control mixes

These results are also presented graphically in Figure 103. Observations indicate that fly ash incorporation increases the porosity of concrete for all tested replacement ratios of fine RCA. This increase is more evident for concrete mixes with 0,50 W/B ratio since at 90 days, the porosity value of mix 21-RA100-FA20 was 24% higher than the control mix and 12% higher than mix 21-RA100, made using only cement as binder. These results are not consistent with the reported by other researchers, who described a reduction in the porosity of concrete by including fly ash [68], however, it is important to notice that commercially sold Colombian cement is more processed, less dense, and usually includes a low replacement ratio of fly ash in its production process. This difference in cement quality could mean that a more optimal fly ash ratio could be determined for reducing the increment of porosity in concrete mixes.

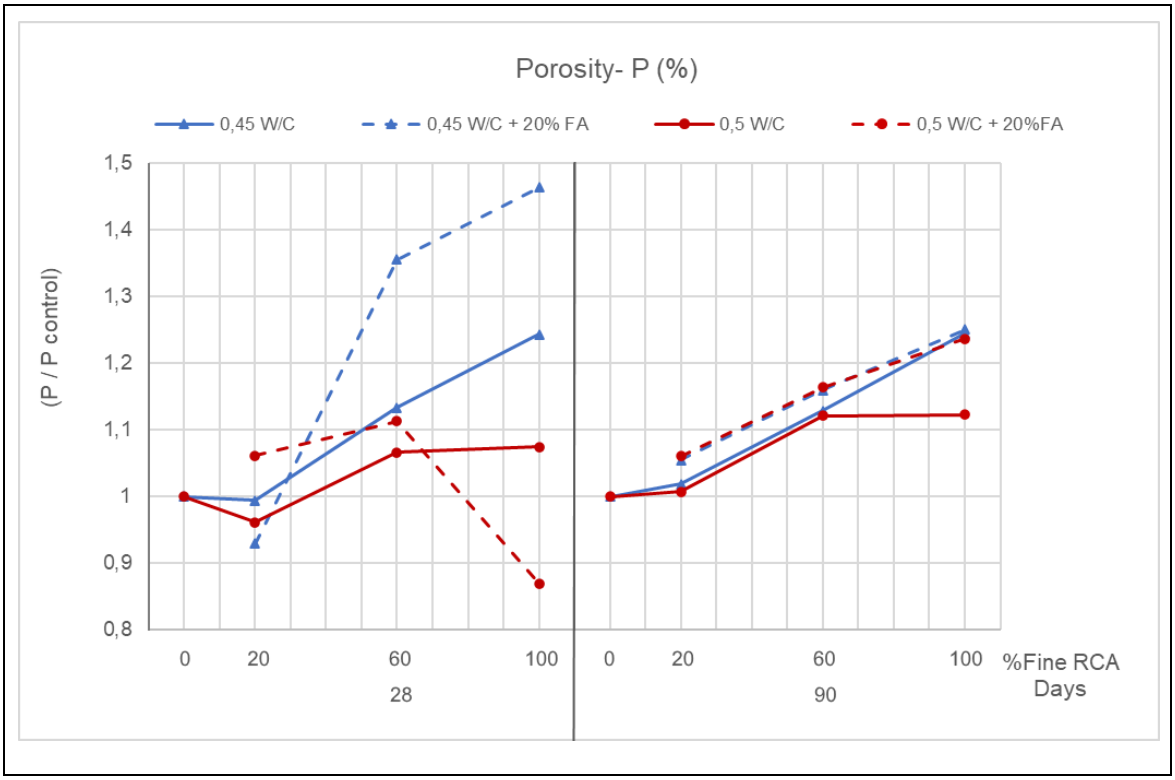

Figure 103 – Porosity of concrete results compared to natural aggregate control mixes.

From this test, it is possible to identify that incorporating fine RCA into concrete mixes will have a detrimental effect in the porosity of concrete for high replacement ratios, but an acceptable increase of porosity could be stablished and accomplished with ratios of incorporation between 20% and 40%. This acceptable increase in porosity should be highly correlated with a tolerable loss in mechanical and durability performance.

8.5 Water Absorption by Immersion

Water absorption by immersion “WA”, was determined for concrete samples after 28 days and 90 days of moist curing. The results obtained after the specified statistical analysis was performed are presented in Table 43.

Mix	Mix	28 Days		90 Days	
ID	Name	WA %	σ %	WA %	σ %
1	28-CONTROL	11,85	0,07	10,73	0,38
2	28-RA20	10,34	0,21	11,39	0,34
3	28-RA60	12,25	0,03	12,68	0,38
4	28-RA100	13,85	0,23	14,38	0,33
5	28-RA20-FA20	10,20	0,01	11,86	0,18
6	28-RA60-FA20	13,49	0,27	13,70	0,13
7	28-RA100-FA20	14,80	0,23	15,05	0,42
8	21-CONTROL	11,59	0,30	10,93	0,16
9	21-RA20	11,20	0,10	11,31	0,07
10	21-RA60	12,82	0,02	12,83	0,44
11	21-RA100	14,42	0,01	13,53	0,30
12	21-RA20-FA20	12,66	0,35	12,80	0,12
13	21-RA60-FA20	13,57	0,30	13,93	0,34
14	21-RA100-FA20	13,18	0,07	14,73	0,26

Table 43 – Water absorption by immersion of concrete test results.

From these results, which are also presented in Figure 104, higher water absorption values are observed for higher fine RCA replacement ratios for both 28 days and 90 days testing ages. The obtained values for 100% fine RCA are 14,38% for 0,45 W/B and 13,53% for 0,50 W/B. These results are similar to the obtained by another researcher where the measured water absorption for concrete specimens with 100% fine RCA incorporation and a W/B ratio of 0.48 was 16,5% [56].

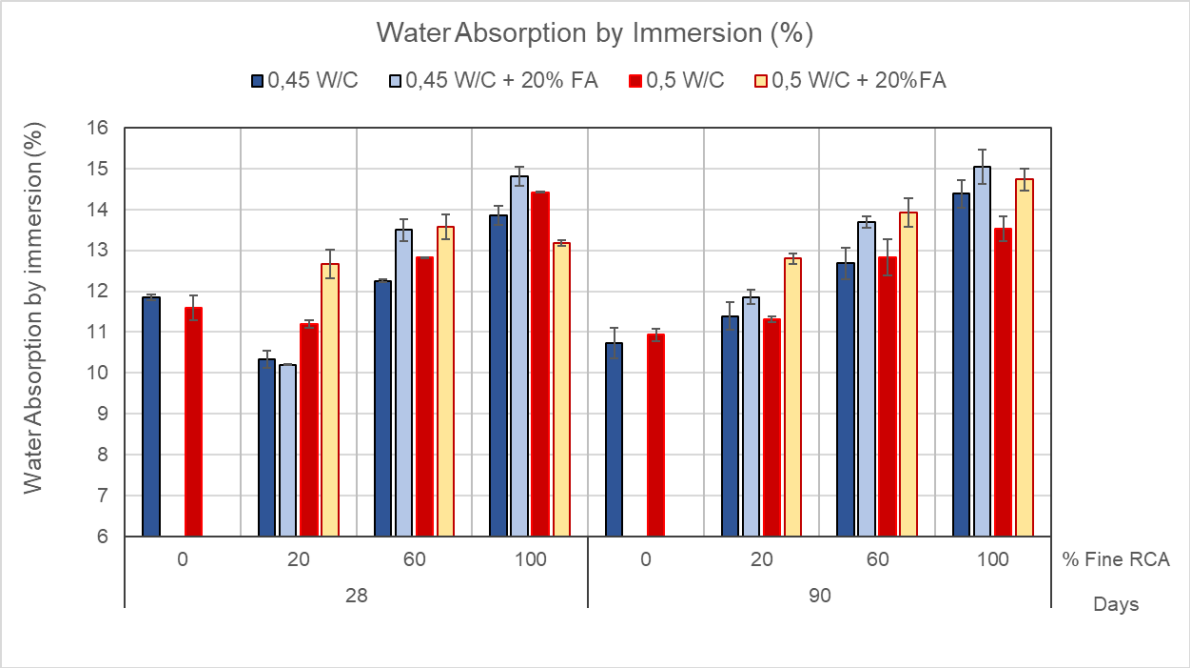

Figure 104 – Water absorption by immersion for increasing replacement ratios of fine RCA at 90 days.

Following the same procedure than previous testing, the results were normalized by dividing by the water absorption value obtained for both control mixes. From these results, presented in Table 44, it is possible to identify that including fine RCA increased water absorption in concrete specimens. Mixes with 20%, 60% and 100% fine RCA replacement presented a growth of 6%, 18% and 34% respectively for 0,45 W/B mixes and 4%, 17% and 24% respectively in 0,50 W/B mixes. Since water absorption by immersion is one of the most described properties in recycled aggregate concrete research internationally, as numerous researchers have observed its correlation with mechanical and durability performance, this growth in water absorption by including fine RCA is consistent with the observations made by other researchers [56].

Recycled aggregates have a high absorption value due to the presence of non-hydrated old-attached mortar, lower particle size with higher surface area and a more porous microstructure than natural aggregates, due to these factors, the resulting concrete mixes are expected to present higher water absorption [50].

Mix ID	Mix W/B	Mix Name	28 Days $\frac{WA}{WA_{ctrl}}$	90 Days $\frac{WA}{WA_{ctrl}}$
1		28-CONTROL	1,00	1,00
2		28-RA20	0,87	1,06
3		28-RA60	1,03	1,18
4	0,45	28-RA100	1,17	1,34
5		28-RA20-FA20	0,86	1,11
6		28-RA60-FA20	1,14	1,28
7		28-RA100-FA20	1,25	1,40
8		21-CONTROL	1,00	1,00
9		21-RA20	0,97	1,04
10		21-RA60	1,11	1,17
11	0,50	21-RA100	1,24	1,24
12		21-RA20-FA20	1,09	1,17
13		21-RA60-FA20	1,17	1,27
14		21-RA100-FA20	1,14	1,35

Table 44 – Water Absorption by Immersion results compared to natural aggregate control mixes.

The results from Table 44 are also presented graphically in Figure 105. When comparing to control mixtures at 28 days, 0,45 W/B concrete specimens presented lower water absorption values at 90 days than 0,50 W/B specimens. However, at 90 days water absorption was higher for 0,45 W/B mixes. This may be the result of the hydration of the old-attached mortar in more recycled particles at early ages due to free water content in 0,50 W/B mixes.

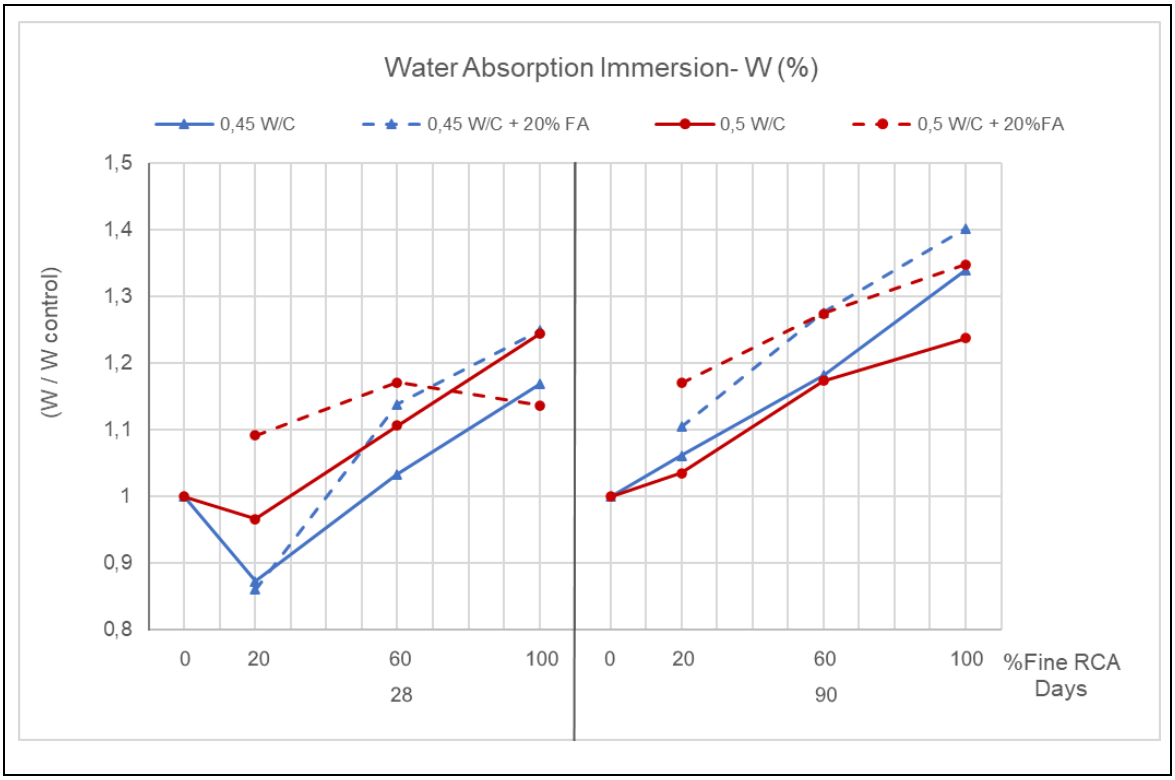

Figure 105 – Water absorption by immersion results compared to natural aggregate control mixes.

Since it has been noted in previous testing that fly ash presented a delayed effect in the hydration process of the studied concrete specimens, the effects of using it as a mineral addition in water absorption by immersion will be assessed after 90 days of curing. It was observed that fly ash increased water absorption by immersion for both groups of RAC mixes. The water absorption values for mixes 28-RA100-FA20 and 21-RA100-FA20 were 40% and 35% higher respectively than each control mix and 6% and 9% higher respectively than mixes made with the same ratio of fine RCA and only cement as binder. Similar behavior was observed for every other mix incorporating fine RCA. These results are not consistent with the work made by other researchers, who have reported that fly ash reduced water absorption when using fine RCA due to the filling of pores, pozzolanic reaction, and its positive effect in density [68], [82], the source of these differences may be the used binder material since it was noted than commercially available cement made in Colombia is less dense and more processed than the cement used in these research works.

Despite the negative effect of incorporating fine RCA in water absorption of concrete, the inclusion of 20% only increased water absorption by an average of 5% for both mix groups. Since water absorption is a property directly correlated with the mechanical and durability properties of concrete, an optimal replacement ratio that increases water absorption by and acceptable margin could be determined and implemented based on its correlation with other concrete properties.

8.6 Rapid Chloride Penetration Test – RCPT

Rapid Chloride Penetration Tests were performed in concrete specimens after 28 days and 90 days of moist curing. In this test, the total charge passed (C) in Coulombs is determined after a 6-hour testing period. The results for every concrete mix and the population standard deviation are summarized in Table 45.

Mix	Mix	28 Days		90 Days	
ID	Name	Charge Passed Coulombs	σ Coulombs	Charge Passed Coulombs	σ Coulombs
1	28-CONTROL	6.221	286	3.011	85
2	28-RA20	6.633	36	3.309	86
3	28-RA60	7.354	23	3.477	96
4	28-RA100	8.629	128	4.713	17
5	28-RA20-FA20	5.608	37	2.978	69
6	28-RA60-FA20	5.648	115	2.568	36
7	28-RA100-FA20	5.747	198	3.062	41
8	21-CONTROL	5.830	135	3.603	94
9	21-RA20	6.945	30	3.779	39
10	21-RA60	6.539	133	3.971	36
11	21-RA100	6.794	61	4.041	58
12	21-RA20-FA20	7.729	54	3.633	106
13	21-RA60-FA20	7.532	18	4.229	174
14	21-RA100-FA20	6.996	2	3.237	83

Table 45 – Rapid Chloride Penetration Test results.

These results are also presented in Figure 106, the classification limits defined in ASTM C1202 and presented in Table 29 are also included. It is possible to identify that the increase in fine RCA replacement increased the total charge passed in concrete specimens from both mix groups. A clear reduction in chloride migration was observed from 28 days to 90 days in all concrete mixes, for the first testing age, all concrete specimens presented a “High” chloride classification according to ASTM C1202 with values higher than 4000 Coulombs. At 90 days, a “Moderate” classification was obtained for most mixes with values between 2000 and 4000 Coulombs. These results are consistent with the work carried by other research programs, in which the inclusion of fine RCA increased the total charge passed [81].

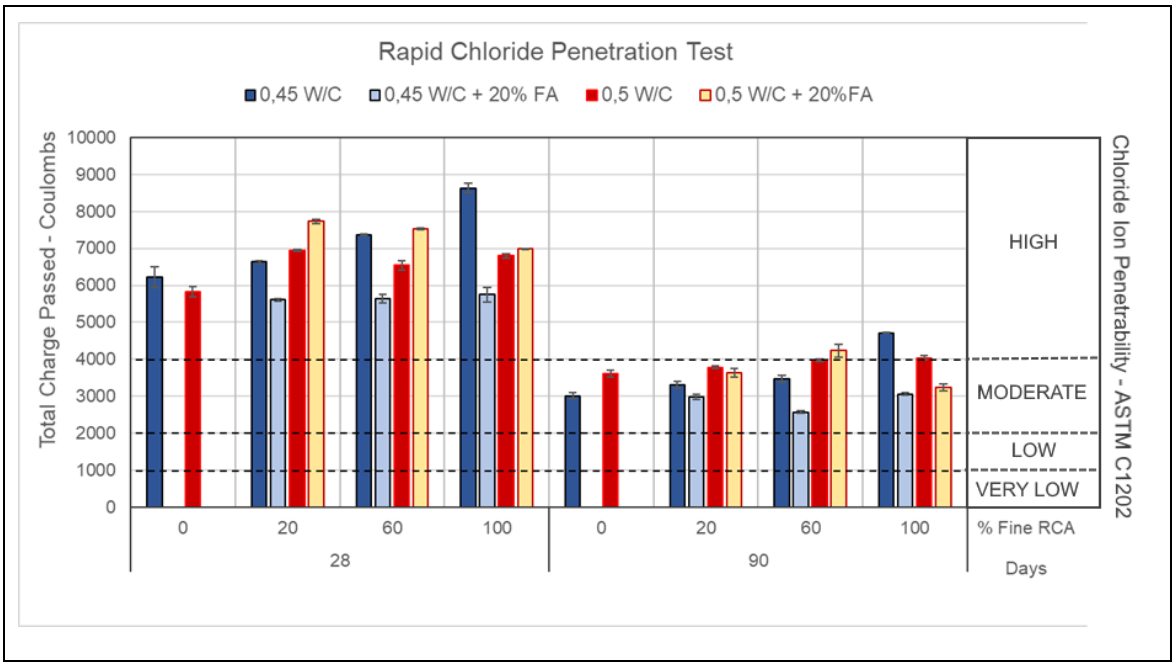

Figure 106 – Rapid Chloride Penetration Test for increasing replacement ratios of fine RCA at 28 and 90 days.

Following the same normalization procedure, comparative values between each obtained result and the value from the control mixes were obtained, these results are presented in Table 46 and graphically in Figure 107. Chloride migration testing results showed an increase in charge passed for both mix groups at 28 days and 90 days, however, the 90-day results are considered a more reliable indicator of durability of concrete since at 28

days the specimens are still relatively young and further testing indicated delayed hydration effects.

Mix ID	Mix W/B	Mix Name	28 Days $\frac{C}{C_{ctrl}}$	90 Days $\frac{C}{C_{ctrl}}$
1		28-CONTROL	1,00	1,00
2		28-RA20	1,07	1,10
3		28-RA60	1,18	1,15
4	0,45	28-RA100	1,39	1,57
5		28-RA20-FA20	0,90	0,99
6		28-RA60-FA20	0,91	0,85
7		28-RA100-FA20	0,92	1,02
8		21-CONTROL	1,00	1,00
9		21-RA20	1,19	1,05
10		21-RA60	1,12	1,10
11	0,50	21-RA100	1,17	1,12
12		21-RA20-FA20	1,33	1,01
13		21-RA60-FA20	1,29	1,17
14		21-RA100-FA20	1,20	0,90

Table 46 – Total charge passed results (C) compared to natural aggregate control mixes.

At 90 days, the incorporation of 20%, 60% and 100% fine RCA increased the charge passed by 10%, 15% and 57% for 0,45 W/B mixes respectively and 5%, 10% and 12% for 0,50 W/B respectively. Literature review shows that these results are consistent with other performed research in which the increase of fine RCA resulted in higher charge passed or electrical conductance [30], [84], [205].

The negative effect of incorporating fine RCA was more notorious for the 0,45 W/B mixes, especially for 100% incorporation of recycled aggregates. As it has been noted in previous testing, the free water content in the concrete mixes could have enhanced a hydration process of old-attached mortar which may have had a positive effect in the 0,50 W/B concrete's permeability to ions.

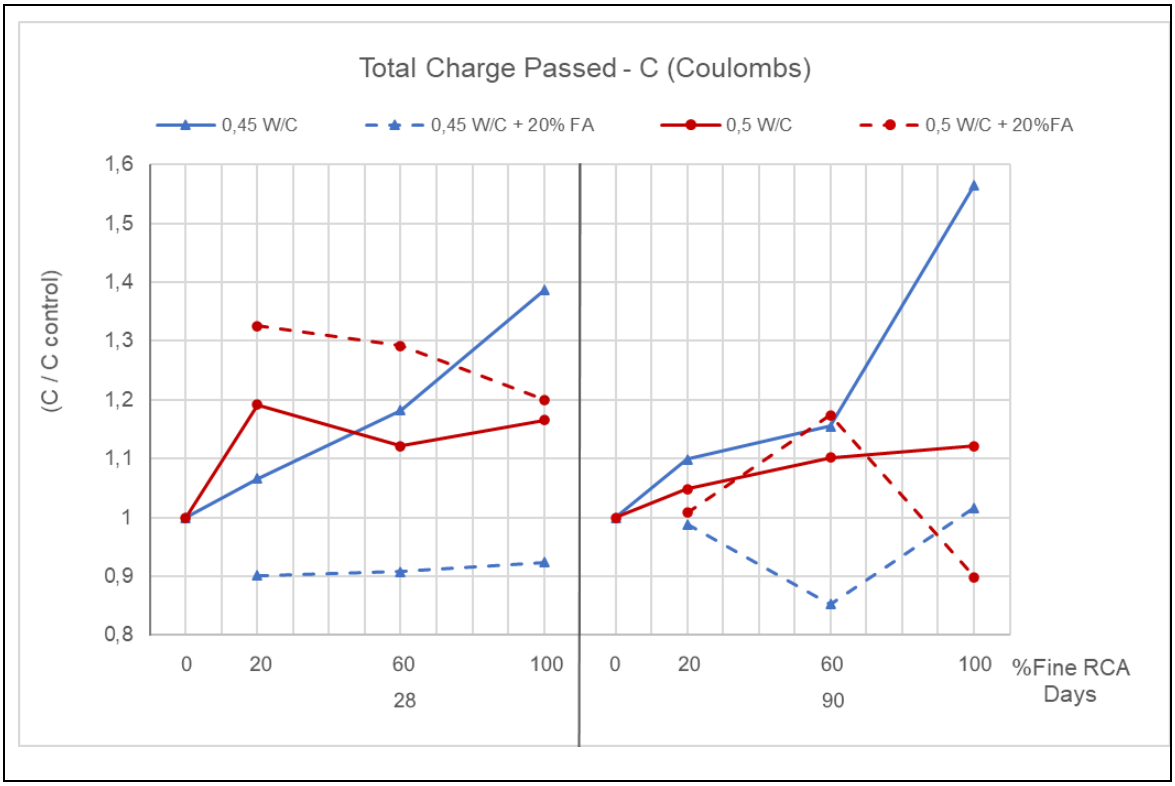

Figure 107 – Total charge passed results compared to natural aggregate control mixes.

In contrast with mechanical and physical property testing, the use of fly ash had a positive effect in the charge passed results at 90 days. For 100% fine RCA replacement, mix 28-RA100-FA20 presented a charge passed reduction of 55% and mix 21-RA100-FA20 presented a reduction of 22% when compared to their respective correspondent mixes without fly ash. When compared to the control mixes, the use of fly ash and full replacement of fine RCA resulted in similar charge passed values at 90 days, effectively being a mitigator for the detrimental effects of incorporating recycled aggregates. This effect was also noted for low and medium replacement ratios. Multiple researchers had already noted the positive effect of incorporating fly ash in the reduction of charge passed and in consequence, the reduction of chloride ion migration [68], [84], according to these works, since fly ash has a pozzolanic positive effect, a less permeable microstructure will be obtained from the reaction between FA and the $Ca(OH)_2$ in RCA. This research program obtained higher porosity and lower relative density for mixes including fly ash, from this point of view, the positive effect of fly ash in reducing electrical conductance of concrete would be more

dependent on the pozzolanic reactions of specimens with fly ash rather than on its filler properties alone. Based on these results, a low level of recycled aggregate replacement (up to 20%) could be implemented without significantly reducing the durability of concrete to chloride ion penetration and a medium content (up to 60%) could be implemented when using fly ash as a mitigator for the detrimental effects of incorporating fine RCA. The acceptable incorporation ratio should be defined based on the level of exposure to chloride ions and the required performance related to other mechanical and durability properties.

8.7 Non-Steady-State Chloride Migration Coefficient

The Non-Steady-State Chloride Migration Coefficient (D_{ns}) was determined for concrete specimens after 28 and 90 days of moist curing. This test is very similar to the rapid chloride migration test, but it is based on the measurement of the penetration depth of chloride ions directly evaluated in concrete specimens. The obtained results after statistical analysis and the population deviation standard are presented in Table 47.

Mix	Mix	28 Days		90 Days	
ID	Name	D_{ns} x 10^{-12} m^2/s	σ x 10^{-12} m^2/s	D_{ns} x 10^{-12} m^2/s	σ x 10^{-12} m^2/s
1	28-CONTROL	24,29	2,16	12,64	0,08
2	28-RA20	21,14	2,08	12,62	1,98
3	28-RA60	21,06	1,56	15,73	0,66
4	28-RA100	19,96	0,99	15,83	1,27
5	28-RA20-FA20	25,89	3,36	13,22	0,49
6	28-RA60-FA20	22,67	0,08	12,63	0,98
7	28-RA100-FA20	21,77	6,90	6,63	0,71
8	21-CONTROL	28,40	3,34	15,63	0,07
9	21-RA20	29,27	0,92	17,66	0,22
10	21-RA60	19,17	1,11	18,23	0,43
11	21-RA100	19,53	0,64	14,85	2,70
12	21-RA20-FA20	30,76	2,10	15,96	0,51
13	21-RA60-FA20	28,59	0,56	17,74	0,43
14	21-RA100-FA20	23,60	2,83	14,02	1,58

Table 47 – non-steady-state migration coefficient test results.

The calculated non-steady-state chloride migration coefficients are also presented in Figure 108. Comparably to the RCPT test, a clear reduction in chloride migration was observed from 28 days to 90 days in all concrete mixes. From this assessment, chloride migration will be reduced as the hydration process continues for older specimen samples and both this test and RCPT should be evaluated at long-term periods for durability assessment. At 28 days, the incorporation of fine RCA reduced D_{ns} for most RAC mixes, revealing a faster hydration process when compared to conventional concrete mixes, this effect has also been observed in previous mechanical testing. At 90 days, higher incorporation of fine RCA increased the non-steady-state migration coefficient of concrete specimens.

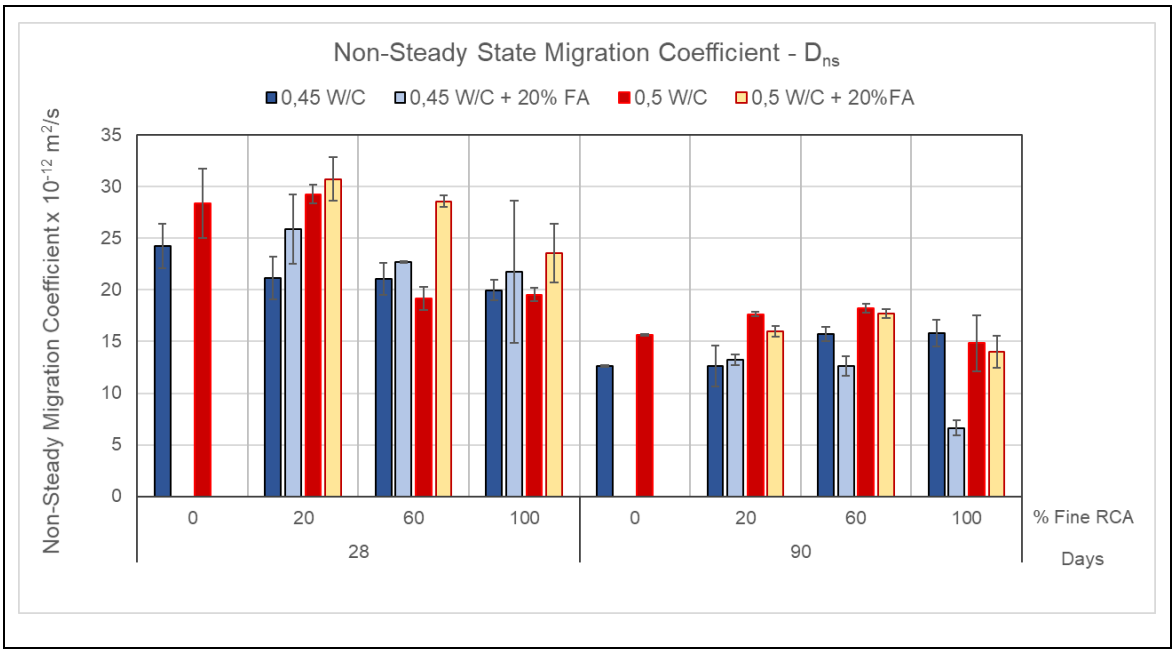

Figure 108 – non-steady-state migration coefficient for increasing replacement ratios of fine RCA at 28 and 90 days.

To compare the results from each mixture with its corresponding control mix, each result was divided by the result obtained for the mixture using only natural aggregates, as shown in Table 48 and Figure 109. Different behaviors in the increment of D_{ns} were observed for mixes of both 0,45 W/B and 0,50 W/B groups. For higher recycled aggregate replacement, mixes with the lower W/B ratio presented higher increments when compared to their control mixes at 90 days, as D_{ns} of mixes with 20%, 60% and 100% fine RCA presented increments

of 1%, 24% and 25% respectively for 0,45 W/B and 13%, 17% and a reduction of 5% respectively for 0,50 W/B mixes. From these values it was possible to identify that the migration coefficient did not change or even was reduced when comparing mixes with 60% and 100% fine RCA.

The obtained results are partially consistent with other researchers who also noted an increment in chloride penetration for higher replacement ratios but did not obtain lower values for the full inclusion of fine RCA [17], [45], [47], [51], [56]. According to these authors, as incorporating fine RCA produces a more porous microstructure with capillary connections, the resulting concrete mixes will be more permeable to chloride penetration.

Mix ID	Mix W/B	Mix Name	28 Days $\frac{D_{ns}}{D_{ns_{ctrl}}}$	90 Days $\frac{D_{ns}}{D_{ns_{ctrl}}}$
1		28-CONTROL	1,00	1,00
2		28-RA20	0,87	1,01
3		28-RA60	0,87	1,24
4	0,45	28-RA100	0,82	1,25
5		28-RA20-FA20	1,07	1,05
6		28-RA60-FA20	0,93	1,00
7		28-RA100-FA20	0,90	0,52
8		21-CONTROL	1,00	1,00
9		21-RA20	1,03	1,13
10		21-RA60	0,67	1,17
11	0,50	21-RA100	0,69	0,95
12		21-RA20-FA20	1,08	1,02
13		21-RA60-FA20	1,01	1,14
14		21-RA100-FA20	0,83	0,90

Table 48 – non-steady-state migration coefficient results (D_{ns}) compared to natural aggregate control mixes.

From the 90-day results, it was also noted that the inclusion of fly ash had a positive effect of reducing D_{ns} of every RAC mix. When including fly ash and 20%, 60% and 100% fine RCA, the migration coefficient was reduced by 11%, 3% and 5% respectively for 0,50 W/B mixes while the 0,45 W/B group also presented a noticeable reduction, especially for 60% and 100% replacement ratios. This positive effect is consistent with the results reported by other researchers, who also obtained lower values of D_{ns} for RAC mixes incorporating

incremental ratios of fine RCA and fly ash [68]. According to these works, fly ash reacts with $Ca(OH)_2$ and produces water insoluble hydration products that reduce permeability by filling voids, resulting in a denser microstructure with less flowable paths for chloride migration.

This positive effect has also been noted by other authors using coarse RCA who reported a decrease from approximately $15x10^{-12}$ m^2/s to $5x10^{-12}$ m^2/s for mixes incorporating 100% recycled aggregates and 30% fly ash, revealing very similar values to the obtained in this work regardless of the aggregate size distribution [38].

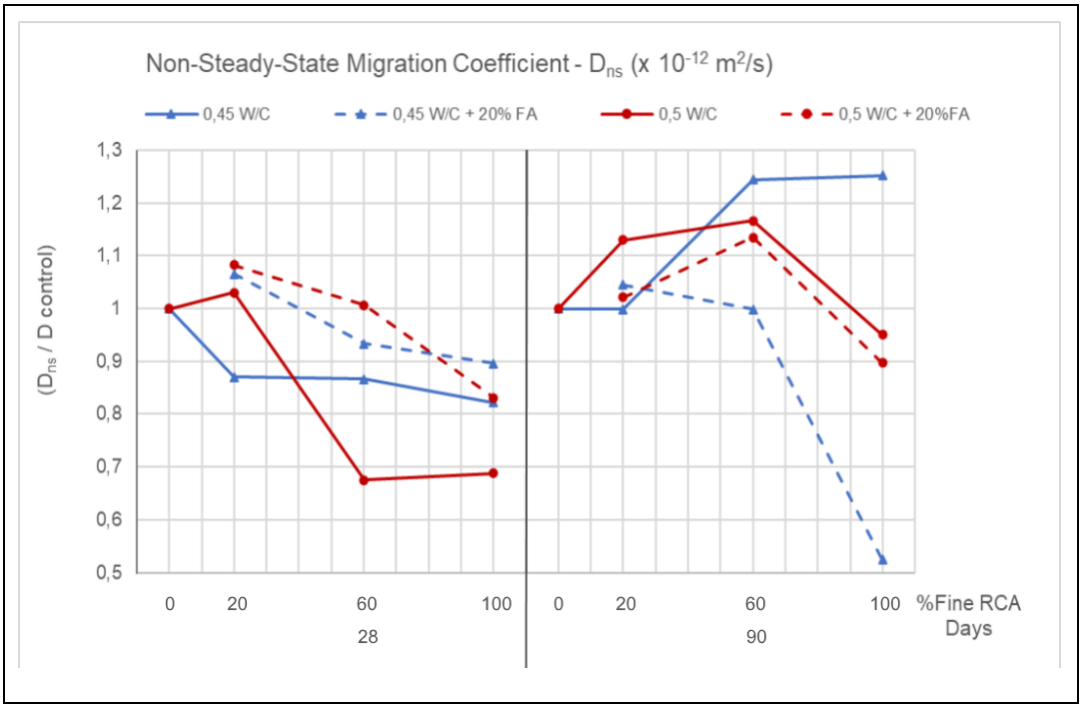

Figure 109 - non-steady-state migration coefficient results (D_{ns}) compared to natural aggregate control mixes.

In this research program, fly ash did not improve the apparent density of concrete specimens nor its mechanical properties, but it was favorable for the reduction of both the total charge passed and the NSTMC. This could mean that the enhancement of chloride ion resistance due to the incorporation of fly ash could be more related to a change in concrete's chemical composition or the reduction of its capillarity than the overall densification of the specimen's microstructure.

Based on these results, a low replacement ratio of recycled aggregates (up to 20%) could be implemented without increasing the permeability of chloride ions in concrete mixes. Higher ratios up to 60% could be also implemented if fly ash is used as a mineral addition and the negative mechanical effects are considered in the mix design process. While replacing 100% and using fly ash reduced the non-steady-state migration coefficient, this effect could not be observed in fine RCA from different sources and should be further assessed.

8.8 Concrete Electrical Impedance

The electrical impedance of concrete specimens cured in corrosive conditions was tested during 4 months as a parameter for the calculation of steel polarization resistance and corrosion rate. While these results are not a part of the experimental program, the obtained impedance values for a frequency of 10 kHz are presented in Table 49, as they give an indicator of the hydration process and permeability reduction in concrete specimens. The electrical resistivity, defined as the resistance per unit of length (Ω m) should also be determined since its value is obtained considering the specimens dimensions which allows direct comparison with results from other works. However, the used experimental setup does not allow to stablish a clear concrete geometry were the electrical current flows and hence the impedance value is presented only as an indicator.

Mix	Mix	28 Days		56 Days		90 Days		120 Days	
ID	Name	Ω Ohm	σ Ohm	Ω Ohm	σ Ohm	Ω Ohm	σ Ohm	Ω Ohm	σ Ohm
1	28-CONTROL	316,35	2,87	514,20	55,01	680,87	4,06	864,30	44,03
2	28-RA20	255,68	12,07	419,36	32,31	622,25	45,48	761,95	60,25
3	28-RA60	233,51	10,80	370,75	19,41	577,30	25,92	691,68	36,16
4	28-RA100	274,48	5,12	328,96	16,70	461,28	8,34	567,55	35,31
5	28-RA20-FA20	264,85	10,27	352,38	22,14	567,77	57,69	835,21	48,19
6	28-RA60-FA20	265,84	14,41	420,16	20,06	567,15	22,69	836,48	5,13
7	28-RA100-FA20	261,26	1,19	383,20	13,98	506,21	21,40	713,99	26,82
8	21-CONTROL	262,47	25,83	364,87	34,90	462,61	40,19	583,74	51,48
9	21-RA20	274,88	0,26	476,11	27,63	541,54	45,29	624,46	58,69
10	21-RA60	274,05	2,51	405,68	12,46	477,87	9,09	548,58	9,45
11	21-RA100	222,48	3,34	383,93	9,18	486,49	7,78	539,14	14,82
12	21-RA20-FA20	194,46	12,02	385,32	7,18	535,44	10,73	609,21	39,11
13	21-RA60-FA20	186,51	2,48	352,37	10,00	502,50	6,19	587,28	3,95
14	21-RA100-FA20	238,35	0,55	337,86	7,25	481,38	4,23	588,78	8,83

Table 49 – Electrical impedance (Ω) test results.

These results are also shown in Figure 110. As expected, natural aggregate concrete mixes with lower W/B ratios presented higher electrical resistance. The incorporation of fine RCA modified concrete impedance depending on the W/B ratio, as 0,45 W/B mixes 28-RA20, 28-RA60 and 28-RA100 presented a clear reduction in electrical impedance at all testing ages as the replacement ratio of fine RCA increased. On the other hand, 0,50 W/B mixes 21-RA20 and 21-RA60 presented similar impedance at all testing ages while a slight reduction was observed for mix 21-RA100.

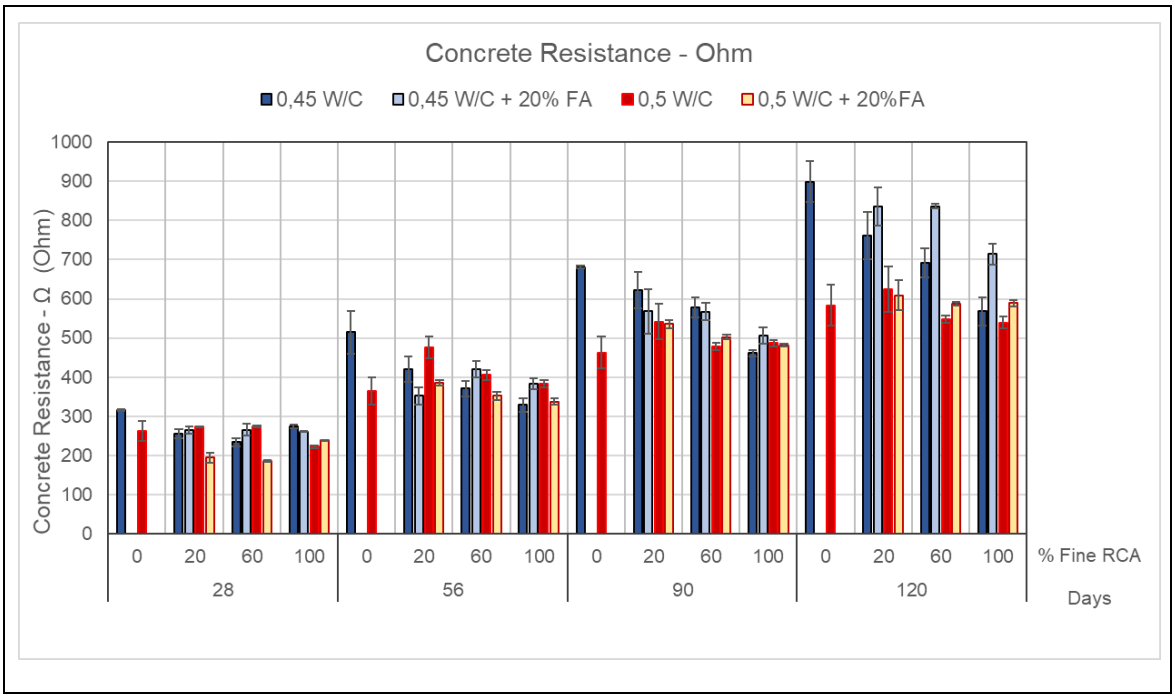

Figure 110 – Concrete electrical impedance for increasing replacement ratios of fine RCA at 28 and 90 days.

Figure 111 presents the electrical impedance development curve for both groups of concrete mixes. From these results, it is possible to identify that concrete impedance increased with the specimen age despite the corrosive curing conditions. After 120 days, a linear development of impedance was observed for the 0,45 W/B mixes and no sign of a reduction in electrical resistance gain rate seemed to occur. On the other hand, the impedance of 0,50 W/B mixes appeared to develop electrical resistance during the first 2 months at a faster rate. At 120 days, a maximum impedance value of approximately 624 ohms was observed for 0,50 W/B mix 21-RA20 while the 0,45 W/B group developed a maximum value of approximately 864 ohms for the control mix 28-CONTROL.

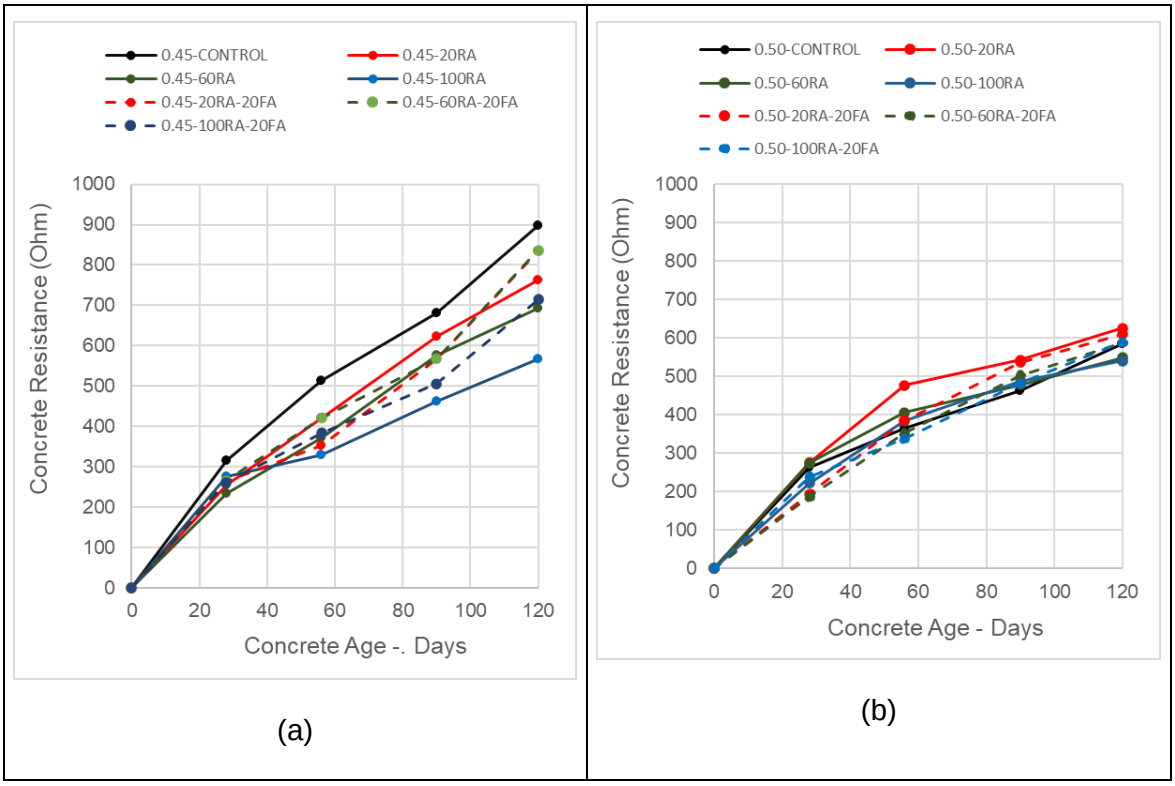

Figure 111 – Concrete electrical impedance development curves for (a) 0,45 W/B mixes. (b) 0,50 W/B mixes.

To perform a more quantitative comparison between control mixes and concrete containing fine RCA and fly ash, Table 50 presents the results of dividing the values by the respective impedance obtained for each control mix. As discussed before, measurements at 28, 56 and 90 days indicated that the inclusion of fine RCA increased electrical resistance for 0,50 W/B mixes but reduced it for the 0,45 W/B mixes. At 120 days, all mixes except 21-RA20 presented lower impedance than their respective control mixes. As the effects of chloride migration and corrosion would be noticeable in field conditions at long-term, the results obtained for 120 days are considered the best indicator of durability performance in the studied concrete mixes.

Mix	Mix	28 Days	56 Days	90 Days	120 Days
ID	Name	$\frac{\Omega}{\Omega_{ctrl}}$	$\frac{\Omega}{\Omega_{ctrl}}$	$\frac{\Omega}{\Omega_{ctrl}}$	$\frac{\Omega}{\Omega_{ctrl}}$
1	28-CONTROL	1,00	1,00	1,00	1,00
2	28-RA20	0,81	0,82	0,91	0,85
3	28-RA60	0,74	0,72	0,85	0,77
4	28-RA100	0,87	0,64	0,68	0,63
5	28-RA20-FA20	0,84	0,69	0,83	0,93
6	28-RA60-FA20	0,84	0,82	0,83	0,93
7	28-RA100-FA20	0,83	0,75	0,74	0,79
8	21-CONTROL	1,00	1,00	1,00	1,00
9	21-RA20	1,05	1,30	1,17	1,07
10	21-RA60	1,04	1,11	1,03	0,94
11	21-RA100	0,85	1,05	1,05	0,92
12	21-RA20-FA20	0,74	1,06	1,16	1,04
13	21-RA60-FA20	0,71	0,97	1,09	1,01
14	21-RA100-FA20	0,91	0,93	1,04	1,01

Table 50 – Electrical impedance (Ω) results compared to natural aggregate control mixes.

The results from Table 50 are presented graphically in Figure 112. At 120 days, 0,45 W/B mixes incorporating 20%, 60% and 100% of fine RCA presented a reduction in electrical impedance of 15%, 23% and 37% respectively. For 0,50 W/B mixes, the addition of 20% fine RCA increased the electrical impedance by 7% while the results of the mixes with 60% and 100% decreased 6% and 8% respectively. This indicates that concrete impedance is directly affected by the presence of free water in the mix, and when using fine RCA, the loss of electrical resistance reported by other authors [47], [82], could be compensated by designing concrete mixes with slightly higher W/B ratios.

The use of fly ash seemed to have different effects depending on the specimen age, at 28 days, it only clearly improved the impedance of the 0,45 W/B mix group, while at 120 days, bot mix groups were benefited by using this mineral addition. At 120 days, mixes 28-RA20-FA20, 28-RA60-FA20 and 28-RA100-FA20 presented an increase in electrical impedance of 8%, 16% and 13% when compared to their correspondent mixes without fly ash. These improvement values compared to mixes without fly ash were 3%, 7% and 9% for the 0,50 W/B mixes incorporating 20%, 60% and 100% fine RCA respectively. These results confirm that fly ash may have a delayed positive effect in recycled aggregate concrete mixes,

representing an effective mitigator for durability-related issues. According to other works, the resistivity of concrete increases for greater incorporations of FA due to the chemical composition of FA (High amount of SO_2 and Al_2O_3 and low content of CaO), which at long-term modifies the original microstructure of concrete due to the kinetic reaction between the soluble ions, the particles and the hydrates; reducing in consequence the pore diameter and the ionic mobility in the electrolytic solutions [82].

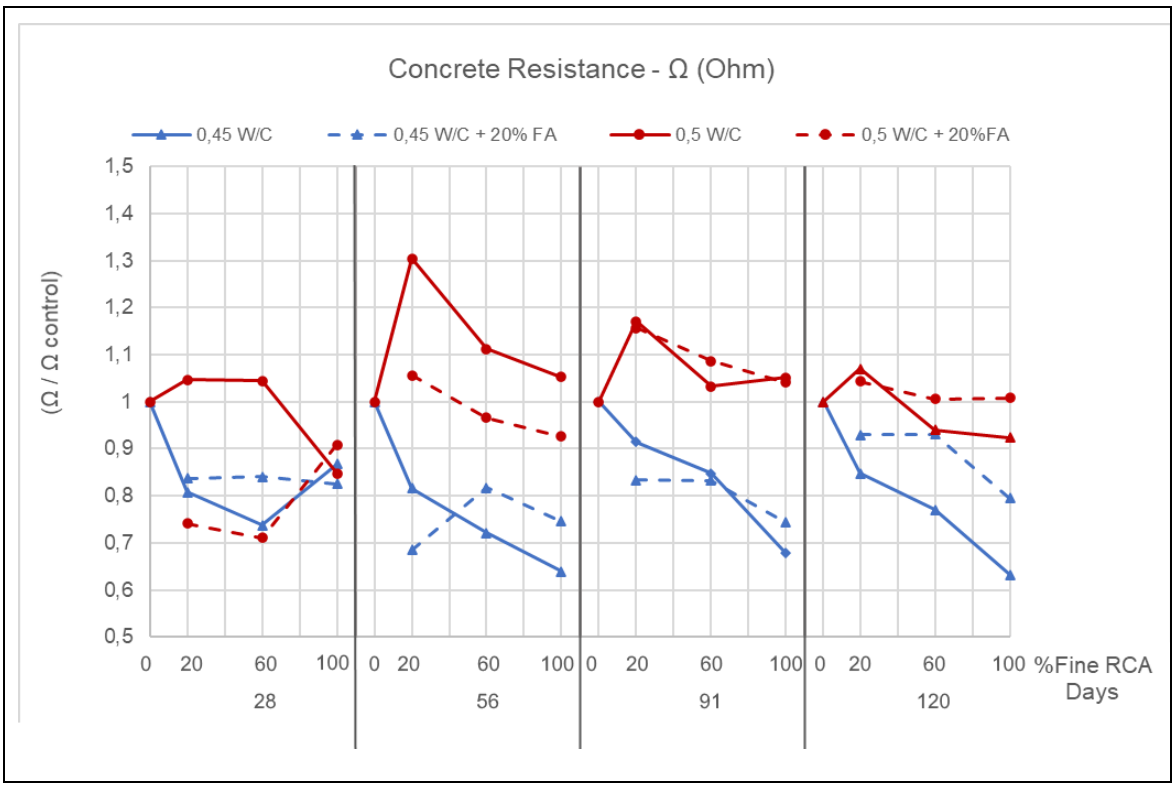

Figure 112 – Electrical impedance (Ω) results compared to natural aggregate control mixes.

While a detrimental effect in concrete electrical resistance was observed from incorporating fine RCA, it is important to notice that replacement ratios up to 60% could be formulated, specially for mixes with a higher W/B ratio, without significantly reducing impedance. The use of fly ash also proved to be an effective mitigator, obtaining practically equal results for low and medium fine RCA replacement ratios when comparing to the control mixes. An optimal fine RCA and fly ash ratio should be defined also based on the effects in other concrete mechanical and durability-related properties.

8.9 Corrosion current density and rate of corrosion

Electrochemical Impedance Spectroscopy (EIS) and Polarization Resistance measurements were made in concrete specimens cured in tap water for 28 days and subsequently submerged in a corrosive chloride solution for 3 months. The obtained current density results and the population standard deviation (σ) are presented in Table 51.

Mix	Mix	28 Days		56 Days		90 Days		120 Days	
ID	Name	Current Density µA/cm²	σ µA/cm²	Current Density µA/cm²	σ µA/cm²	Current Density µA/cm²	σ µA/cm²	Current Density µA/cm²	σ µA/cm²
1	28-CONTROL	0,06	0,02	0,09	0,03	0,18	0,00	1,14	0,07
2	28-RA20	0,23	0,02	0,17	0,01	0,09	0,04	0,12	0,05
3	28-RA60	0,20	0,02	0,08	0,01	0,17	0,04	0,27	0,04
4	28-RA100	0,28	0,06	0,12	0,03	0,18	0,05	0,15	0,04
5	28-RA20-FA20	0,16	0,01	0,12	0,02	0,13	0,03	0,17	0,07
6	28-RA60-FA20	0,17	0,01	0,13	0,02	0,16	0,03	0,15	0,02
7	28-RA100-FA20	0,26	0,08	0,13	0,02	0,16	0,05	0,18	0,06
8	21-CONTROL	0,24	0,06	0,12	0,02	0,12	0,01	0,08	0,01
9	21-RA20	0,18	0,00	0,20	0,06	0,18	0,05	0,38	0,08
10	21-RA60	0,28	0,09	0,08	0,01	0,08	0,01	0,11	0,01
11	21-RA100	0,27	0,01	0,14	0,02	0,14	0,01	0,12	0,01
12	21-RA20-FA20	0,15	0,04	0,14	0,01	0,13	0,01	0,11	0,01
13	21-RA60-FA20	0,13	0,05	0,34	0,23	0,14	0,02	0,13	0,02
14	21-RA100-FA20	0,34	0,02	0,18	0,02	0,30	0,03	0,18	0,03

Table 51 – Current density results at different specimen ages.

The measured corrosion current density and the corrosion risk classification limits are presented graphically in Figure 113, since only one mix at one testing age (28-CONTROL for 120 days) presented an atypical “very high” classification, Figure 114 presents the other results without this value to allow better evaluation.

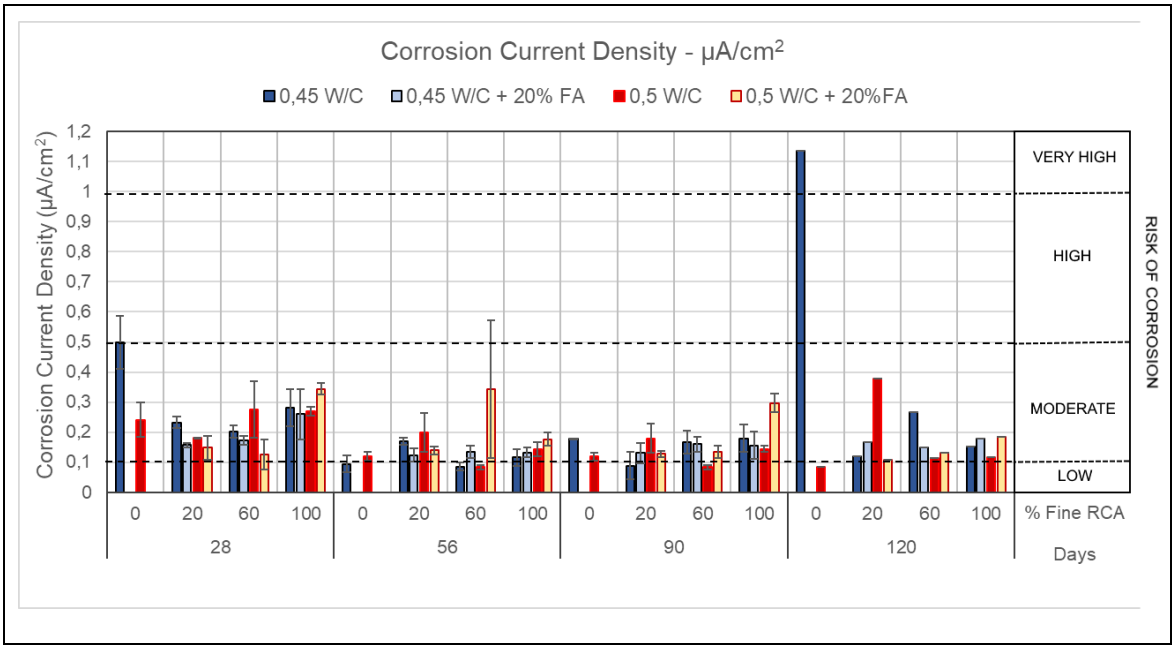

Figure 113 – Corrosion current density for increasing replacement ratios of fine RCA.

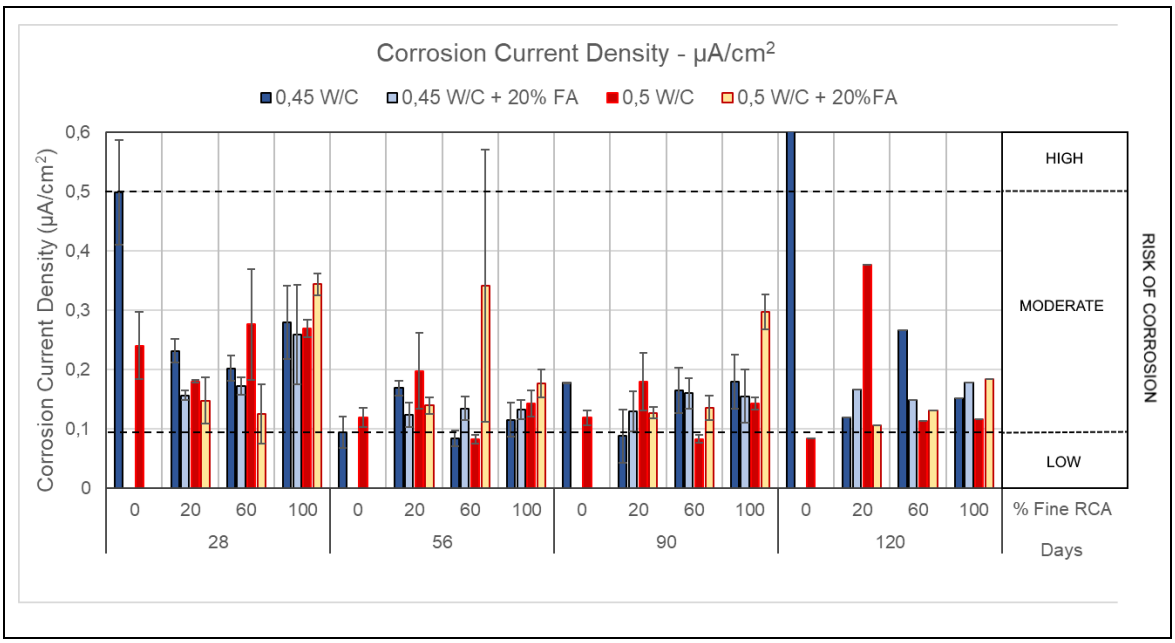

Figure 114 – Detailed corrosion current density for increasing replacement ratios of fine RCA.

Results indicate that most concrete mixes presented a “moderate” corrosion risk at all testing ages, and higher corrosion current density was measured for most mixes at 28 days. A clear negative effect of incorporating incrementing levels of fine RCA could not be determined. For the 0,45 W/B ratio, at younger ages RAC mixes presented higher corrosion current density, but as the specimen increased, the difference between mixes with fine RCA and control mixes was less notorious. For the 0,50 W/B ratio, the control mix presented the lower corrosion current density at 120 days, however a detrimental corrosion effect couldn’t be determined from the incorporation of fine RCA since the measurements of mixes 21-CONTROL and 21-RA100 were very similar for all testing ages. Since this property had not been measured before in mixes incorporating fine RCA, no reference could be found in previous research works, however, it has been observed that reducing the W/B ratio will reduce corrosion current density as higher resistivity in concrete mixes will increase polarization resistance and result in lesser corrosion current density.

A comparison between the results of each concrete mix with its respective control mix is presented in Table 52 and Figure 115.

Mix	Mix	28 Days	56 Days	90 Days	120 Days
ID	Name	$\frac{CD}{CD_{ctrl}}$	$\frac{CD}{CD_{ctrl}}$	$\frac{CD}{CD_{ctrl}}$	$\frac{CD}{CD_{ctrl}}$
1	28-CONTROL	1,00	1,00	1,00	1,00
2	28-RA20	3,73	1,79	0,50	0,11
3	28-RA60	3,25	0,90	0,93	0,23
4	28-RA100	4,51	1,22	1,01	0,13
5	28-RA20-FA20	2,52	1,31	0,73	0,15
6	28-RA60-FA20	2,78	1,42	0,90	0,13
7	28-RA100-FA20	4,17	1,41	0,87	0,16
8	21-CONTROL	1,00	1,00	1,00	1,00
9	21-RA20	0,75	1,66	1,51	4,45
10	21-RA60	1,15	0,70	0,70	1,33
11	21-RA100	1,12	1,20	1,20	1,37
12	21-RA20-FA20	0,62	1,17	1,07	1,26
13	21-RA60-FA20	0,52	2,86	1,14	1,55
14	21-RA100-FA20	1,43	1,48	2,50	2,17

Table 52 – Corrosion current density (CD) results compared to natural aggregate control mixes.

From Figure 115 it is also possible to identify that the corrosion current density for 0,45 W/B mixes incorporating 20%, 60% and 100% fine RCA was 373%, 325% and 451% higher respectively at 28 days, however, at 90 days a reduction of 50%, 7% and 1% was observed for the same mixes. Compared to the 0,50 W/B control mix at 28, 56, 90 and 120 days, the specimens from 21-RA100 presented an increase of 12%, 20%, 20% and 37% respectively. This would suggest that a full replacement of recycled aggregates while using higher W/B ratios could increase corrosion current density and corrosion risk.

The effects of using fly ash varied depending on the age of the specimen. While at 28 days all mixes from the 0,45 W/B group presented a reduction in corrosion current density from incorporating fly ash, this behavior was less evident for older specimens. Incorporating fly ash in mixes from the 0,50 W/B group with a higher fine RCA replacement ratio than 60% had a detrimental effect after the curing period in NaCl solution started. Different studies of corrosion in steel bars embedded in fly ash concrete have noted that this mineral addition could reduce corrosion rate as the modification of pH inside concrete provides passive protection to the steel bar and reduces chloride penetration [38], [77], however, in this research program, these positive effects were different depending on the W/B ratio, the age of the specimen and the fine RCA replacement ratio.

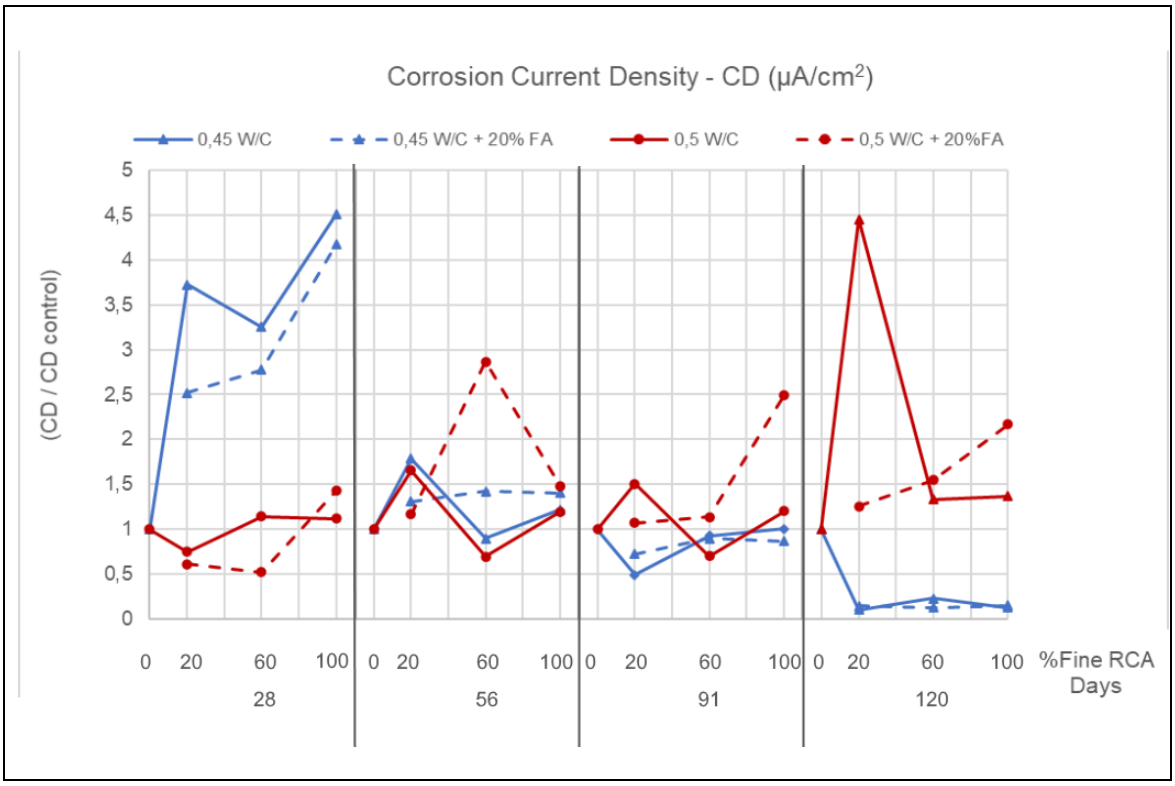

Figure 115 - Corrosion current density (CD) results compared to natural aggregate control mixes.

The corrosion rate of the embedded steel bars for different concrete specimen ages was also obtained from the current density and the results are presented in Table 53 and Figure 116. For simple analysis, this corrosion rate was calculated in micrometers per year (µm/y) and can be interpreted as the steel bar radius that would be affected each year by corrosion. From these results it was possible to identify that corrosion rate of steel bars is not a directly time-dependent property. This is expected as it corresponds to a steel property rather than a concrete property and no negative effect should be observed in this testing period scale unless corrosive reactions are triggered.

Mix ID	Mix Name	28 Days CR μm/y	56 Days CR μm/y	90 Days CR μm/y	120 Days CR μm/y
1	28-CONTROL	0,7	1,1	2,1	13,2
2	28-RA20	2,7	2,0	1,0	1,4
3	28-RA60	2,3	1,0	1,9	3,1
4	28-RA100	3,3	1,3	2,1	1,8
5	28-RA20-FA20	1,8	1,4	1,5	1,9
6	28-RA60-FA20	2,0	1,6	1,9	1,7
7	28-RA100-FA20	3,0	1,5	1,8	2,1
8	21-CONTROL	2,8	1,4	1,4	1,0
9	21-RA20	2,1	2,3	2,1	4,4
10	21-RA60	3,2	1,0	1,0	1,3
11	21-RA100	3,1	1,7	1,7	1,3
12	21-RA20-FA20	1,7	1,6	1,5	1,2
13	21-RA60-FA20	1,5	4,0	1,6	1,5
14	21-RA100-FA20	4,0	2,1	3,5	2,1

Table 53 – Corrosion rates (μm/y) calculated for each concrete mix.

Results also indicate that for all concrete mixes, the corrosion rate of steel bars presented values between 0,7 μm/y and 4,4 μm/y with an average value of 2,3 μm/y except for one atypically high measurement at 120 days for mix 28-CONTROL. The steel bars of RAC specimens did not present higher corrosion rates than control mixes and the use of fly ash and modification of W/B ratio did not significantly alter this property. From these results it could be noted that the corrosion rate of steel bars was not modified by using fine RCA for the measured time, and additionally, since no clear negative tendency could be observed and all mixes had a “moderate” risk classification, it could not be concluded that incorporating fine RCA would accelerate corrosion the embedded steel bars when comparing to conventional concrete, even for corrosive environments.

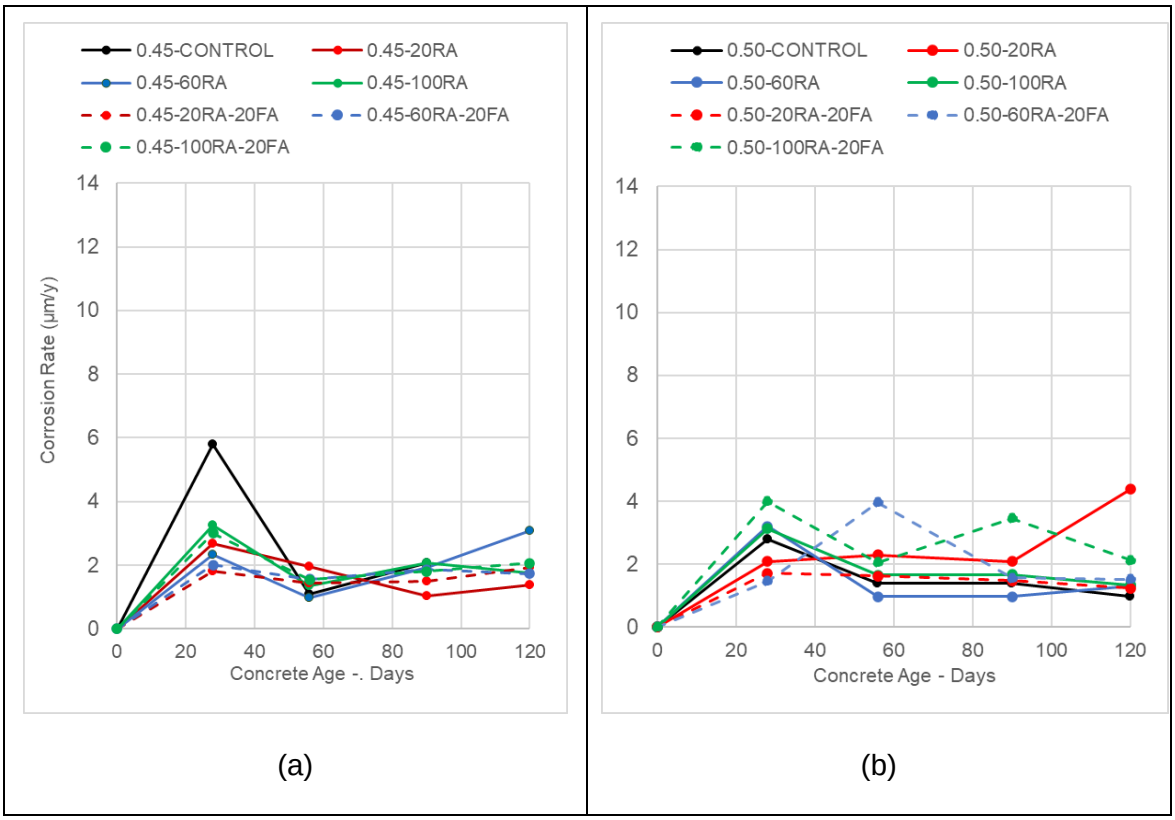

Figure 116 – Measured corrosion rate at different specimen ages for (a). 0,45 W/B mixes and (b). 0,50 W/B mixes.

From the obtained rates, the number of years for corroding 1 mm of the embedded steel bars radius was calculated. The results are presented in Table 54. All results indicate time periods longer than the design lifespan of any concrete structure used in international building practice, obtaining a minimum value of 228 years. It is also important to notice that these values were obtained for 6 mm diameter steel bars imbedded in 76 mm diameter concrete cylinders, representing an approximate concrete cover of 35 mm which is a lower value than the specified for aggressive environments in most building codes. Since the measurements at 120 days were made after 3 months of immersing the specimens in an aggressive 3% NaCl solution, recycled aggregate concrete used in regular buildings with an average lifespan of 100 years will not have steel corrosion levels that would represent a risk in the structural integrity when adequate cover is provided.

Mix ID	Mix Name	28 Days CR y/mm	56 Days CR y/mm	90 Days CR y/mm	120 Days CR y/mm
1	28-CONTROL	1385	911	483	-
2	28-RA20	372	510	972	719
3	28-RA60	426	1014	520	324
4	28-RA100	307	746	480	567
5	28-RA20-FA20	549	695	662	519
6	28-RA60-FA20	499	639	538	578
7	28-RA100-FA20	332	648	554	485
8	21-CONTROL	358	721	723	1016
9	21-RA20	477	435	479	228
10	21-RA60	312	1037	1032	762
11	21-RA100	319	601	601	741
12	21-RA20-FA20	581	617	675	809
13	21-RA60-FA20	685	252	637	657
14	21-RA100-FA20	250	487	290	468

Table 54 – Years required for corrosion of 1 mm of the embedded steel bar radius for each control mix.

Measurements were also made to estimate the corrosion electric potential (E_{CORR}), also called the open circuit potential, which corresponds to the potential measured when no (net) current is flowing in the absence of electrical connections. This potential is measured against the reference calomel electrode, and the results are negative since a relative excess of electrons is present in the embedded steel bar due to the oxidation reactions in the interface. Higher electrical potential values are an indicator of higher rates of corrosion due to an increase in electron exchange. The obtained results are presented in Table 55.

Mix	Mix	28 Days	56 Days	90 Days	120 Days
ID	Name	E_{corr} mV	E_{corr} mV	E_{corr} mV	E_{corr} mV
1	28-CONTROL	-357	-321	-539	-533
2	28-RA20	-159	-320	-302	-295
3	28-RA60	-253	-318	-275	-193
4	28-RA100	-261	-193	-301	-268
5	28-RA20-FA20	-238	-184	-177	-158
6	28-RA60-FA20	-189	-245	-243	-214
7	28-RA100-FA20	-310	-265	-328	-246
8	21-CONTROL	-243	-227	-168	-170
9	21-RA20	-207	-228	-194	-396
10	21-RA60	-285	-172	-195	-152
11	21-RA100	-293	-163	-164	-202
12	21-RA20-FA20	-338	-197	-178	-167
13	21-RA60-FA20	-385	-244	-195	-173
14	21-RA100-FA20	-426	-368	-356	-195

Table 55 – Corrosion Potential (E_{CORR}) measurements at different specimen ages.

Figure 117 was obtained by plotting the absolute value of the corrosion potential of each concrete mix against the specimen age for both mix groups. In this figure, similar values of corrosion potential can be observed for mixes made with 0,45 and 0,50 W/B ratios, obtaining absolute results between 0,2 V and 0,425 V. Similarly to the corrosion rate results, no clear relationship could be established between the replacement ratio of fine RCA and the corrosion potential of steel bars. The corrosion electrical potential did not increase with specimen age since after 3 months of curing in an aggressive environment, the measured corrosion potential was similar for mixes made with natural and recycled aggregates.

Since corrosion is a slow process, longer measurements should be made after years of exposure to very aggressive environments. However, as no significant differences were noticed on this test or the other chloride-penetration related tests that would reject the use of fine RCA in concrete from corrosion related problems, the assessed aggregate cannot be stablished as a corrosive material that enhances this reaction in reinforcement steel bars.

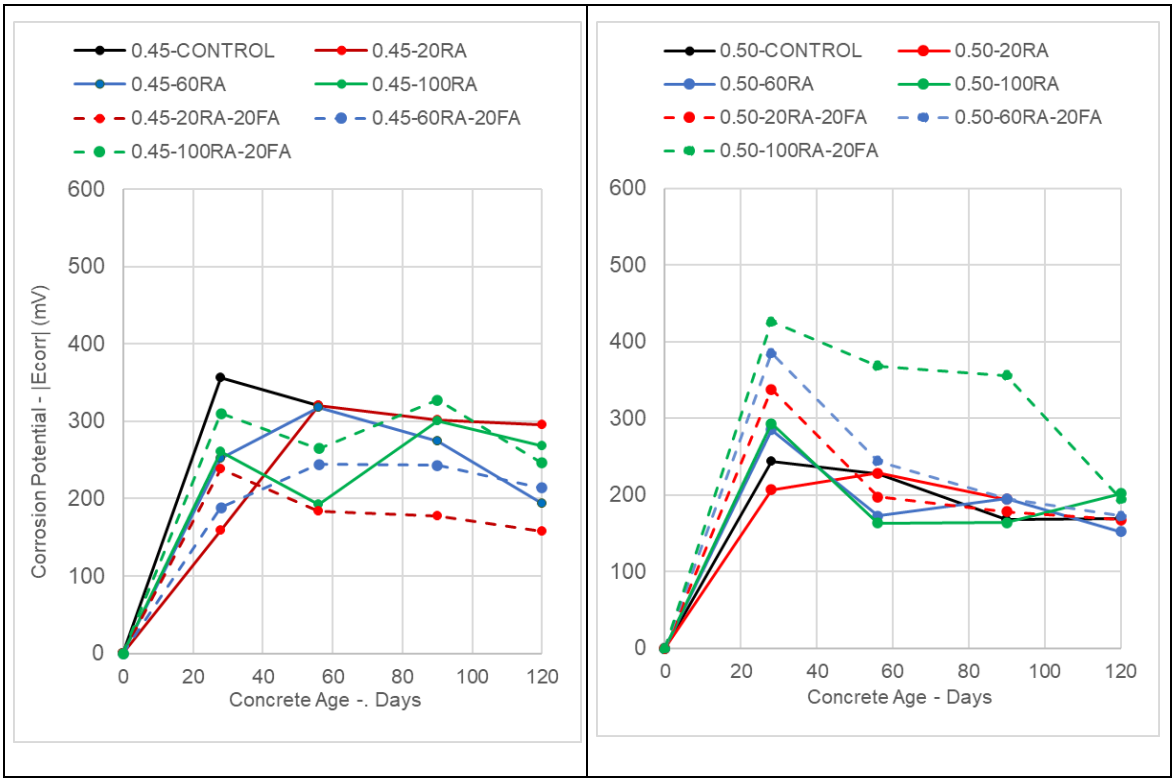

Figure 117 - Corrosion Potential ($|E_{CORR}|$) measurements at different specimen ages for (a). 0,45 W/B Mixes. (b). 0,50 W/B mixes.

8.10 Concrete Permeability to Air Coefficient – KT

The concrete permeability to air coefficient – KT was determined after 28 days and 90 days of moist curing. As discussed in previous sections, this property was measured using a PermeaTORR device in concrete 15x15x15 cm cubical samples and the results are presented in Table 56 and Figure 118.

Mix ID	Mix Name	28 Days		90 Days	
		KT x 10^{16} m^2	σ x 10^{16} m^2	KT x 10^{16} m^2	σ x 10^{16} m^2
1	28-CONTROL	0,155	0,098	0,146	0,077
2	28-RA20	0,118	0,063	0,314	0,162
3	28-RA60	0,107	0,049	0,148	0,153
4	28-RA100	0,122	0,071	0,338	0,179
5	28-RA20-FA20	0,145	0,065	0,119	0,039
6	28-RA60-FA20	0,559	0,309	0,183	0,053
7	28-RA100-FA20	0,705	0,334	0,241	0,150
8	21-CONTROL	0,178	0,068	0,402	0,194
9	21-RA20	0,223	0,113	0,202	0,102
10	21-RA60	0,139	0,070	0,183	0,090
11	21-RA100	0,147	0,070	0,400	0,230
12	21-RA20-FA20	0,308	0,135	0,328	0,195
13	21-RA60-FA20	0,548	0,282	0,447	0,141
14	21-RA100-FA20	0,442	0,195	0,106	0,063

Table 56 – Air permeability coefficient KT test results.

The test results do not indicate a clear increase in the KT coefficient from incorporating fine RCA in concrete mixes. Both at 28 days and 90 days, similar values were obtained for mixtures regardless of replacement ratio of recycled aggregates. It is also possible to identify that the W/B ratio did not have a significant effect in the tested air permeability coefficient for RAC mixes and was mostly notorious when comparing the results from the control mixes. To compare the air permeability coefficient with the natural aggregate concrete mixes, each value was divided by the result of the respective control mix, obtaining the results presented in Table 57 and Figure 119.

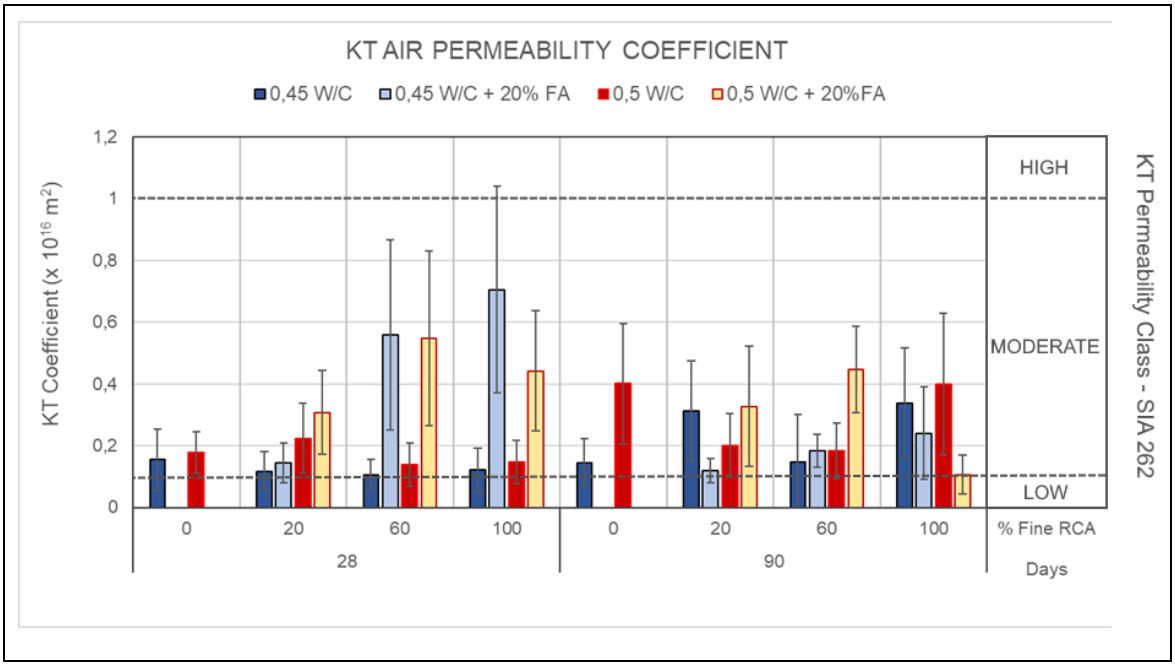

Figure 118 – Air permeability coefficient for increasing replacement ratios of fine RCA at 28 and 90 days.

When comparing the mixes without fly ash incorporation, increasing the fine RCA replacement ratio did not have a negative impact in the 0,45 W/B mixes at 28 days, while at 90 days incorporating 20%, 60% and 100% recycled aggregates resulted in an increase of the KT coefficient by 215%, 1% and 232% when comparing to the control mix. This effect was not observed for 0,50 W/B mixes at 90 days, as the same replacement ratios of fine RCA reduced the KT permeability coefficient by 50%, 54% and less than 1% respectively. While the KT air permeability coefficient has not been measured using this method in RAC mixes with only fine recycled aggregates, other research has been performed that concluded that the intrinsic permeability of concrete increases with the increasing RCA content and reduces with extended curing periods [10], this was attributed to the continuation of the hydration process and the narrowing of the capillary spaces in concrete microstructure. This is partially consistent with the obtained results, as all RAC mixes presented higher air permeability values. Results also indicated that the KT coefficient was higher for some 0,50 W/B mixes when comparing to the 0,45 W/B mixes with the same fine RCA replacement.

Mix ID	Mix W/B	Mix Name	28 Days $\frac{KT}{KT_{ctrl}}$	90 Days $\frac{KT}{KT_{ctrl}}$
1		28-CONTROL	1,00	1,00
2		28-RA20	0,76	2,15
3		28-RA60	0,69	1,01
4	0,45	28-RA100	0,79	2,32
5		28-RA20-FA20	0,94	0,82
6		28-RA60-FA20	3,61	1,25
7		28-RA100-FA20	4,56	1,65
8		21-CONTROL	1,00	1,00
9		21-RA20	1,25	0,50
10		21-RA60	0,78	0,46
11	0,50	21-RA100	0,83	1,00
12		21-RA20-FA20	1,73	0,82
13		21-RA60-FA20	3,07	1,11
14		21-RA100-FA20	2,48	0,26

Table 57 – Air permeability coefficient (KT) results compared to natural aggregate control mixes.

The inclusion of fly ash did not have a positive effect in reducing the KT coefficient in concrete mixes with fine RCA. At 28 days, both 0,45 W/B and 0,50 W/B mix groups with fly ash presented a higher KT coefficient, notably for mixes containing more than 60% recycled aggregates. At 120 days, incorporating fly ash had a positive effect when comparing mixes with 100% recycled aggregates since the air permeability coefficient for mixes 28-RA100-FA20 and 21-RA100-FA20 was reduced by 67% and 74% when comparing to their counterparts without fly ash.

It is also important to notice that this test is highly dependent on the surface conditions and dimensions of the tested specimen. A high deviation was observed depending on the testing face of the cubical specimen and very different values were obtained if the surface presented small-sized pores or discontinuities. Concrete mixes with fly ash have a higher water demand and lower workability that usually results in the presence of a more porous microstructure near to the surface that could have affected the measurements.

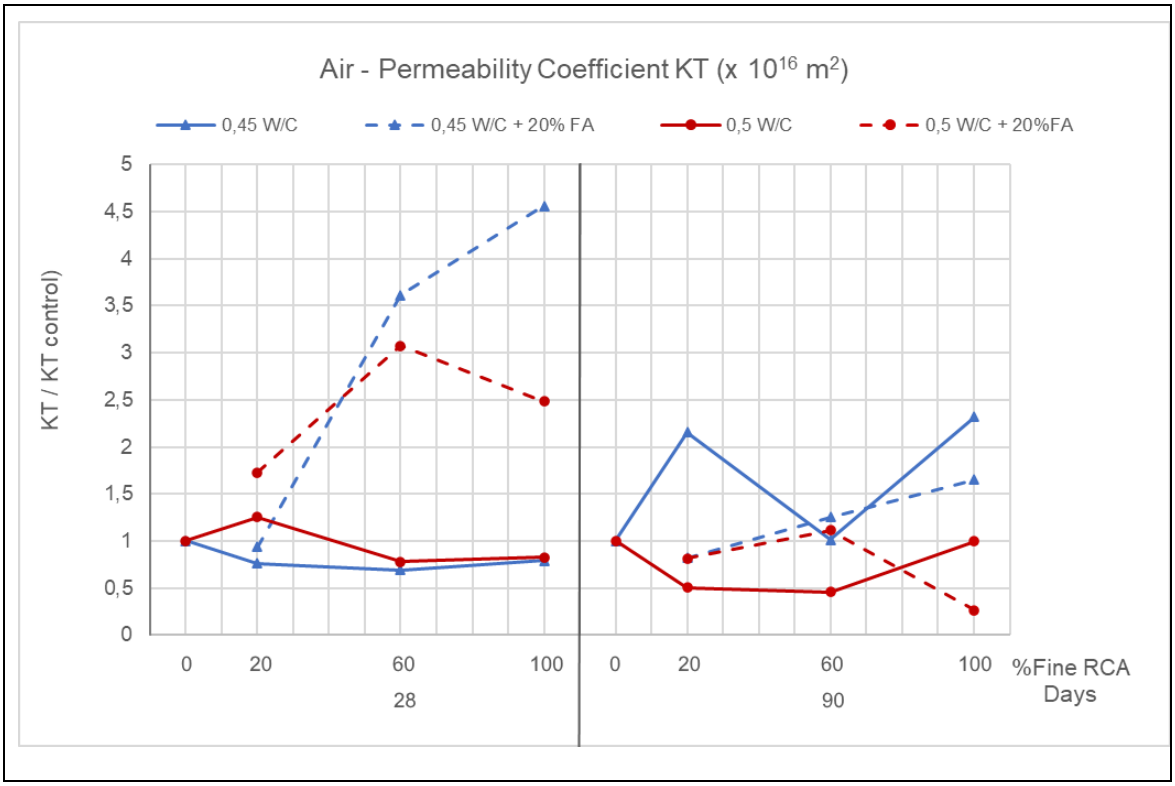

Figure 119 - Air permeability coefficient (KT) results compared to natural aggregate control mixes.

Since this test results did not indicate a clear reduction in concrete's performance from incorporating fine RCA, no conclusive assessment can be made. However, it is important to notice that all concrete mixes presented a "Moderate" permeability according to the reference international standard. Further research could be implemented using different specimens such as concrete slabs that could guarantee a more uniform air flow when performing the test. Since the PermeaTORR device is used superficially in concrete specimens, special attention should be taken to assure equal surface conditions.

8.11 Overall performance of concrete mixes with fine RCA

After performing 2 mechanical tests and 8 durability tests in concrete specimens from recycled aggregate mixes, a summary of the effects of incorporating 20%, 60% and 100% fine RCA (f-RCA) and 20% fly ash (FA) for the assessed W/B ratios is presented in Table 58. When the classification is followed by a percentage, different effects were identified for this specified fine RCA addition. Since mechanical, permeability and chloride related properties were obtained at 28 days and 90 days while electrochemical corrosion measurements were made each month for 120 days, this classification represents a general trend in the observed behavior from incorporating these materials in concrete mixes for the most relevant testing age. For mechanical testing, the same effects were observed at both testing ages, while for durability and electrochemical testing, it is considered that long-term results are more important since they are related with the deterioration of concrete and steel bar rebars that would take years to have significant effect in the structural integrity of any construction.

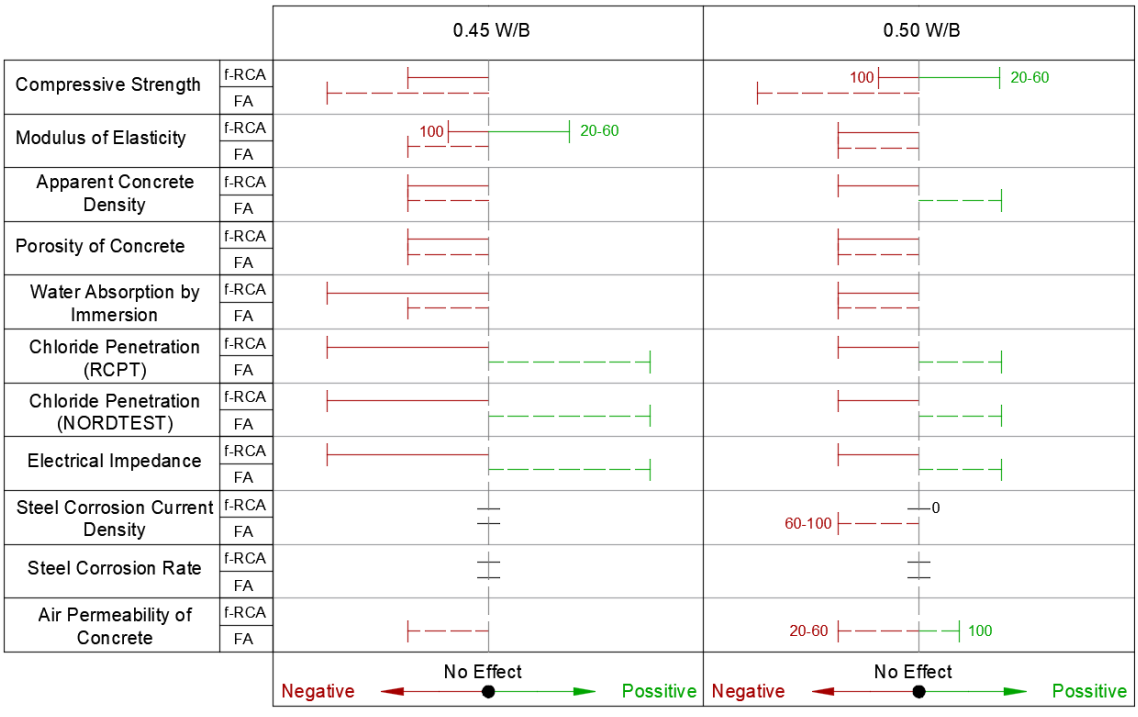

Table 58 – Summary of the effects of incorporating fine RCA (f-RCA) and fly ash (FA) in different durability and mechanical tests.

8.11.1 Physical and Mechanical Properties

In general, and as it has been observed by other research works, the incorporation of fine recycled concrete aggregates had detrimental effects in the mechanical properties of concrete. In this research, fine RCA was used in 20%, 60% and 100% ratios and in most tests, concrete mixes with 100% fine RCA presented the worst performance. It was observed however, that this negative effect was lower for the 0,50 W/B mix group.

Concrete specimens from this group, showed higher water absorption than 0,45 W/B mixes at 28 days but lower at 90 days, suggesting an early fast hydration process that resulted in accelerated densification. At 90 days, mixes from this group presented lesser porosity and had achieved and surpassed the design compressive strength of 21 MPa, reaching values of 25 MPa for mixes made with only fine RCA and 30 MPa for 20% fine RCA incorporation. For the 0,50 W/B group, incorporating 60% fine RCA only reduced the modulus of elasticity by 6% and for the 0,45 W/B group, including 20% and 60% fine RCA increased the modulus of elasticity by 8% and 2% respectively.

Based on a mechanical perspective, including fine RCA would be feasible for structural purposes, and the possible loss of strength could be compensated with adequate mix design and trial testing. Compressive strength testing revealed that these aggregates could be implemented for replacement ratios of even 100% if an adequate mix design is formulated. Higher strength values can be achieved for lower W/B ratios; however, a better performance was observed for mixes with fine RCA and a 0,50 W/B ratio which highly surpassed the strength design value. The modulus of elasticity will be reduced by high contents of fine RCA; however, it could be implemented up to 60% without significantly reducing this property. From a practical point of view, if the modulus of elasticity can be determined for a conventional concrete mix, similar values can be expected for replacement ratios of fine RCA between 20% and 60% Higher contents would require testing in concrete trial mixes and any significant reduction should be considered in the structural design of concrete elements. The presence of fly ash will reduce mechanical performance, specially at early ages, however, this can be controlled with the mix design process and early trial mixes as it has very positive effects in the durability of concrete.

While the porosity, density and water absorption of concrete mixes are not a direct measurement of its mechanical or durability performance, the results have shown that the RAC mixes with 0,50 W/B ratio presented more similar physical properties to the control mix than the 0,45 W/B group. The higher free water content may compensate the high absorption of fine RCA particles and allow a better hydration process. Since the assessed physical properties are very similar between concrete mixes, no correlation could be made between them and chloride related properties. Physical testing indicated that higher contents of fine RCA in concrete would require higher W/B ratios and curing to guarantee and adequate hydration process, however, incorporating a fine RCA content between 20% and 60% and fly ash could be acceptable.

8.11.2 Durability-related Properties

Both the RCPT and NT tests revealed a reducing effect of incorporating fine RCA in chloride permeability, with more noticeable effects in the 0,45 W/B group, especially for full aggregate replacement. For these cases, the use of fly ash had a very positive effect of reducing chloride penetration. However, it is very important to notice that according to the ASTM C1202, at 90 days the permeability classification for all mixes up to 60% fine RCA without fly was “Moderate”, and all mixes with 100% and fly ash also presented this category. This reveals that the increase in chloride penetration due to recycled aggregates can be mitigated with fly ash and very satisfactory performance can be obtained for mixes with fly ash and aggregate replacements between 20% and 60%.

The measurements of concrete electrical impedance after 4 months confirmed this positive effect of using fly ash and revealed a delayed effect since for younger specimens the effects were not as notorious. This is important when using this mineral for durability purposes since the benefits will be more evident at long-term testing and the mechanical performance at younger ages will be affected. Electrical impedance also revealed that the inclusion of high contents of fine RCA is more viable with higher W/B content since similar impedance values were obtained for 0,45 W/B and 0,50 W/B specimens with 100% fine RCA. From this test, it is evident that using a fine RCA incorporation between 20% to 60% and fly ash would mitigate the negative effects of these aggregates, specially for lower W/B ratios.

The polarization resistance testing indicated that for most mixes, including control mixes, the embedded steel bars presented a “Moderate” corrosion risk, and no clear correlation could be stablished between the corrosion current density and the contents of fly ash and fine RCA. From rate of corrosion calculations, the time required to lose 1 mm of bar radius (16% of effective diameter) by this reaction would be between 250 years and 1037 years for RAC mixes, while the maximum obtained for control mixes was 1385 years. This would mean that the inclusion of fine RCA does not trigger corrosive reactions and provides similar protection than conventional concrete and the concrete constructions made with this material could easily have a lifespan of more than 100 years.

A clear increase in the air permeability coefficient was not stablished, however, all of the concrete mixes including 21-CONTROL and 28-CONTROL presented a “moderate” permeability classification, suggesting that no significant variation in air permeability results from incorporating fine RCA.

8.11.3 Structural Uses in the Future

Based on all these results, a reference concrete mix with a fine RCA replacement ratio between 20% and 60% and 20% fly ash designed for a 0,50 W/B ratio could be formulated for structural purposes. This mix would be expected to present lower mechanical performance at lower ages but have achieved the design compressive strength between 28 days and 90 days. This optimal mix would also present similar physical properties and the same chloride penetration classification and corrosion risk at long term than conventional concrete with the same mix design. This would mean that for low and medium strength requirements with a normal exposure condition, recycled concrete with partial or full fine RCA incorporation could be implemented and present a satisfactory structural performance. The use of this material for higher mechanical requirements or more aggressive conditions could be allowed if trial testing is conducted.

8.12 Durability Performance According to International Standards and Regulations

In this research work, 14 mixes with different replacement levels of fine RCA and fly ash were assessed for 2 W/B ratios. The mechanical and durability testing indicated that mixes with a fine RCA incorporation between 20% and 60% would have an acceptable performance when compared to conventional concrete, and the use of fly ash would decrease chloride permeability and corrosion risk. However, the use of these kind of aggregates is not allowed in every international building code and different requirements in composition, physical properties and applications are defined. In this section, an assessment of this optimal mix according to multiple international codes is performed.

To identify the viability of using fine recycled aggregates in concrete mixes, different aggregate classifications according to international building standards were identified and compiled by *Rosero Alvarez, (2019)* [206]. In this work, the aggregates were classified according to their possible incorporation in structural concrete, non-structural concrete, pavements and base or filler material for road construction. Since the scope of this work is the evaluation of using fine RCA for structural concrete, based on *Rosero Alvarez, (2019)* [206]**,** 20 recycled aggregate classifications for structural applications were identified in building standards from 12 different countries. The names, description and reference standard are presented in Table 59.

ID	Country	Aggregate Classification	Classification Description	National Standard
1	Spain	ARH	Recycled concrete aggregates	*GEAR - Guía Española de Áridos Reciclados procedentes de residuos de construcción y demolición (RCD)*
2		ARMh	Recycled concrete aggregates mixed with ceramics (high)	
3		ARMc	Recycled concrete aggregates mixed with ceramics (low)	
4	U.K	CCA	Coarse Crushed concrete Aggregate	*British Standard - BS 8500*
5	Portugal	ARB1	Recycled concrete aggregates	*Portuguese Standards E471, E472, E473 & E474 - 2009*
6		ARB2	Recycled concrete aggregates with masonry	
7	Germany	T1	Recycled concrete aggregates	*DIN 4226-102:2017-08*
8		T2	Recycled concrete aggregates with masonry	
9	Netherlands	T1	Recycled concrete aggregates	*CUR - NEN 5905:2010*
10		T2	Recycled concrete aggregates with masonry	
11	Belgium	T1	Recycled concrete aggregates	*PTV 406 Technical Prescription: Recycled Aggregates from construction and demolition waste. NBN EN 206:2013+A1:2016*
12		T2	Recycled concrete aggregates with masonry	
13	Australia	1A(RCA)	Recycled concrete aggregates	*HB 155 - 2002 Guide to the use of recycled concrete and masonry materials*
14	U.S.A	T1-High	Crushed concrete aggregates	*ACI 555R-01 Removal and Reuse of Hardened Concrete.*
15		T2-Med		

ID	Country	Aggregate Classification	Classification Description	National Standard
16		T3-Low		
17	Peru	T1	Crushed concrete aggregates	*NTP 400,053 Manejo de residuos de la actividad de construccion. Reciclaje de concreto de demolición. Norma E.060 Concreto Armado*
18	Italy	T1	Crushed concrete aggregates	*NTC2008 - Italian Building Code*
19	Hong Kong	T1	Crushed concrete aggregates	*Aggregates for Concrete, Construction Standard CS3:2016*
20	Switzerland	T1	Crushed concrete aggregates	*SIA 162/4 Béton de recyclage*

Table 59 – Recycled aggregate classification in multiple international building standards. – Adapted from *Rosero Alvarez, (2019)* [206].

For each one of these aggregate classifications, requirements regarding waste composition are defined. Most international building codes require a concrete composition between 70% and 100%, and limit the content of masonry waste, organic materials, and floating fine contaminants. These requirements and the legend of each component are summarized in Table 60 and Table 61.

ID	Material Constituents
C	Concrete waste
M	Masonry waste
A	Asphaltic waste
MAT	Aditional materials waste
D	Contaminants such as organic materials
FF	Material finer than sieve No. 200
FM	Floating Materials such as wood, plastic, paper or similar.

Table 60 – Definition of each composition material. Adapted from *Rosero Alvarez, (2019)* [206].

ID	Country	Aggregate Classification	C %	M %	A %	MAT %	D %	FF %	FM %
1	Spain	ARH	>90	<10	<5	<1	<0.6	-	<2
2		ARMh	>70	<30	<5	<1	<0.6	-	<2
3		ARMc	<70	>30	<5	<1	<0.6	-	<2
4	U.K	CCA	>90	<10	<5	<1	-	<4	<2
5	Portugal	ARB1	>90	<10	<5	<0.5	-	<3	<2
6		ARB2	>70	<30	<5	<1	-	<3	<2
7	Germany	T1	>90	<10	<1	<2	<1	<4	-
8		T2	>70	<10	<1	<3	<1	<4	-
9	Netherlands	T1	>95	<5	0	<1.5	-	-	-
10		T2	<55	>65	0	<2	-	<4	-
11	Belgium	T1	>95	<10	<5	<5	<1	<5	-
12		T2	>40	>10	<5	<10	<1	<3	-
13	Australia	1A(RCA)	>95	0	<1	-	<1	-	-
14	U.S.A	T1-High	100	0	0	0	-	-	-
15		T2-Med	100	0	0	0	-	-	-
16		T3-Low	100	0	0	0	-	-	-
17	Peru	T1	100	0	0	0	-	-	-
18	Italy	T1	100	0	0	0	-	-	-
19	Hong Kong	T1	≤100	0	0	-	<1	<4	-
20	Switzerland	T1	≤100	<3	0	-	<1	-	-

Table 61 – Composition requirements (% By mass) for structural use of recycled aggregates in different building standards. Adapted from *Rosero Alvarez, (2019)* [206].

These international standards also define a requirement for various physical properties such as aggregate density, minimum particle size and aggregate absorption, as presented in Table 62. Most international standards for coarse aggregates, also include shape requirements such as the flakiness and elongation index, however, they are not included since these parameters are not easily determined in fine particles. From these regulations, it is possible to identify that some building codes do not allow the use of fine RCA from a particle size point of view, while others limit aggregate absorption and particle density. Since it is expected that fine RCA presents higher water absorption as a result of the porous nature of the old attached mortar [49], the particle size distribution can be controlled through limitations of this property.

ID	Country	Aggregate Classification	Aggregate Density	Mix. Or Max. Size	%Passes Sieve 4 mm	Aggregate Absorption
			(g/cm^3)	(mm)		%
1	Spain	ARH	-	>4	<35	≤5
2		ARMh	-	>4	<35	≤5
3		ARMc	-	>4	<35	≤5
4	U.K	CCA	-	-	-	-
5	Portugal	ARB1	≥2,2	-	-	≤7
6		ARB2	≥2,2	-	-	≤7
7	Germany	T1	≥2,0	-	-	≤10
8		T2	≥2,0	-	-	≤15
9	Netherlands	T1	≥2,1	-	-	-
10		T2	≥2,0	-	-	-
11	Belgium	T1	≥2,1	-	-	≤9
12		T2	≥1,6	-	-	≤18
13	Australia	1A(RCA)	≥2,1	>4	-	≤6
14	U.S.A	T1-High	≥2,0	>4	-	≤12
15		T2-Med	≥2,0	>4	-	≤12
16		T3-Low	≥2,0	>4	-	≤12
17	Peru	T1	-	-	-	-
18	Italy	T1	-	-	-	-
19	Hong Kong	T1	≥2,0	-	≤5	≤10
20	Switzerland	T1	-	-	-	-

Table 62 – Physical requirements of recycled aggregates for structural use according to different building codes. Adapted from *Rosero Alvarez, (2019)* [206].

The compressive strength of concrete made with a maximum RCA incorporation is also defined in these international building codes and compiled in Table 63. Most standards only allow the use of RCA for low or medium strength requirements for incorporation ratios usually lower than 25% and limit the use of recycled aggregate concrete to low exposure categories as a safety factor against the observed negative durability effects of incorporating RCA. The limitations of Table 63 are considered very restrictive as countries like Spain, Australia and the U.S.A do not allow the use of particles with a size lower than 4 mm and the requirements are usually made only considering the use of coarse recycled aggregates.

ID	Country	Aggregate Classification	F'c	% RCA Incorporation	Additional Restrictions
			(MPa)	%	
1	Spain	ARH	≤30	≤20	Low exposure category
2		ARMh	≤30	≤20	
3		ARMc	≤30	≤20	
4	U.K	CCA	>20 ≤40	≤20	Low exposure category
5	Portugal	ARB1	≤40	≤25	Low exposure category
6		ARB2	≤35	≤20	
7	Germany	T1	≤25 ≤30	≤35 ≤25	Low exposure category
8		T2	≤25 ≤30	≤35 ≤25	
9	Netherlands	T1	≤35	≤20	-

ID	Country	Aggregate Classification	F'c	% RCA Incorporation	Additional Restrictions
			(MPa)	%	
10		T2	≤35	≤10	-
11	Belgium	T1	≤25 ≤30 ≤20	≤20 ≤25 ≤35	Max. 20% incorporation if exposed outdoor
12		T2	≤25 ≤30 ≤20	≤20 ≤25 ≤35	
13	Australia	1A(RCA)	≤40	≤30	-
14	U.S.A	T1-High	≥ 34	≤100	-
15		T2-Med	≥27 - <34	≤100	-
16		T3-Low	≥12 - <27	≤100	-
17	Peru	T1	-	-	-
18	Italy	T1	≤30 ≤20 ≤45	≤30 ≤60 ≤15	-
19	Hong Kong	T1	≤35	≤20	-
20	Switzerland	T1	≤25 ≤30 ≤20	≤20	Max. 25 MPa. for outdoor use

Table 63 – Structural recycled aggregate concrete strength requirements and maximum RCA incorporation in different building codes. Adapted from *Rosero Alvarez, (2019)* [206].

The properties of the fine RCA used in this research work for concrete mixes are presented in Table 64. When comparing these values with the specified requirements of the referenced building codes, these particles could be used for structural concrete from a composition point of view, since they were obtained from prefabricated demolished slabs and their composition does not include possible masonry particles nor organic materials.

Based on their physical properties, the aggregate density is sufficient for use in all countries except Portugal, but the size distribution and aggregate absorption wouldn't allow their use in Spain, Belgium, Australia, U.S.A and Hong Kong.

Aggregate Property	Value
Concrete Composition – %	>95%
Aggregate Density - g/cm^3	2,12
Max Size - mm	4,75 mm
Min Size – mm	0,15 mm
Particles finer than Sieve No.200 (0,075 mm) - %	9,40
Aggregate Absorption - %	9,48

Table 64 – Used fine RCA properties relevant for building codes classifications.

The use of fine RCA for structural applications would require particles composed of 95% of concrete and with minimum clay, masonry, and organic contaminants. While this may sound restrictive, these values could be achieved by adequate demolition and processing methods and could be controlled by parameters such as aggregate density and aggregate absorption which are strongly correlated with the resulting properties of concrete [59]. For example, other researchers have also obtained satisfactory mechanical and durability performance for a maximum replacement of 30% fine RCA when the particles presented an absorption close to 9% [53], [100] and a density lower than 2,5 g/cm^3 [50], [51]. Research has also been carried in Colombia for fine RCA with an absorption close to 9% and an apparent density of 2,2% [147], revealing that these parameters may also be applied for national regulations.

From a mechanical point of view, the concrete mixes were formulated with a design strength of 21 MPa and 28 MPa, and at 90 days, all mixes incorporating 20%, 60% and 100% fine

RCA achieved their respective strength value. Based on these results and the limitations described in Table 63, higher replacement ratios could be implemented for an eventual use of fine RCA since the compressive strength can be achieved with an adequate mix design procedure regardless of the replacement ratio.

From a durability point of view, the use of fine RCA can be achieved if a mitigator is used and the concrete exposure category is controlled. A maximum incorporation of RCA of 60% could be implemented easily with satisfactory durability performance if a mineral addition such as fly ash is incorporated in the concrete mix for low exposure levels. Different studies have also noticed that fine RCA benefits from FA incorporation in terms of carbonation resistance, a property which was not assessed but also has an important effect in rebar corrosion, obtaining building lifespans of at least 50 years [78]. European Standards EN 197-1 limits the incorporation of fly ash to 35% by cement mass, this limit could be adopted for RAC since different studies have suggested that using FA values between 20% and 35% will reduce chloride penetration without significantly reducing the mechanical performance or increasing the carbonation depth [68].

Results also showed that concrete mixes with recycled aggregates do not trigger corrosive reactions in the embedded steel bars when exposed to aggressive curing conditions, so these aggregates could be incorporated with similar precautions than conventional concrete. Based on this research and other works, a proposed classification to allow the use of fine RCA is presented in Figure 120.

Concrete Waste	>92%
Masonry Waste	<5%
Asphaltic Waste	<5%
Additional Materials	<1%
Contaminants	<1%

Aggregate Density (g/cm^3)	>2.1
Aggregate Absorption	<9.5%
Particles Finer than Sieve No.200	<10%

F'c (MPa)	% Fine RCA incorporation	Additional Requirements*	Exposure Category
≤ 30	≤ 25	Enhancement method such as 20% Fly Ash.	Low Exposure
≤ 25	≤50	Enhancement method such as 20% Fly Ash.	Low Exposure
≤ 25	≤ 20	-	Low or Medium Exposure

** Fly ash can be replaced by other enhancement method or mitigator.*

Figure 120 – Proposed fine RCA requirements for the use in structural concrete.

It is important to notice that this research achieved adequate mechanical and durability performance when also incorporating a super-plasticizer in the mix for a target slump of 152,4 mm (6 in), however, lower required workability values should also include water-reducing admixtures and perform trial testing for an optimal content depending on the requirements of each project as water reducing admixtures decrease the effective W/B ratio and can even improve the properties of concrete made with recycled aggregates [62].

International building codes have a restrictive use of coarse RCA in concrete mixes and most of them don't allow the use of fine RCA particles, however, results have shown that an adequate performance can be achieved if the material is composed mostly of crushed concrete and a durability mitigator such as fly ash is incorporated. In a larger scale, this would require a more selective demolition process, however, the environmental effects of reincorporating fine RCA and the possible reduction in concrete production costs could possibly balance the additional processes required in fine RCA selection.

In the case of Colombia, the national standard NTC 6421 “*Coarse recycled aggregates for use in concrete”* is being formulated for the first time. This standard will only allow the use of coarse aggregates for structural use for a minimum content of 92% concrete, a maximum absorption of 5% and a maximum incorporation of 20% for elements with a design compressive strength lesser than 35 MPa. For non-structural elements, replacing 100% will be allowed for a less strict composition and absorption. While this test is only formulated for the use of coarse aggregates, it sets a favorable precedent for the use of recycled aggregates in the country, since most of the national construction is performed for concrete mixes with a compressive strength lesser than 35 MPa, which will allow the use of these aggregates in a large scale. The standardization of the use of coarse aggregates will also improve the demolition and RCA processing methods since new technologies and procedures will be implemented in Colombia to maximize the commercial potential of these aggregates. The international use of fine RCA is still restrictive, but as this research and others have proved, a satisfactory mechanical performance can be achieved for buildings with extended lifespans using concrete mixes with an adequate mix design and the use of enhancement techniques such as the inclusion of fly ash.

9. Conclusions and Recommendations

9.1 Conclusions

Since concrete production is not currently a fully sustainable practice, this research work aimed to assess the effects of incorporating incremental levels of fine recycled concrete aggregates (RCA) in the durability properties of concrete with different water/binder ratio (W/B) related to steel rebar corrosion and the possible enhancing effects of using fly ash. The incorporation of recycled aggregates in concrete mixes would drastically reduce the negative environmental effects of mining activities and land encroachment while possibly reducing production costs associated with extraction and transportation in expanding cities located far from aggregate sources like Bogotá, Colombia. The use of other by-products such as fly ash and the implementation of different sustainable enhancing methods like CO_2 treatments could also further improve the environmental viability of recycled concrete.

In this research, an extensive literature review was performed, followed by a full characterization of the properties of cementitious materials, natural and recycled aggregates. The test results in concrete were compared to international building regulations to study the viability of incorporating fine RCA in national and international construction practice and a possible mix composition incorporating fine RCA was proposed. The main conclusions obtained from the mechanical and durability assessments are the following:

- The assessed fine recycled aggregates presented higher absorption, higher voids in aggregates and lesser specific gravity than natural aggregates. This aggregate loss in performance is the responsible for the observed reduction in concrete's fresh state and hardened state properties.
- Aggregate testing also indicated that the employed fine RCA is potentially expansive from Alkali-Silica reactions, however, the use of fly ash was an effective mitigator against this detrimental reaction. Since this reaction is dependent on the composition of the aggregates from the parent concrete, the use of fine RCA for

structural concrete should require Alkali-aggregate testing and mitigation assessment using supplementary cementitious materials.

- While increasing the content of fine RCA reduced the slump value of concrete in fresh-state, the target slump was achieved during testing using a high-range superplasticizer (SP). For concrete mixes with 0,45 and 0,50 W/B, a higher content of SP was used to achieve the desired workability for higher fine RCA replacements. This indicates that modern chemical addition technology allows the use of aggregates and cementitious materials with high-absorption values while still achieve adequate fresh-state properties. Nevertheless, compatibility tests should always be performed when incorporating chemical additions.
- Both mechanical and durability testing revealed a better relative performance of incorporating fine RCA for the 0,50 W/B ratio. At early ages, the higher free water content balanced the absorption rate of fine RCA and probably contributed to the hydration of old-attached mortar and reduction of the effective W/B ratio in the mix, resulting in a lesser difference between compressive strength, modulus of elasticity, porosity, water absorption and density of mixes with 60% and 100% fine RCA incorporation than the 0,45 W/B group. The inclusion of 20% fine RCA had a positive effect in most tested physical and mechanical properties.
- Testing revealed that fine RCA can be incorporated in concrete for low or medium replacement ratios without significantly reducing the mechanical properties, and the desired compressive strength can be achieved at long-term with an adequate mix design. The incorporation of Fly Ash had a negative effect at early ages, however, at 90 days the difference was lower, and some mixes achieved the design strength.
- Chloride penetration tests revealed a detrimental effect of incorporating fine RCA in concrete, presenting higher charge passed and non-steady-state migration coefficient. However, the use of 20% fly ash proved to be a highly effective mitigator in reducing chloride permeability, obtaining at 90 days a “moderate” risk classification according to the ASTM C1202 for mixes made with even 100% fine RCA.
- Electrochemical measurements revealed that the use of fly ash reduces the electrical conductance of recycled concrete and has a very positive effect in long-

term durability. This effect was more notorious for mixes with low W/B ratios. This is consistent with the observed results in chloride penetration testing and reveals that the use of supplementary cementitious materials can reduce the negative effects of incorporating fine RCA and allow the use of these materials in structural concrete.

- Electrochemical corrosion measurements revealed that the use of fine RCA is not a corrosion trigger by itself. At early and later ages, all concrete mixes with both natural and recycled aggregates presented a “moderate” risk of corrosion even when exposed to a corrosive environment with high chloride presence. Corrosion testing also revealed that concrete made with fine RCA may be used for a service lifespan of more than 100 years without risk of corrosion for low exposure categories.
- When the recycled aggregates are derived of concrete sorted without organic contaminants and masonry or ceramic waste, international building codes could allow the use of fine RCA in replacement ratios of 20% and up to 60% if a mitigator such as fly ash is implemented for structural concrete with low or medium strength requirements and a regular service lifespan of 50 to 100 years. Even higher ratios could be implemented if an adequate mechanical and durability performance is demonstrated. The physical properties of the aggregates are related to the hardened state properties of concrete, requiring the control of variables such as particle absorption and density, however, a satisfactory performance was obtained from fine aggregates that were crushed and sorted without expensive technologies. If a sorting protocol is made in the demolition process, the aggregates could be used for structural concrete without requiring additional processing. If an aggregate does not meet the proposed physical requirements, literate review has shown that mechanical, chemical, or thermal processes could be implemented to remove old-attached mortar, reducing water absorption, and increasing the aggregate’s density.
- A recycled concrete producer with fine RCA could easily implement a mechanical performance-tracking system, identifying the optimal values of recycled aggregate and fly ash to be used depending on the design characteristic of concrete. From a

durability point of view, periodic chloride penetration tests could be performed but the results from this research show that the incorporation of fine RCA by itself is not a trigger for corrosion and the concrete mixes can have similar permeability values than conventional concrete. For low exposure areas, fine RCA between 20% and 60% could be implemented with fly ash for structural purposes with low or medium strength requirements and a regular lifespan of 100 years.

- The growing international concern for sustainability will continue to promote the use of recycled materials. This research has shown that the re-use of fine recycled concrete aggregates for structural use is possible if an adequate mitigation technique is provided form a mechanical and durability point of view as target resistance can be achieved when using fine recycled aggregates and corrosion risk due to chlorides is not higher than conventional concrete.

9.2 Recommendations for further research

- This research assessed the effects of recycled aggregates obtained from crushed prefabricated slabs. Further research must be performed assessing the effects of multiple sources of fine RCA and the correlation between the properties of RCA and hardened concrete. If the viability of using recycled aggregates with a different composition than the proposed is identified, the use of fine RCA could be implemented without strict demolition and sorting protocols.
- While alkali-aggregate testing was performed, literature review indicates that further research regarding this reaction and possible mitigators must be performed.
- This research was conducted for different fine recycled aggregate replacement ratios between 0% and 100%. However, further research must be performed for a narrower substitution between 0% and 25% regarding mechanical and durability-related properties since no apparent negative effect was observed in this range.
- The modulus of elasticity was determined at 90 days for most mixes and a estimation factor was discussed for this age. However, since it is an important

design parameter that could affect the dimension of structural elements, further research should be performed at different ages and employing multiple sources of fine RCA.

- Further research should be performed regarding the rheological properties of concrete made with recycled aggregates due to their higher water absorption including the use of super plasticizers and water reducing admixtures.
- Further research should be performed regarding cyclic loading and energy dissipation capacity for structural elements made with RCA in general, since many countries, such as Colombia, that would benefit for their use have higher seismic activity.
- Further research should be performed regarding the economic viability of employing different replacement ratios of fine RCA in Colombia, performing a life cycle assessment and establishing a comparative price analysis between RAC, RAC with enhancing methods and conventional concrete.
- To further enhance the positive environmental effects of using RCA, further research regarding supplementary cementing materials (SCM) should be performed.

10. References

[1] B. Estanqueiro, J. Dinis Silvestre, J. de Brito, and M. Duarte Pinheiro, “Environmental life cycle assessment of coarse natural and recycled aggregates for concrete,” *Eur. J. Environ. Civ. Eng.*, vol. 22, no. 4, pp. 429–449, 2018.

[2] C. M. Grădinaru, “The Environmental Impact of Concrete Production and the Necessity of its Greening,” *Resilient Soc. Multidiscip. Contrib. from Econ. Law, Policy, Eng. Agric. Life Sci. Fields*, no. June, 2017.

[3] A. Melo, A. Gonçalves, and I. Martins, “Construction and demolition waste generation and management in Lisbon (Portugal),” *Resour. Conserv. Recycl. - RESOUR Conserv Recycl*, vol. 55, pp. 1252–1264, 2011.

[4] J. Xiao, *Recycled Aggregate Concrete Structures*. 2018.

[5] J. De Brito, F. Agrela, and R. V. Silva, *Construction and Demolition Waste*. Elsevier Ltd, 2019.

[6] L. W. Zhang, A. O. Sojobi, V. K. R. Kodur, and K. M. Liew, “Effective utilization and recycling of mixed recycled aggregates for a greener environment,” *J. Clean. Prod.*, vol. 236, p. 117600, 2019.

[7] B. B. Mukharjee and S. V. Barai, “Mechanical and microstructural characterization of recycled aggregate concrete containing silica nanoparticles,” *J. Sustain. Cem. Mater.*, vol. 6, no. 1, pp. 37–53, 2017.

[8] K. P. Verian, W. Ashraf, and Y. Cao, “Properties of recycled concrete aggregate and their influence in new concrete production,” *Resour. Conserv. Recycl.*, vol. 133, no. October 2017, pp. 30–49, 2018.

[9] H. Guo *et al.*, “Durability of recycled aggregate concrete – A review,” *Cem. Concr. Compos.*, vol. 89, pp. 251–259, 2018.

[10] W. H. Kwan, M. Ramli, K. J. Kam, and M. Z. Sulieman, “Influence of the amount of recycled coarse aggregate in concrete design and durability properties,” *Constr. Build. Mater.*, vol. 26, no. 1, pp. 565–573, 2012.

[11] D. Matias, J. De Brito, A. Rosa, and D. Pedro, “Mechanical properties of concrete

produced with recycled coarse aggregates - Influence of the use of superplasticizers," *Constr. Build. Mater.*, vol. 44, pp. 101–109, 2013.

[12] J. Xiao, W. Li, Y. Fan, and X. Huang, "An overview of study on recycled aggregate concrete in China (1996-2011)," *Constr. Build. Mater.*, vol. 31, pp. 364–383, 2012.

[13] J. Pacheco, J. de Brito, C. Chastre, and L. Evangelista, "Experimental investigation on the variability of the main mechanical properties of concrete produced with coarse recycled concrete aggregates," *Constr. Build. Mater.*, vol. 201, pp. 110–120, 2019.

[14] R. Kurda, J. De Brito, and J. D. Silvestre, "Indirect evaluation of the compressive strength of recycled aggregate concrete with high fly ash ratios," *Mag. Concr. Res.*, vol. 70, no. 4, pp. 204–216, 2018.

[15] F. Rodrigues, M. T. Carvalho, L. Evangelista, and J. De Brito, "Physical-chemical and mineralogical characterization of fine aggregates from construction and demolition waste recycling plants," *J. Clean. Prod.*, vol. 52, pp. 438–445, 2013.

[16] S. Lotfi, M. Eggimann, E. Wagner, R. Mróz, and J. Deja, "Performance of recycled aggregate concrete based on a new concrete recycling technology," *Constr. Build. Mater.*, vol. 95, pp. 243–256, 2015.

[17] D. Pedro, J. de Brito, and L. Evangelista, "Evaluation of high-performance concrete with recycled aggregates: Use of densified silica fume as cement replacement," *Constr. Build. Mater.*, vol. 147, pp. 803–814, 2017.

[18] R. V. V Silva, J. De Brito, R. K. K. Dhir, J. de Brito, and R. K. K. Dhir, "Use of recycled aggregates arising from construction and demolition waste in new construction applications," *J. Clean. Prod.*, vol. 236, p. 117629, 2019.

[19] P. Marco, *A conceptual model to design recycled aggregate concrete for structural applications*. 2014.

[20] V. S. Babu, A. K. Mullick, K. K. Jain, and P. K. Singh, "Strength and durability characteristics of high-strength concrete with recycled aggregate-influence of processing," *J. Sustain. Cem. Mater.*, vol. 4, no. 1, pp. 54–71, 2014.

[21] C. Shi, Y. Li, J. Zhang, W. Li, L. Chong, and Z. Xie, "Performance enhancement of

recycled concrete aggregate - A review," *J. Clean. Prod.*, vol. 112, pp. 466–472, 2016.

[22] B. J. Zhan, D. X. Xuan, W. Zeng, and C. S. Poon, "Carbonation treatment of recycled concrete aggregate: Effect on transport properties and steel corrosion of recycled aggregate concrete," *Cem. Concr. Compos.*, vol. 104, no. July, p. 103360, 2019.

[23] C. M. Nwakaire, S. P. Yap, C. C. Onn, C. W. Yuen, and H. A. Ibrahim, "Utilisation of recycled concrete aggregates for sustainable highway pavement applications ; a review," *Constr. Build. Mater.*, vol. 235, p. 117444, 2020.

[24] R. Wang, N. Yu, and Y. Li, "Methods for improving the microstructure of recycled concrete aggregate : A review," *Constr. Build. Mater.*, vol. 242, p. 118164, 2020.

[25] K. Mcneil and T. H. Kang, "Recycled Concrete Aggregates : A Review," vol. 7, no. 1, pp. 61–69, 2013.

[26] L. Evangelista and J. De Brito, "Concrete with fine recycled aggregates: A review," *Eur. J. Environ. Civ. Eng.*, vol. 18, no. 2, pp. 129–172, 2014.

[27] M. Pepe, R. D. Toledo Filho, E. A. B. Koenders, and E. Martinelli, "Alternative processing procedures for recycled aggregates in structural concrete," *Constr. Build. Mater.*, vol. 69, pp. 124–132, 2014.

[28] G. Dimitriou, P. Savva, and M. F. Petrou, "Enhancing mechanical and durability properties of recycled aggregate concrete." 2017.

[29] S. M. S. Kazmi, M. J. Munir, Y.-F. Wu, I. Patnaikuni, Y. Zhou, and F. Xing, "Influence of different treatment methods on the mechanical behavior of recycled aggregate concrete: A comparative study," *Cem. Concr. Compos.*, vol. 104, no. July, p. 103398, 2019.

[30] Y. Kim, A. Hanif, S. M. S. Kazmi, M. J. Munir, and C. Park, "Properties enhancement of recycled aggregate concrete through pretreatment of coarse aggregates - Comparative assesssment of assorted techniques." 2018.

[31] S. Ismail and M. Ramli, "Engineering properties of treated recycled concrete aggregate (RCA) for structural applications," *Constr. Build. Mater.*, vol. 44, pp. 464–476, 2013.

[32] A. Akbarnezhad, K. C. G. Ong, M. H. Zhang, C. T. Tam, and T. W. J. Foo, “Microwave-assisted beneficiation of recycled concrete aggregates,” *Constr. Build. Mater.*, vol. 25, no. 8, pp. 3469–3479, 2011.

[33] H. Choi, M. Lim, H. Choi, R. Kitagaki, and T. Noguchi, “Using Microwave Heating to Completely Recycle Concrete,” *J. Environ. Prot. (Irvine,. Calif).*, vol. 05, no. 07, pp. 583–596, 2014.

[34] K. Bru, S. Touzé, F. Bourgeois, N. Lippiatt, and Y. Ménard, “Assessment of a microwave-assisted recycling process for the recovery of high-quality aggregates from concrete waste,” *Int. J. Miner. Process.*, vol. 126, no. January 2014, pp. 90–98, 2014.

[35] M. S. de Juan and P. A. Gutiérrez, “Study on the influence of attached mortar content on the properties of recycled concrete aggregate,” *Constr. Build. Mater.*, vol. 23, no. 2, pp. 872–877, 2009.

[36] F. S. Khalid, N. B. Azmi, K. A. S. M. Sumandi, and P. N. Mazenan, “Mechanical properties of concrete containing recycled concrete aggregate (RCA) and ceramic waste as coarse aggregate replacement,” *AIP Conf. Proc.*, vol. 1891, no. 2017, 2017.

[37] S. Kabir, A. Al-Shayeb, and I. M. Khan, “Recycled Construction Debris as Concrete Aggregate for Sustainable Construction Materials,” *Procedia Eng.*, vol. 145, pp. 1518–1525, 2016.

[38] K. Kim, M. Shin, and S. Cha, “Combined effects of recycled aggregate and fly ash towards concrete sustainability,” *Constr. Build. Mater.*, vol. 48, pp. 499–507, 2013.

[39] Y. Wang, P. Hughes, H. Niu, and Y. Fan, “A new method to improve the propierties of recycled aggregate concrete: Composite addition of basalt fiber and nano-silica.” 2019.

[40] A. Abd Elhakam, A. E. Mohamed, and E. Awad, “Influence of self-healing, mixing method and adding silica fume on mechanical properties of recycled aggregates concrete,” *Constr. Build. Mater.*, vol. 35, pp. 421–427, 2012.

[41] B. A. Tayeh, D. M. Al, and R. Alyousef, “The utilization of recycled aggregate in high performance concrete : a review,” *Integr. Med. Res.*, vol. 9, no. 4, pp. 8469–8481,

2020.

[42] M. Gomes and J. De Brito, “Structural concrete with incorporation of coarse recycled concrete and ceramic aggregates: Durability performance,” *Mater. Struct. Constr.*, vol. 42, no. 5, pp. 663–675, 2009.

[43] V. W. Y. Tam, D. Kotrayothar, and J. Xiao, “Long-term deformation behaviour of recycled aggregate concrete,” *Constr. Build. Mater.*, vol. 100, pp. 262–272, 2015.

[44] S. Seara-paz, B. González-fonteboa, F. Martínez-abella, and I. González-taboada, “Time-dependent behaviour of structural concrete made with recycled coarse aggregates . Creep and shrinkage,” *Constr. Build. Mater.*, vol. 122, pp. 95–109, 2016.

[45] D. Pedro, J. de Brito, and L. Evangelista, “Structural concrete with simultaneous incorporation of fine and coarse recycled concrete aggregates: Mechanical, durability and long-term properties,” *Constr. Build. Mater.*, vol. 154, pp. 294–309, 2017.

[46] R. V. Silva, J. De Brito, and R. K. Dhir, “Properties and composition of recycled aggregates from construction and demolition waste suitable for concrete production,” *Constr. Build. Mater.*, vol. 65, pp. 201–217, 2014.

[47] L. Evangelista and J. De Brito, “Durability of crushed fine recycled aggregate concrete assessed by permeability-related properties,” *Mag. Concr. Res.*, vol. 71, no. 21, pp. 1142–1150, 2019.

[48] J. J. de Oliveira Andrade, E. Possan, J. Z. Squiavon, and T. L. P. Ortolan, “Evaluation of mechanical properties and carbonation of mortars produced with construction and demolition waste,” *Constr. Build. Mater.*, vol. 161, pp. 70–83, 2018.

[49] L. Evangelista, M. Guedes, J. De Brito, A. C. Ferro, and M. F. Pereira, “Physical, chemical and mineralogical properties of fine recycled aggregates made from concrete waste,” *Constr. Build. Mater.*, vol. 86, pp. 178–188, 2015.

[50] S. Ghorbani, S. Sharifi, S. Ghorbani, V. W. Tam, J. de Brito, and R. Kurda, “Effect of crushed concrete waste’s maximum size as partial replacement of natural coarse aggregate on the mechanical and durability properties of concrete,” *Resour. Conserv. Recycl.*, vol. 149, no. November 2018, pp. 664–673, 2019.

[51] M. Bravo *et al.*, “Durability performance of concrete with recycled aggregates from construction and demolition waste plants,” *Constr. Build. Mater.*, vol. 77, pp. 357–369, 2015.

[52] F. Cartuxo, J. De Brito, L. Evangelista, J. R. Jiménez, and E. F. Ledesma, “Increased durability of concrete made with fine recycled concrete aggregates using superplasticizers,” *Materials (Basel).*, vol. 9, no. 2, 2016.

[53] C. J. Zega and Á. A. Di Maio, “Use of recycled fine aggregate in concretes with durable requirements,” *Waste Manag.*, vol. 31, no. 11, pp. 2336–2340, 2011.

[54] L. Evangelista and J. de Brito, “Mechanical behaviour of concrete made with fine recycled concrete aggregates,” *Cem. Concr. Compos.*, vol. 29, no. 5, pp. 397–401, 2007.

[55] Z. Guo, C. Chen, D. E. Lehman, W. Xiao, S. Zheng, and B. Fan, “Mechanical and durability behaviours of concrete made with recycled coarse and fine aggregates,” *Eur. J. Environ. Civ. Eng.*, vol. 8189, pp. 1–19, 2017.

[56] L. Evangelista and J. de Brito, “Durability performance of concrete made with fine recycled concrete aggregates,” *Cem. Concr. Compos.*, vol. 32, no. 1, pp. 9–14, 2010.

[57] S. Sadati and K. H. Khayat, “Field performance of concrete pavement incorporating recycled concrete aggregate,” *Constr. Build. Mater.*, vol. 126, pp. 691–700, 2016.

[58] C. Thomas, J. Setién, J. A. Polanco, P. Alaejos, and M. Sánchez De Juan, “Durability of recycled aggregate concrete,” *Constr. Build. Mater.*, vol. 40, pp. 1054–1065, 2013.

[59] S. Omary, E. Ghorbel, and G. Wardeh, “Relationships between recycled concrete aggregates characteristics and recycled aggregates concretes properties,” *Constr. Build. Mater.*, vol. 108, pp. 163–174, 2016.

[60] Y. A. Fawzy, “Impact of recycled gravel obtained from low or medium concrete grade on concrete properties,” *HBRC J.*, vol. 14, no. 1, pp. 1–8, 2018.

[61] L. Ferreira, J. De Brito, and M. Barra, “Influence of the pre-saturation of recycled coarse concrete aggregates on concrete properties,” *Mag. Concr. Res.*, vol. 63, no. 8, pp. 617–627, 2011.

[62] A. Barbudo, J. De Brito, L. Evangelista, M. Bravo, and F. Agrela, “Influence of water-reducing admixtures on the mechanical performance of recycled concrete,” *J. Clean. Prod.*, vol. 59, pp. 93–98, 2013.

[63] L. Ferreira, J. de Brito, and M. Barra, “Influence of the pre-saturation of recycled coarse concrete aggregates on concrete properties,” *Mag. Concr. Res.*, vol. 63, no. 8, pp. 617–627, 2011.

[64] C. Ulsen, H. Kahn, G. Hawlitschek, E. A. Masini, S. C. Angulo, and V. M. John, “Production of recycled sand from construction and demolition waste,” *Constr. Build. Mater.*, vol. 40, pp. 1168–1173, 2013.

[65] R. V. Silva, J. De Brito, and N. Saikia, “Influence of curing conditions on the durability-related performance of concrete made with selected plastic waste aggregates,” *Cem. Concr. Compos.*, vol. 35, no. 1, pp. 23–31, 2013.

[66] C. Alexandridou, G. N. Angelopoulos, and F. A. Coutelieris, “Mehcanical and durability performance of concrete produced with recycled aggregates from Greek construction and demolition waste plants.” 2017.

[67] J. Xiao, D. Lu, and J. Ying, “Durability of recycled aggregate concrete: An overview,” *J. Adv. Concr. Technol.*, vol. 11, no. 12, pp. 347–359, 2013.

[68] R. Kurda, J. de Brito, and J. D. Silvestre, “Combined influence of recycled concrete aggregates and high contents of fly ash on concrete properties,” *Constr. Build. Mater.*, vol. 157, pp. 554–572, 2017.

[69] M. J. McGinnis, M. Davis, A. de la Rosa, B. D. Weldon, and Y. C. Kurama, “Strength and stiffness of concrete with recycled concrete aggregates,” *Constr. Build. Mater.*, vol. 154, pp. 258–269, 2017.

[70] D. Pedro, J. De Brito, and L. Evangelista, “Influence of the use of recycled concrete aggregates from different sources on structural concrete,” *Constr. Build. Mater.*, vol. 71, no. 2014, pp. 141–151, 2014.

[71] C. C. Fan, R. Huang, H. Hwang, and S. J. Chao, “The effects of different fine recycled concrete aggregates on the properties of Mortar,” *Materials (Basel).*, vol. 8, no. 5, pp. 2658–2672, 2015.

[72] Z. Li, *Advanced Concrete Technology*. Wiley, 2011.

[73] A. André, J. De Brito, A. Rosa, and D. Pedro, “Durability performance of concrete incorporating coarse aggregates from marble industry waste,” *J. Clean. Prod.*, vol. 65, pp. 389–396, 2014.

[74] R. V. Silva, R. Neves, J. De Brito, and R. K. Dhir, “Carbonation behaviour of recycled aggregate concrete,” *Cem. Concr. Compos.*, vol. 62, pp. 22–32, 2015.

[75] S. Macdonald, *Concrete: Building Pathology*. Wiley, 2008.

[76] A. M. Neville and J. J. Brooks, *Concrete Technology*. Prentice Hall, 2010.

[77] S.-C. Kou and C.-S. Poon, “Long-term mechanical and durability properties of recycled aggregate concrete prepared with the incorporation of fly ash,” *Cem. Concr. Compos.*, vol. 37, pp. 12–19, 2013.

[78] R. Kurda, J. De Brito, and J. D. Silvestre, “Carbonation of concrete made with high amount of fly ash and recycled concrete aggregates for utilization of CO2,” *J. CO2 Util.*, vol. 29, no. November 2018, pp. 12–19, 2019.

[79] M. C. Limbachiya, T. Leelawat, and R. K. Dhir, “RCA CONCRETE: A STUDY OF PROPERTIES IN THE FRESH STATE, STRENGTH DEVELOPMENT AND DURABILITY,” in *Sustainable Construction: Use of Recycled Concrete Aggregate*, pp. 227–237.

[80] S. C. Kou, “Influence of Fly Ash as Cement Replacement on the Properties of Recycled Aggregate Concrete,” *ASCE Libr.*, 2007.

[81] S. C. Kou, C. S. Poon, and H. W. Wan, “Properties of concrete prepared with low-grade recycled aggregates,” *Constr. Build. Mater.*, vol. 36, pp. 881–889, 2012.

[82] R. Kurda, J. de Brito, and J. D. Silvestre, “Water absorption and electrical resistivity of concrete with recycled concrete aggregates and fly ash,” *Cem. Concr. Compos.*, vol. 95, no. October 2018, pp. 169–182, 2019.

[83] J. Sim and C. Park, “Compressive strength and resistance to chloride ion penetration and carbonation of recycled aggregate concrete with varying amount of fly ash and fine recycled aggregate,” *Waste Manag.*, vol. 31, no. 11, pp. 2352–2360, 2011.

[84] R. V. Silva, J. De Brito, R. Neves, and R. Dhir, “Prediction of chloride ion penetration of recycled aggregate concrete,” *Mater. Res.*, vol. 18, no. 2, pp. 427–440, 2015.

[85] S. Taner, C. Meyer, and S. Herfellner, “Effects of internal curing on the strength , drying shrinkage and freeze – thaw resistance of concrete containing recycled concrete aggregates,” *Constr. Build. Mater.*, vol. 91, pp. 288–296, 2015.

[86] Y. Cheng, X. Shang, and Y. Zhang, “Experimental research on durability of recycled aggregate concrete under freeze- thaw cycles,” 2017.

[87] S. Lotfi, J. Deja, P. Rem, R. Mróz, E. Van Roekel, and H. Van Der Stelt, “Mechanical recycling of EOL concrete into high-grade aggregates,” *"Resources, Conserv. Recycl.*, vol. 87, pp. 117–125, 2014.

[88] J. Wu, X. Jing, and Z. Wang, “Uni-axial compressive stress-strain relation of recycled coarse aggregate concrete after freezing and thawing cycles,” *Constr. Build. Mater.*, vol. 134, pp. 210–219, 2017.

[89] Z. Li, Z. Deng, H. Yang, and H. Wang, “Bond behavior between recycled aggregate concrete and deformed rebar after Freeze-thaw damage,” *Constr. Build. Mater.*, vol. 250, p. 118805, 2020.

[90] A. Richardson, K. Coventry, and J. Bacon, “Freeze / thaw durability of concrete with recycled demolition aggregate compared to virgin aggregate concrete,” *J. Clean. Prod.*, vol. 19, no. 2–3, pp. 272–277, 2011.

[91] J. A. Bogas, J. De Brito, and D. Ramos, “Freeze e thaw resistance of concrete produced with fi ne recycled concrete aggregates,” *J. Clean. Prod.*, vol. 115, pp. 294–306, 2016.

[92] R. Zaharieva, “Frost resistance of recycled aggregate concrete,” vol. 34, pp. 1927–1932, 2004.

[93] K. Liu, J. Yan, Q. Hu, Y. Sun, and C. Zou, “Effects of parent concrete and mixing method on the resistance to freezing and thawing of air-entrained recycled aggregate concrete,” *Constr. Build. Mater.*, vol. 106, pp. 264–273, 2016.

[94] A. Gokce, S. Nagataki, T. Saeki, and M. Hisada, “Freezing and thawing resistance of air-entrained concrete incorporating recycled coarse aggregate: The role of air

content in demolished concrete," *Cem. Concr. Res.*, vol. 34, no. 5, pp. 799–806, 2004.

[95] M. Bravo, J. De Brito, J. Pontes, and L. Evangelista, "Shrinkage and creep performance of concrete with recycled aggregates from CDW plants," *Mag. Concr. Res.*, vol. 69, no. 19, pp. 974–995, 2017.

[96] R. V. Silva, J. De Brito, and R. K. Dhir, "Prediction of the shrinkage behavior of recycled aggregate concrete: A review," *Constr. Build. Mater.*, vol. 77, pp. 327–339, 2015.

[97] Y. Geng, Y. Wang, and J. Chen, "Creep behaviour of concrete using recycled coarse aggregates obtained from source concrete with different strengths," *Constr. Build. Mater.*, vol. 128, pp. 199–213, 2016.

[98] Y. Geng, M. Zhao, H. Yang, and Y. Wang, "Creep model of concrete with recycled coarse and fine aggregates that accounts for creep development trend difference between recycled and natural aggregate concrete," *Cem. Concr. Compos.*, vol. 103, no. October 2018, pp. 303–317, 2019.

[99] F. Cartuxo, J. De Brito, L. Evangelista, J. R. Jiménez, and E. F. Ledesma, "Rheological behaviour of concrete made with fine recycled concrete aggregates - Influence of the superplasticizer," *Constr. Build. Mater.*, vol. 89, pp. 36–47, 2015.

[100] S. Manzi, C. Mazzotti, and M. C. Bignozzi, "Short and long-term behavior of structural concrete with recycled concrete aggregate," *Cem. Concr. Compos.*, vol. 37, no. 1, pp. 312–318, 2013.

[101] C. Thomas, J. De Brito, A. Cimentada, and J. A. Sainz-aja, "Macro- and micro-properties of multi-recycled aggregate concrete," *J. Clean. Prod.*, vol. 245, p. 118843, 2020.

[102] P. Zhu, Y. Hao, H. Liu, D. Wei, L. Shaofeng, and L. Gu, "Durability evaluation of three generations of 100% repeatedly recycled coarse aggregate concrete." 2019.

[103] V. Abreu, L. Evangelista, and J. de Brito, "The effect of multi-recycling on the mechanical performance of coarse recycled aggregates concrete." 2018.

[104] A. Poursaee, *Corrosion of Steel in Concrete Structures*, 1st ed. Elsevier, 2016.

[105] S. F. U. Ahmed, “Properties of Concrete Containing Recycled Fine Aggregate and Fly Ash,” *J. Solid Waste Technol. Manag.*, vol. 40, no. 1, pp. 70–78, 2014.

[106] Q. Ren, Y. Wu, X. Zhang, and Y. Wang, “Effects of fly ash on the mechanical and impact properties of recycled aggregate concrete after exposure to high temperature,” *Eur. J. Environ. Civ. Eng.*, vol. 0, no. 0, pp. 1–17, 2019.

[107] R. V. Silva, J. de Brito, and R. K. Dhir, “Comparative analysis of existing prediction models on the creep behaviour of recycled aggregate concrete,” *Eng. Struct.*, vol. 100, pp. 31–42, 2015.

[108] M. Limbachiya, M. S. Meddah, and Y. Ouchagour, “Use of recycled concrete aggregate in fly-ash concrete,” *Constr. Build. Mater.*, vol. 27, no. 1, pp. 439–449, 2012.

[109] K. P. Verian, “Using recycled concrete as coarse aggregate in pavement concrete,” no. April 2012, p. 192, 2012.

[110] B. Fonteboa and F. Abella, “Concretes with aggregates from demolition waste and silica fume. Materials and mechanical properties,” *Build. Environ.*, vol. 43, pp. 429–437, 2008.

[111] M. Gesoglu, E. Güneyisi, H. Ö. Öz, I. Taha, and M. T. Yasemin, “Failure characteristics of self-compacting concretes made with recycled aggregates,” *Constr. Build. Mater.*, vol. 98, pp. 334–344, 2015.

[112] Y. Wang, P. Hughes, H. Niu, and Y. Fan, “A new method to improve the properties of recycled aggregate concrete: Composite addition of basalt fiber and nano-silica,” *J. Clean. Prod.*, vol. 236, p. 117602, 2019.

[113] M. Stefanidou and I. Papayianni, “Influence of nano-SiO2 on the Portland cement pastes,” *Compos. Part B Eng.*, vol. 43, pp. 2706–2710, 2012.

[114] Z. Luo, W. Li, V. W. Y. Tam, J. Xiao, and S. P. Shah, “Current progress on nanotechnology application in recycled aggregate concrete,” *J. Sustain. Cem. Mater.*, vol. 8, no. 2, pp. 79–96, 2019.

[115] J. Ying, B. Zhou, and J. Xiao, “Pore structure and chloride diffusivity of recycled

aggregate concrete with nano-SiO2 and nano-TiO2," *Constr. Build. Mater.*, vol. 150, pp. 49–55, 2017.

[116] P. Hosseini, A. Booshehrian, and A. Madari, "Developing Concrete Recycling Strategies by Utilization of Nano-SiO2 Particles," *Waste and Biomass Valorization*, vol. 2, no. 3, pp. 347–355, 2011.

[117] M. A. Chandak and P. Y. Pawade, "Influence of Metakaolin in Concrete Mixture : A Review," no. May, pp. 37–41, 2018.

[118] P. min Zhan *et al.*, "Utilization of nano-metakaolin in concrete: A review," *J. Build. Eng.*, vol. 30, no. January, p. 101259, 2020.

[119] R. Muduli and B. B. Mukharjee, "Performance assessment of concrete incorporating recycled coarse aggregates and metakaolin: A systematic approach," *Constr. Build. Mater.*, vol. 233, p. 117223, 2020.

[120] J. Xie *et al.*, "Effect of nano metakaolin on compressive strength of recycled concrete," *Constr. Build. Mater.*, vol. 256, 2020.

[121] A. Sadeghi-Nik, J. Berenjian, S. Alimohammadi, O. Lotfi-Omran, A. Sadeghi-Nik, and M. Karimaei, "The Effect of Recycled Concrete Aggregates and Metakaolin on the Mechanical Properties of Self-Compacting Concrete Containing Nanoparticles," *Iran. J. Sci. Technol. - Trans. Civ. Eng.*, vol. 43, no. s1, pp. 503–515, 2019.

[122] R. Muduli and B. B. Mukharjee, "Effect of incorporation of metakaolin and recycled coarse aggregate on properties of concrete," *J. Clean. Prod.*, vol. 209, pp. 398–414, 2019.

[123] V. N. Patel, C. D. Modhera, M. M. Chavda, and M. M. Panseriya, "Effect of metakaolin on mechanical properties of different grades concretes inclusion of recycled aggregates from C & D waste and ceramic waste," *Int. J. Eng. Technol.*, vol. 7, no. 3, pp. 138–142, 2018.

[124] N. K. Bui, T. Satomi, and H. Takahashi, "Effect of mineral admixtures on properties of recycled aggregate concrete at high temperature," *Constr. Build. Mater.*, vol. 184, pp. 361–373, 2018.

[125] K. Kapoor, S. P. Singh, and B. Singh, “Permeability of self-compacting concrete made with recycled concrete aggregates and metakaolin,” *J. Sustain. Cem. Mater.*, vol. 6, no. 5, pp. 293–313, 2017.

[126] N. Singh and S. P. Singh, “Carbonation and electrical resistance of self compacting concrete made with recycled concrete aggregates and metakaolin,” *Constr. Build. Mater.*, vol. 121, pp. 400–409, 2016.

[127] N. Singh and S. P. Singh, “Carbonation resistance and microstructural analysis of Low and High Volume Fly Ash Self Compacting Concrete containing Recycled Concrete Aggregates,” *Constr. Build. Mater.*, vol. 127, pp. 828–842, 2016.

[128] A. Mardani-Aghabaglou, C. Yüksel, A. Beglarigale, and K. Ramyar, “Improving the mechanical and durability performance of recycled concrete aggregate-bearing mortar mixtures by using binary and ternary cementitious systems,” *Constr. Build. Mater.*, vol. 196, pp. 295–306, 2019.

[129] V. S. Babu, A. K. Mullick, K. K. Jain, and P. K. Singh, “Strength and durability characteristics of high-strength concrete with recycled aggregate-influence of processing,” *J. Sustain. Cem. Mater.*, vol. 4, no. 1, pp. 54–71, 2014.

[130] S.-C. Kou, B. Zhan, and C.-S. Poon, “Use of a CO2 curing step to improve the properties of concrete prepared with recycled aggregates,” *Cem. Concr. Compos.*, vol. 45, pp. 22–28, 2014.

[131] B. Zhan, C. S. Poon, Q. Liu, S. Kou, and C. Shi, “Experimental study on CO2 curing for enhancement of recycled aggregate properties,” *Constr. Build. Mater.*, vol. 67, pp. 3–7, 2014.

[132] B. Lu, C. Shi, Z. Cao, M. Guo, and J. Zheng, “Effect of carbonated coarse recycled concrete aggregate on the properties and microstructure of recycled concrete,” *J. Clean. Prod.*, vol. 233, pp. 421–428, 2019.

[133] Z. Zhao, S. Wang, L. Lu, and C. Gong, “Evaluation of pre-coated recycled aggregate for concrete and mortar,” *Constr. Build. Mater.*, vol. 43, pp. 191–196, 2013.

[134] F. Martirena, T. Castaño, A. Alujas, R. Orozco-Morales, L. Martinez, and S. Linsel, “Improving quality of coarse recycled aggregates through cement coating,” *J. Sustain. Cem. Mater.*, vol. 6, no. 1, pp. 69–84, 2017.

[135] Y. C. Liang, Z. M. Ye, F. Vernerey, and Y. Xi, “Development of processing methods to improve strength of concrete with 100% recycled coarse aggregate,” *J. Mater. Civ. Eng.*, vol. 27, no. 5, pp. 1–9, 2015.

[136] J. Qiu, D. Q. S. Tng, and E.-H. Yang, “Surface treatment of recycled concrete aggregates through microbial carbonate precipitation,” *Constr. Build. Mater.*, vol. 57, pp. 144–150, 2014.

[137] A. M. Grabiec, J. Klama, D. Zawal, and D. Krupa, “Modification of recycled concrete aggregate by calcium carbonate biodeposition,” *Constr. Build. Mater.*, vol. 34, pp. 145–150, 2012.

[138] Z. Feng, Y. Zhao, W. Zeng, Z. Lu, and S. P. Shah, “Using microbial carbonate precipitation to improve the properties of recycled fine aggregate and mortar,” *Constr. Build. Mater.*, vol. 230, p. 116949, 2020.

[139] K. K. Sahoo, M. Arakha, P. Sarkar, D. P. Robin, and S. Jha, “Enhancement of properties of recycled coarse aggregate concrete using bacteria,” *Int. J. Smart Nano Mater.*, vol. 7, no. 1, pp. 22–38, 2016.

[140] J. Wang, B. Vandevyvere, S. Vanhessche, J. Schoon, N. Boon, and N. De Belie, “Microbial carbonate precipitation for the improvement of quality of recycled aggregates,” *J. Clean. Prod.*, vol. 156, pp. 355–366, 2017.

[141] V. W. Y. Tam, X. F. Gao, and C. M. Tam, “Microstructural analysis of recycled aggregate concrete produced from two-stage mixing approach,” *Cem. Concr. Res.*, vol. 35, no. 6, pp. 1195–1203, 2005.

[142] V. W. Y. Tam and C. M. Tam, “Assessment of durability of recycled aggregate concrete produced by two-stage mixing approach,” *J. Mater. Sci.*, vol. 42, no. 10, pp. 3592–3602, May 2007.

[143] J. P. Barreto Delgado and D. A. Cufiño Melo, “Influencia del porcentaje de agregado reciclado en la penetrabilidad al ión cloruro y en la permeabilidad al agua para concretos reciclados,” *Univ. La Gran Colomb.*, no. c, 2014.

[144] A. Laverde and N. Torres Castellanos, “Propiedades mecáncias, eléctricas y de durabilidad de concretos con agregados reciclados,” p. 87, 2017.

[145] S. A. Gil, J. J. M. Barrero, and C. D. T. Bello, “Evaluación de la resistencia a la compresión y flexión de concretos de 28 MPA con RA y Ceniza Volante,” *Univ. La Gran Colomb.*, vol. 53, no. 9, pp. 1689–1699, 2017.

[146] N. R. Bojacá Castañeda, “Propiedades Mecánicas Y De Durabilidad De Concretos Con Agregado Reciclado,” *ECI*, p. 119, 2013.

[147] A. F. de J. Muñoz Cuellar, “Carbonatación acelerada de agregados finos reciclados y su influencia en mezclas de mortero,” *Tesis Maest. Esc. Colomb. Ing. Julio Garavito Colomb. Bogotá*, p. 296, 2017.

[148] ICONTEC - Instituto Colombiano de Normas Técnicas, “NTC 6421 - Agregados gruesos reciclados para uso en el concreto hidráulico.” ICONTEC - Instituto Colombiano de Normas Técnicas, 2021.

[149] ICONTEC - Instituto Colombiano de Normas Técnicas, “NTC 6422 - Ensayo de clasificación de los componentes de los agregados gruesos reciclados,” 2021.

[150] A. Poursaee, “Corrosion of steel bars in saturated Ca(OH)2 and concrete pore solution,” *Chall. J. Concr. Res. Lett.*, vol. 1, no. 3, 2010.

[151] A. Poursaee and C. M. Hansson, “Reinforcing steel passivation in mortar and pore solution,” *Cem. Concr. Res.*, vol. 37, no. 7, pp. 1127–1133, 2007.

[152] O. M. Jensen, P. F. Hansen, A. M. Coats, and F. P. Glasser, “Chloride ingress in cement paste and mortar,” *Cem. Concr. Res.*, vol. 29, no. 9, pp. 1497–1504, 1999.

[153] P. Ghods, O. B. Isgor, G. McRae, and T. Miller, “The effect of concrete pore solution composition on the quality of passive oxide films on black steel reinforcement,” *Cem. Concr. Compos.*, vol. 31, no. 1, pp. 2–11, 2009.

[154] A. J. Bard and M. V Mirkin, *Scanning electrochemical microscopy*. CRC Press, 2001.

[155] B. Martín-Pérez, H. Zibara, R. D. Hooton, and M. D. A. Thomas, “Study of the effect of chloride binding on service life predictions,” *Cem. Concr. Res.*, vol. 30, no. 8, pp. 1215–1223, 2000.

[156] S. Ahmad, “Reinforcement corrosion in concrete structures, its monitoring and service life prediction—a review,” *Cem. Concr. Compos.*, vol. 25, no. 4, pp. 459–471, 2003.

[157] K. Tuutti, “Corrosion of Steel in Concrete,” *Swedish Cem. Concr. Res. Inst.*, 1982.

[158] D. A. Jones, *Principles and Prevention of Corrosion*. Prentice Hall, 1996.

[159] J. L. Marriaga and P. Claisse, “The influence of the blast furnace slag replacement on chloride penetration in concrete,” *Ing. e Investig.*, vol. 31, no. 2, pp. 38–47, 2011.

[160] NT Build 492, “Concrete, mortar and cement-based repair materials: Chloride migration coefficient from non-steady-state migration experiments,” *Measurement*, pp. 1–8, 1999.

[161] R. J. Torrent, “A two-chamber vacuum cell for measuring the coefficient of permeability to air of the concrete cover on site,” *Mater. Struct.*, vol. 25, no. 6, pp. 358–365, 1992.

[162] T. Vieira, A. Alves, J. de Brito, J. R. Correia, and R. V. Silva, “Durability-related performance of concrete containing fine recycled aggregates from crushed bricks and sanitary ware,” *Mater. Des.*, vol. 90, pp. 767–776, 2016.

[163] ASTM International, “ASTM C1157 / C1157M-20a, Standard Performance Specification for Hydraulic Cement,” 2020.

[164] ICONTEC - Instituto Colombiano de Normas Técnicas, “NTC 121 - Especificación de desempeño para cemento hidráulico,” 2021.

[165] ICONTEC - Instituto Colombiano de Normas Técnicas, “NTC 220 - Cementos. Determinación de la resistencia de morteros de cemento hidráulico a la compresión, usando cubos de 50 mm o 2 pulgadas de lado,” 2021.

[166] ASTM International, “ASTM C109 / C109M-21, Standard Test Method for Compressive Strength of Hydraulic Cement Mortars (Using 2-in. or [50 mm] Cube Specimens),” 2021.

[167] ICONTEC - Instituto Colombiano de Normas Técnicas, “NTC 111 - Cementos. Especificaciones para la mesa de flujo usada en ensayos de cemento hidráulico,” 2021.

[168] ICONTEC - Instituto Colombiano de Normas Técnicas, “NTC 3937 - CEMENTOS. ARENA NORMALIZADA PARA ENSAYOS DE CEMENTO HIDRÁULICO,” 2019.

[169] ASTM International, “ASTM C778-17, Standard Specification for Standard Sand,” 2017.

[170] ICONTEC - Instituto Colombiano de Normas Técnicas, “NTC 1776 - MÉTODO DE ENSAYO PARA DETERMINAR EL CONTENIDO TOTAL DE HUMEDAD EVAPORABLE POR SECADO DE LOS AGREGADOS,” 2019.

[171] ICONTEC - Instituto Colombiano de Normas Técnicas, “NTC 176 - Método de ensayo para determinar la densidad relativa (gravedad específica) y la absorción del agregado grueso,” 2019.

[172] ICONTEC - Instituto Colombiano de Normas Técnicas, “NTC 92 - MÉTODO DE ENSAYO PARA LA DETERMINACIÓN DE LA DENSIDAD VOLUMÉTRICA (MASA UNITARIA) Y VACÍOS EN AGREGADOS,” 2019.

[173] ASTM International, “ASTM C566-19, Standard Test Method for Total Evaporable Moisture Content of Aggregate by Drying,” 2019.

[174] ASTM International, “ASTM C127- Standard Test Method for Density, Relative Density (Specific Gravity), and Absorption of Coarse Aggregate,” *Annu. B. ASTM Stand.*, pp. 1–5, 2004.

[175] ASTM International, “ASTM C29, Standard Test Method for Bulk Density (‘ Unit Weight ’) and Voids in Aggregate,” *ASTM Int.*, vol. i, no. c, pp. 1–5, 2009.

[176] ICONTEC - Instituto Colombiano de Normas Técnicas, “NTC 78 - MÉTODO DE ENSAYO PARA DETERMINAR POR LAVADO EL MATERIAL QUE PASA EL TAMIZ 75 µm (No. 200) EN AGREGADOS MINERALES,” 2019.

[177] ICONTEC - Instituto Colombiano de Normas Técnicas, “NTC 237 - Método de ensayo para determinar la densidad relativa (gravedad especifica) y la absorción del agregado fino,” 2020.

[178] ASTM International, “ASTM C117-17, Standard Test Method for Materials Finer than 75-µm (No. 200) Sieve in Mineral Aggregates by Washing,” 2017.

[179] ASTM International, “ASTM C128-15, Standard Test Method for Relative Density (Specific Gravity) and Absorption of Fine Aggregate,” 2015.

[180] ASTM International, “ASTM C87 / C87M-17, Standard Test Method for Effect of

Organic Impurities in Fine Aggregate on Strength of Mortar," 2017.

[181] ASTM International, "ASTM C136 / C136M-19, Standard Test Method for Sieve Analysis of Fine and Coarse Aggregates," vol. i, no. 200, pp. 1–5, 2019.

[182] ASTM International, "ASTM C33 / C33M-18, Standard Specification for Concrete Aggregates," 2018.

[183] ASTM International, "ASTM C295 / C295M-19, Standard Guide for Petrographic Examination of Aggregates for Concrete," 2019.

[184] ICONTEC - Instituto Colombiano de Normas Técnicas, "NTC 3773 - Guía para la inspección petrográfica de agregados para concreto," 1995.

[185] B. Fournier and M.-A. Bérubé, "Alkali-aggregate reaction in concrete: a review of basic concepts and engineering implications," *Can. J. Civ. Eng.*, vol. 27, no. 2, pp. 167–191, 2011.

[186] M. B. Santos, J. De Brito, and A. S. Silva, "A review on alkali-silica reaction evolution in recycled aggregate concrete," *Materials (Basel).*, vol. 13, no. 11, 2020.

[187] ASTM International, "ASTM C1260-14 Standard Test Method for Potential Alkali Reactivity of Aggregates (Mortar-Bar Method)," *Annu. B. ASTM Stand. Vol. 04.02*, pp. 1–5, 2014.

[188] ASTM International, "ASTM C1567-21, Standard Test Method for Determining the Potential Alkali-Silica Reactivity of Combinations of Cementitious Materials and Aggregate (Accelerated Mortar-Bar Method)," *Annu. B. ASTM Stand.*, vol. 04.02, pp. 774–778, 2021.

[189] Y. Zhu, A. Zahedi, L. F. M. Sanchez, B. Fournier, and S. Beauchemin, "Overall assessment of alkali-silica reaction affected recycled concrete aggregate mixtures derived from construction and demolition waste," *Cem. Concr. Res.*, vol. 142, no. November 2020, p. 106350, 2021.

[190] C. Trottier, R. Ziapour, A. Zahedi, L. Sanchez, and F. Locati, "Microscopic characterization of alkali-silica reaction (ASR) affected recycled concrete mixtures induced by reactive coarse and fine aggregates," *Cem. Concr. Res.*, vol. 144, no.

March, p. 106426, 2021.

[191] ASTM International, “ASTM D7348-13, Standard Test Methods for Loss on Ignition (LOI) of Solid Combustion Residues,” 2013.

[192] ASTM International, “ASTM C618-19, Standard Specification for Coal Fly Ash and Raw or Calcined Natural Pozzolan for Use in Concrete,” 2019.

[193] ASTM International, “ASTM C494 / C494M-19, Standard Specification for Chemical Admixtures for Concrete,” 2019.

[194] ACI - American Concrete Institute, “ACI PRC-211.1-91: Standard Practice for Selecting Proportions for Normal, Heavyweight, and Mass Concrete,” 2002.

[195] ASTM International, “ASTM C192 / C192M-19, Standard Practice for Making and Curing Concrete Test Specimens in the Laboratory,” pp. 1–8, 2007.

[196] ASTM International, “ASTM C143 / C143M-20, Standard Test Method for Slump of Hydraulic-Cement Concrete,” 2020.

[197] ASTM International, “ASTM C511-19, Standard Specification for Mixing Rooms, Moist Cabinets, Moist Rooms, and Water Storage Tanks Used in the Testing of Hydraulic Cements and Concretes,” 2019.

[198] ASTM International, “ASTM C39 / C39M-21, Standard Test Method for Compressive Strength of Cylindrical Concrete Specimens,” 2021.

[199] ASTM International, “ASTM C469 / C469M-14e1, Standard Test Method for Static Modulus of Elasticity and Poisson’s Ratio of Concrete in Compression,” 2014.

[200] ASTM International, “ASTM C1202-19, Standard Test Method for Electrical Indication of Concrete’s Ability to Resist Chloride Ion Penetration,” 2019.

[201] ASTM International, “ASTM C642-13, Standard Test Method for Density, Absorption, and Voids in Hardened Concrete,” 2013.

[202] Swiss Society of Engineers and Architects, “SIA 262/1 - Construction en béton - Spécifications complémentaires,” 2013.

[203] ASTM International, “ASTM G59-97(2020), Standard Test Method for Conducting Potentiodynamic Polarization Resistance Measurements,” 2020.

[204] R. López *et al.*, “Durabilidad De La Infraestructura De Concreto Reforzado Expuesta a Diferentes Ambientes Urbanos De México,” vol. 292, no. July 2017, p. 149, 2006.

[205] G. H. N. Suarez, “Propiedades mecánicas y de durabilidad del concreto elaborado con agregados finos reciclados sometidos a carbonatación acelerada,” *ECI*, vol. 4, pp. 9–15, 2017.

[206] D. M. Rosero Alvarez, “Propuesta de guía de uso de los agregados reciclados en colombia provenientes de rcd, basado en normativa internacional y en el desarrollo de investigaciones de universidades colombianas,” *Univ. Nac. Colomb.*, 2019.